

Determining fate of aquatic herbicides by quantifying environmentally relevant degradation pathways in whole-lake treatments

By

Amber Marie White

A dissertation submitted in partial fulfillment of the requirements for the degree of

Doctor of Philosophy
(Environmental Chemistry and Technology Program)

at the

UNIVERSITY OF WISCONSIN-MADISON

2022

Date of final oral examination: 08/23/2022

This dissertation is approved by the following members of the Final Oral Committee:

Christina Remucal, Associate Professor, Civil and Environmental Engineering
Katherine McMahon, Professor, Civil and Environmental Engineering
James Hurley, Professor, Civil and Environmental Engineering
Paul Koch, Assistant Professor, Plant Pathology
Michelle Nault, Water Resources Specialist, Wisconsin Department of Natural Resources

Abstract

Determining fate of aquatic herbicides by quantifying environmentally relevant degradation pathways in whole-lake treatments

By

Amber Marie White

Doctor of Philosophy- Environmental Chemistry and Technology Program

University of Wisconsin-Madison

Associate Professor Christina K. Remucal

Professor Katherine D. McMahon

The environmental fate and persistence of polar organic compounds, such as pesticides and personal care products, is driven by the sum of all transformation and physical transport processes that act upon them. Aquatic herbicides, a class of polar organic compounds, are commonly used in lakes, rivers, and reservoirs for the control of invasive and nuisance plants. Here, field and laboratory experiments are combined to quantify the degradation and identify the dominant environmental transformation pathways of three aquatic herbicides: 2,4-dichlorophenoxyacetic acid (2,4-D), flurpyrauxifen-benzyl (FPB), and fluridone. Laboratory experiments quantify photodegradation, biodegradation, sorption, and hydrolysis under isolated conditions. Lab experiments are combined with mass balance modeling and transformation product tracking across the laboratory and field data to draw conclusions about specific chemical fate processes and to identify strategies for translating laboratory transformation studies to environmental systems.

Irradiation studies show that 2,4-D, FPB, and fluridone all undergo direct photodegradation. However, modeling efforts demonstrate that this process is negligible for 2,4-

D under environmental conditions. Biodegradation microcosms constructed using field inocula show that sediment microbial communities are responsible for degradation of 2,4-D in lakes, but fluridone is very resistant to biodegradation. Additional abiotic transformation experiments found that FPB is hydrolyzed to an initial product, florpyrauxifen, which is then biodegraded in the water-sediment microcosms. Attempts to quantify gene copies of the *tfdA* gene, which is responsible for the degradation of 2,4-D, failed in field and lab experiments. Further investigation *in silico* found established primers amplified under 5% of putative degrader sequences but 100% of experimentally verified degraders when allowing for three or one mismatches, respectively, between template and primer sequences.

These results show how the combination of field and laboratory studies can be used to determine a full environmental transformation pathway, identify physical lake processes that may impact chemical fate, and screen for transformation products that warrant further investigation. Our work demonstrates how laboratory experiments can fall short when describing environmental fate, typically due to inaccurately replicating environmental conditions. Finally, this mechanistic understanding of aquatic herbicide fate also helps resource managers make decisions about herbicide use, concentration, and potential risks associated with treatment.

Acknowledgements

There are an incredible number of people who have help me reach this goal of earning my PhD in my personal and professional life. A sincere thank you to everyone I have worked with or talked with my dissertation about. I couldn't have done it without all of you!

First and foremost, a whole-hearted and never ending thank you to my advisers Christy Remucal and Trina McMahon. This dissertation truly would not exist without your thoughtful questioning, critical feedback, and never-ending support of the wild field studies I wanted to carry out. I could not have been luckier to have two incredible role models to learn how to be a scientist from. Thank you for your flexibility and commitment to your students. Our lives are forever changed because of your work.

I would also like to thank my committee members, Paul Koch, Jim Hurley, and Michelle Nault. I am incredibly lucky to have such a wealth of knowledge available to build this dissertation and am eternally grateful for the amount of feedback I have gotten from all of you through paper drafts, preliminary exams, and seminar feedback. An extra thanks to Michelle Nault for guiding my first steps into the aquatic plant management world, with whom I have had the pleasure of attending several lakes management meetings, sharing a cabin in the woods during a power outage, and who provided my first (and only) experience with bear spaghetti.

I would not have made it to the end of my PhD without the mentors I have had along the way. My first introduction to research was through the Searle Biodiesel Lab at Loyola University Chicago, which my mentor Zach Waickman built from the ground up. Zach taught me the basics of working in a lab, designing an experiment, and most importantly how to glue together PVC pipes. I also owe an immense amount of gratitude to my master's adviser Nate Johnson, who taught

me about engineering, writing, mass balances, how to drive a boat, and how to glue together PVC pipes while in a boat.

There are not enough thanks for the members of the Remucal and McMahon labs who have helped me conduct field work, lab work, and maintain some sort of social life during graduate school and a pandemic. Your assistance carrying coolers or canoes and swapping out samples in the HPLC tray is part of the success of this dissertation. An extra thanks to Reid and Jenna for volunteering to do field work, even though we got trapped in a thunderstorm or were gone for 18 hours. Additional thanks and gratitude are due to the past members of the lab and Water Science and Engineering Lab, who provided good conversation, coffee runs, ice cream adventures, and a passion to get outside. An extra special thanks to Ben Peterson for being a good lab mate and great friend. Thank you for all your efforts teaching this chemist more microbiology and thank you for including me in yours and Hannah's life, it has been an honor to feed the cats.

I had the privilege of mentoring four students during my time at UW-Madison, and this dissertation would not have been completed without their help in lab and in the field. Ellie, Sydney, Josie, and Angie- thank you for everything!

This dissertation would not be complete without the unending patience and commitment to student success of James Lazarcik. Your passion for good analytical techniques, methods, and high-quality control are woven throughout the core of this dissertation and are skills I will use forever.

Marissa Kneer will never receive enough credit for her support during my entire grad school experience. When we first started working together in 2016 on mercury, I could not have imagined where we could have ended up today. Thank you for the coffee runs, bike rides, field sampling at 4 am, and road trips that made the last 6 years fun.

To my lockdown companion and close (but far away) friend Elizabeth McDaniel, thank you for everything. From finding our apartment to helping take care of Ivy while I was doing field work, this dissertation is founded in your work and support. I will always be grateful of our game nights, movie nights, and piano nights that made graduate school much more enjoyable. Thank you for sharing Millie with me.

Thank you to my wonderful partner Doug, who I met during graduate school, and who has a infinite amount of patience for my spills, dropped things, and general disarray during stressful times. I am eternally grateful for our time together, and hope to continue exploring, traveling, and trying new experiences now that I am done with school. Thank you for the sacrifices you have made to support me so far- they are not taken lightly.

Finally, thank you to my parents, who have never said no to my dreams and have helped me move across the country for school and research several times, often putting my needs before them. Thank you for teaching me to chase my dreams and never give up, how to make anything happen, and how to push through a difficult situation. To my sister Angela, who has known me as a college student for as long as she can literally remember: it's your turn now. Reach for the stars and chase your dreams. You never know where they'll take you, but I know you have the power to make anything happen.

Table of Contents

Abstract	i
Acknowledgements	iii
List of Figures	x
List of Tables	xvi
Chapter 1	1
<i>1.1 Motivation</i>	<i>1</i>
<i>1.2 Aquatic Herbicides</i>	<i>1</i>
<i>1.3 Herbicide Mode of Action</i>	<i>3</i>
<i>1.4 Herbicide Tolerance and Resistance</i>	<i>3</i>
<i>1.5 Herbicide Formulations</i>	<i>4</i>
<i>1.6 Policy Related to Aquatic Herbicides</i>	<i>5</i>
<i>1.7 Environmental Transformation Processes and Quantification Methods</i>	<i>7</i>
1.7.1 Hydrolysis	<i>8</i>
1.7.2 Photodegradation	<i>9</i>
1.7.3 Microbial Degradation.....	<i>10</i>
1.7.4 Limitations of Laboratory and Field Transformation Testing.....	<i>12</i>
<i>1.8 Environmental Fate of Three Aquatic Herbicides</i>	<i>13</i>
1.8.1 2,4-Dichlorophenoxyacetic Acid	<i>14</i>
1.8.2 Florpyrauxifen-benzyl.....	<i>16</i>
1.8.3 Fluridone	<i>18</i>
<i>1.9 Knowledge Gaps</i>	<i>18</i>
<i>1.10 Research Objectives</i>	<i>20</i>
<i>1.11 References</i>	<i>22</i>
Chapter 2	36
<i>2.1 Details on Collaboration</i>	<i>36</i>
<i>2.2 Abstract</i>	<i>36</i>
<i>2.3 Introduction</i>	<i>37</i>
<i>2.4 Materials and Methods</i>	<i>40</i>
2.4.1 Chemicals.....	<i>40</i>
2.4.2 Field Sampling.....	<i>40</i>
2.4.3 Photochemical Irradiation Experiments.....	<i>42</i>
2.4.4 Microcosm Incubations.....	<i>43</i>

2.4.5 tfdA Analysis	44
2.4.6 Analytical Methods	44
2.4.7 Mass Balance Calculations	44
2.5 <i>Results and Discussion</i>	45
2.5.1 2,4-D Persistence During Lake Applications.....	45
2.5.2 Photochemical Degradation	50
2.5.3 Photochemical Modeling	52
2.5.4 Microbial Degradation of 2,4-D in Aquatic Systems	53
2.6 <i>Environmental Implications</i>	57
2.7 <i>Acknowledgements</i>	59
2.8 <i>References</i>	59
Chapter 3	67
3.1 <i>Details on Collaboration</i>	67
3.2 <i>Abstract</i>	67
3.3 <i>Importance</i>	68
3.4 <i>Introduction</i>	68
3.5 <i>Results</i>	71
3.5.1 Confirming Specificity of 81 and 215 bp Primers in tfdA Reference Genes	71
3.5.2 Failed Amplicon Cloning and Sequencing of PCR Products	74
3.5.3 Phylogenetic Analysis Leads to Discovery of Putative Degraders.....	76
3.5.4 Failed in silico Amplification With qPCR Primers on Putative Degraders.....	80
3.6 <i>Conclusions</i>	81
3.7 <i>Methods</i>	82
3.7.1 Environmental Sample Collection	82
3.7.2 qPCR Amplification.....	83
3.7.3 Bacterial Strains and tfdA Reference Genes.....	84
3.7.4 TOPO Cloning	85
3.7.5 Accessed Datasets	85
3.7.6 Identification of Putative 2,4-D Degraders	86
3.7.7 Phylogenetic Diversity of Putative 2,4-D Degraders and Functional Annotations	87
3.7.8 Primer Analysis.....	87
3.8 <i>Data availability statement</i>	88
3.9 <i>Acknowledgements</i>	88
3.10 <i>References</i>	89
Chapter 4	96
4.1 <i>Details on Collaboration</i>	96
4.2 <i>Abstract</i>	96

4.3 Introduction.....	97
4.4 Materials and Methods	100
4.4.1 Chemicals.....	100
4.4.2 FPB Sample Preservation and Processing	100
4.4.3 Field Sampling.....	101
4.4.4 Photochemical Irradiation Experiments.....	102
4.4.5 Microcosm Incubations.....	103
4.4.6 Hydrolysis Experiment	104
4.4.7 Analytical Methods.....	104
4.4.8 Mass Balance Calculations	104
4.5 Results and Discussion	105
4.5.1 FPB Degradation and Florpyrauxifen Formation in Lakes.....	105
4.5.2 Photochemical Irradiations and Environmental Photodegradation Modeling.....	110
4.5.3 Microcosm Incubations.....	113
4.5.4 Hydrolysis of FPB	115
4.6 Environmental Implications.....	118
4.7 Acknowledgements.....	119
4.8 References	120
Chapter 5	126
5.1 Contribution Statement.....	126
5.2 Abstract.....	126
5.3 Introduction.....	127
5.4 Materials and Methods	129
5.4.1 Chemicals.....	129
5.4.2 Photochemical Irradiation Experiments.....	130
5.4.3 Microcosm Incubations.....	132
5.4.4 Sediment Fluridone Extractions.....	133
5.4.5 Analytical Methods.....	134
5.5 Results and Discussion	135
5.5.1 Photodegradation of Fluridone in Lake Water.....	135
5.5.2 Microcosm Incubations.....	137
5.5.3 Sediment fluridone extractions	140
5.6 Conclusions and Future Directions	142
5.7 Acknowledgements.....	143
5.8 References	143
Chapter 6	148
6.1 Summary	148
6.2 Suggestions for Future Research.....	151

6.2.1 FPB Degradation in Plants.....	151
6.2.2 Florpyrauxifen Fate and Transformation.....	152
6.2.3 Incorporation of Microbiology Community Analysis Into Standardized Biodegradation Tests	152
6.3 References.....	153
Appendix A.....	156
<i>Section A.1. Bio- and Photodegradation Transformation Pathways and Products.....</i>	<i>156</i>
<i>Section A.2. Materials.....</i>	<i>159</i>
<i>Section A.3. Field Sampling Methods.....</i>	<i>160</i>
<i>Section A.4. Bulk Water Chemistry.....</i>	<i>163</i>
<i>Section A.5. Photodegradation Experiments and Modeling.....</i>	<i>165</i>
<i>Section A.6. Microbial Degradation and tfdA Quantification.....</i>	<i>171</i>
<i>Section A.7. Analytical Methods.....</i>	<i>174</i>
<i>Section A.8. Mass Balance.....</i>	<i>175</i>
<i>Section A.9. Treatment data.....</i>	<i>180</i>
<i>Section A.10. References.....</i>	<i>188</i>
Appendix B.....	191
Appendix C.....	193
<i>Section C.1. Materials and Chemical Structures.....</i>	<i>193</i>
<i>Section C.2. Field Sampling Methods.....</i>	<i>195</i>
<i>Section C.3. Bulk Water Chemistry.....</i>	<i>198</i>
<i>Section C.4. Photochemical Irradiations and Modeling.....</i>	<i>198</i>
<i>Section C.5. Microcosm Incubations.....</i>	<i>202</i>
<i>Section C.6. Hydrolysis Experiments.....</i>	<i>204</i>
<i>Section C.7. Analytical Methods.....</i>	<i>205</i>
<i>Section C.8. Treatment Data.....</i>	<i>208</i>
<i>Section C.9 References.....</i>	<i>213</i>

List of Figures

- Figure 1.1.** Invasive Eurasian watermilfoil matted on surface of South Twin Lake. Picture taken by Amber White in August 2019.2
- Figure 1.2.** Overview of direct and indirect photodegradation of an organic compound (R). PPRI can be ^3DOM , $^1\text{O}_2$, or $\cdot\text{OH}$9
- Figure 1.3.** Chemical structures of (a) 2,4-D, (b) 2,4-dichlorophenol, and (c) 3,5-dichlorocatechol14
- Figure 1.4.** Chemical structure of (a) FPB and expected degradation products (b) florpyrauxifen, (c) X12300837, (d) X11966341, (e) X12131932, and (f) X12393505.....17
- Figure 1.5.** Chemical structure of fluridone.....18
- Figure 2.1.** (a) Epilimnion-wide average 2,4-D concentrations during six large-scale treatments. Error bars represent the standard deviation of 2,4-D concentrations measured in epilimnion samples at each time point. Individual lake data with 2,4-D concentrations at all sampling sites can be found in **Figures A.8-A.13**. (b) 2,4-D concentrations in the epilimnion, nearshore, and hypolimnion of Random Lake.....47
- Figure 2.2.** (a, d) Measured 2,4-D concentrations, (b, e) modeling results compared with average epilimnion concentrations, and (c, f) sample site locations for McCarry and Round Lakes, respectively. Maps created using ArcGIS software (10.6.1) by Esri. Data provided by the National Atlas of the United States, USGS. Error bars in panels (b) and (e) represent the standard deviation of 2,4-D concentrations measured in epilimnion samples at each time point.....48
- Figure 2.3.** (a) Observed 2,4-D laboratory photodegradation rate constants, corrected for light screening, in lake water and corresponding direct photodegradation controls. (b) Observed degradation of 2,4-D in microcosm incubations using sediment and water (Sed) in comparison with abiotic controls (Control) and lake water only (Water) for McCarry (McC), Round (Rnd), and Random (Rdm) Lakes. Error bars represent the standard deviation of triplicate samples. Individual lake microcosm data is presented in **Figure A.6**.....51
- Figure 3.1.** Gel of sediment recovery experiment using a serial dilution of *tfdA* class I gene standard from 10^7 (most left) to 10^1 (most right) (a). Gel of lake sediments and spiked with 10^3 gene copies (white boxes) and unspiked sediments (black boxes) as well as a 10^3 standard (orange box) (b). Ladder in both (a) and (b) is New England biotech 100 bp ladder. Band size is approximately 215 bp.....72
- Figure 3.2.** Electrophoresis gel of a qPCR amplification product of *tfdA* class I 81 bp primer in soil sample collected from the growth chamber study with 100 bp ladder.....73

Figure 3.3. Gel of colonies with gene product from two soil (green letters), one sediment (brown letters), and one water sample (blue letters) after TOPO cloning, incubation in LB and plates at 37°C, and amplified using M13 primers. Expected product size of 215 bp for samples A-R and 81 bp for samples S-W. Ladder size indicated on gel is 100 bp and 1 kbp from left to right.....76

Figure 3.4. Phylogenetic tree of putative *tfdA* degraders (a). Tree color corresponds to phylum and outer ring corresponds to environmental origin. Counts of sequences from each phyla of putative 2,4-D degraders (b). Counts of sequences from each environment of origin of putative 2,4-D degraders (c).....77

Figure 3.5. (a) Amplification success rates using 1604 sequences of putative 2,4-D degraders tested with 81 and 215 bp primers. Zero, one, and three mismatches were allowed. (b) Amplification success rates of 29 experimentally verified 2,4-D degraders with 81 and 215 bp primers.81

Figure 4.1. (a) [FPB] and (b) [florpyrauxifen] in the treatment zone of all treated lakes.....106

Figure 4.2. (a) [FPB] at three sites and (b) epilimnion wide average [FPB], [florpyrauxifen], and [X11966341] in Kettle Moraine Lake. Error bars in (b) represent standard deviation of all epilimnion samples.....107

Figure 4.3. Silver Lake (a) [dissolved organic carbon] (DOC), (b) ratio of absorbance at 265 and 350 nm (b), and (c) SUVA₂₅₄ during 2021 herbicide treatment. Purple sashed lines represents pretreatment values of 4.94, 8.5, and 0.8 for [DOC], E2:E3, and SUVA₂₅₄ respectively.108

Figure 4.4 311 nm irradiation of FPB in (a) ultrapure water and (b,c) Muskellunge Lake water. [FPB] and [florpyrauxifen] on left axis and degradation products (b) X12131932 and (c) X12393505 on right axis, presented as area. Error bars represent standard deviation of triplicate samples.....112

Figure 4.5. Microcosms incubated with FPB in (a-c) Kettle Moraine Lake and (d-f) Lilly Lake. (a, d) Abiotic controls are 0.2 µm filter sterilized, while (b, e) water only microcosms are unfiltered lake water and no sediment. (c, f) Sediment microcosms contain area of degradation product X11966341 due to issues with quantification on LC-MS/MS. Error bars represent the standard deviation of samples from triplicate microcosms113

Figure 4.6. Observed (a) hydrolysis rates plotted against pH for all tested conditions and [FPB] and [florpyrauxifen] at (b) pH 10, (c) pH 7, and (d) pH 4. Error bars represent the standard deviation of samples taken from triplicate reactors.....116

Figure 4.7. Proposed FPB degradation schematic in aquatic environments. Product identified in each reaction by number as follows: 1- field campaign; 2- photodegradation experiments; 3- FPB incubated microcosms; 4- florpyrauxifen incubated microcosm, 5- hydrolysis experiment. Red boxes represent changed functional group after reaction.....117

Figure 5.1. Chemical structure of fluridone.....128

- Figure 5.2.** Absorbance spectra of 20 μM fluridone in ultrapure water.....131
- Figure 5.3.** Irradiation at 311 nm for direct degradation control and six different lake waters including the high (undiluted lake water) and low (diluted to 3 mg-C L⁻¹) dissolved organic carbon concentrations.135
- Figure 5.4.** Rate constants measured during 311 nm irradiation experiments in ultrapure and natural water (corrected for light screening). Error bars represent standard deviation of triplicate samples.....136
- Figure 5.5.** (a) [Fluridone] in microcosms incubated with relevant environmental inocula at an initial concentration of 3 μM . (b) [Fluridone] in unfiltered lake water and water and sediment microcosms normalized to abiotic control [fluridone]. Error bars in (a) represent the standard deviation of triplicate microcosms measurements and in (b) are the standard deviation of the triplicate concentration ratios.....139
- Figure 5.6.** Sorption isotherm for fluridone over concentration range of 1-12 μM . C_w is the concentration in the water and C_s is concentration on the solid.142
- Figure A.1.** Degradation schematic for photodegradation of 2,4-D. The primary product, 2,4-dichlorophenol, can be photodegraded into 2-chloro-1,4-benzoquinone.....156
- Figure A.2.** Biodegradation schematic for 2,4-D via the *tfdA* and *tfdB* genes products. Primary degradation products formed include 2,4-dichlorophenol, glyoxylate, succinate, and carbon dioxide before 2,4-dichlorophenol is further oxidized to 3,5-dichlorocatechol.....157
- Figure A.3.** Location of all lakes sampled in Wisconsin, USA. All maps were created using ArcGIS software (10.6.1) by Esri. Data provided by the National Atlas of the United States, USGS.....161
- Figure A.4.** Molar absorptivity of 2,4-D, 2,4-dichlorocatechol, and 3,5-dichlorocatechol on left y-axis. Bulb intensity of 311 and 365 nm bulbs on right y-axis.....167
- Figure A.5.** Irradiance data for the global horizontal irradiance spectra generated using SMARTS. Early summer treatments show slightly higher intensities than fall treatments.....166
- Figure A.6.** 2,4-D degradation in microcosms. (a) Random, (b) Round, (c) Pleasant, and (d) Okauchee Lakes have been treated with 2,4-D previously, while (e) Pike, (f) Bony, (g) McCarry, and (h) Eagle Lakes have had no previous treatments. Two of three (h) Eagle water-only microcosms were destroyed during incubation so only one microcosm is shown after day 3. One replicate in the (e) Pike Lake water-only microcosm had loss, as shown in the large error bars at day 14 and 28. Error bars represent standard deviation of triplicate microcosms.....171
- Figure A.7.** Modeled [2,4-D] in McCarry Lake using weekly flow measurements compared to average discharge for 70 days of treatment.....177

Figure A.8. [2,4-D] in (a) surface water and (b) porewater for (c) Eagle Lake. Hypolimnion samples were collected at EL1 and peepers were installed at site EL4. EL6 is a culvert under the road and was sampled to monitor advective transport back into Twin Bear Lake. EL7 is Murrays Dam at the outflow of Flynn Lake and was sampled to monitor advective transport downstream. Homeowner volunteers collected weekly samples at EL4 and EL5. Green dashed line in (a) represents application target whole lake concentration of 1.67 μM180

Figure A.9. [2,4-D] in (a) surface water and (b) porewater in (c) McCarry Lake. Hypolimnion collected at ML1. Peepers were installed and volunteer homeowner samples were collected at ML4. Green dashed line in (a) represents target whole lake concentration of 1.58 μM181

Figure A.10. [2,4-D] in (a) surface water and (b) porewater in (c) Round Lake. Hypolimnion samples were collected at RB1 and peepers were installed at RB7. Flow measurements and volunteer homeowner collected samples were made at RB5 and RB6. Green dashed line in (a) represents target bay-wide concentration of 1.63 μM182

Figure A.11. [2,4-D] in (a) surface water and (b) porewater in (c) Pleasant Lake. Peepers were installed at site PL4. PL1 was used as reference for advective transport out of the treated bay. Green dashed line in (a) represents target bay-wide concentration of 14.2 μM . Large error bars in the top peeper wells for days 1, 5, and 7 is likely due to resettling of sediment and suspended solids following peeper placement given the shallowness (1.5 m) of the bay and unconsolidated nature of the sediment. Error bars represent the standard deviation of triplicate porewater samples....183

Figure A.12. (a) [2,4-D] in surface water at all sampling sites for (b) Okauchee Lake. Green dashed line in (a) represents target bay wide concentration of 9 μM . Peepers were not deployed in this lake.184

Figure A.13. [2,4-D] in (a) surface water and (b) porewater in (c) Random Lake. Hypolimnion sample were collected from RL1. Peepers were installed at RL2. Volunteer homeowner water samples and peepers were collected at RL2. Green dashed line in (a) represents target whole lake concentration of 1.17 μM . Three peepers were collected each sampling event for 15 days. Two peepers had a paired top and bottom sample while the third peeper was bottom only. Error bars represent the standard deviation of triplicate (bottom) or duplicate (top) samples.....185

Figure A.14. (a) Temperature and (b) dissolved oxygen depth profiles for Random Lake. The lake was completely mixed at the beginning of treatment and began to stratify by May 29, 2019. Dissolved oxygen remained low in the hypolimnion throughout the entire treatment.....186

Figure A.15. Hypsographs for (a) Eagle, (b) McCarry, (c) Round, and (d) Random Lakes. Pink dashed line represents stratification depth. Area above pink curve represents sediment exposed to epilimnion, while area below the pink line is sediment isolated from epilimnion. Hypsographs for each stratified lake were generated using the rLakeAnalyzer package in R Studio.....187

Figure B.1. Gel visualization of gene product of 215 bp tfdA primer on class I gene standard (a) as well as class II and class III standard (b) in duplicate.....191

- Figure C.1.** Map of lakes sampled during 2021-2022 field campaign. All lakes selected in conjunction with Wisconsin Department of Natural Resources (WDNR). Map made using Leaflet package in RStudio.197
- Figure C.2.** Absorbance spectra of 10 μM FPB (blue) and 20 μM florpyrauxifen (purple).....200
- Figure C.3.** Photochemical irradiation of FPB at 311 nm. Natural log of the ratio of [FPB] at time t to initial [FPB].201
- Figure C.4.** Microcosms kinetics for FPB in (a) Kettle Moraine La and (b) Kettle Moraine Lake as well as florpyrauxifen incubations in (c) Lilly Lake and (d) Kettle Moraine Lake. Error bars represent the standard deviation of triplicate reactors. 202
- Figure C.5.** Microcosms incubated with florpyrauxifen in (a-c) Kettle Moraine Lake and (d-f) Lilly Lake. (a, d) Abiotic controls are 0.2 μm filter sterilized while (b, e) water only microcosms are unfiltered lake water and no sediment. (c, f) Sediment microcosms contain area of degradation product X11966341 due to issues with quantification on LC-MS/MS. Error bars represent the standard deviation of samples from triplicate reactors.....203
- Figure C.6.** [FPB] and [florpyrauxifen] in hydrolysis experiments at (a) pH 10, (b) pH 9, (c) pH 8, (d) pH 7, (e) pH 6, (f) pH 5, (g) pH 4. Three lake waters included at ambient pH: (h) Muskellunge (pH 7.15), (i) Silver Lake (pH 7.22), (j) South Twin Lake (pH 8.62). Error bars represent the standard deviation of triplicate reactors.....204
- Figure C.7.** Absorbance data for florpyrauxifen from pH 2.5-4. pK_a determined by measuring pH at different wavelengths and using least squares regression, which is at pH of 3.18.....205
- Figure C.8.** (a) All sites on Kettle Moraine Lake, (b) [FPB], [florpyrauxifen], and [X11966341] of site KM1. (c) [FPB], (d) [florpyrauxifen], and [X11966341] in all sites. Dashed line is potential lake wide concentration of 1.28 nM. Standards for X11966341 and a quantitative method were only available for the 2022 lakes (Kettle Moraine Lake and Lilly Lake).....208
- Figure C.9.** (a) All sites on Muskellunge Lake, (b) lake wide average [FPB] and [florpyrauxifen]. (c) [FPB], (d) [florpyrauxifen] in all sites. Dashed line is potential lake wide concentration of 0.48 nM. Error bars in (b) represent standard deviation of three samples (one from each site) at each time point. Standards for X11966341 and a quantitative method were only available for the 2022 lakes (Kettle Moraine Lake and Lilly Lake).....209
- Figure C.10.** (a) All sites on Silver Lake, (b) lake wide average [FPB] and [florpyrauxifen]. (c) [FPB], (d) [florpyrauxifen] in all sites. Dashed line is potential lake wide concentration of 0.36 nM. Error bars in (b) represent standard deviation of three samples (one from each site) at each time point. Standards for X11966341 and a quantitative method were only available for the 2022 lakes (Kettle Moraine Lake and Lilly Lake).....210

Figure C.11. (a) All sites on South Twin Lake, (b) lake wide average [FPB] and [florpyrauxifen]. (c) [FPB], (d) [florpyrauxifen] in all sites. Dashed line is potential lake wide concentration of 0.93 nM. Error bars in (b) represent standard deviation of three samples (one from each site) at each time point. Standards for X11966341 and a quantitative method were only available for the 2022 lakes (Kettle Moraine Lake and Lilly Lake).....211

Figure C.12. (a) All sites on Lilly Lake, (b) lake wide average [FPB], [florpyrauxifen], and [X11966341]. (c) [FPB], (d) [florpyrauxifen] in all sites. Dashed line is potential lake wide concentration of 2.16 nM. Error bars in (b) represent standard deviation of three samples (one from each site) at each time point. Standards for X11966341 and a quantitative method were only available for the 2022 lakes (Kettle Moraine Lake and Lilly Lake)..... 212

List of Tables

Table 1.1. Summary of EPA prescribed tests and comparable OECD tests investigating fate and transformation of polar organic compounds.	8
Table 2.1. Summary of sampled lakes including waterbody identification code (WBIC), herbicide application area, treatment date, target concentration, and treatment history. Trophic status is designated as eutrophic (E), mesotrophic (M), or oligotrophic (O). Target 2,4-D concentration is from treatment permit application. When not stated on permit application, target concentration was calculated from lake/bay volume and amount of herbicide applied as listed on treatment record. Treated bays are indicated by a ^ and listed as the treatment area size. Asterisk (*) indicates Secchi depth measurement hit lake bottom.....	41
Table 2.2. Summary of observed half-lives in large-scale 2,4-D applications, microcosm experiments, and photodegradation experiments. Field half-life is calculated from observed epilimnion wide averages. Microcosm half-life is calculated from observed concentrations in reactors. Photodegradation half-life is calculated by using modeled in-lake photodegradation rates. Bony and Pike Lakes are included as no-treatment controls and have never been treated with 2,4-D. Asterisk (*) for McCarry Lake indicates half-life after degradation started.....	46
Table 3.1. Characteristics of four environmental samples used in TOPO cloning including environmental origin, number of colonies sequenced from each parent sample, and primer used for PCR amplification.....	71
Table 3.2. Recovery of <i>tfdA</i> class I gene in sediments unexposed to 2,4-D. Expected gene recoveries are calculated based on sediment mass and water content.....	74
Table 4.1. Summary of sampled lakes including waterbody identification code (WBIC), herbicide application area, treatment date, target concentration, and treatment history. Trophic status is designated as eutrophic (E), mesotrophic (M), or oligotrophic (O). Target 2,4-D concentration is from treatment permit application. When not stated on permit application, target concentration was calculated from lake/bay volume and amount of herbicide applied as listed on treatment record.....	101
Table 4.2. Half-lives of FPB in field study and laboratory experiments.....	106
Table 5.1. Summary of literature reports of field, photodegradation, biodegradation, and sorption studies of fluridone	130
Table 5.2. Time segments for gradient method used to analyze fluridone on HPLC.....	134
Table 5.3. Instrument parameters for detection of 2-nitrobenzaldehyde and fluridone in water..	134
Table 5.4. Recovery and standard deviation of triplicate fluridone sediment extractions measured during method development.	140

Table 5.5. Recovery and standard deviation of triplicate fluridone sediment extractions measured in microcosms. Each microcosm had 1 kg of sediment was incubated with a total of 6 μM fluridone.....	141
Table A.1. Summary of 2,4-D transformation pathways and rates for field and lab studies. Half-lives, formulation, and study type with important details are summarized. All studies were completed using the 2,4-D anion except the field studies, which used a 2,4-D dimethylamine salt formulation that dissociates immediately. Asterisk indicates two half-lives provided that are not directly applicable to our study system based on experimental conditions but are included for completeness.....	158
Table A.2. Summary of all sample types collected during field campaign.....	162
Table A.3. Dissolved carbon, $E_2:E_3$ (absorbance at 250 nm divided by absorbance at 365 nm), and $SUVA_{254}$ (specific UV absorbance at 254 nm) for all lakes visited during field sampling.....	163
Table A.4. Bulk water chemistry for all lakes visited during the field campaign. ND indicates concentrates were below the limit of detection.....	164
Table A.5. Measured quantum yields for 2,4-D, 2,4-dichlorophenol, and 3,5-dichlorocatechol at pH 7. Quantum yields are calculated from 311 nm exposures using the ultrapure water (direct degradation) control.....	167
Table A.6. SMARTS Modeling input parameters for the in-lake photolysis degradation of 2,4-D. Each lakes modeling conditions, such as date, time, and location of treatment, is included. CO_2 concentration is from measurements from January 2019.....	168
Table A.7. Thermocycler conditions for qPCR amplification of a portion of the <i>tfdA</i> gene adapted from Baelum et al. 2008. Conditions were optimized for our thermocycler.....	173
Table A.8. Flow rates, aqueous buffer ratios, and detection wavelengths for each compound analyzed via HPLC.....	174
Table A.9. Water flow and depth observations at culvert discharging McCarry Lake.....	178
Table A.10. Water flow and depth observations at culvert discharging Round Lake.....	179
Table A.11. Predicted sediment [2,4-D] using lake/bay-wide 24-hour surface water [2,4-D], sediment organic carbon concentrations, and $K_{oc} = 61.7$ to 78 mL g^{-1}	186
Table A.12. Summary physical parameters distributions for each lake expressed as percent of lake area under 6 m and 1 m as well as mean depth.....	187
Table B.1. NCBI BLAST hits for top pairwise alignments between <i>tfdA</i> classes I, II, and III genes and sequenced plasmids.....	192

Table C.1. Chemical structures, formulas, and molecular weight of floryrauxifen-benzyl and five degradation products.....	194
Table C.2. Precursor and product ion information for FPB, internal standard, and degradation products.....	206
Table C.3. Gradient chromatography details for analytical method of FPB, internal standard, and degradation products.	206
Table C.4. Method information for quantification of 2-nitrobenzaldehyde via high pressure liquid chromatography.	207

Chapter 1

Introduction

1.1 Motivation

This dissertation investigates the fate and transport of three aquatic herbicides, 2,4-dichlorophenoxyacetic acid (2,4-D), florypyrauxifen-benzyl (FPB), and fluridone, and how they can be used as tools to connect laboratory transformation experiments to actual environmental fate. Aquatic herbicides are used frequently across the United States to treat invasive and nuisance plants in lakes, rivers, and reservoirs to maintain their recreational, navigational, and aesthetic properties. The planned applications, precise dosing, and extended exposure times make aquatic herbicides an excellent tool to study the relationship between laboratory studies and environmental fate, especially because aquatic systems are complex environments with competing transformation mechanisms. Additionally, a rise in herbicide tolerance to canonical aquatic herbicides requires a mechanistic understanding of the processes that contribute to transformation to support responsible herbicide use.

1.2 Aquatic Herbicides

Aquatic herbicides are used ubiquitously across the United States for the control of invasive and nuisance plants in lakes, rivers, and reservoirs.¹⁻³ Invasive plants are of particular concern because of their ability to negatively impact native communities,⁴⁻⁷ decrease home and property values,⁸⁻¹⁰ and impede recreational use of the lake,¹¹ costing millions of dollars of “benefit” to the waterbody and surrounding property.¹²⁻¹⁴ Aquatic herbicides are used to treat several different

plants,¹⁵ including the invasive Eurasian watermilfoil (*Myriophyllum spicatum*; **EWM**; **Figure 1.1**),¹⁶⁻²⁰ and Hydrilla (*Hydrilla verticillate*).^{21,22} While treatment methods include biological control like weevil release²³ and physical hand pulling,¹⁵ herbicide treatment is often preferred because of its effectiveness at long term control.^{18,24-26} Herbicides can also be selective based on the mechanism of action and timing of herbicide application to target pests.^{15,27}

The State of Wisconsin collectively spends approximately \$9.3 million on management of invasive and nuisance plants annually, which includes homeowner, state, county, and local government contributions, demonstrating the widespread engagement of stakeholders in nuisance plant management.¹⁵ EWM is present in 911 lakes and rivers across the State of Wisconsin,²⁸ abatement of which accounted for 81% of herbicide treatment permit requests in the 2015-2016 application cycle.¹⁵



Figure 1.1. Invasive Eurasian watermilfoil matted on surface of South Twin Lake. Picture taken by Amber White in August 2019.

1.3 Herbicide Mode of Action

There are several different herbicides approved for aquatic use in the United States. Broadly, herbicides can be categorized as systemic or contact. Systemic herbicides are taken up through leaves or roots and translocated to the site of toxicity within a plant. In contrast, contact herbicides act on the part of the plant they physically touch.^{15,27,29} Herbicides can be further classified into categories beyond contact or systemic based on their mode of action within the plant. Currently, there are 34 recognized groups of herbicide modes of action; this dissertation will focus on Group 4 (Auxin Mimics) and Group 12 (Inhibition of Phytoene Desaturase).^{30–32} Group 4 herbicides, such as 2,4-D, florypyrauxifen-benzyl, florypyrauxifen, and halauxifen work by stimulating rapid growth in the plant that is not supported by the available nutrients, causing leaves and stems to disintegrate.^{27,30,31,33} Group 12 herbicides, such as fluridone, work by disrupting the formation of molecules that protect chlorophyll from UV light, bleaching the chloroplasts and disrupting photosynthesis.^{15,34,35} In order for any chemical treatment to be effective, the herbicide must meet certain concentration (i.e., contact) exposure time minimums. This exposure is determined by the specific herbicide, mechanism of action, and plant of concern.^{17,20,21,36–38}

1.4 Herbicide Tolerance and Resistance

The repeated and prevalent use of herbicides has led to a resistance or tolerance to certain herbicides. EWM is of particular concern with increased documentation of tolerance to 2,4-D and fluridone,^{19,20,24,39,40} likely due to crossbreeding with the native Northern watermilfoil to form a hybrid. Best practices in weed and pest management recommend alternating different modes of action to prevent the selection for herbicide tolerant plants and to retain effectiveness of herbicides as tools in the aquatic plant management toolbox.^{27,29,32,41} Thus, resource managers and agrochemical companies are interested in developing new mode of action herbicides and

understanding the mechanisms that control herbicide degradation in the environment to limit the development of herbicide resistance.

1.5 Herbicide Formulations

Commercial herbicide solutions are available as a mixture of active ingredients that carry out the toxic action and inert ingredients that support the active ingredient. Active ingredients are legally defined as “any substance ... that will prevent, destroy, repel or mitigate any pest, or that functions as a plant regulator, desiccant, defoliant, or nitrogen stabilizer.”⁴² The precise formulation of the active ingredient and inert ingredients varies based on the product and intended use. For example, one solid formulation of 2,4-dichlorophenoxyacetic acid contains 27.6% 2,4-D butoxyethylester and 72.4% inert ingredients,⁴³ while a liquid formulation contains 46.8% 2,4-D dimethylamine salt and 53.2% inert ingredients.⁴⁴ These differences in formulation change the environmental fate of the active ingredient with respect to both initial release (e.g., solid formulations can be “slow release”) and degradation/transformation processes within the environment.^{33,45–47}

Conversely, inert ingredients are “any substance ... other than the active ingredient, which is intentionally included in a pesticide product.”⁴² While the exact composition of inert ingredients is not required to be disclosed on an herbicide label, the percentage of inert ingredients in the total product is disclosed and can comprise a significant portion of the commercial herbicide solution.⁴⁸ These ingredients can be used to improve herbicide effectiveness or extend shelf-life, but are not part of the intended toxic mechanism of the solution.^{33,46,49,50} However, the inert components can be independently toxic or can create an enhanced toxicity to the target or non-target organisms.^{33,48,50–52} Despite the ubiquitous use of inert compounds, their high percentage of

composition in commercial solutions, and potential to also have negative/toxic effects, regulation and registration of active and inactive ingredients is different at the federal level.

1.6 Policy Related to Aquatic Herbicides

In the United States, the Environmental Protection Agency (EPA) is responsible for the review and registration of all pesticides under the Federal Insecticide, Fungicide, and Rodenticide Act (FIFRA).⁴² Manufacturers submitting a new pesticide registration are required to submit data assessing the safety and efficacy of the active ingredient, such as data related to the physical properties, stability, human toxicology, environmental fate, and potential effects on nontarget organisms.⁵³ A set of standardized tests for each of these categories are published by the USEPA and are discussed in Section 1.7. It is important to note that these tests assess the active ingredient and not the end-use formulation.

Inert ingredients are assessed independently of the active ingredients and new data may not be required for new pesticide registration if the compound is already recognized by EPA.⁵³ New pesticide registrations containing an existing inert ingredient must list the inert components, any potential chemical reactions with the new active ingredient, and the ratio of inert ingredients in the end-use formulation, but additional toxicology or environmental fate data for the inert ingredients is not required.^{42,53} This modular review process, while streamlined for moving new pesticide products to market, ignores the combined effects of the active and inert ingredients. Although these compounds are also subject to review on a regular basis like the active ingredients, the review process for inert ingredients requires less data than active ingredient registration.⁵¹

Because aquatic herbicides are applied directly to water, their use is also subject to compliance with the Clean Water Act.⁵⁴ The Clean Water Act is the dominant federal policy

regulating the discharge of pollutants and regulating surface water quality. While pesticides are not described as “pollutants” under FIFRA, they are treated as “pollutants” under the Clean Water Act because they can cause “death, disease, [and] physiological malfunctions in organisms.”⁵⁴ This means any application of an herbicide requires a permit through the National Pollution Discharge Elimination System,⁵⁵ which is administered at the state level and approved on an individual treatment basis.^{55,56}

If an herbicide treatment is planned on a waterbody used for drinking water or is near a drinking water intake pump, some considerations of the Safe Drinking Water Act should be made. Several commonly used aquatic herbicides, including copper, 2,4-D, endothall, diquat, and glyphosate, are regulated in drinking water under this Safe Drinking Water Act, although the enforcement/implementation occurs in the distribution of treated water and not the source of drinking water.⁵⁷ For example, Wisconsin has a “set-back distance” requiring any herbicide treatments to occur at least 400 meters away from any drinking water intakes, although this does not apply to private wells.⁵⁶

The patchwork of federal statutes regulating the use of aquatic herbicides demonstrates the complexity of their use, especially in aquatic settings. Whether they are considered “pollutants” or not depends on the specific statute being invoked since they can cause a toxic response in some organisms by design. Additionally, the inert components of end-use formulations are evaluated separately and independently from the active components, obscuring any antagonistic effects to target or non-target organisms. Importantly, there is also no discussion of transformation product risk assessment.

1.7 Environmental Transformation Processes and Quantification Methods

A significant amount of data related to the environmental fate of an herbicide is required for EPA registration, described in in the Fate, Transport, and Transformation Test Guidelines (Series 835).⁵⁸ Not every test is required, but the guidelines are designed to standardize the data received with new pesticide registrations. Most of the tests (**Table 1.1**) are conducted under controlled laboratory conditions (Groups A-E), while three categories of tests have field requirements (Groups F-H). The EPA prescribed tests are closely aligned with tests developed by the Organization for Economic Co-operation and Development (OECD), an international organization dedicated to supporting standardized policies and procedures for improved international collaboration. These tests are designed to evaluate the photodegradation, biodegradation, sorption, hydrolysis, and volatilization of the chemical of interest under stringent test conditions.⁵⁹ Like the individual assessment of active and inert ingredients of a pesticide, each transformation pathway is assessed individually (except in the field studies) and rates are combined through mass balance modeling for risk assessment.⁵⁸⁻⁶⁰ Most assessments describe chemical transformation in terms of half-life, or the amount of time for the concentration to decrease by half and assume pseudo-first order kinetics for degradation rates (Equation 1.1)^{59,60} where k is the measured first-order rate (sec^{-1}). Below is an overview of each transformation mechanism and the associated testing guidelines.

$$t_{1/2} = \frac{\ln 2}{k} \quad (\text{Eq. 1.1})$$

Table 1.1. Summary of EPA prescribed tests⁶⁰ and comparable OECD⁵⁹ tests investigating fate and transformation of polar organic compounds.

Test category	Transport mechanism investigated	Comparable OECD Tests
Group A — Laboratory Transport Test Guidelines	Sorption, leaching, and volatilization	106, 312
Group B — Laboratory Abiotic Transformation Test Guidelines	Hydrolysis, direct photodegradation in water and air	111
Group C — Laboratory Biological Transformation Test Guidelines	Aerobic and anaerobic biodegradation in minimal salt media, soil, water, activated sludge	301, 302, 303, 304, 306, 309, 311, 314
Group D — Transformation in Water and Soil Test Guidelines	Aerobic and anaerobic biodegradation in soil and water	307 and 308
Group E — Transformation Chemical-Specific Test Guideline	Indirect photodegradation screening, subsurface anaerobic biodegradation	None
Group F — Field Dissipation Test Guidelines	Dissipation studies in terrestrial, aquatic, or forested systems	None
Group G — Ground Water Monitoring Test Guidelines	Leaching into groundwater	None
Group H — Volatility from Soil Test Guidelines	Volatilization from treated soils	None

1.7.1 Hydrolysis

Hydrolysis is an abiotic degradation reaction that results from a nucleophilic attack of a water molecule on an organic compound.⁶¹ While hydrolysis can occur at any pH, it can also be acid or base catalyzed, meaning an enhanced rate of hydrolysis occurs under either acidic or basic conditions. Compounds especially susceptible to hydrolysis include esters, epoxides, amides, carbamates, and aliphatic/allylic halides.^{62,63} Hydrolysis is investigated using OECD Test 111⁶⁴ and EPA Tests 835.2120⁶⁵ and 835.2130.⁶⁶ Generally, sterile water is buffered at pH 4, 7, and 9 and incubated with the compound of interest, which is quantified regularly until 90% of the compound is gone.

1.7.2 Photodegradation

Photodegradation is an important environmental transformation pathway for many organic compounds⁶⁷⁻⁶⁹ and can proceed through two different mechanisms: direct or indirect photodegradation (**Figure 1.2**). Direct photodegradation involves a photon of light being absorbed by a chemical and inducing a structural change.^{61,70,71} Compounds that are susceptible to environmental photodegradation (i.e., absorb light > 290 nm) will also have a quantifiable quantum yield (Φ) that describes the likelihood of a single photon causing a reaction.⁷² Indirect photodegradation relies on photochemically produced reactive intermediates (PPRI) being excited by a photon and subsequently degraded the compound of interest.^{68,73} PPRI are most commonly produced by the photoexcitation of naturally present dissolved organic matter (DOM). There are three primary PPRI in aquatic environments: triple state dissolved organic matter (³DOM), singlet oxygen (¹O₂), and hydroxyl radical ([•]OH).⁷⁴⁻⁷⁷ The abundance and composition of these PPRI in water will depend on the background concentration and composition of the dissolved organic matter in the aquatic environment of interest.⁷⁸⁻⁸⁰

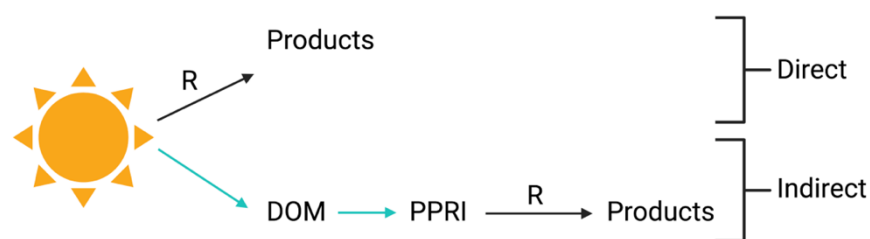


Figure 1.2. Overview of direct and indirect photodegradation of an organic compound (R). PPRI can be ³DOM, ¹O₂, or [•]OH.

Photodegradation assessment is described by OECD test 316⁸¹ and EPA tests 853.2210⁸² and 853.2240,⁸³ all of which involve a two-tiered theoretical and experimental approach. First, a

maximum potential photodegradation rate is calculated based on light absorbance of the compound, a quantum yield of 1, and simulated environmental light. If the compound has a half-life below a certain threshold (i.e., 30 days in OECD test 316), then experiments quantifying direct photolysis will proceed. Broadly, the compound of interest is irradiated using light in the environmentally relevant spectrum (> 290 nm) over a period of time that allows enough loss to occur for kinetic calculations, usually one to two half-lives at minimum. Direct photodegradation rates are measured in ultrapure water, while dark controls (i.e., the compound in ultrapure water but not exposed to light) are used to quantify any additional abiotic transformation.^{81,83} Interestingly, neither OECD 316 nor EPA test guidelines require an assessment of indirect photodegradation, although EPA has guidelines to screen for indirect photodegradation.⁸⁴ Indirect photodegradation is measured by irradiating the compound of interest in natural water (i.e. water with dissolved organic matter)^{68,85,86} All tests require the use of a chemical actinometer, which is a chemical that photodegrades at a known rate and is used to quantify light intensity during the experiment.^{87,88} At this stage, any major (>10 % applied chemical) transformation products should be identified and modeling used to predict half-lives in water in natural sunlight assuming 40° N latitude during midsummer and 12 hours a day of sunlight.⁸¹⁻⁸³ Modeling field photodegradation does not require calculation of chemical specific quantum yield. Instead, a value of 1 (i.e., a 100% reaction efficiency) can be used to calculate the maximum photodegradation rate in natural waters.

1.7.3 Microbial Degradation

Microbial degradation of polar organic compounds is a well-documented and ubiquitous environmental transformation mechanism.^{5,89-99} Biodegradation rate is highly dependent on the chemical itself as well as the environmental conditions, such as oxygen availability,¹⁰⁰⁻¹⁰⁴

temperature,^{105–107} pH,^{105,106,108} nutrient availability,¹⁰⁹ and microbial community structure.^{110–112} Because of this, biodegradation of the three herbicides of interest in this dissertation are discussed individually in Section 1.8.

The biodegradation of organic compounds is assessed through a series of protocols in a tiered system similar to the photodegradation studies. This tiered system breaks degradation down into different environmental matrices under different conditions and are discussed at length in Kowalczyk et al. 2015¹¹³ and Lapertot and Pulgarin 2006.¹¹⁴ The first tier is the Ready Biodegradability (i.e. OECD 301 and EPA 835.3110 and 835.3410) test, which uses high concentration chemical spiking, a minimal salt media, and (usually) sewage treatment plant derived biomass to measure complete respiration of a compound through changes in dissolved organic carbon or carbon dioxide generation.^{115–117} Compounds that fail the ready biodegradability tests are moved to the second tier, inherent biodegradability, which lowers concentration of the spiked compound, adds additional nutrients, and introduces different test options depending on the environmental matrix.^{59,113,114} The third tier is simulation tests, which attempt to simulate actual degradation in the environment. These tests investigate the degradation in a compartmentalized simulation test that measures aerobic and anaerobic biodegradation in water, soil, and sediment separately,^{113,114,118} and as such there are several options depending on matrix, oxygen constraints, etc. The most important tests for biodegradation in the freshwater aquatic environment are OECD 308¹¹⁹ and 309¹²⁰ and EPA tests 835.3190,¹²¹ 835.4300,¹²² and 835.4400,¹²² which use surface water and sediments from aquatic environments to test biodegradation under simulated environmental conditions.

1.7.4 Limitations of Laboratory and Field Transformation Testing

There are several criticisms in the literature of the existing simulation tests and their relevance to true environmental transport. First, photodegradation studies do not require modeling for all compounds nor quantify potential indirect photodegradation, which can be an important environmental pathway.^{68,85,123} Additionally, seasonality and depth integrated photodegradation rates are not calculated, which can change photodegradation rates substantially.¹²³ Biodegradation is isolated to either water or sediment microbial communities, which oversimplifies sediment-water dynamics and disrupts the ambient nutrients, oxygen, and light trends the microbial populations maybe have been conditioned before.^{109,124–126} Additionally, techniques used to keep incubations oxygenated, such as shaking or stirring sediments, as well as high ratios of sediment to water can influence how chemicals of interest and their degradation products sorb in a way that is not environmentally relevant.^{110,124,127} Lastly, spiking incubations with higher chemical concentrations than observed in the environment can change the degradation kinetics, underscoring the importance of using relevant inoculum and relevant environmental concentrations.^{109,128–131}

While the biodegradation tests solely focus on the chemical kinetics, there is no investigation into the microbial community carrying out the degradation process.^{113,126} Currently, there are several tools available to investigate the microbial population responsible for biodegradation. Enrichment, isolation, and culturing of specific strains of bacteria that can degradation contaminants either in mixtures or as the sole carbon source are ideal for identifying specific transformation products and identifying complete transformation pathways,^{100,113,132,133} but likely 1) mischaracterize the possible degrading community due to culture techniques, if they can be cultured at all, or 2) eliminate co-metabolism of chemicals by populations of

microbes.^{102,134–136} Other techniques investigating the molecular abundance of a gene or transcripts associated with specific compound degradation can be used to describe the degrading population, such as qPCR, 16S rRNA sequencing, metagenomic, or meta-transcriptomic approaches depending on the amount of information known about the specific microorganisms and biochemical pathways.^{94,95,99,125,137–142} Thus, the lack of any characterization of the biodegrading population beyond cell counts may contribute to the difficulties in translating the laboratory studies to field fate and needs additional exploration.

Field degradation studies are often difficult to carry out due to limitations in understanding source and input rates of chemicals of interest, as well as low detection limits, competing transformation mechanisms, and difficulties in quantifying compounds in complex matrices.^{123,128–130,143,144} Thus, laboratory-based studies are likely to remain the predominant tool to study transformation of polar organic compounds when field studies are not possible, even though they often fall short of accurately describing true environmental fate.^{130,145,146} Understanding the limitations of the laboratory studies, however, is critical for risk management and assessment of new chemicals entering the environment.

1.8 Environmental Fate of Three Aquatic Herbicides

There are three commonly used aquatic herbicides used in Wisconsin for the management of invasive and nuisance plants: 2,4-dichlorophenoxyacetic acid (2,4-D, **Figure 1.3a**), floryprauxifen-benzyl (FPB, **Figure 1.4a**), and fluridone (**Figure 1.5**). These three herbicides have been registered through FIFRA as described previously and permitted for use in large-scale treatments in Wisconsin. However, the increased reports of herbicide tolerance to 2,4-D requires resistance/tolerance recommend alternating different mode of action herbicides,^{15,147} such as

fluridone and FPB, both of which have documented success treating EWM and the hybrid watermilfoil.^{15,36,37} A brief description of all three herbicides environmental fate is described below, specifically pertaining to applications in freshwater lakes.

1.8.1 2,4-Dichlorophenoxyacetic Acid

2,4-D (**Figure 1.3a**) is used at high rates globally^{148–153} and is the most commonly used herbicide for invasive Eurasian watermilfoil treatment in Wisconsin.¹⁵ While 2,4-D is effective for controlling Eurasian watermilfoil at low concentrations in whole-lake applications (0.45 – 10 μM), the degradation of 2,4-D in lakes is variable and can result in extended exposure periods that are harmful to non-target organisms.^{7,18,47,154,155} 2,4-D is susceptible to both photolysis and biodegradation, and the combination of both degradation mechanisms is suspected to influence 2,4-D persistence.^{18,24,156,157} 2,4-D photodegradation in aquatic environments is expected to be relatively slow, with half-lives in ultrapure water being about 13-32 days in natural and simulated sunlight.^{86,158,159} 2,4-D can also be degraded by hydroxyl radical, but indirect photodegradation in natural waters has not been quantified and could be an important component of environmental photodegradation.^{68,79,86,160,161} The primary expected photodegradation product is 2,4-dichlorophenol (**Figure 1.3b**).^{45,156} Sorption and volatilization are expected to be negligible.^{45,156,158,159}

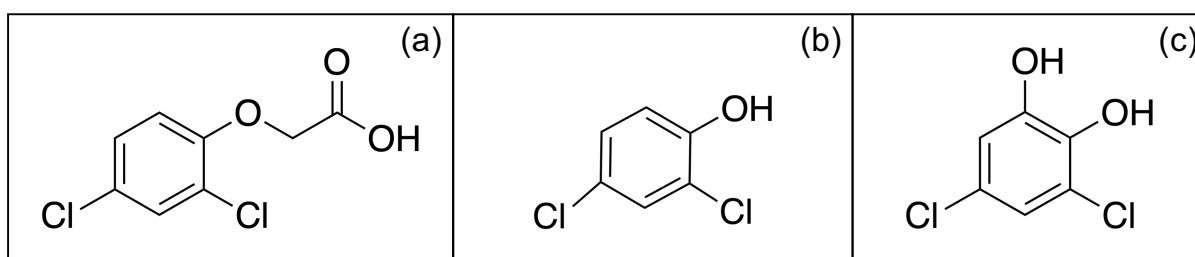


Figure 1.3. Chemical structures of (a) 2,4-D, (b) 2,4-dichlorophenol, and (c) 3,5-dichlorocatechol.

2,4-D is degraded by bacteria using the *tfd* gene cluster.^{153,162–165} Biodegradation is expected to occur in two phases: a lag or acclimation during phase followed by a rapid degradation phase.^{101,166} Repeated exposure to 2,4-D shortens the acclimation phase of microbes, suggesting that repeated use of 2,4-D over several months promotes more rapid microbial degradation.^{101,156,166,167} Biodegradation is faster in aerobic conditions ($t_{1/2}$ = of 7-50 days) compared to anaerobic conditions ($t_{1/2}$ = 331 days).^{156,158} Biodegradation is initiated by *tfdA*, which encodes an alpha-ketoglutarate dependent oxygenase that uses Fe(II) to catalyze the reaction into 2,4-dichlorophenol, carbon dioxide, and succinate.¹⁶⁸ This is considered the rate limiting step because *tfdA* is transcribed separately from the downstream *tfdBCDEF*, of which there are two copies, but only one copy of the *tfdA* gene.¹⁶⁹ This duplication is likely due to the need for rapid degradation of 2,4-D transformation products that are toxic to bacteria.¹⁶⁷ Complete mineralization primarily produces 2,4-dichlorophenol (**Figure 1.3b**) and 3,5-dichlorocatechol (**Figure 1.3c**) before being shuttled into the citric acid cycle.^{167,168}

There are many documented 2,4-D degraders in the phyla of Alpha, Beta, and Gammaproteobacteria that have been isolated from soil systems,^{132,133,170,171} including several strains capable of using 2,4-D as their sole carbon source.^{133,164,165} There are three gene classes of *tfdA* classes, but because the gene can be horizontally transferred¹⁷² these classes are distributed throughout different bacterial phyla. However, the genetic sequence is expected to be well conserved *tfdA* gene within individual classes.¹⁷¹ The *tfd* gene has been extensively studied on the JMP134 plasmid in *Cupriavidus pinatubonesis*, previously named *Cupriavidus necator*, *Alcaligenes eutrophus*, and *Ralstonia eutropha*.^{168,171,173,174}

A set of qPCR primers (81 or 215 bp fragment) were developed for the quantitative detection of *tfdA* in pure cultures and from the environment¹⁷⁵ and have been applied predominantly in soil environments,^{101,174,176–178} but have limited applications in aquatic environments.^{101,179} These qPCR primers were developed from cultured representatives of soil and environments that may miss other environmental representatives. Additionally, no previous studies have applied metagenomic analyses to the *tfdA* gene in any environments, suggesting the diversity of environmental degraders at present is limited to what has been detected through culturing.

1.8.2 Florpyrauxifen-benzyl

Like 2,4-D, FPB is a new auxin mimic herbicide registered in 2017 predominantly for use in aquatic environments.¹⁸⁰ Commonly used to combat hydrilla, Eurasian watermilfoil, and other broadleaf plants, FPB was developed to address increasing tolerance to previously used herbicides such as 2,4-D^{19,29,39,41} and fluridone^{22,32,40} by creating an alternative mode of action compound.¹⁸¹ Few peer-reviewed studies of laboratory or field quantification of FPB are available, likely due to the recent development of this compound. FPB photodegradation is rapid ($t_{1/2} = 0.07$ days at 40 °N latitudes in pH 4) with negligible volatilization.¹⁸² Hydrolysis at pH 7 is slow ($t_{1/2} = 111$ days) but significantly faster at pH 9 ($t_{1/2} = 1.3$ days).¹⁸³ Solubility is low (i.e., 34 nM) and correspondingly sorption potential is high; FPB has an octanol-water partitioning coefficient ($\log K_{ow}$) of 5.5 and water-soil carbon partitioning coefficient ($\log K_{oc}$) of 4.53 mL g⁻¹.¹⁸² Aerobic and anaerobic microbial degradation is expected to be faster at low and neutral pH with aquatic metabolism half-lives of 2-6 days.^{180,182} There are no documented bacteria associated with FPB degradation at this time.

Lastly, there are several possible degradation products that could form from FPB. These products are novel in that they do not have common names or CAS number. They are, however, expected to have same or lesser toxicity as FPB.^{180,184,185} The primary degradation product is florpyrauxifen,^{36,185} while products X12131932 and X12393505 are expected to form predominantly through photodegradation and products X11966341 and X12300837 are likely to form in water and sediment environments.¹⁸⁵

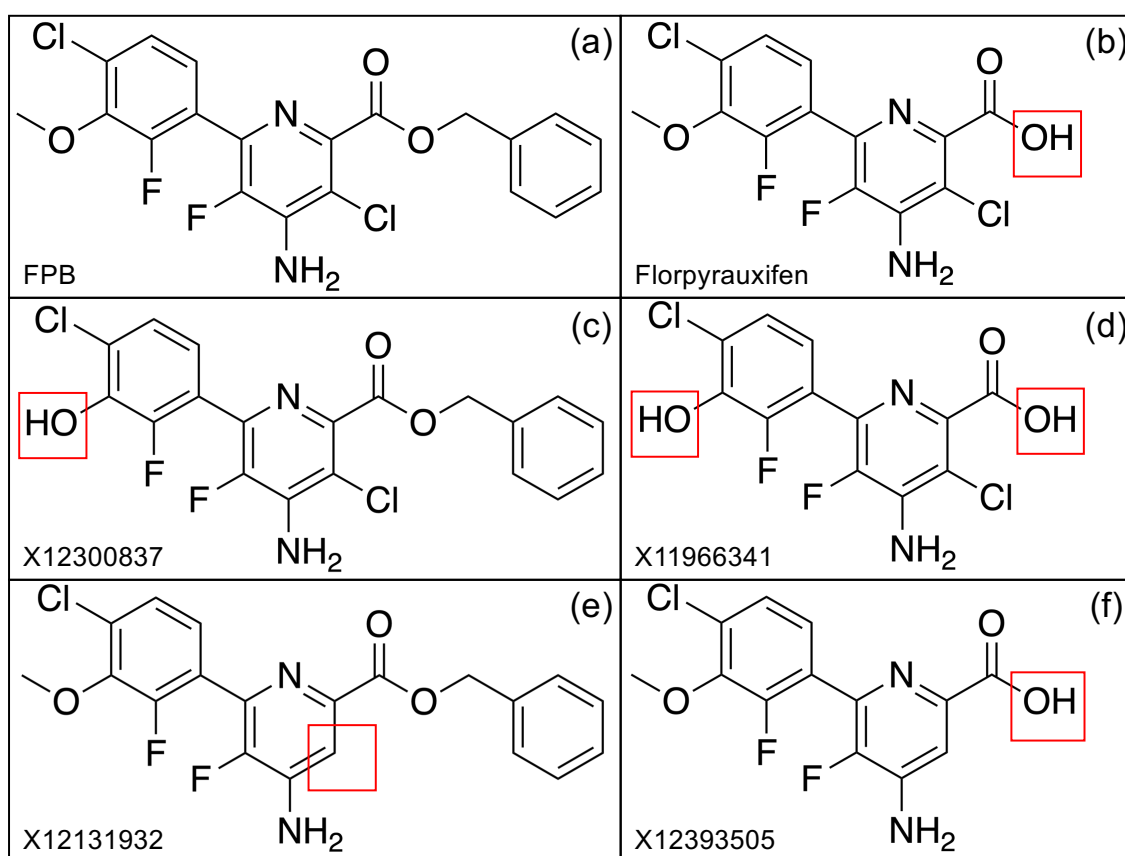


Figure 1.4. Chemical structure of (a) FPB and expected degradation products (b) florpyrauxifen, (c) X12300837, (d) X11966341, (e) X12131932, and (f) X12393505.

1.8.3 Fluridone

Fluridone (**Figure 1.5**) is a systemic herbicide that prevents the synthesis of important biomolecules that protect the plant from photobleaching.^{34,35} For fluridone to be effective, a low concentration (6-36 nM)^{21,38,186} is applied for the entire growing season (>100 days) and often requires multiple applications to maintain an effective concentration.^{15,186-188} Fluridone is known to undergo rapid photolysis with a half-life of 28 hours – 12 days in ultrapure water and lake water, respectively.¹⁸⁹⁻¹⁹¹ Microbial degradation is slow but no specific microbes or metabolic pathways have been associated with its degradation.^{188,192,193} Fluridone also has a high affinity for binding to sediments⁴⁶ and has been found to persist for up to a year following initial treatment,^{3,188,194} suggesting sediments are a possible sink for unreacted fluridone that is available for future resuspension or uptake.

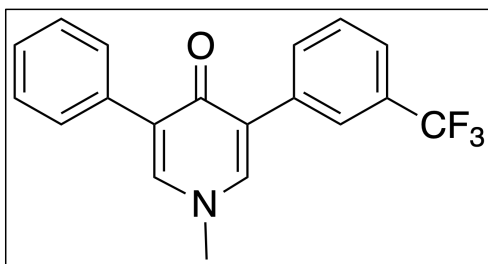


Figure 1.5. Chemical structure of fluridone.

1.9 Knowledge Gaps

Currently, the environmental fate and transformation of polar organic compounds is assessed predominantly through laboratory studies. These studies isolate the active ingredient from the inactive components and isolate individual transformation mechanisms from each other to

calculate predicted environmental half-lives. However, laboratory-based assessments fall short of accurately predicting environmental fate due to challenges mimicking physical transport processes (i.e., sediment interaction, flow, and light) and chemical conditions (i.e., oxygen and nutrient concentrations) that would exist in the natural environment. Additionally, there is a lack of field studies connecting laboratory studies to environmental fate due to the technical and logistical challenges with conducting large scale field investigations. Lastly, modular testing schemes emphasize degradation kinetics of the active herbicide ingredient without consideration of the role of the inactive ingredients, transformation products, or the microbial community carrying out the degradation. Thus, there is a critical need for research that investigates the link between environmental fate and laboratory tests that describe environmental fate in a comprehensive and holistic manner.

There is also a critical knowledge gap in the understanding of the aquatic fate of the three commonly used herbicides: 2,4-D, FPB, and fluridone. Despite the prevalence and historic use of 2,4-D, most of the existing field and laboratory transformation studies were conducted in terrestrial or cultured systems. On the other hand, FPB was developed for use in aquatic systems, but is understudied largely due to the recent development and registration of the herbicide. Lastly, fluridone requires long exposure times and is expected to be degraded via photodegradation; however, no studies have investigated the specific removal of fluridone from lake water via indirect photodegradation. Thus, the planned and coordinated direct application of these aquatic herbicides to lakes provides a unique opportunity to mechanistically link the environmental transformation of these herbicides to laboratory studies describing individual transformation mechanisms.

1.10 Research Objectives

A summary of the research chapters found in this dissertation is described in this section. Chapters 2-5 are the main data chapters, all of which are intended for publication. Chapters 2 and 3 focus on 2,4-D, specifically the environmental fate and degradation in lakes (Chapter 2) and the bacteria that degrade 2,4-D across all environmental matrices (Chapter 3). Chapter 4 focuses on FPB, the production and transformation of several FPB degradation products, and the effects of the inactive formulation ingredients on lake chemistry. Chapter 5 discusses fluridone and the role of photodegradation, specifically direct photodegradation, in removing fluridone from surface waters. Chapter 6 is a summary of the results found in this dissertation as well as discussion of future directions for both individual herbicide fate and environmental fate and transport research as a whole.

In Chapter 2, mass balance modeling is used to relate measurements of 2,4-D in lakes to laboratory scale investigations of biodegradation and photodegradation. Six large-scale 2,4-D lake treatments were quantified during Summer 2019 with an emphasis on characterizing physical processes in the lakes, such as outflow of unreacted 2,4-D and exchange of herbicide across sediment-water interface. Paired laboratory biodegradation and photodegradation studies were used to individually assess degradation in surface water only, water-sediment suspensions, direct photodegradation irradiations, and indirect photodegradation irradiations to determine the primary environmental degradation pathway. The planned herbicide applications at homogenous lake wide concentrations allowed intensive field campaigns to capture spatially and temporally detailed degradation data for comparison to the laboratory data.

Chapter 3 builds on the chemical kinetics quantified in Chapter 2 by investigating the microbial community responsible for degradation of 2,4-D using molecular and computational

techniques. Quantitative investigation of *tfdA* gene copies using qPCR measured degrader abundance in environmental samples known to degrade 2,4-D. Metagenomic analyses used publicly available genome sequences to identify putative 2,4-D degraders. Lastly, *in silico* modeling investigated qPCR primer fidelity across the putative degrading community. Metagenomic microbial community characterization, *in silico* modeling, and quantitative qPCR with known 2,4-D degrading samples compares culture-based tools to non-culture-based tools for biodegradation studies.

Chapter 4 provides a detailed description of the transformation pathways of FPB through intensive field campaigns and laboratory experiments. Five large-scale FPB treatments during 2021 and 2022 were studied to quantify FPB, transformation products, and inactive ingredient composition and concentration over two field seasons. Like 2,4-D, the planned treatments allowed paired photodegradation, biodegradation, and hydrolysis experiments to be used to contextualize field data and to identify the environmentally relevant degradation pathway. Changes in chemical properties compared to 2,4-D, specifically larger partitioning coefficients, hydrolysis potential as a carboxylic acid ester, and rapid expected photodegradation, allow a different set of degradation processes to be investigated.

Chapter 5 expands from auxin mimic herbicides into a photobleaching herbicide, fluridone, that has a significantly longer exposure time requirement. Laboratory studies investigate direct and indirect photodegradation as well as biodegradation in water only or sediment-water suspensions. Here, we use laboratory experiments to quantify specific biodegradation, photodegradation, and sorption rates and compare to the existing literature related to fluridone fate in lakes.

Finally, Chapter 6 provides a summary of the four research chapters and discusses the future directions of the research. Conclusions about the specific fate of each herbicide as well as

broad recommendations for the incorporation of field and laboratory data to understand chemical fate are discussed.

1.11 References

- (1) TRC Environmental. Supplemental Environmental Impact Statement for State of Washington Aquatic Plant and Algae Management <https://fortress.wa.gov/ecy/publications/documents/1710020.pdf>. (accessed 2020 -05 -10).
- (2) Northeast Aquatic Research. Tuxedo Lake, Wee Wah, and Little Wee Wah Aquatic Plant Sampling Report [http://www.tpfyi.com/docs/NEAR Aquatic Plant Sampling Report 1-24-2020.pdf](http://www.tpfyi.com/docs/NEAR_Aquatic_Plant_Sampling_Report_1-24-2020.pdf). (accessed 2020 -05 -10).
- (3) Muir, D. C. G.; Grift, N. P. Fate of fluridone in sediment and water in laboratory and field experiments. *J. Agric. Food Chem.* **1982**, *30* (2), 238–244. <https://doi.org/10.1021/jf00110a006>.
- (4) Boylen, C. W.; Eichler, L. W.; Madsen, J. D. Loss of native aquatic plant species in a community dominated by Eurasian watermilfoil. *Hydrobiologia.* **1999**, *415*, 207–211. <https://doi.org/10.1023/A:1003804612998>.
- (5) Ghisalba, O.; Cevey, P.; Kuenzi, M.; Schar, H.-P. Biodegradation of chemical waste by specialized methylotrophs, an alternative to physical methods of waste disposal. *Conservation & Recycling.* **1985**, *8*, 47–71.
- (6) Madsen, J. D.; Sutherland, J. W.; Bloomfield, J. A.; Eichler, L. W.; Boylen, C. W. The decline of native vegetation under dense Eurasian watermilfoil canopies. *J. Aquat. Plant Manage.* **1991**, *29*, 94–99.
- (7) Schleppebach, B. T.; Matzke, G.; Shaw, S. L.; Sass, G. G. Fish and zooplankton community responses to the cessation of long-term invasive Eurasian watermilfoil (*Myriophyllum spicatum*) chemical treatments in a north-temperate, USA lake. *Fishes* **2022**, *7* (4), 165. <https://doi.org/10.3390/fishes7040165>.
- (8) Horsch, E. J.; Lewis, D. J. The effects of aquatic invasive species on property values: Evidence from a quasi-experiment. *Land Economics.* **2009**, *85*, 391–409. <https://doi.org/10.3368/le.85.3.391>.
- (9) Olden, J. D.; Tamayo, M. Incentivizing the public to support invasive species management: Eurasian milfoil reduces lakefront property values. *PLoS ONE.* **2014**, *9* (10), e110458. <https://doi.org/10.1371/journal.pone.0110458>.
- (10) Lovell, S. J.; Stone, S. F.; Fernandez, L. The economic impacts of aquatic invasive species: A review of the literature. *Agricultural and Resource Economics Review* **2006**, *35*, 195–208. <https://doi.org/10.1017/S1068280500010157>.
- (11) Smith, C. S.; Barko, J. W. Ecology of Eurasian watermilfoil. *J. Aquat. Plant Manage.* **1990**, *28*, 55–64.
- (12) Adams, D. C.; Lee, D. J.; Schardt, J.; Schmitz, D.; Ludlow, J. Estimating the value of invasive aquatic plant control: A bioeconomic analysis of 13 public lakes in Florida. *Journal of Agricultural and Applied Economics* **2007**, *39*, 97–109.
- (13) Adams, D. C.; Bucaram, S.; Lee, D. J.; Hodges, A. W. Public preferences and values for management of aquatic invasive plants in state parks. *Lake and Resvr. Mange.* **2010**, *26* (3), 185–193. <https://doi.org/10.1080/07438141.2010.504319>.

- (14) Havel, J. E.; Kovalenko, K. E.; Thomaz, S. M.; Amalfitano, S.; Kats, L. B. Aquatic invasive species: Challenges for the future. *Hydrobiologia*. **2015**, *750*, 147–170. <https://doi.org/10.1007/s10750-014-2166-0>.
- (15) Blanke, C.; Mikulyuk, A.; Nault, M.; Provost, S.; Schaal, C.; Egeren, S. van; Williams, M.; Mednick, A. Strategic Analysis of Aquatic Plant Management in Wisconsin https://dnr.wi.gov/topic/EIA/documents/APMSA/APMSA_Final_2019-06-14.pdf (accessed 2020 -05 -15).
- (16) Bartodziej, W.; Ludlow, J. Aquatic vegetation monitoring by natural resources agencies in the United States. *Lake and Resvr. Mange.* **1997**, *13* (2), 109–117. <https://doi.org/10.1080/07438149709354302>.
- (17) Slade, J. G.; Poovey, A. G.; Netherland, M. D. Efficacy of fluridone on Eurasian and hybrid watermilfoil. *J. Aquat. Plant. Manage.* **2007**, *45* (2), 116–118.
- (18) Frater, P.; Mikulyuk, A.; Barton, M.; Nault, M.; Wagner, K.; Hauxwell, J.; Kujawa, E. Relationships between water chemistry and herbicide efficacy of Eurasian watermilfoil management in Wisconsin lakes. *Lake and Resvr. Mange.* **2017**, *33* (1), 1–7. <https://doi.org/10.1080/10402381.2016.1235634>.
- (19) Moody, M. L.; Les, D. H. Evidence of hybridity in invasive watermilfoil (*Myriophyllum*) populations. *PNAS*. **2002**, *99* (23), 14867–14871. <https://doi.org/10.1073/pnas.172391499>.
- (20) Glomski, L. M.; Netherland, M. D. Response of Eurasian and hybrid watermilfoil to low use rates and extended exposures of 2,4-D and triclopyr. *J. Aquat. Plant. Manage.* **2010**, *48*, 12–14.
- (21) Netherland, M. D.; Getsinger, K. D.; Turner, E. G. Fluridone concentration and exposure time requirements for control of Eurasian watermillfoil and hydrilla. *J. Aquat. Plant. Manage.* **1993**, *31*, 189–194.
- (22) Netherland, M. D.; Jones, D. Fluridone-resistant hydrilla (*Hydrilla verticillata*) is still dominant in the Kissimmee Chain of Lakes, Fl . *Invasive Plant Science and Management* **2015**, *8* (2), 212–218. <https://doi.org/10.1614/ipsm-d-14-00071.1>.
- (23) Havel, J. E.; Knight, S. E.; Maxson, K. A. A field test on the effectiveness of milfoil weevil for controlling Eurasian watermilfoil in Wisconsin lakes. *Hydrobiologia*. **2017**, *800* (1), 81–97. <https://doi.org/10.1007/s10750-017-3142-2>.
- (24) Nault, M. E.; Barton, M.; Hauxwell, J.; Heath, E.; Hoyman, T.; Mikulyuk, A.; Netherland, M. D.; Provost, S.; Skogerboe, J.; van Egeren, S. Evaluation of large-scale low-concentration 2,4-D treatments for Eurasian and hybrid watermilfoil control across multiple Wisconsin lakes. *Lake and Resvr. Mange.* **2018**, *34* (2), 115–129. <https://doi.org/10.1080/10402381.2017.1390019>.
- (25) Kujawa, E. R.; van Egeren, S.; Mikulyuk, A.; Nault, M. E.; Barton, M.; Hauxwell, J.; Frater, P. Lessons from a decade of lake management: effects of herbicides on Eurasian watermilfoil and native plant communities. *Ecosphere*. **2017**, *8* (4), 1–11. <https://doi.org/10.1002/ecs2.1718>.
- (26) Nault, M. E.; Netherland, M. D.; Mikulyuk, A.; Skogerboe, J. G.; Asplund, T.; Hauxwell, J.; Toshner, P. Efficacy, selectivity, and herbicide concentrations following a whole-lake 2,4-D application targeting Eurasian watermilfoil in two adjacent northern Wisconsin lakes. *Lake and Resvr. Mange.* **2014**, *30* (1), 1–10. <https://doi.org/10.1080/10402381.2013.862586>.
- (27) Grossmann, K. Auxin herbicides: Current status of mechanism and mode of action. *Pest Mgmt. Sci.* **2010**, *66* (2), 113–120. <https://doi.org/10.1002/ps.1860>.

- (28) Wisconsin Department of Natural Resources. Wisconsin Eurasian watermilfoil locations <https://dnr.wi.gov/lakes/invasives/AISLists.aspx?species=EWM&location=ANY> (accessed 2022 -08 -11).
- (29) Richardson, R. J. Aquatic plant management and the impact of emerging herbicide resistance issues. *Weed Tech.* **2008**, 22 (1), 8–15. <https://doi.org/10.1614/wt-07-034.1>.
- (30) Herbicide Resistance Action Committee <https://hracglobal.com/tools/classification-lookup> (accessed 2022 -08 -02).
- (31) Weed Science Society of America <https://wssa.net/wssa/weed/herbicides/> (accessed 2022 -08 -02).
- (32) Mallory-Smith, C. A.; Retzinger Jr., E. J. Revised classification of herbicides by site of action for weed resistance management strategies. *Weed Tech.* **2003**, 17 (3), 605–619. [https://doi.org/10.1614/0890-037x\(2003\)017\[0605:rcohbs\]2.0.co;2](https://doi.org/10.1614/0890-037x(2003)017[0605:rcohbs]2.0.co;2).
- (33) Peterson, M. A.; McMaster, S. A.; Riechers, D. E.; Skelton, J.; Stahlman, P. W. 2,4-D past, present, and future: A review. *Weed Tech.* **2016**, 30 (2), 303–345. <https://doi.org/10.1614/wt-d-15-00131.1>.
- (34) Arnold, W. R. Fluridone: A new aquatic herbicide. *J. Aquat. Plant. Manage.* **1979**, 17, 30–33.
- (35) Bartels, P. G.; Watson, C. W. Inhibition of carotenoid synthesis by fluridone and norflurazon. *Weed Sci* **1978**, 26 (2), 198–203. <https://doi.org/10.1017/s0043174500049675>.
- (36) Netherland, M. D.; Richardson, R. J. Evaluating sensitivity of five aquatic plants to a novel arylpicolinate herbicide utilizing an organization for economic cooperation and development protocol. *Weed Sci.* **2016**, 64 (1), 181–190. <https://doi.org/10.1614/ws-d-15-00092.1>.
- (37) Beets, J.; Heilman, M.; Netherland, M. D. Large-scale mesocosm evaluation of florpyrauxifen-benzyl, a novel arylpicolinate herbicide, on Eurasian and hybrid watermilfoil and seven native submersed plants. *J. Aquat. Plant. Manage.* **2019**, 57, 49–55.
- (38) Netherland, M. D.; Getsinger, K. D.; Skogerboe, J. D. Mesocosm evaluation of the species-selective potential of fluridone. *J. Aquat. Plant. Manage.* **1997**, 35 (2), 41–50.
- (39) Larue, E. A.; Zuellig, M. P.; Netherland, M. D.; Heilman, M. A.; Thum, R. A. Hybrid watermilfoil lineages are more invasive and less sensitive to a commonly used herbicide than their exotic parent (Eurasian watermilfoil). *Evolutionary Applications.* **2013**, 6 (3), 462–471. <https://doi.org/10.1111/eva.12027>.
- (40) Berger, S. T.; Netherland, M. D.; MacDonald, G. E. Laboratory documentation of multiple-herbicide tolerance to fluridone, norflurazon, and topiramazone in a hybrid watermilfoil (*Myriophyllum spicatum* × *M. sibiricum*) population. *Weed Sci.* **2015**, 63 (1), 235–241. <https://doi.org/10.1614/ws-d-14-00085.1>.
- (41) Busi, R.; Goggin, D. E.; Heap, I. M.; Horak, M. J.; Jugulam, M.; Masters, R. A.; Napier, R. M.; Riar, D. S.; Satchivi, N. M.; Torra, J.; Westra, P.; Wright, T. R. Weed resistance to synthetic auxin herbicides. *Pest Mgmt. Sci.* **2018**, 74 (10), 2265–2276. <https://doi.org/10.1002/ps.4823>.
- (42) USEPA. Federal Insecticide, Fungicide, and Rodenticide Act <https://www.epa.gov/laws-regulations/summary-federal-insecticide-fungicide-and-rodenticide-act> (accessed 2022 -08 -04).

- (43) Applied Biochemists. Navigate chemical label <http://www.lakerestoration.com/pdf/Navigatelabel.pdf> (accessed 2021 -10 -24). <https://doi.org/http://www.lakerestoration.com/pdf/Navigatelabel.pdf>.
- (44) NuFarm. Weedar 64 chemical label <http://www.cdms.net/ldat/ld08K005.pdf> (accessed 2021 -10 -24). <https://doi.org/http://www.cdms.net/ldat/ld08K005.pdf>.
- (45) Zepp, R. G.; Wolfe, N. L.; Gordon, J. A.; Baughman, G. L. Dynamics of 2,4-D esters in surface waters: Hydrolysis, photolysis, and vaporization. *Environ. Sci. Technol.* **1975**, *9* (13), 1144–1150. <https://doi.org/10.1021/es60111a001>.
- (46) Mossler, M. A.; Shilling, D. G.; Milgram, K. E.; Haller, W. T. Interaction of formulation and soil components on the aqueous concentration of fluridone. *J. Aquat. Plant. Manage.* **1993**, *31*, 257–260.
- (47) DeQuattro, Z. A.; Karasov, W. H. Impacts of 2,4-dichlorophenoxyacetic acid aquatic herbicide formulations on reproduction and development of the fathead minnow (*Pimephales promelas*). *Environ. Toxicol. and Chem.* **2016**, *35* (6), 1478–1488. <https://doi.org/10.1002/etc.3293>.
- (48) Surgan, M.; Condon, M.; Cox, C. Pesticide risk indicators: Unidentified inert ingredients compromise their integrity and utility. *Environmental Management.* **2010**, *45* (4), 834–841. <https://doi.org/10.1007/s00267-009-9382-9>.
- (49) Polli, E. G.; Alves, G. S.; de Oliveira, J. V.; Kruger, G. R. Physical–chemical properties, droplet size, and efficacy of dicamba plus glyphosate tank mixture influenced by adjuvants. *Agronomy.* **2021**, *11* (7). <https://doi.org/10.3390/agronomy11071321>.
- (50) Tominack, R. L. Herbicide formulations. *Clinical Toxicology.* **2000**, *38* (2), 129–135.
- (51) Cox, C.; Surgan, M. Unidentified inert ingredients in pesticides: Implications for human and environmental health. *Environmental Health Perspectives.* **2006**, *114* (12), 1803–1806. <https://doi.org/10.1289/ehp.9374>.
- (52) Straw, E. A.; Thompson, L. J.; Leadbeater, E.; Brown, M. J. F. Inert ingredients are understudied, potentially dangerous to bees and deserve more research attention. *Proc. R. Soc. B.* **2022**, *289*, 20212353. <https://doi.org/10.1098/rspb.2021.2353>.
- (53) USEPA. Pesticide Registration Manual <https://www.epa.gov/pesticide-registration/pesticide-registration-manual> (accessed 2022 -08 -02).
- (54) USEPA. Clean Water Act. <https://www.epa.gov/laws-regulations/summary-clean-water-act> (accessed 2022-08-04)
- (55) USEPA. National Pollutant Discharge Elimination System (NPDES) Permit Basics <https://www.epa.gov/npdes/npdes-permit-basics> (accessed 2022 -08 -04).
- (56) WI Dept. of Natural Resources; Dept. of Health and Human Services; Dept. of Agriculture, T. and C. Protect. Frequently Asked Questions about Aquatic Herbicide Use in Wisconsin <https://dnr.wi.gov/lakes/plants/factsheets/GeneralherbicideFAQ.pdf> (accessed 2022 -08 -15).
- (57) USEPA. Safe Drinking Water Act. <https://www.epa.gov/sdwa> (accessed 2022-08-02)
- (58) USEPA. Series 835 - Fate, Transport and Transformation Test Guidelines <https://www.epa.gov/test-guidelines-pesticides-and-toxic-substances/series-835-fate-transport-and-transformation-test> (accessed 2022 -08 -04).
- (59) OECD. *Revised Introduction to the OECD Guidelines for Testing of Chemicals, Section 3*; OECD, 2006. <https://doi.org/10.1787/9789264030213-en>.
- (60) USEPA. Principles and Strategies Related to Biodegradation Testing of Organic Chemicals under the Toxic Substances Control Act (TSCA)

- <https://www.regulations.gov/document/EPA-HQ-OPPT-2009-0152-0002> (accessed 2022 -08 -04).
- (61) Schwarzenbach, R. P.; Gschwend, P. M.; Imboden, D. M. *Environmental Organic Chemistry*, 3rd ed.; **2017**.
- (62) Stefanidis, D.; Jencks, W. P. General base catalysis of ester hydrolysis. *J. Am. Chem. Soc* **1993**, *115*, 6045–6050.
- (63) Mabey, W.; Mill, T. Critical review of hydrolysis of organic compounds in water under environmental conditions. *Journal of Physical and Chemical Reference Data* **1978**, *7* (2), 383–415. <https://doi.org/10.1063/1.555572>.
- (64) OECD. *Test No. 111: Hydrolysis as a Function of pH*; OECD, 2004. <https://doi.org/10.1787/9789264069701-en>.
- (65) USEPA. Hydrolysis <https://www.regulations.gov/document/EPA-HQ-OPPT-2009-0152-0009> (accessed 2022 -08 -04).
- (66) USEPA. Hydrolysis as a function of pH and temperature <https://www.regulations.gov/document/EPA-HQ-OPPT-2009-0152-0010> (accessed 2022 -08 -04).
- (67) Boreen, A. L.; Arnold, W. A.; McNeill, K. Photodegradation of pharmaceuticals in the aquatic environment: A review. *Aquat. Sci.* **2003**, *65* (4), 320–341. <https://doi.org/10.1007/s00027-003-0672-7>.
- (68) Remucal, C. K. The role of indirect photochemical degradation in the environmental fate of pesticides: A review. *Environ. Sci. Processes Impacts.* **2014**, *16* (4), 628–653. <https://doi.org/10.1039/c3em00549f>.
- (69) Sud, D.; Kaur, P. Heterogeneous photocatalytic degradation of selected organophosphate pesticides: A review. *Critical Reviews in Environmental Science and Technology.* **2012**, *42* (22), 2365–2407. <https://doi.org/10.1080/10643389.2011.574184>.
- (70) Zafiriou, O. C.; Jousot-Dubien, J.; Zepp, R. G.; Zika, R. G. Photochemistry of natural waters. *Environ. Sci. Technol.* **1984**, *18* (12), 358–371.
- (71) Mill, T. Predicting photoreaction rates in surface waters. *Chemosphere.* **1999**, *38* (6), 1379–1390.
- (72) Leifer, A. *The Kinetics of Environmental Aquatic Photochemistry: Theory and Practice*; American Chemical Society, 1988.
- (73) Wenk, J.; von Gunten, U.; Canonica, S. Effect of dissolved organic matter on the transformation of contaminants induced by excited triplet states and the hydroxyl radical. *Environ. Sci. Technol.* **2011**, *45* (4), 1334–1340. <https://doi.org/10.1021/es102212t>.
- (74) McNeill, K.; Canonica, S. Triplet state dissolved organic matter in aquatic photochemistry: Reaction mechanisms, substrate scope, and photophysical properties. *Environ. Sci. Processes Impacts.* **2016**, *18* (11), 1381–1399. <https://doi.org/10.1039/C6EM00408C>.
- (75) Haag, W.; Hoigné, J. Photo-sensitized oxidation in natural water via •OH radicals. *Chemosphere.* **1985**, *14* (11–12), 1659–1671. [https://doi.org/10.1016/0045-6535\(85\)90107-9](https://doi.org/10.1016/0045-6535(85)90107-9).
- (76) Zepp, R. G.; Wolfe, N. L.; Baughman, G. L.; Hollis, R. C. Singlet oxygen in natural waters. *Nature.* **1977**, *267* (5610), 421–423. <https://doi.org/10.1038/267421a0>.
- (77) Haag, W. R.; Hoigne, J.; Gassman, E.; Braun, A. Singlet oxygen in surface waters — Part II: Quantum yields of its production by some natural humic materials as a function of wavelength. *Chemosphere.* **1984**, *13* (5–6), 641–650. [https://doi.org/10.1016/0045-6535\(84\)90200-5](https://doi.org/10.1016/0045-6535(84)90200-5).

- (78) Maizel, A. C.; Remucal, C. K. Molecular composition and photochemical reactivity of size-fractionated dissolved organic matter. *Environ. Sci. Technol.* **2017**, *51* (4), 2113–2123. <https://doi.org/10.1021/acs.est.6b05140>.
- (79) Maizel, A. C.; Li, J.; Remucal, C. K. Relationships between dissolved organic matter composition and photochemistry in lakes of diverse trophic status. *Environ. Sci. Technol.* **2017**, *51* (17), 9624–9632. <https://doi.org/10.1021/acs.est.7b01270>.
- (80) Berg, S. M.; Whiting, Q. T.; Herrli, J. A.; Winkels, R.; Wammer, K. H.; Remucal, C. K. The role of dissolved organic matter composition in determining photochemical reactivity at the molecular level. *Environ. Sci. Technol.* **2019**, *53* (20), 11725–11734. <https://doi.org/10.1021/acs.est.9b03007>.
- (81) OECD. *Test No. 316: Phototransformation of Chemicals in Water – Direct Photolysis*; OECD, 2008. <https://doi.org/10.1787/9789264067585-en>.
- (82) USEPA. Direct Photolysis Rate in Water by Sunlight. <https://www.regulations.gov/document/EPA-HQ-OPPT-2009-0152-0011> (accessed 2022 -08 -04).
- (83) USEPA. Photodegradation in Water. <https://www.regulations.gov/document/EPA-HQ-OPPT-2009-0152-0012> (accessed 2022 -08 -04).
- (84) USEPA. Indirect Photolysis Screening Test <https://www.regulations.gov/document/EPA-HQ-OPPT-2009-0152-0031> (accessed 2022 -08 -07).
- (85) McConville, M. B.; Mezyk, S. P.; Remucal, C. K. Indirect photodegradation of the lampricides TFM and niclosamide. *Environ. Sci. Processes Impacts.* **2017**, *19* (8), 1028–1039. <https://doi.org/10.1039/c7em00208d>.
- (86) Wang, Y.; Roddick, F. A.; Fan, L. Direct and indirect photolysis of seven micropollutants in secondary effluent from a wastewater lagoon. *Chemosphere.* **2017**, *185*, 297–308. <https://doi.org/10.1016/j.chemosphere.2017.06.122>.
- (87) Galbavy, E. S.; Ram, K.; Anastasio, C. 2-Nitrobenzaldehyde as a chemical actinometer for solution and ice photochemistry. *J. Photochem. Photobio. A: Chem* **2010**, *209* (2–3), 186–192. <https://doi.org/10.1016/j.jphotochem.2009.11.013>.
- (88) Laszakovits, J. R.; Berg, S. M.; Anderson, B. G.; O'Brien, J. E.; Wammer, K. H.; Sharpless, C. M. *p*-Nitroanisole/pyridine and *p*-nitroacetophenone/pyridine actinometers revisited: Quantum yield in comparison to ferrioxalate. *Environ. Sci. Technol. Lett.* **2017**, *4* (1), 11–14. <https://doi.org/10.1021/acs.estlett.6b00422>.
- (89) Watson, J. R. Seasonal variation in the biodegradation of 2,4-D in river water. *Water Res.* **1977**, *11*, 153–157. [https://doi.org/10.1016/0043-1354\(77\)90120-8](https://doi.org/10.1016/0043-1354(77)90120-8).
- (90) Buerge, I. J.; Kasteel, R.; Bächli, A.; Poiger, T. Behavior of the chiral herbicide imazamox in soils: Enantiomer composition differentiates between biodegradation and photodegradation. *Environ. Sci. Technol.* **2019**, *53* (10), 5733–5740. <https://doi.org/10.1021/acs.est.8b07210>.
- (91) Luo, Y.; Atashgahi, S.; Rijnaarts, H. H. M.; Comans, R. N. J.; Sutton, N. B. Influence of different redox conditions and dissolved organic matter on pesticide biodegradation in simulated groundwater systems. *Sci. Total Environ.* **2019**, *677*, 692–699. <https://doi.org/10.1016/j.scitotenv.2019.04.128>.
- (92) Rodríguez-Cruz, M. S.; Bælum, J.; Shaw, L. J.; Sørensen, S. R.; Shi, S.; Aspray, T.; Jacobsen, C. S.; Bending, G. D. Biodegradation of the herbicide mecoprop-p with soil depth and its relationship with class III *tfdA* genes. *Soil Biology and Biochemistry.* **2010**, *42* (1), 32–39. <https://doi.org/10.1016/j.soilbio.2009.09.018>.

- (93) Simsimn, G. v.; Chesters, G. Persistence of endothall in the environment. *Water, Air, and Soil Pollution*. **1975**, *4*, 399–413. <https://doi.org/10.1007/BF00280725>.
- (94) Huang, X.; He, J.; Yan, X.; Hong, Q.; Chen, K.; He, Q.; Zhang, L.; Liu, X.; Chuang, S.; Li, S.; Jiang, J. Microbial catabolism of chemical herbicides: Microbial resources, metabolic pathways and catabolic genes. *Pesticide Biochemistry and Physiology* **2017**, *143*, 272–297. <https://doi.org/10.1016/j.pestbp.2016.11.010>.
- (95) Wang, S.; Miltner, A.; Muskus, A. M.; Nowak, K. M. Microbial activity and metamitron degrading microbial communities differ between soil and water-sediment systems. *Journal of Hazardous Materials*. **2021**, *408* (15), 124293. <https://doi.org/10.1016/j.jhazmat.2020.124293>.
- (96) Schwartz, H. G. Microbial degradation of pesticides in aqueous solutions. *J. Water Pollution Control Federation*. **1967**, *39* (10), 1701 – 1714.
- (97) Paris, D. F.; Steen, W. C.; Baughman, G. L.; Barnett, J. T. Second-order model to predict microbial degradation of organic compounds in natural waters. *Appl. Environ. Microbiol.* **1981**, *41* (3), 603–609.
- (98) Zhou, X.; Jin, W.; Sun, C.; Gao, S. H.; Chen, C.; Wang, Q.; Han, S. F.; Tu, R.; Latif, M. A.; Wang, Q. Microbial degradation of *N,N*-dimethylformamide by *Paracoccus sp.* strain DMF-3 from activated sludge. *Chemical Engineering Journal*. **2018**, *343*, 324–330. <https://doi.org/10.1016/j.cej.2018.03.023>.
- (99) Barbosa da Costa, N.; Fugère, V.; Hébert, M. P.; Xu, C. C. Y.; Barrett, R. D. H.; Beisner, B. E.; Bell, G.; Yargeau, V.; Fussmann, G. F.; Gonzalez, A.; Shapiro, B. J. Resistance, resilience, and functional redundancy of freshwater bacterioplankton communities facing a gradient of agricultural stressors in a mesocosm experiment. *Molec. Eco.* **2021**, *30* (19), 4771–4788. <https://doi.org/10.1111/mec.16100>.
- (100) Jog, K. v.; Hess, K. Z.; Field, J. A.; Krzmarzick, M. J.; Sierra-Alvarez, R. Aerobic biodegradation of emerging azole contaminants by return activated sludge and enrichment cultures. *Journal of Hazardous Materials*. **2021**, *417*, 126151. <https://doi.org/10.1016/j.jhazmat.2021.126151>.
- (101) de Liphthay, J. R.; Tuxen, N.; Johnsen, K.; Hansen, L. H.; Albrechtsen, H. J.; Bjerg, P. L.; Aamand, J. In situ exposure to low herbicide concentrations affects microbial population composition and catabolic gene frequency in an aerobic shallow aquifer. *Appl. Environ. Microbiol.* **2003**, *69* (1), 461–467. <https://doi.org/10.1128/AEM.69.1.461-467.2003>.
- (102) Peterson, B. D.; McDaniel, E. A.; Schmidt, A. G.; Lepak, R. F.; Janssen, S. E.; Tran, P. Q.; Marick, R. A.; Ogorek, J. M.; DeWild, J. F.; Krabbenhoft, D. P.; McMahon, K. D. Mercury methylation genes identified across diverse anaerobic microbial guilds in a eutrophic sulfate-enriched lake. *Environ. Sci. Technol.* **2020**, *54*, 15840. <https://doi.org/10.1021/acs.est.0c05435>.
- (103) Elder, D. J. E.; Kelly, D. J. The bacterial degradation of benzoic acid and benzenoid compounds under anaerobic conditions: Unifying trends and new perspectives. *FEMS Microbiology Reviews*. **1994**, *13* (4), 441–468. [https://doi.org/10.1016/0168-6445\(94\)90064-7](https://doi.org/10.1016/0168-6445(94)90064-7).
- (104) Nijenhuis, I.; Nikolausz, M.; Köth, A.; Felföldi, T.; Weiss, H.; Drangmeister, J.; Großmann, J.; Kästner, M.; Richnow, H. H. Assessment of the natural attenuation of chlorinated ethenes in an anaerobic contaminated aquifer in the Bitterfeld/Wolfen area using stable isotope techniques, microcosm studies and molecular biomarkers. *Chemosphere*. **2007**, *67* (2), 300–311. <https://doi.org/10.1016/j.chemosphere.2006.09.084>.

- (105) Peleg, M. A new look at models of the combined effect of temperature, pH, water activity, or other factors on microbial growth rate. *Food Engineering Reviews*. **2022**, *14*, 31–44. <https://doi.org/10.1007/s12393-021-09292-x>.
- (106) Koseki, S.; Nonaka, J. Alternative approach to modeling bacterial lag time, using logistic regression as a function of time, temperature, pH, and sodium chloride concentration. *Appl. Environ. Microbiol.* **2012**, *78* (17), 6103–6112. <https://doi.org/10.1128/AEM.01245-12>.
- (107) Chalifour, A.; Walser, J. C.; Pomati, F.; Fenner, K. Temperature, phytoplankton density, and bacteria diversity drive the biotransformation of micropollutants in a lake ecosystem. *Water Res.* **2021**, *202*, 117412. <https://doi.org/10.1016/j.watres.2021.117412>.
- (108) Buerge, I. J.; Bächli, A.; Kasteel, R.; Portmann, R.; López-Cabeza, R.; Schwab, L. F.; Poiger, T. Behavior of the chiral herbicide imazamox in soils: pH-dependent, enantioselective degradation, formation and degradation of several chiral metabolites. *Environ. Sci. Technol.* **2019**, *53* (10), 5725–5732. <https://doi.org/10.1021/acs.est.8b07209>.
- (109) Li, J.; Shimizu, K.; Sakharkar, M. K.; Utsumi, M.; Zhang, Z.; Sugiura, N. Comparative study for the effects of variable nutrient conditions on the biodegradation of microcystin-LR and concurrent dynamics in microcystin-degrading gene abundance. *Bioresource Technology*. **2011**, *102* (20), 9509–9517. <https://doi.org/10.1016/j.biortech.2011.07.112>.
- (110) Seller, C.; Honti, M.; Singer, H.; Fenner, K. Biotransformation of chemicals in water-sediment suspensions: Influencing factors and implications for persistence assessment. *Environ. Sci. Technol. Lett.* **2020**, *7* (11), 854–860. <https://doi.org/10.1021/acs.estlett.0c00725>.
- (111) Groffman, P. M.; Voos, G. Relationships between microbial biomass and dissipation of 2,4-D and dicamba in soil. *Bio. Fert. Soils* **1997**, *24* (1), 106–110. <https://doi.org/10.1007/s003740050216>.
- (112) Ahtiainen, J.; Aalto, M.; Pessala, P. Biodegradation of chemicals in a standardized test and in environmental conditions. *Chemosphere*. **2003**, *51* (6), 529–537. [https://doi.org/10.1016/S0045-6535\(02\)00861-5](https://doi.org/10.1016/S0045-6535(02)00861-5).
- (113) Kowalczyk, A.; Martin, T. J.; Price, O. R.; Snape, J. R.; van Egmond, R. A.; Finnegan, C. J.; Schäfer, H.; Davenport, R. J.; Bending, G. D. Refinement of biodegradation tests methodologies and the proposed utility of new microbial ecology techniques. *Ecotoxicology and Environmental Safety*. **2015**, *111*, 9–22. <https://doi.org/10.1016/j.ecoenv.2014.09.021>.
- (114) Lapertot, M. E.; Pulgarin, C. Biodegradability assessment of several priority hazardous substances: Choice, application and relevance regarding toxicity and bacterial activity. *Chemosphere*. **2006**, *65* (4), 682–690. <https://doi.org/10.1016/j.chemosphere.2006.01.046>.
- (115) Reuschenbach, P.; Pagga, U.; Strotmann, U. A critical comparison of respirometric biodegradation tests based on OECD 301 and related test methods. *Water Res.* **2003**, *37*, 1571–1582.
- (116) USEPA. Ready Biodegradability <https://www.regulations.gov/document/EPA-HQ-OPPT-2009-0152-0018> (accessed 2022 -08 -07).
- (117) OECD. *Test No. 301: Ready Biodegradability*; OECD, 1992. <https://doi.org/10.1787/9789264070349-en>.
- (118) Wennberg, A. C.; Meland, S.; Grung, M.; Lillicrap, A. Unravelling reasons for variability in the OECD 306 marine biodegradation test. *Chemosphere*. **2022**, *300*, 134476. <https://doi.org/10.1016/j.chemosphere.2022.134476>.

- (119) OECD. *Test No. 308: Aerobic and Anaerobic Transformation in Aquatic Sediment Systems*; OECD, 2002. <https://doi.org/10.1787/9789264070523-en>.
- (120) OECD. *Test No. 309: Aerobic Mineralization in Surface Water – Simulation Biodegradation Test*; OECD, 2004. <https://doi.org/10.1787/9789264070547-en>.
- (121) USEPA. *Aerobic Mineralization in Surface Water – Simulation Biodegradation Test* <https://www.regulations.gov/document/EPA-HQ-OPPT-2009-0152-0032> (accessed 2022 -08 -07).
- (122) USEPA. *Aerobic and Anaerobic Aquatic Metabolism* <https://www.regulations.gov/document/EPA-HQ-OPPT-2009-0152-0039> (accessed 2022 -08 -07).
- (123) McConville, M. B.; Cohen, N. M.; Nowicki, S. M.; Lantz, S. R.; Hixson, J. L.; Ward, A. S.; Remucal, C. K. A field analysis of lampricide photodegradation in Great Lakes tributaries. *Environ. Sci. Processes Impacts*. **2017**, *19* (7), 891–900. <https://doi.org/10.1039/c7em00173h>.
- (124) Honti, M.; Hahn, S.; Hennecke, D.; Junker, T.; Shrestha, P.; Fenner, K. Bridging across OECD 308 and 309 data in search of a robust biotransformation indicator. *Environ. Sci. Technol.* **2016**, *50* (13), 6865–6872. <https://doi.org/10.1021/acs.est.6b01097>.
- (125) Trigo, A.; Valencia, A.; Cases, I. Systemic approaches to biodegradation. *FEMS Microbiology Reviews*. **2009**, *33* (1), 98–108. <https://doi.org/10.1111/j.1574-6976.2008.00143.x>.
- (126) Thouand, G.; Durand, M. J.; Maul, A.; Gancet, C.; Blok, H. New concepts in the evaluation of biodegradation/persistence of chemical substances using a microbial inoculum. *Front. Microbiol.* **2011**, *2*, 1-6. <https://doi.org/10.3389/fmicb.2011.00164>.
- (127) Shrestha, P.; Junker, T.; Fenner, K.; Hahn, S.; Honti, M.; Bakkour, R.; Diaz, C.; Hennecke, D. Simulation studies to explore biodegradation in water-sediment systems: From OECD 308 to OECD 309. *Environ. Sci. Technol.* **2016**, *50* (13), 6856–6864. <https://doi.org/10.1021/acs.est.6b01095>.
- (128) Li, Z.; McLachlan, M. Comparing non-targeted chemical persistence assessed using an unspiked OECD 309 test to field measurements. *Environ. Sci. Processes Impacts*. **2020**, *22* (5), 1233–1242. <https://doi.org/10.1039/c9em00595a>.
- (129) Li, Z.; McLachlan, M. S. Biodegradation of chemicals in unspiked surface waters downstream of wastewater treatment plants. *Environ. Sci. Technol.* **2019**, *53* (4), 1884–1892. <https://doi.org/10.1021/acs.est.8b05191>.
- (130) Honti, M.; Fenner, K. Deriving persistence indicators from regulatory water-sediment studies - Opportunities and limitations in OECD 308 data. *Environ. Sci. Technol.* **2015**, *49* (10), 5879–5886. <https://doi.org/10.1021/acs.est.5b00788>.
- (131) Mezzanotte, V.; Bertani, R.; Innocenti, F. D.; Tosin, M. Influence of inocula on the results of biodegradation tests. *Polymer Degradation and Stability*. **2005**, *87* (1), 51–56. <https://doi.org/10.1016/j.polyimdeggradstab.2004.06.009>.
- (132) Marron-Montiel, E.; Ruiz-Ordaz, N.; Rubio-Graados, C.; Juarez-Ramirez, C.; Galindez-Mayer, C. J. Isolation, kinetic characterization in batch and continuous culture and application for bioaugmenting an activated sludge microbial community. *Process Biochemistry*. **2006**, *41*, 1521–1528. <https://doi.org/10.1016/j.procbio.2006.02.012>.
- (133) Musarrat, J.; Bano, N. Isolation and characterization of 2,4-dichlorophenoxyacetic acid-catabolizing bacteria and their biodegradation efficiency in soil. *Word Jrnl. Micro. Biotech.* **2000**, *16*, 495–497.

- (134) Soulas, G. Evidence for the existence of different physiological groups in the microbial community responsible for 2,4-D mineralization in soil. *Soil Bio. Biochem.* **1993**, *25* (4), 443449. [https://doi.org/10.1016/0038-0717\(93\)90069-N](https://doi.org/10.1016/0038-0717(93)90069-N).
- (135) Vallaeys, T.; Persello-Cartieaux, F.; Rouard, N.; Lors, C.; Laguerre, G.; Soulas, G. PCR-RLFP analysis of 16s rRNA, *tfdA* and *tfdB* genes reveals a diversity of 2,4-D degraders in soil aggregates. *FEMS Micro. Eco.* **2006**, *24* (3), 269–278. <https://doi.org/10.1111/j.1574-6941.1997.tb00444.x>.
- (136) McDaniel, E. A.; Peterson, B. D.; Stevens, S. L. R.; Tran, P. Q.; Anantharaman, K.; McMahon, K. D. Expanded phylogenetic diversity and metabolic flexibility of mercury-methylating microorganisms. *mSystems.* **2020**, *5* (4), e00299-20. <https://doi.org/10.1128/msystems.00299-20>.
- (137) Cao, Y.; Yu, M.; Dong, G.; Chen, B.; Zhang, B. Digital PCR as an emerging tool for monitoring of microbial biodegradation. *Molecules.* **2020**, *25*, 706. <https://doi.org/10.3390/molecules25030706>.
- (138) Beach, N. K.; Noguera, D. R. Design and assessment of species-level qPCR primers targeting Comammox. *Front. Microbiol.* **2019**, *10*, 1–15. <https://doi.org/10.3389/fmicb.2019.00036>.
- (139) Pinto, A. J.; Marcus, D. N.; Ijaz, U. Z.; Bautista-de los Santos, Q. M.; Dick, G. J.; Raskin, L. Metagenomic evidence for the presence of Comammox *Nitrospira*-like bacteria in a drinking water system. *mSphere.* **2016**, *1* (1), e00054-15. <https://doi.org/10.1128/msphere.00054-15>.
- (140) Ann Moran, M. Metatranscriptomics: Eavesdropping on complex microbial communities large-scale sequencing of mRNAs retrieved from natural communities provides insights into microbial activities and how they are regulated. *Microbes.* **2018**, *4* (7), 329–335.
- (141) Stenuit, B.; Eyers, L.; Schuler, L.; Agathos, S. N.; George, I. Emerging high-throughput approaches to analyze bioremediation of sites contaminated with hazardous and/or recalcitrant wastes. *Biotechnology Advances.* **2008**, *26* (6), 561-575. <https://doi.org/10.1016/j.biotechadv.2008.07.004>.
- (142) Zhang, Y.; Sei, K.; Toyama, T.; Ike, M.; Zhang, J.; Yang, M.; Kamagata, Y. Changes of catabolic genes and microbial community structures during biodegradation of nonylphenol ethoxylates and nonylphenol in natural water microcosms. *Biochemical Engineering Journal.* **2008**, *39* (2), 288–296. <https://doi.org/10.1016/j.bej.2007.09.015>.
- (143) Zhi, H.; Miannecki, A. L.; Kolpin, D. W.; Klaper, R. D.; Iwanowicz, L. R.; LeFevre, G. H. Tandem field and laboratory approaches to quantify attenuation mechanisms of pharmaceutical and pharmaceutical transformation products in a wastewater effluent-dominated stream. *Water Res.* **2021**, *203*, 117537. <https://doi.org/10.1016/j.watres.2021.117537>.
- (144) White, A. M.; Nault, M. E.; McMahon, K. D.; Remucal, C. K. Synthesizing laboratory and field experiments to quantify dominant transformation mechanisms of 2,4-dichlorophenoxyacetic acid (2,4-D) in aquatic environments. *Environ. Sci. Technol.* **2022**, *56* (15), 10838–10848. <https://doi.org/10.1021/acs.est.2c03132>.
- (145) ter Horst, M. M. S.; Koelmans, A. A. Analyzing the limitations and the applicability domain of water-sediment transformation tests like OECD 308. *Environ. Sci. Technol.* **2016**, *50* (19), 10335–10342. <https://doi.org/10.1021/acs.est.6b02906>.
- (146) Unice, K.; Bare, J.; Kreider, M.; Panko, J. Experimental methodology for assessing the environmental fate of organic chemicals in polymer matrices using column leaching studies

- and OECD 308 water/sediment systems: Application to tire and road wear particles. *Sci. Total Environ.* **2015**, *533*, 476–487. <https://doi.org/10.1016/j.scitotenv.2015.06.053>.
- (147) DOW. Rinskor Active Technical Bulletin http://storage.dow.com.edgesuite.net/dowagro/rinskor/Rinskor_Tech_Bulletin.pdf. (accessed 2020-05-15).
- (148) Zuanazzi, N. R.; Ghisi, N. de C.; Oliveira, E. C. Analysis of global trends and gaps for studies about 2,4-D herbicide toxicity: A scientometric review. *Chemosphere.* **2020**, *241*, 125016. <https://doi.org/10.1016/j.chemosphere.2019.125016>.
- (149) Liu, W.; Li, H.; Tao, F.; Li, S.; Tian, Z.; Xie, H. Formation and contamination of PCDD/FS, PCBS, PECBZ, HZCBZ and polychlorophenols in the production of 2,4-D products. *Chemosphere* **2013**, *92* (3), 304–308. <https://doi.org/10.1016/j.chemosphere.2013.03.031>.
- (150) Islam, F.; Wang, J.; Farooq, M. A.; Khan, M. S. S.; Xu, L.; Zhu, J.; Zhao, M.; Muñoz, S.; Li, Q. X.; Zhou, W. Potential impact of the herbicide 2,4-dichlorophenoxyacetic acid on human and ecosystems. *Environment International.* **2018**, *111*, 332–351. <https://doi.org/10.1016/j.envint.2017.10.020>.
- (151) Atwood, D.; Paisley-Jones, C. *US EPA - Pesticides Industry Sales and Usage 2008 - 2012; 2017.* https://www.epa.gov/sites/default/files/2017-01/documents/pesticides-industry-sales-usage-2016_0.pdf. (accessed 2022-06-15).
- (152) Barbosa, A. M. C.; Solano, M. de L. M.; Umbuzeiro, G. de A. Pesticides in drinking water – The Brazilian monitoring program. *Front Public Health.* **2015**, *3*, 246. <https://doi.org/10.3389/fpubh.2015.00246>.
- (153) Paszko, T.; Muszyński, P.; Materska, M.; Bojanowska, M.; Kostecka, M.; Jackowska, I. Adsorption and degradation of phenoxyalkanoic acid herbicides in soils: A review. *Environ. Toxicol. and Chem.* **2016**, *35* (2), 271–286. <https://doi.org/10.1002/etc.3212>.
- (154) Dehnert, G. K.; Freitas, M. B.; Sharma, P. P.; Barry, T. P.; Karasov, W. H. Impacts of subchronic exposure to a commercial 2,4-D herbicide on developmental stages of multiple freshwater fish species. *Chemosphere.* **2021**, *263*, 127638. <https://doi.org/10.1016/j.chemosphere.2020.127638>.
- (155) Dehnert, G. K.; Freitas, M. B.; DeQuattro, Z. A.; Barry, T.; Karasov, W. H. Effects of low, subchronic exposure of 2,4-dichlorophenoxyacetic acid (2,4-D) and commercial 2,4-D formulations on early life stages of fathead minnows (*Pimephales promelas*). *Environ. Toxicol. and Chem.* **2018**, *37* (10), 2550–2559. <https://doi.org/10.1002/etc.4209>.
- (156) Aly, O. M.; Faust, S. D. Studies on the fate of 2,4-D and ester derivatives in natural surface waters. *J. Agric. Food Chem.* **1964**, *12* (6), 541–546. <https://doi.org/10.1021/jf60136a016>.
- (157) Aly, O. M.; Faust, S. D. Removal of 2,4-dichlorophenoxyacetic acid derivatives from natural waters. *J Am Water Works Assoc.* **1965**, *57* (2), 221–230. <https://doi.org/10.1002/j.1551-8833.1965.tb01390.x>.
- (158) Walters, J. Environmental fate of 2,4-dichlorophenoxyacetic acid. **1999**. <http://citeseerx.ist.psu.edu/viewdoc/download?doi=10.1.1.639.4289&rep=rep1&type=pdf> (accessed 2020-05-15)
- (159) EPA. Reregistration Eligibility Decision for 2,4-D https://archive.epa.gov/pesticides/reregistration/web/pdf/24d_red.pdf (accessed 2020-05-15). https://doi.org/https://archive.epa.gov/pesticides/reregistration/web/pdf/24d_red.pdf. (accessed 2020-05-15)
- (160) Berg, S. M.; Whiting, Q. T.; Herrli, J. A.; Winkels, R.; Wammer, K. H.; Remucal, C. K. The role of dissolved organic matter composition in determining photochemical reactivity

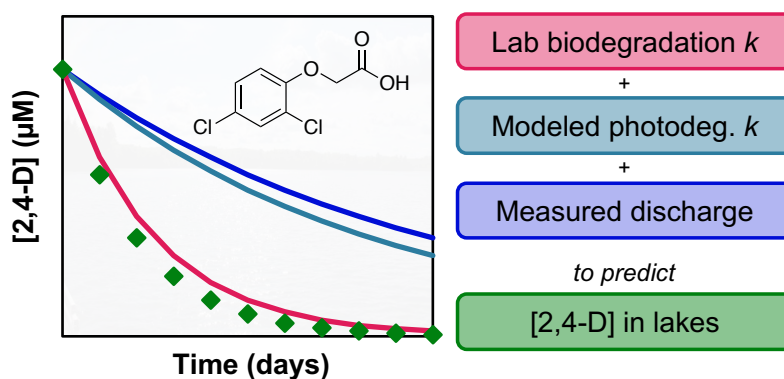
- at the molecular level. *Environ. Sci. Technol.* **2019**, *53* (20), 11725–11734. <https://doi.org/10.1021/acs.est.9b03007>.
- (161) Armbrust, K. L. Pesticide hydroxyl radical rate constants: Measurements and estimates of their importance in aquatic environments. *Environ. Toxicol. and Chem.* **2000**, *19* (9), 2175–2180. <https://doi.org/10.1002/etc.5620190905>.
- (162) Chavez Rodriguez, L.; Ingalls, B.; Schwarz, E.; Streck, T.; Uksa, M.; Pagel, H. Gene-centric model approaches for accurate prediction of pesticide biodegradation in soils. *Environ. Sci. Technol.* **2020**, *54* (21), 13638–13650. <https://doi.org/10.1021/acs.est.0c03315>.
- (163) Ogram, A. v.; Jessup, R. E.; Ou, L. T.; Rao, P. S. C. Effects of sorption on biological degradation rates of (2,4-dichlorophenoxy)acetic acid in soils. *Appl. Environ. Microbiol.* **1985**, *49* (3), 582–587. <https://doi.org/10.1128/aem.49.3.582-587.1985>.
- (164) Han, L.; Zhao, D.; Li, C. Isolation and 2,4-D-degrading characteristics of *Cupriavidus campinensis* bJ71. *Braz. J. Microbiol* **2015**, *46* (2), 433–441.
- (165) Zabaloy, M. C.; Gómez, M. A. Isolation and characterization of indigenous 2,4-D herbicide degrading bacteria from an agricultural soil in proximity of Sauce Grande river, Argentina. *Annals Micro.* **2014**, *64* (3), 969–974. <https://doi.org/10.1007/s13213-013-0731-9>.
- (166) Macur, R. E.; Wheeler, J. T.; Burr, M. D.; Inskeep, W. P. Impacts of 2,4-D application on soil microbial community structure and on populations associated with 2,4-D degradation. *Microbiological Research.* **2007**, *162* (1), 37–45. <https://doi.org/10.1016/j.micres.2006.05.007>.
- (167) Kumar, A.; Trefault, N.; Olaniran, A. O. Microbial degradation of 2,4-dichlorophenoxyacetic acid: Insight into the enzymes and catabolic genes involved, their regulation and biotechnological implications. *Crit. Rev. Micro.* **2016**, *42* (2), 194–208. <https://doi.org/10.3109/1040841X.2014.917068>.
- (168) Fukumori, F.; Hausinger, R. P. *Alcaligenes eutrophus* JMP134 “2,4-dichlorophenoxyacetate monooxygenase” is an α -ketoglutarate-dependent dioxygenase. *J. Bact.* **1993**, *175* (7), 2083–2086. <https://doi.org/10.1128/jb.175.7.2083-2086.1993>.
- (169) Laemmli, C. M.; Leveau, J. H. J.; Zehnder, A. J. B.; Roelof Van Der Meer, J. Characterization of a second *tfd* gene cluster for chlorophenol and chlorocatechol metabolism on plasmid pJP4 in *Ralstonia eutropha* JMP134(pJP4). *J. Bact.* **2000**, *182* (15), 4165–4172. <https://doi.org/10.1128/JB.182.15.4165-4172.2000>.
- (170) Chaudhry, G. R.; Huang, G. H. Isolation and characterization of a new plasmid from a *Flavobacterium sp.* which carries the genes for degradation of 2,4-dichlorophenoxyacetate. *J. Bact.* **1988**, *170* (9).
- (171) Baelum, J.; Jacobsen, C. S.; Holben, W. E. Comparison of 16s rRNA gene phylogeny and functional *tfdA* gene distribution in thirty-one different 2,4-dichlorophenoxyacetic acid and 4-chloro-2-methylphenoxyacetic acid degraders. *Systematic and Applied Microbiology* **2010**, *33* (2), 67–70. <https://doi.org/10.1016/j.syapm.2010.01.001>.
- (172) McGowan, C.; Fulthorpe, R.; Wright, A.; Tiedje, J. M. Evidence for interspecies gene transfer in the evolution of 2,4-dichlorophenoxyacetic acid degraders. *Appl. Environ. Microbiol* **1998**, *64* (10), 4089–4092.
- (173) Lerch, T. Z.; Dignac, M. F.; Barriuso, E.; Bardoux, G.; Mariotti, A. Tracing 2,4-D metabolism in *Cupriavidus necator* JMP134 with ¹³C-labelling technique and fatty acid profiling. *J. Micro. Methods* **2007**, *71* (2), 162–174. <https://doi.org/10.1016/j.mimet.2007.08.003>.

- (174) Nicolaisen, M. H.; Bælum, J.; Jacobsen, C. S.; Sørensen, J. Transcription dynamics of the functional *tfdA* gene during MCPA herbicide degradation by *Cupriavidus necator* AEO106 (pRO101) in agricultural soil. *Environ. Microbiol.* **2008**, *10* (3), 571–579. <https://doi.org/10.1111/j.1462-2920.2007.01476.x>.
- (175) Bælum, J.; Jacobsen, C. S. TaqMan probe-based real-time PCR assay for detection and discrimination of class I, II, and III *tfdA* genes in soils treated with phenoxy acid herbicides. *Appl. Environ. Microbiol.* **2009**, *75* (9), 2969–2972. <https://doi.org/10.1128/AEM.02051-08>.
- (176) Bælum, J.; Nicolaisen, M. H.; Holben, W. E.; Strobel, B. W.; Sørensen, J.; Jacobsen, C. S. Direct analysis of *tfdA* gene expression by indigenous bacteria in phenoxy acid amended agricultural soil. *ISME.* **2008**, *2* (6), 677–687. <https://doi.org/10.1038/ismej.2008.21>.
- (177) Batioğlu-Pazarbaşı, M.; Bælum, J.; Johnsen, A. R.; Sørensen, S. R.; Albrechtsen, H. J.; Aamand, J. Centimeter-scale vertical variability of phenoxy acid herbicide mineralization potential in aquifer sediment relates to the abundance of *tfdA* genes. *FEMS Micro. Eco.* **2012**, *80* (2), 331–341. <https://doi.org/10.1111/j.1574-6941.2012.01300.x>.
- (178) Batoğlu-Pazarbaş, M.; Milosevic, N.; Malaguerra, F.; Binning, P. J.; Albrechtsen, H. J.; Bjerg, P. L.; Aamand, J. Discharge of landfill leachate to streambed sediments impacts the mineralization potential of phenoxy acid herbicides depending on the initial abundance of *tfdA* gene classes. *Environmental Pollution.* **2013**, *176*, 275–283. <https://doi.org/10.1016/j.envpol.2013.01.050>.
- (179) de Liphay, J. R.; Aamand, J.; Barkay, T. Expression of *tfdA* genes in aquatic microbial communities during acclimation to 2,4-dichlorophenoxyacetic acid. *FEMS Micro. Eco.* **2006**, *40* (3), 205–214. <https://doi.org/10.1111/j.1574-6941.2002.tb00953.x>.
- (180) USEPA. Final Registration Decision on the New Active Ingredient Florpyrauxifen-benzyl <https://www.regulations.gov/document/EPA-HQ-OPP-2016-0560-0065> (accessed 2022 -07 -25).
- (181) Epp, J. B.; Alexander, A. L.; Balko, T. W.; Buysse, A. M.; Brewster, W. K.; Bryan, K.; Daeuble, J. F.; Fields, S. C.; Gast, R. E.; Green, R. A.; Irvine, N. M.; Lo, W. C.; Lowe, C. T.; Renga, J. M.; Richburg, J. S.; Ruiz, J. M.; Satchivi, N. M.; Schmitzer, P. R.; Siddall, T. L.; Webster, J. D.; Weimer, M. R.; Whiteker, G. T.; Yerkes, C. N. The discovery of Arylex™ active and Rinskor™ active: Two novel auxin herbicides. *Bioorganic and Medicinal Chemistry* **2016**, *24* (3), 362–371. <https://doi.org/10.1016/j.bmc.2015.08.011>.
- (182) Corteva Agriscience. Rinskor Active Technical Bulletin https://www.corteva.com/content/dam/dpagco/corteva/global/corporate/general/files/active-ingredients/DF_Rinskor-TechBulletin_12-14-18.pdf (accessed 2022 -07 -25).
- (183) SePRO. ProcellaCOR EC SDS https://sepro.com/Documents/ProcellaCOR_EC--SDS.pdf (accessed 2022 -08 -15).
- (184) Battelle. Independent Laboratory Validation of a Dow AgroSciences Method for the Determination of XDE-848 Benzyl Ester and Five Metabolites (X11438848, X12300837, X11966341, X12131932 and X12393505) in Water. https://www.epa.gov/sites/production/files/2017-09/documents/ilv_-_florpyrauxifen-benzyl_degradates_in_water_-_mrid_49677802.pdf. (accessed 2020 -05 -15).
- (185) Arena, M.; Auteri, D.; Barmaz, S.; Brancato, A.; Brocca, D.; Bura, L.; Carrasco Cabrera, L.; Chaideftou, E.; Chiusolo, A.; Civitella, C.; Court Marques, D.; Crivellente, F.; Ctverackova, L.; de Lentdecker, C.; Egsmose, M.; Erdos, Z.; Fait, G.; Ferreira, L.; Goumenou, M.; Greco, L.; Ippolito, A.; Istace, F.; Jarrah, S.; Kardassi, D.; Leuschner, R.;

- Lostia, A.; Lythgo, C.; Magrans, J. O.; Medina, P.; Mineo, D.; Miron, I.; Molnar, T.; Padovani, L.; Parra Morte, J. M.; Pedersen, R.; Reich, H.; Sacchi, A.; Santos, M.; Serafimova, R.; Sharp, R.; Stanek, A.; Streissl, F.; Sturma, J.; Szentes, C.; Tarazona, J.; Terron, A.; Theobald, A.; Vagenende, B.; van Dijk, J.; Villamar-Bouza, L. Peer review of the pesticide risk assessment of the active substance florpyrauxifen (variant assessed florpyrauxifen-benzyl). *EFSA Journal*. **2018**, *16* (8). <https://doi.org/10.2903/j.efsa.2018.5378>.
- (186) Onterra. Silver Lake Management Plan. https://www.townshipofmarion.com/wp-content/uploads/2018/01/SilverWaushara_HWMmonitorReport2017_v1-1.pdf. (accessed 2020 -05 -15)
- (187) Osborne, J. A.; West, S. D.; Cooper, Raymond, B.; Schmitz, D. C.; Cooper B., R.; Schmitz, D. C. Fluridone and N-methylformaide residue determination in ponds. *J. Aquat. Plant. Manage.* **1989**, *27*, 74–78.
- (188) West, S. D.; Burger, R. O.; Poole, G. M.; Mowrey, D. H. Bioconcentration and field dissipation of the aquatic herbicide fluridone and its degradation products in aquatic environments. *J. Agric. Food Chem.* **1983**, *31* (3), 579–585. <https://doi.org/10.1021/jf00117a028>.
- (189) Macdonald, G. E.; Haller, W. T.; Shilling, D. G. UV-B filtration to reduce photolysis of fluridone in experimental tanks. *J. Aquat. Plant. Manage.* **1996**, *34* (2), 78–80.
- (190) Saunders, D. G.; Mosier, J. W. Photolysis of the aquatic herbicide fluridone in aqueous solution. *J. Agric. Food Chem.* **1983**, *31* (2), 237–241. <https://doi.org/10.1021/jf00116a013>.
- (191) Mossler, M. A.; Shilling, D. G.; Haller, W. T. Photolytic degradation of fluridone. *J. Aquat. Plant. Manage.* **1989**, *27*, 69–73.
- (192) Mossler, M. A.; Shillings, D. G.; Albrecht, S. L.; Haller, W. T. Microbial degradation of fluridone. *J. Aquat. Plant. Manage.* **1991**, *29*, 77–80.
- (193) Schroeder, J.; Banks, P. A. Persistence of fluridone in five Georgia soils. *Weed Sci.* **1986**, *34* (4), 612–616. <https://doi.org/10.1017/s0043174500067539>.
- (194) Muir, D.; Grift, N. P.; Blouw, A. P.; Lockhart, W. L. Persistence of fluridone in small ponds. *Journal of Environmental Quality.* **1980**, *9* (1), 151–156.

Chapter 2

Synthesizing laboratory and field experiments to quantify dominant transformation mechanisms of 2,4-dichlorophenoxyacetic acid (2,4-D) in aquatic environments



2.1 Details on Collaboration

Chapter 2 is a collaboration between Amber White, Michelle Nault, Katherine McMahon, and Christy Remucal. AW collected the samples, analyzed the samples, and wrote the manuscript with input from all coauthors. This paper is published in *Environmental Science and Technology*, 2022, (56) 15, 10939 – 10848, <https://pubs.acs.org/doi/full/10.1021/acs.est.2c03132>.

2.2 Abstract

Laboratory studies used to assess the environmental fate of organic chemicals such as pesticides fail to replicate environmental conditions, resulting in large errors in predicted transformation rates. We combined laboratory and field data to identify the dominant loss processes of the herbicide 2,4-dichlorophenoxyacetic acid (2,4-D) in lakes for the first time.

Microbial and photochemical degradation were individually assessed using laboratory-based microcosms and irradiation studies, respectively. Field campaigns were conducted in six lakes to quantify 2,4-D loss following large-scale herbicide treatments. Irradiation studies showed that 2,4-D undergoes direct photodegradation, but modeling efforts demonstrated that this process was negligible under environmental conditions. Microcosms constructed using field inocula showed that sediment microbial communities are responsible for degradation of 2,4-D in lakes. Attempts to quantify transformation products were unsuccessful in both laboratory and field studies, suggesting their persistence is not a major concern. The synthesis of laboratory and field experiments is used to demonstrate best practices in designing laboratory persistence studies and in using those results to mechanistically predict contaminant fate in complex aquatic environments.

2.3 Introduction

Understanding the environmental fate and transformation of polar organic compounds is critical for accurately assessing risk to ecosystems. Laboratory-based persistence studies are used to inform regulatory decisions for chemicals but are difficult to translate to the ecosystem scale, often resulting in wide variability in predicted persistence and environmental half-lives.¹⁻⁵ For example, photochemical degradation rates observed in laboratories may be orders of magnitude slower than rates observed in lakes or rivers due to differences in pathlength (i.e., water depth) and light intensity.⁶ Similarly, biodegradation rates observed in laboratories vary with inoculum source (i.e., sediment, water, or sludge) and target compound concentration,^{5,7,8} making extrapolation to the environment challenging. Furthermore, laboratory studies often fail to consider additional environmental conditions that control chemical fate, such as pH,⁹ microbial community composition,^{1,10,11} and season.^{6,12}

Assessing organic compound persistence and transformation pathways in the field presents other challenges. Many of these compounds are present at low concentrations with unknown input rates to lakes or rivers.^{4,13} Transformation processes, such as photo- and biodegradation, occur simultaneously alongside physical processes, making it impossible to isolate individual reactions.^{7,13,14} While quantification of known degradation products and genetic markers of biodegradation can provide insight to *in situ* transformations, information on specific pathways, transformation processes, and genetic data is needed for them to be successful.¹⁵⁻¹⁷

Aquatic herbicides offer a unique opportunity to quantitatively study transformation pathways of polar organic compounds under field conditions. Herbicides, such as 2,4-dichlorophenoxyacetic acid (2,4-D),¹⁸⁻²³ are directly applied to lakes to control nuisance plants, dosing the waterbody to homogenous concentrations for weeks to months.^{21,24-28} Despite its prevalent use in terrestrial environments,²⁹⁻³² little is known about 2,4-D fate in aquatic systems. Additionally, commercial formulations for terrestrial applications are often different than aquatic applications.³²⁻³⁵ Observed 2,4-D half-lives in Wisconsin lakes range from 4 - 76 days (**Table A.1**);^{20,22,23} this wide range cannot be explained solely by lake physicochemical differences and can result in unintended exposure to non-target organisms. Additionally, the extensive use of 2,4-D has led to increased herbicide resistance or tolerance within invasive aquatic plant populations,³⁶⁻³⁸ further underscoring the need for a mechanistic understanding of 2,4-D aquatic transformation processes.

Our current understanding of 2,4-D environmental fate is based on laboratory studies or field studies in soil environments. Potential degradation processes in lakes include photodegradation and biodegradation, while sorption, hydrolysis, and volatilization are negligible.³⁹⁻⁴¹ 2,4-D undergoes photodegradation under laboratory conditions to produce 2,4-

dichlorophenol as a major product (**Figure A.1**).^{39,42} Photodegradation in freshwater is variable, with predicted direct photodegradation half-lives of 13 to 32 days in simulated and natural sunlight experiments (**Table A.1**).^{39,43} While 2,4-D is susceptible to degradation via hydroxyl radical ($\cdot\text{OH}$),^{44,45} indirect 2,4-D photodegradation has not yet been quantified in lake water. Indirect photodegradation is a major loss mechanism for many polar organic contaminants⁴⁶⁻⁴⁹ and warrants further investigation.

2,4-D biodegradation mechanisms have been widely studied in soil.^{50,51} Biodegradation occurs in two phases: a slow degradation acclimation phase followed by a rapid degradation phase.^{52,53} Repeated exposure to 2,4-D in soil systems shortens the acclimation phase, suggesting repeated 2,4-D use promotes more rapid biodegradation, potentially by increasing the abundance of key degraders and transcription of the *tfdA* gene.⁵⁴⁻⁵⁷ 2,4-D transformation into 2,4-dichlorophenol (**Figure A.2**) is considered the rate limiting biodegradation step, followed by rapid biodegradation of 2,4-dichlorophenol to 3,5-dichlorocatechol.^{56,58,59} The key known enzyme required for aerobic 2,4-D metabolism is an alpha-ketoglutarate-dependent dioxygenase encoded by the *tfdA* gene, discovered in bacteria isolated using 2,4-D as a sole carbon source.^{60,61} Additionally, qPCR primers were developed to detect the *tfdA* gene.^{62,63} However, these primers have been used predominantly in soil and pure cultures, with limited application to aquatic environments.⁵⁷

Direct 2,4-D application to lakes represents an opportunity to study processes impacting herbicides under well-characterized field conditions. Furthermore, the lack of 2,4-D fate studies in aquatic systems is a critical knowledge gap for resource managers who oversee responsible herbicide use. Thus, the goal of our study was to quantify 2,4-D transformation pathways in lakes following direct herbicide application. Our study combines field quantification of 2,4-D with

laboratory bio- and photodegradation experiments to quantify specific transformation rates. We also test indicators of *in situ* transformation processes using molecular indicators of biodegradation and pathway-specific transformation products. This study provides a holistic framework for combining laboratory experiments, field measurements, and modeling to determine dominant transformation processes of polar organic compounds in aquatic environments.

2.4 Materials and Methods

2.4.1 Chemicals

Chemicals were used as received and are described in detail in **Section A2**. All commercial 2,4-D solutions used in lake treatments were the dimethylamine salt formulation (46.8%¹⁹ or 47.3%⁶⁴ 2,4-D), while laboratory experiments used pure 2,4-D. Ultrapure water (18.2 MΩ cm) was obtained from an ultrapure water purification system.

2.4.2 Field Sampling

Six large-scale 2,4-D treatments in Wisconsin, USA were studied from May to October 2019 (**Table 2.1; Figure A.3**). These treatments use 2,4-D concentrations that could affect aquatic plants lake wide (i.e., >0.45 μM).^{21,22} Lakes were selected in collaboration with the Wisconsin Department of Natural Resources (WDNR) to study how geographic/climatic factors and repeated 2,4-D applications impact transformation rates.

Table 2.1. Summary of sampled lakes including waterbody identification code (WBIC), herbicide application area, treatment date, target concentration, and treatment history. Trophic status is designated as eutrophic (E), mesotrophic (M), or oligotrophic (O). Target 2,4-D concentration is from treatment permit application. When not stated on permit application, target concentration was calculated from lake/bay volume and amount of herbicide applied as listed on treatment record. Treated bays are indicated by a ^ and listed as the treatment area size. Asterisk (*) indicates Secchi depth measurement hit lake bottom.

Lake (WBIC)	Herbicide application area (m ²)	Trophic Status	Treatment Date	Water temp (°C)	Secchi (m)	Target conc. (ppm)/(µM)	Treatment history
Random 30300	857,934	E	May 20, 2019	17	1.63	0.26/1.17	Several whole-lake treatments, including 2018
Eagle 2902900	655,591	O	June 10, 2019	21	6.38	0.37/1.67	Small-scale treatment (< 2020 m ²) in 2009, 2012, 2013
McCarry 2903400	129,499	M	June 10, 2019	24	2.25	0.35/1.58	None
Round 2395600	785,090^	O	June 25, 2019	19	5.38	0.36/1.62	Several small-scale treatments
Pleasant 741500	32,901^	M	Sept. 16, 2019	20	1.5 *	3.14/14.22	Several small-scale treatments
Okauchee 850300	38,445^	M	Sept. 23, 2019	22	1.75*	2.00/9.04	Several bay-wide and large-scale treatments, including 2018

Pretreatment surface water, sediment, and microbial biomass were collected from the epilimnion, hypolimnion, and nearshore area \leq 72 hours prior to treatment and stored at 4°C until processing (**Section A3**). Pretreatment samples were used for bulk water chemistry measurements (**Section A4**), photochemical irradiations (**Section A5**), and microcosm incubations (**Section A6**).

Water samples were collected immediately after 2,4-D applications (0-6 hours after treatment), 1, 3, 5, and 7 days after treatment, and weekly thereafter. At each sampling event, surface water was collected for 2,4-D quantification from several sites to quantify advective transport. Porewater samples were collected using passive sampling devices⁶⁵ in all lakes except Okauchee and simultaneously captured [2,4-D] at the sediment water interface and top 0-4 cm of sediment (**Section A3**). Biomass for *tfdA* abundance measurements was collected via surface water grab sampling for filtering from the epilimnion, hypolimnion, and nearshore sites, while sediment was collected by hand-coring at the nearshore site (**Section A3**). Discharge from McCarry and Round Lakes was measured using a flow meter (**Sections A3 and A8**).

2.4.3 Photochemical Irradiation Experiments

Photodegradation experiments were conducted in a Rayonet merry-go-round photoreactor equipped with sixteen bulbs that emit light at 311 nm (± 22 nm width at half-max) or 365 nm (± 10 nm; **Figure A.4**).⁶⁶ Both bulbs emit light in the solar spectrum.^{67,68} The 311 nm bulbs were used to quantify direct photodegradation while the 365 nm bulbs were used to isolate indirect photodegradation because 2,4-D absorbs light in the range of the 311 nm bulbs (**Figure A.4**). Irradiation experiments in borosilicate glass tubes were conducted in triplicate using buffered (pH 7, 10 mM phosphate buffer) solutions of 20 μM (4.4 ppm) 2,4-D in ultrapure water (direct photodegradation) or 3 mg-C L⁻¹ lake water (indirect photodegradation) alongside dark controls. This [2,4-D] is representative of maximum herbicide application rates (4.0 ppm).^{19,64,69} Additional experiments with 20 μM 2,4-dichlorophenol and 3,5-dichlorocatechol were conducted at 311 nm to quantify direct and indirect photodegradation rates of the expected transformation products. 2-

Nitrobenzaldehyde⁷⁰ and *para*-nitroanisole/pyridine⁷¹ actinometers were used at 311 and 365 nm, respectively (**Section A5**).

Direct quantum yields for 2,4-D, 2,4-dichlorophenol, and 3,5-dichlorocatechol were calculated relative to the actinometer as described previously.^{49,66,68} The calculated quantum yield for 2,4-D was combined with solar irradiance modeling using the Simple Model of Atmospheric Transfer of Sunshine⁶⁷ to calculate 2,4-D half-lives in sunlight (**Section A5**).

2.4.4 Microcosm Incubations

Water and sediment were collected from six study lakes in the field campaign and two untreated lakes to serve as no-treatment controls for microcosms biodegradation studies (**Table 2.2**). Containers were suspended in the dark in Lake Mendota water through a lake inlet in the Water Science and Engineering Laboratory, Madison, WI to keep microcosms controlled at lake temperature (13.5 to 21.1°C). Degradation by the water column microbial community was quantified in triplicate microcosms with unfiltered lake water (5 L) while degradation by the sediment microbial community was quantified in microcosms with filtered lake water (2 L) and sediment (1 kg). Abiotic loss processes were assessed in control microcosms with filtered lake water (2 L). Microcosms were incubated with 10 µM (2.2 ppm) 2,4-D, which is representative of the lower end of 2,4-D application rates (2-4 ppm).^{19,64,69} Samples were collected for up to 150 days, syringe filtered to remove particulates and microbes (0.45 µm), and analyzed for 2,4-D, 2,4-dichlorophenol, and 3,5-dichlorocatechol.

2.4.5 *tfdA* Analysis

Efforts to measure *tfdA* using qPCR and gene cloning are described in **Section A6**. Briefly, DNA was extracted using an MP Bio Fast DNA Spin Kit and amplified using ThermoFisher SYBR Green Master Mix on an iCycler thermocycler (Bio-Rad, Hercules, CA) and non-class specific *tfdA* primers intended to amplify a 215 bp fragment (**Table A.7**).^{62,63} Amplicons were cloned and sequenced using Sanger sequencing technology.

2.4.6 Analytical Methods

2,4-D, 2,4-dichlorophenol, 3,5-dichlorocatechol, 2-nitrobenzaldehyde, and *p*-nitroanisole were quantified by high-performance liquid chromatography using a diode-array detector. Samples with [2,4-D] below 0.1 μM were quantified by liquid chromatography-tandem mass spectrometry. Ultraviolet-visible light spectra for each lake were collected from 200-800 nm. Sediment carbon concentrations were measured using EPA method 160.4⁷² and a ThermoFisher Lindberg Blue muffle furnace. Bulk water chemistry was analyzed using ion chromatography, inductively coupled-plasma optical emission spectrometry, and total organic carbon analysis (**Tables A.3** and **A.4**). Methods details provided in **Section A7**.

2.4.7 Mass Balance Calculations

Mass balances for Round and McCarry Lakes were conducted using measured lake discharge (i.e., physical loss), photodegradation, and biodegradation rates in the following equation:

$$C_t = C_0 \times e^{-\left(\frac{Q_{avg}}{V} + k_{photodegradation} + k_{biodegradation}\right) t} \quad \text{eq. 1}$$

where C_t is [2,4-D] at time t , C_0 is initial [2,4-D], Q_{avg} is average discharge over treatment period, V is lake volume, $k_{\text{photodegradation}}$ is the modeled direct photodegradation rate, and $k_{\text{biodegradation}}$ is the biodegradation rate calculated using microcosm incubations. Our model assumes simple first-order biodegradation loss despite observations of variable lag times in a subset of the microcosms. While more mechanistic studies into biodegradation would require models that include these lag times (e.g., logistic,^{73,74} Gompertz,^{74–76} or second order⁷⁷ models), we use a first-order loss model based on the absence of observable lag times in the lake 2,4-D data. Details on mass balance derivation are provided in **Section A8**.

2.5 Results and Discussion

2.5.1 2,4-D Persistence During Lake Applications

2,4-D degradation was quantified in six lakes that underwent large-scale treatments (**Table 2.1**). [2,4-D] ranged from $< 0.1 \mu\text{M}$ to $19.9 \mu\text{M}$ over the course of all treatments (**Figure 2.1a**). Half-lives ranged 6 – 24 days (**Table 2.2**), which is within the range of previous large-scale 2,4-D treatments in Wisconsin (range of 4 – 76 days, median half-life of 16 days; **Table A.1**). Okauchee Lake had significant advective transport away from the treatment area (**Figure A.12**), never achieved an epilimnetic homogenous [2,4-D] (**Figure 2.1a**), and is excluded from in-lake degradation analysis.

Eagle, McCarry, and Round Lakes stratified prior to 2,4-D treatment in June 2019 and achieved epilimnion-wide mixing of 2,4-D three to seven days after treatment. Target concentrations for Eagle, McCarry, and Round Lakes were 1.67 , 1.58 , and $1.63 \mu\text{M}$, respectively. Herbicide transport into the hypolimnion was negligible (**Figures A.8-A.10**), suggesting all

herbicide degradation occurred in the epilimnion. 2,4-D half-lives were ~16 days in all three lakes (Table 2.2).

In contrast to the stratified lakes, Random Lake was thermally mixed prior to treatment and stratified two weeks after treatment. As a result, 2,4-D persisted in the suboxic hypolimnion (DO <3 mg L⁻¹; Figure A.14) longer than the epilimnion (Figure 2.1b). The target concentration for Random Lake was 1.18 µM. While the epilimnion sustained [2,4-D] of 0.99 ± 0.06 µM for 15 days, the hypolimnion maintained [2,4-D] of 0.87 ± 0.02 µM for 25 days. By the end of sampling (day 65), 2,4-D was not detected in the epilimnion (half-life = 24 days) but was 0.22 µM in the hypolimnion (half-life = 41 days). Differences between the epilimnion and hypolimnion are potentially due to a longer hypolimnion residence time, slower biodegradation 2,4-D under suboxic conditions, and/or negligible photodegradation.^{35,78}

Table 2.2. Summary of observed half-lives in large-scale 2,4-D applications, microcosm experiments, and photodegradation experiments. Field half-life is calculated from observed epilimnion wide averages. Microcosm half-life is calculated from observed concentrations in reactors. Photodegradation half-life is calculated by using modeled in-lake photodegradation rates. Bony and Pike Lakes are included as no-treatment controls and have never been treated with 2,4-D. Asterisk (*) for McCarry Lake indicates half-life after degradation started.

Lake	$t_{1/2}$ field (days)	$t_{1/2}$ microcosm (days)	$t_{1/2}$ photodegradation (days)	$t_{1/2}$ predicted from lab experiments + flow (days)
Random	24	25	184	25
McCarry	15	100; 37*	184	25
Eagle	16	37	184	36.5
Round	15	6	183	5.5
Pleasant	6	7	226	6
Bony	-	10	-	-
Pike	-	12	-	-

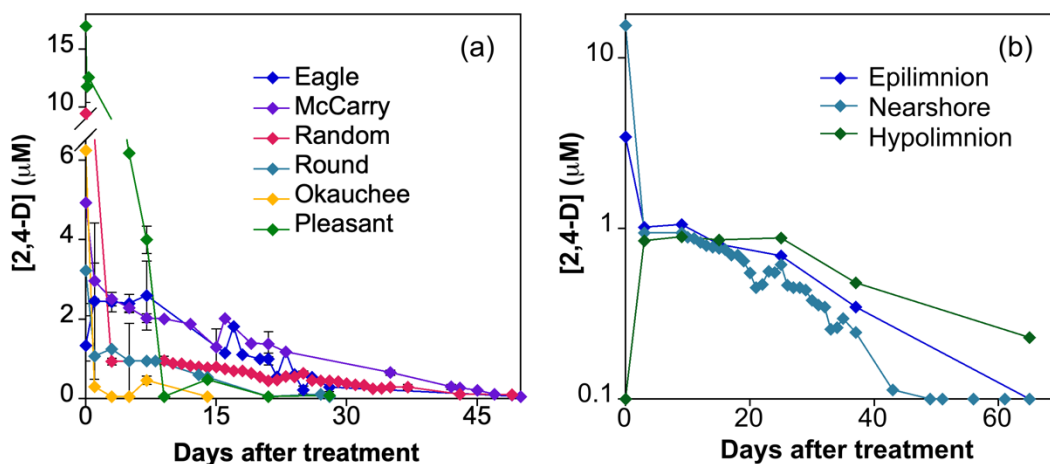


Figure 2.1. (a) Epilimnion-wide average 2,4-D concentrations during six large-scale treatments. Error bars represent the standard deviation of 2,4-D concentrations measured in epilimnion samples at each time point. Individual lake data with 2,4-D concentrations at all sampling sites can be found in **Figures A.8-A.13**. (b) 2,4-D concentrations in the epilimnion, nearshore, and hypolimnion of Random Lake.

Pleasant Lake had a large-scale treatment in a thermally mixed bay (maximum depth 2 m), with an average [2,4-D] of 12.55 ± 5.53 μM within 24 hours of application. Minimal transport of 2,4-D out of the bay was observed, with out-of-bay concentrations ranging 0.05 and 0.81 μM for 28 days (**Figure A.11**). 2,4-D half-life in Pleasant Lake was 6 days, the fastest of all treatments.

2,4-D was detected in sediment porewater in shallow, nearshore sites (**Figures A.8-A.11, A.13**), suggesting 2,4-D was completely mixed into the sediments. [2,4-D] in the top 0-4 cm of water overlying the sediment were comparable to that of the mixed epilimnion. Integrated 0-4 cm porewater concentrations were slightly lower, ranging 0.05 to 2 μM throughout all treatments. Round Lake did not have porewater 2,4-D accumulation (**Figure A.10**), likely due to the placement of peepers in a sandy, high traffic area. In the stratified lakes, significant portions of the sediment were exposed to the mixed epilimnion (**Figure A.15** and **Table A.12**); 56% of McCarry Lake had

water depths less than 1 m, while 69-96% of Eagle, Random, and treated areas of Round Lakes had water depths less than 6 m. Each stratified lake had a mean depth less than the stratified depth, suggesting a high rate of epilimnion interaction with sediments.

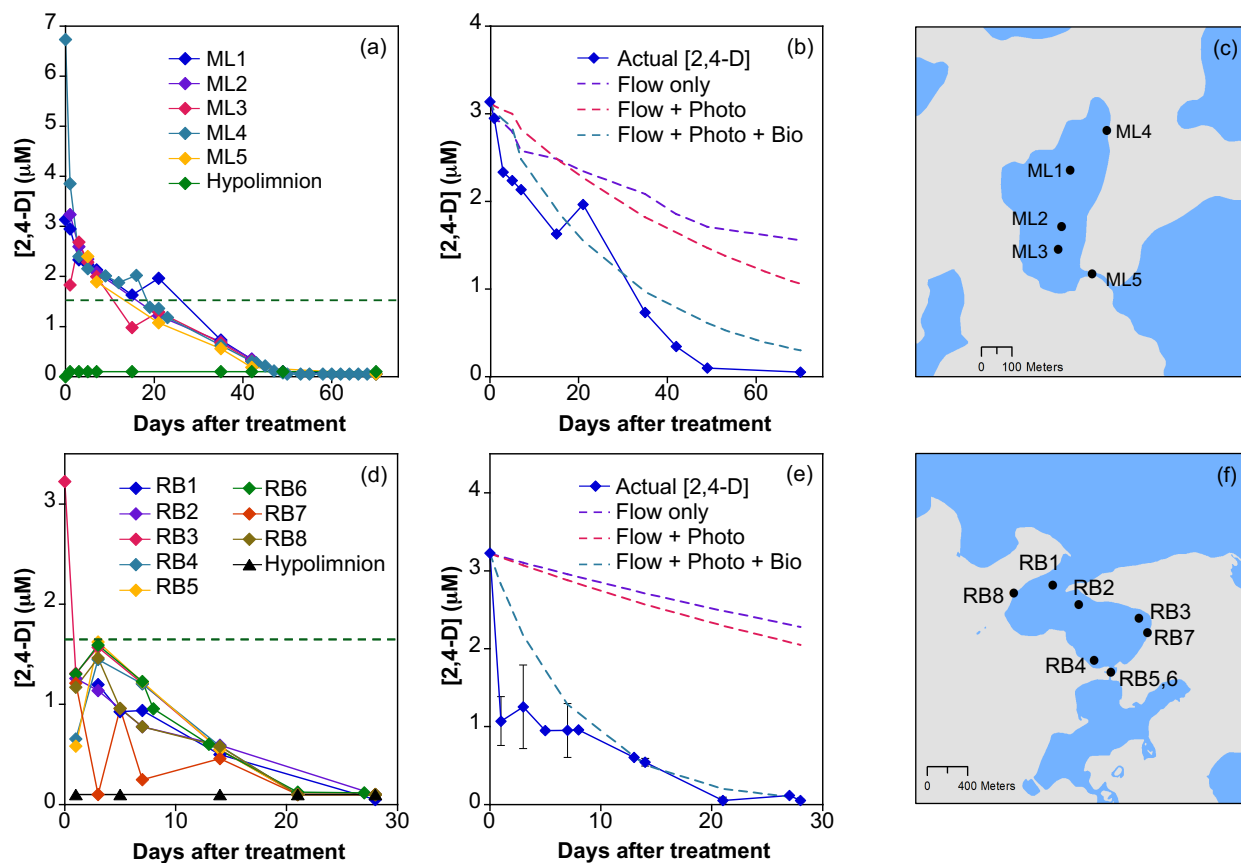


Figure 2.2. (a, d) Measured 2,4-D concentrations, (b, e) modeling results compared with average epilimnion concentrations, and (c, f) sample site locations for McCarry and Round Lakes, respectively. Maps created using ArcGIS software (10.6.1) by Esri. Data provided by the National Atlas of the United States, USGS. Error bars in panels (b) and (e) represent the standard deviation of 2,4-D concentrations measured in epilimnion samples at each time point.

Investigation into specific transformation and physical loss processes is needed to identify the dominant loss pathway of 2,4-D in lakes. 2,4-D is potentially susceptible to both photodegradation and biodegradation, as well as physical flow out of lakes. Previous studies report laboratory direct photodegradation half-lives of 13-32 days while biodegradation studies report

half-lives of 7-38 days (**Table A.1**), suggesting photodegradation and biodegradation contribute similarly to 2,4-D degradation under laboratory conditions.

During our field study, we measured discharge from two lakes to quantify non-destructive 2,4-D loss. Using lake 2,4-D concentrations and flow rates, physical discharge accounted for 22.5% and 29.2% of 2,4-D lost in McCarry and Round Lakes, respectively (i.e., half-lives of 59 and 56 days; **Figures 2.2b** and **2.2e**). Given the difference in size (0.13 vs. 0.79 km²) and flow (1.05 x 10⁶ vs. 2.24 x 10⁷ L d⁻¹; **Tables A.9** and **A.10**), we expect these values to be representative of the range of discharge possible in the other studied lakes and therefore conclude that discharge is not the dominant loss mechanism of 2,4-D.

Attempts to quantify expected 2,4-D transformation products as *in situ* indicators of transformation pathways were unsuccessful. 2,4-Dichlorophenol is expected to form as both a photodegradation product³⁹ and biodegradation product,⁶¹ but rapid 2,4-dichlorophenol transformation into 3,5-dichlorocatechol by the *tfdB* gene product implies 3,5-dichlorocatechol may be a better indicator of biodegradation (**Figure A.1-A.2**).⁷⁸ While additional biodegradation products have been identified,⁷⁸⁻⁸⁰ we chose 2,4-dichlorophenol and 3,5-dichlorocatechol as our products of interest because they are formed in the *tfdA* pathway and could pair qPCR analysis with product formation. However, neither 2,4-dichlorophenol nor 3,5-dichlorocatechol (**Figure A.2**) were detected (HPLC limits of detection = 0.3 μM and 0.8 μM, respectively; **Table A.8**) in surface water or porewater samples. While this result does not identify specific transformation pathways, it suggests neither product accumulates in surface waters following large-scale 2,4-D treatments, a novel result unreported in previous 2,4-D studies.^{20,23,27} Because we could not detect transformation products in the field, we used laboratory experiments to isolate and quantify photo- and biodegradation rates.

2.5.2 Photochemical Degradation

2,4-D undergoes direct photodegradation under 311 nm irradiation with an observed first-order loss rate constant of $(9.74 \pm 0.02) \times 10^{-5} \text{ s}^{-1}$ (**Figure 2.3a**), which corresponds to a quantum yield (Φ) of $(3.12 \pm 0.01) \times 10^{-3}$. This Φ is between reported values of 9.5×10^{-3} measured at 254 nm (pH 7)⁴⁴ and 6.7×10^{-4} determined using simulated sunlight ($> 290 \text{ nm}$; pH 7).³¹ Differences between these quantum yields are likely due to differences in irradiance wavelengths and their overlap with the 2,4-D absorbance spectrum (**Figure A.4**).

We investigated indirect photodegradation of 2,4-D using water collected from four study lakes. The observed photodegradation rate constants were identical to direct photodegradation rate constants under both 311 and 365 nm irradiation with values of $(9.8 \pm 0.2) \times 10^{-5} \text{ s}^{-1}$ ($t_{1/2} = 2 \text{ hours}$) and $(3.0 \pm 1.2) \times 10^{-7} \text{ s}^{-1}$ ($t_{1/2} = 27 \text{ days}$), respectively, after correcting for light screening (**Figure 2.3a**). Thus, 2,4-D is not susceptible to dissolved organic matter (DOM)-mediated indirect photodegradation under these conditions.

The inability of 2,4-D to undergo indirect photodegradation conflicts with previous literature. Several studies have found direct photodegradation to be significantly slower than degradation via hydroxyl radical generated by the photolysis of hydrogen peroxide or nitrate under simulated sunlight $> 290 \text{ nm}$ (**Table A.1**),^{44,45,81} suggesting that indirect photodegradation is the dominant transformation mechanism. However, these studies did not use $[\cdot\text{OH}]$ expected in freshwater environments. While we did not quantify $\cdot\text{OH}$ production, previous measurements using the same light source and similar natural waters detected $[\cdot\text{OH}]_{\text{ss}}$ of 10^{-16} to 10^{-18} M under near surface conditions.^{47,49,82} When combined with the reported bimolecular rate constant of $3.24 \times 10^9 \text{ M}^{-1} \text{ s}^{-1}$ for 2,4-D and $\cdot\text{OH}$ ⁸¹ estimate a maximum pseudo-first order loss rate constant of $3.24 \times 10^{-7} \text{ s}^{-1}$ under our experimental conditions ($t_{1/2} = 25 \text{ days}$) in the top 1 cm of the water column;

this half-life will increase with depth due to light screening and become negligible when integrated over the epilimnion. Thus, $[\cdot\text{OH}]_{\text{ss}}$ in natural water systems is likely too low for this pathway to dominate. Lastly, the absence of an observed enhancement of 2,4-D photodegradation in the presence of DOM similarly rules out other photochemically produced reactive intermediates, such as singlet oxygen or triplet state DOM. Thus, we conclude direct photodegradation is the dominant photodegradation transformation pathway in natural waters with typical $[\cdot\text{OH}]_{\text{ss}}$ (e.g., in the absence of elevated nitrite or nitrate).

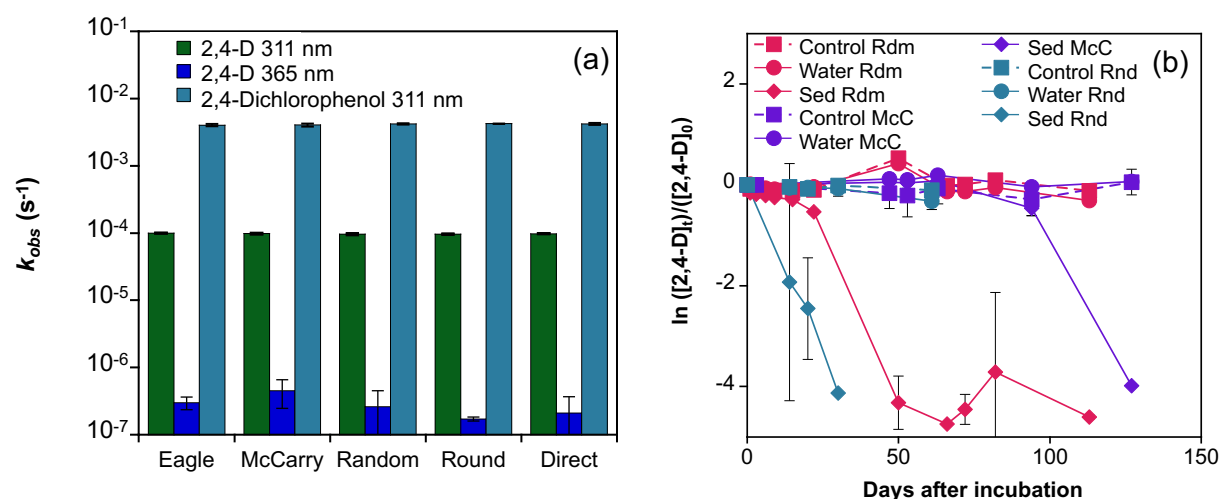


Figure 2.3. (a) Observed 2,4-D laboratory photodegradation rate constants, corrected for light screening, in lake water and corresponding direct photodegradation controls. (b) Observed degradation of 2,4-D in microcosm incubations using sediment and water (Sed) in comparison with abiotic controls (Control) and lake water only (Water) for McCarry (McC), Round (Rnd), and Random (Rdm) Lakes. Error bars represent the standard deviation of triplicate samples. Individual lake microcosm data is presented in **Figure A.6**.

The photodegradation product 2,4-dichlorophenol was not detected. 2,4-Dichlorophenol absorbs light at the same wavelengths as 2,4-D (**Figure A.4**), suggesting it could be susceptible to photodegradation. To test this hypothesis, we irradiated 2,4-dichlorophenol at 311 nm and observed a photodegradation rate constant of $(4.17 \pm 0.16) \times 10^{-3} \text{ s}^{-1}$ ($\Phi = (7.9 \pm 0.3) \times 10^{-2}$). The

observed loss rate constant of 2,4-dichlorophenol is two orders of magnitude faster than that of 2,4-D (**Figure 2.3a**), demonstrating that this 2,4-D photoproduct is unlikely to accumulate. This finding agrees with previous observations of rapid photodegradation of 2,4-dichlorophenol in ultrapure water under 254 nm light and natural sunlight.^{42,56} The measured quantum yield is lower than the previously reported value of 0.26 (>300 nm, pH 8),⁸³ likely due to differences in pH because 2,4-dichlorophenol quantum yield increases with increasing pH.⁸³

2.5.3 Photochemical Modeling

In-lake photodegradation half-lives were calculated using modeled light intensity at noon on the day of treatment for each lake (**Section A5**) and measured quantum yields (**Table A.5**) assuming direct photodegradation is the primary photodegradation pathway. Estimated 2,4-D photodegradation half-lives in the top 1 cm of water ranged 183 to 226 days (**Table 2.2; Figures 2.2b and 2.2d**). These slow photodegradation rates overestimate the rates expected in freshwater lakes because light intensity is not constant over a 24-hour period and varies seasonally. Importantly, rates will decrease exponentially with depth due to light attenuation over the 3 to 6 m epilimnion.^{6,84} These overestimated photodegradation rates show photodegradation accounts for < 1% of the observed 2,4-D loss in the six lakes. Half-lives observed in large-scale treatments (6-24 days; **Table 2.2**) were up to 16 times faster than those calculated in photodegradation modeling (183-226 days, **Table 2.2, Figure 2.2b and 2.2c**). Thus, we conclude photodegradation of 2,4-D is negligible in lakes.

In contrast to our results, previous studies predict faster 2,4-D photodegradation with half-lives of 2-4 weeks, suggesting 2,4-D is a moderately photolabile compound. For example, U.S. EPA registration documents predict aquatic half-life of 12.9 calendar days based on laboratory

experiments in pH 5 buffered water.⁴³ Similar direct photodegradation half-lives of 19 and 32 days have been reported using constant simulated sunlight³¹ and natural sunlight,⁸¹ respectively. Our results demonstrate laboratory-measured rates overpredict the rates of 2,4-D photodegradation expected in lakes after correcting for light intensity, even when factors like pathlength or diurnal variability in sunlight are not considered. Thus, while previous laboratory experiments demonstrate rapid 2,4-D photodegradation under certain conditions, the extrapolation from laboratory to field transformation rates can lead to inaccurate assessments of photolability when environmental conditions are not carefully considered.

2.5.4 Microbial Degradation of 2,4-D in Aquatic Systems

2,4-D degradation was only observed in laboratory microcosms incubated with sediment (**Table 2.2**; **Figures 2.3b** and **A.6**). No loss was observed in the filtered controls or unfiltered lake water incubations over 28-140 days (**Figures 2.3b** and **A.6**). Because 2,4-D has a high solubility (0.1 M)^{35,56,85} and low carbon-water partitioning coefficient (K_{oc}) of 61.7 to 78 mL g⁻¹ (**Table A.11**),^{43,86} we concluded that loss in the microcosms was due to biodegradation by microbes in the sediment. This observation is consistent with previous reports of 2,4-D⁵⁶ and other polar organic compound⁵ degradation in water/sediment systems. The lack of degradation in the water-only microcosms is likely attributable to insufficient biomass compared to sediment-water suspensions.^{2,4,87-89}

2,4-D half-lives ranged 5 to 100 days in the microcosms (average of 25 days; **Table 2.2**), which was a similar order of magnitude as field observations. The McCarry Lake microcosm had the longest and most pronounced acclimation phase (i.e., 100 days; **Table 2.2**; **Figure 2.3b**) despite

having an average 2,4-D half-life in the lake (i.e., 15 days; **Table 2.2**). Once degradation started, 2,4-D half-life was 37 days, which is comparable to other microcosms.

Repeated 2,4-D exposure in previous studies increased degradation rates in soil microcosms and cultures (**Table A.1**), suggesting repeated 2,4-D applications could decrease half-lives in subsequent herbicide applications.^{54–57,90} Thus, we hypothesized degradation would be fastest in Random (frequent large-scale) and Pleasant Lakes (frequent small-scale) because of their treatment histories (**Table 2.1**). However, there were no clear difference in half-lives in microcosms using inoculum from previously treated lakes (6-25 days) compared to microcosms created from untreated lakes (10-37 days; **Table 2.2**; **Figure 2.3b**). This suggests that previous annual treatments are not sufficient to drive a lasting 2,4-D degrader enrichment in lake microbial communities.

Attempts to quantify *tfdA* gene copies as an indicator of microbial degradation were unsuccessful in laboratory and field experiments. qPCR amplification produced non-specific gene products and smearing on the agarose gel in both water and sediment samples, despite efforts to optimize the reaction (**Section A6**). Cloning and sequencing of PCR amplicons generated 23 sequences of approximately 180 bp each, which is shorter than the expected product of 215 bp. Analysis with BLASTN confirmed the sequences were fragments of the cloning vector rather than *tfdA* gene product (**Section A6**). Previous work has demonstrated challenges in applying primers derived from cultured representatives to environmental samples,^{91–94} and our work shows the previously published *tfdA* qPCR primers failed to accurately detect aquatic environmental representatives. While an alternative degradation pathway has recently been described using the *cad* genes,⁹⁵ this pathway is less studied and has only been found in cultured representatives. More

appropriate primers for this gene are needed to capture the abundance of 2,4-D degrading bacteria in freshwater systems.

The biodegradation products 3,5-dichlorocatechol and 2,4-dichlorophenol (**Figure A.2**) were not detected in laboratory or field studies. We hypothesize that once the rate limiting step of converting 2,4-D into 2,4-dichlorophenol was completed, degradation products were quickly used for metabolic operations.⁷⁸ Therefore, intermediate metabolites such as 3,5-dichlorocatechol were likely too transient to quantify.

While 2,4-D half-lives in the microcosms were similar to field half-life measurements (**Table 2.2**), they were not directly correlated. 2,4-D half-lives in Random and Pleasant Lake microcosms were nearly identical to field measurements. However, 2,4-D half-lives in microcosms were twice as long as the field measurements for Eagle and McCarry Lake (i.e., 15 – 16 days in lake versus 37 days in microcosms). Conversely, 2,4-D half-life in Round Lake was twice as fast in the microcosms (6 days) as the lake (15 days). Additionally, some trends in the microcosms, such as the long lag period in McCarry Lake (**Figure 2.3b**), were not replicated in the field study, demonstrating the limitations of solely relying on laboratory-based measurements to predict environmental fate.

Lake biodegradation rates were estimated from microcosm measurements as a first approximation in the mass balance. In McCarry Lake, biodegradation corresponds to 70% of 2,4-D loss by day 70, for a total loss of 93% with physical flow (22.5%) and photodegradation (<1%; **Table 2.2**). This is likely an underestimate of biodegradation due to the extended acclimation period and long degradation half-life observed in the microcosms. Similarly, incorporating the biodegradation rate for Round Lake predicts 96% of 2,4-D loss (**Figure 2.2d**), including physical flow (29%) and photodegradation (<1%). The biodegradation estimate in Round Lake is likely an

overestimate, stemming from a rapid observed biodegradation half-life of 6 days. While directly translating the microcosm rates from the laboratory experiments into the model over-simplifies the effects of other environmental factors, the addition of the biodegradation rate closely models actual 2,4-D loss compared to flow or photodegradation. Thus, we propose microbial degradation is the dominant degradation pathway of 2,4-D in lakes. Biodegradation is expected to be most rapid in the sediment based on our results given the high percentage of epilimnion lake area in contact with sediment (**Figure A.15**).

While the half-lives in the field and microcosm studies were not directly correlated, both data sets demonstrate no effect of treatment history on degradation rate (**Table 2.2**; **Figure A.6**). This observation has two potential implications. First, these low frequency (annually or less), low concentration chemical treatments may not significantly change microbial community composition in contrast with higher frequency or concentration pesticide applications.⁹⁶ Alternatively, other factors influencing lake microbial community structure might overpower a small perturbation, highlighting the importance of a resilient ecosystem.⁹⁷ This finding further demonstrates how laboratory studies can inaccurately predict environmental fate by failing to replicate environmental conditions, in this case not considering realistic application patterns for aquatic systems.

Our model includes parameters for microbial degradation, photodegradation, and flow, but does not include plant uptake or sediment sorption. Plant uptake is required for a lethal response, but 2,4-D is not degraded in the process⁹⁸ and does not accumulate in plants.^{99,100} Based on measured sediment carbon concentrations and the reported K_{oc} ,^{29,43} sediment sorption is negligible in all studied lakes (**Table A.11**). Porewater [2,4-D] was comparable to overlying water

concentrations (**Figures A.8-11, A.13**), suggesting 2,4-D was dissolved and available for biodegradation.

2.6 Environmental Implications

We used laboratory experiments to isolate and quantify specific transformation mechanisms and model loss following large-scale 2,4-D applications to lakes. While this study is specific to 2,4-D, these results can be used to design field transformation studies based on laboratory studies and vice versa. Our synthesis of laboratory and field experiments underscores the importance of both approaches for mechanistically understanding contaminant fate in complex aquatic environments. While our study investigated the active ingredient of 2,4-D (>46% 2,4-D in commercial solutions used in this study), the commercial formulation can potentially impact how a compound moves through the environment and should be considered when designing fate and transport studies with other compounds.

Our results reveal major limitations in the standard approach of using laboratory measurements to predict the environmental fate of organic compounds. Laboratory-based photodegradation studies and modeling demonstrated 2,4-D photodegradation rates are too slow to be relevant, in contrast with previous studies, including U.S. EPA registration documents,^{42,43,56,101} that note the photolability of 2,4-D. Similarly, laboratory-based microcosm experiments incubated at lake temperatures with relevant inoculum demonstrated 2,4-D biodegradation is associated with sediment-derived microbial communities but did not capture physical processes that affected 2,4-D fate, specifically the role of advective transport and lake stratification. Collectively, the observed discrepancies clearly demonstrate that laboratory measurements cannot be directly applied to predict field transformation rates.

Using laboratory measurements to elucidate dominant transformation mechanisms is also prone to error. Previous studies indicated bio- and photodegradation of 2,4-D have similar half-lives,^{31,43,56,81,102,103} yet our holistic approach clearly showed that biodegradation was dominant in lakes. We attempted to quantify transformation products and specific genes to further distinguish between these processes in the field. However, the absence of quantifiable transformation products, even when high initial parent compound concentrations were used, suggests that similar attempts to elucidate mechanisms of similar organic compounds under field conditions will be challenging. Additionally, previously described primers for the *tfdA* gene failed to detect the presence of known degraders, demonstrating the importance of validating primers constructed from cultured representatives.

Laboratory experiments can never fully represent field conditions and therefore it is ideal to validate conclusions using field measurements. While this labor-intensive approach is limited to unique situations (e.g., when compounds are intentionally added to aquatic systems),^{6,22,23,68} these cases can be used to demonstrate best practices, such as those outlined here, in extrapolating laboratory measurements to field conditions. These data can also be used to highlight factors that warrant careful consideration in designing laboratory experiments, which we anticipate will continue to be the standard approach in predicting contaminant fate. Laboratory photodegradation rate measurements must be combined with modeled sunlight and site-specific conditions (e.g., water depth, variability in light) to evaluate this process under environmental conditions. Similarly, biodegradation experiments should be conducted with representative inocula at relevant temperatures and using molecular tools validated with environmental samples. While we often justify experimental conditions as being “environmentally relevant”, this phrase can have a range

of meanings and site-specific factors that must be considered to make future studies relevant to environmental conditions.

2.7 Acknowledgements

We thank Scott Van Egeren, Pamela Toshner, Heidi Bunk, Craig Helker, Arthur Watkinson, and Amanda Schmitz at Wisconsin Department of Natural Resources (WDNR) for assistance selecting and sampling field sites. Marissa Kneer, Sydney Van Frost, and Ellie Kimlinger provided field and laboratory support. Sampling supported by Onterra, LLC, homeowners of Pike Lake Chain of Lakes Association, Random Lake Association, and Round Lake Property Owners Association. We thank Naila Barbosa de Costa for optimizing the qPCR method and Jonathan Remucal for GIS assistance. Funding provided by WDNR, National Science Foundation Graduate Research Fellowship (A.M.W.), and an Anna Grant Birge Memorial Award. Any use of trade or product names is for descriptive purposes and does not imply endorsement by the U.S. Government or State of Wisconsin.

2.8 References

- (1) Seller, C.; Honti, M.; Singer, H.; Fenner, K. Biotransformation of chemicals in water-sediment suspensions: Influencing factors and implications for persistence assessment. *Environ. Sci. Technol. Lett.* **2020**, *7* (11), 854–860. <https://doi.org/10.1021/acs.estlett.0c00725>.
- (2) Honti, M.; Fenner, K. Deriving persistence indicators from regulatory water-sediment studies - Opportunities and limitations in OECD 308 data. *Environ. Sci. Technol.* **2015**, *49* (10), 5879–5886. <https://doi.org/10.1021/acs.est.5b00788>.
- (3) Unice, K.; Bare, J.; Kreider, M.; Panko, J. Experimental methodology for assessing the environmental fate of organic chemicals in polymer matrices using column leaching studies and OECD 308 water/sediment systems: Application to tire and road wear particles. *Sci. Total Environ.* **2015**, *533*, 476–487. <https://doi.org/10.1016/j.scitotenv.2015.06.053>.
- (4) Li, Z.; McLachlan, M. Comparing non-targeted chemical persistence assessed using an unspiked OECD 309 test to field measurements. *Environ. Sci. Processes Impacts* **2020**, *22* (5), 1233–1242. <https://doi.org/10.1039/c9em00595a>.

- (5) Zhi, H.; Miannecki, A. L.; Kolpin, D. W.; Klaper, R. D.; Iwanowicz, L. R.; LeFevre, G. H. Tandem field and laboratory approaches to quantify attenuation mechanisms of pharmaceutical and pharmaceutical transformation products in a wastewater effluent-dominated stream. *Water Res.* **2021**, *203*. <https://doi.org/10.1016/j.watres.2021.117537>.
- (6) McConville, M. B.; Cohen, N. M.; Nowicki, S. M.; Lantz, S. R.; Hixson, J. L.; Ward, A. S.; Remucal, C. K. A field analysis of lampricide photodegradation in Great Lakes tributaries. *Environ. Sci. Processes Impacts.* **2017**, *19* (7), 891–900. <https://doi.org/10.1039/c7em00173h>.
- (7) Whale, G.; Parsons, J.; van Ginkel, K.; Davenport, R.; Vaiopoulou, E.; Fenner, K.; Schaeffer, A. Improving our understanding of the environmental persistence of chemicals. *Integ. Environ. Assess. Mgmt.* **2021**, *17* (6), 1123–1135. <https://doi.org/10.1002/ieam.4438>.
- (8) Davenport, R.; Curtis-Jackson, P.; Dalkmann, P.; Davies, J.; Fenner, K.; Hand, L.; McDonough, K.; Ott, A.; Ortega-Calvo, J. J.; Parsons, J. R.; Schäffer, A.; Sweetlove, C.; Trapp, S.; Wang, N.; Redman, A. Scientific concepts and methods for moving persistence assessments into the 21st century. *Integ. Environ. Assess. Mgmt.* **2022**, *0* (0), 1–34. <https://doi.org/10.1002/ieam.4575>.
- (9) Buerge, I. J.; Bächli, A.; Kasteel, R.; Portmann, R.; López-Cabeza, R.; Schwab, L. F.; Poiger, T. Behavior of the chiral herbicide imazamox in soils: pH-dependent, enantioselective degradation, formation, and degradation of several chiral metabolites. *Environ. Sci. Technol.* **2019**, *53* (10), 5725–5732. <https://doi.org/10.1021/acs.est.8b07209>.
- (10) Ahtiainen, J.; Aalto, M.; Pessala, P. Biodegradation of chemicals in a standardized test and in environmental conditions. *Chemosphere.* **2003**, *51* (6), 529–537. [https://doi.org/10.1016/S0045-6535\(02\)00861-5](https://doi.org/10.1016/S0045-6535(02)00861-5).
- (11) Groffman, P. M.; Voos, G. Relationships between microbial biomass and dissipation of 2,4-D and dicamba in soil. *Bio. Fert. Soils.* **1997**, *24* (1), 106–110. <https://doi.org/10.1007/s003740050216>.
- (12) Watson, J. R. Seasonal variation in the biodegradation of 2,4-D in river water. *Water Res.* **1977**, *11*, 153–157. [https://doi.org/10.1016/0043-1354\(77\)90120-8](https://doi.org/10.1016/0043-1354(77)90120-8).
- (13) Fenner, K.; Elsner, M.; Lueders, T.; McLachlan, M. S.; Wackett, L. P.; Zimmermann, M.; Drewes, J. E. Methodological advances to study contaminant biotransformation: New prospects for understanding and reducing environmental persistence? *ACS ES&T Water.* **2021**, *1* (7), 1541–1554. <https://doi.org/10.1021/acsestwater.1c00025>.
- (14) Fenner, K.; Canonica, S.; Wackett, L. P.; Elsner, M. Evaluating pesticide degradation in the environment: Blind spots and emerging opportunities. *Science.* **2013**, *341*, 752–758.
- (15) Chavez Rodriguez, L.; Ingalls, B.; Schwarz, E.; Streck, T.; Uksa, M.; Pagel, H. Gene-centric model approaches for accurate prediction of pesticide biodegradation in soils. *Environ. Sci. Technol.* **2020**, *54* (21), 13638–13650. <https://doi.org/10.1021/acs.est.0c03315>.
- (16) Buerge, I. J.; Kasteel, R.; Bächli, A.; Poiger, T. Behavior of the chiral herbicide imazamox in soils: Enantiomer composition differentiates between biodegradation and photodegradation. *Environ. Sci. Technol.* **2019**, *53* (10), 5733–5740. <https://doi.org/10.1021/acs.est.8b07210>.
- (17) Ahtiainen, J.; Aalto, M.; Pessala, P. Biodegradation of chemicals in a standardized test and in environmental conditions. *Chemosphere.* **2003**, *51* (6), 529–537. [https://doi.org/10.1016/S0045-6535\(02\)00861-5](https://doi.org/10.1016/S0045-6535(02)00861-5).
- (18) Blanke, C.; Mikulyuk, A.; Nault, M.; Provost, S.; Schaal, C.; Egeren, S. van; Williams, M.; Mednick, A. Strategic Analysis of Aquatic Plant Management in Wisconsin

- https://dnr.wi.gov/topic/EIA/documents/APMSA/APMSA_Final_2019-06-14.pdf
(accessed 2020-05-15).
- (19) NuFarm. Weedar 64 chemical label <http://www.cdms.net/ldat/ld08K005.pdf> (accessed 2021-10-24).
 - (20) Frater, P.; Mikulyuk, A.; Barton, M.; Nault, M.; Wagner, K.; Hauxwell, J.; Kujawa, E. Relationships between water chemistry and herbicide efficacy of Eurasian watermilfoil management in Wisconsin lakes. *Lake Resvr. Mgmt.* **2017**, *33* (1), 1–7. <https://doi.org/10.1080/10402381.2016.1235634>.
 - (21) Glomski, L. M.; Netherland, M. D. Response of Eurasian and hybrid watermilfoil to low use rates and extended exposures of 2,4-D and triclopyr. *J. Aquat. Plant. Mgmt.* **2010**, *48*, 12–14.
 - (22) Nault, M. E.; Barton, M.; Hauxwell, J.; Heath, E.; Hoyman, T.; Mikulyuk, A.; Netherland, M. D.; Provost, S.; Skogerboe, J.; van Egeren, S. Evaluation of large-scale low-concentration 2,4-D treatments for Eurasian and hybrid watermilfoil control across multiple Wisconsin lakes. *Lake and Resvr. Mgmt.* **2018**, *34* (2), 115–129. <https://doi.org/10.1080/10402381.2017.1390019>.
 - (23) Nault, M. E.; Netherland, M. D.; Mikulyuk, A.; Skogerboe, J. G.; Asplund, T.; Hauxwell, J.; Toshner, P. Efficacy, selectivity, and herbicide concentrations following a whole-lake 2,4-D application targeting Eurasian watermilfoil in two adjacent northern Wisconsin lakes. *Lake and Resvr. Mgmt.* **2014**, *30* (1), 1–10. <https://doi.org/10.1080/10402381.2013.862586>.
 - (24) Reinert, K. H.; Rodgers, J. H. Fate and persistence of aquatic herbicides. *Rev. of Environ. Cont. and Tox.* **1987**, 61–89. https://doi.org/10.1007/978-1-4612-4700-5_3.
 - (25) Busi, R.; Goggin, D. E.; Heap, I. M.; Horak, M. J.; Jugulam, M.; Masters, R. A.; Napier, R. M.; Riar, D. S.; Satchivi, N. M.; Torra, J.; Westra, P.; Wright, T. R. Weed resistance to synthetic auxin herbicides. *Pest Mgmt. Sci.* **2018**, *74* (10), 2265–2276. <https://doi.org/10.1002/ps.4823>.
 - (26) Arnold, W. R. Fluridone: A new aquatic herbicide. *J. Aquat. Plant. Mgmt.* **1979**, *17*, 30–33.
 - (27) Kujawa, E. R.; van Egeren, S.; Mikulyuk, A.; Nault, M. E.; Barton, M.; Hauxwell, J.; Frater, P. Lessons from a decade of lake management: effects of herbicides on Eurasian watermilfoil and native plant communities. *Ecosphere* **2017**, *8* (4), 1–11. <https://doi.org/10.1002/ecs2.1718>.
 - (28) Valley, R. D.; Crowell, W.; Welling, C. H.; Proulx, N. Effects of a low-dose fluridone treatment on submersed aquatic vegetation in a eutrophic Minnesota lake dominated by Eurasian watermilfoil and coontail. *J. Aquat. Plant. Mgmt.* **2006**, *44*, 19–25.
 - (29) Gaultier, J.; Farenhorst, A.; Crow, G. Spatial variability of soil properties and 2,4-D sorption in a hummocky field as affected by landscape position and soil depth. *Cand. J. Soil Sci.* **2006**, No. 86, 89–95. <https://doi.org/10.4141/S04-074>.
 - (30) Góngora-Echeverría, V. R.; Martin-Laurent, F.; Quintal-Franco, C.; Lorenzo-Flores, A.; Giacomán-Vallejos, G.; Ponce-Caballero, C. Dissipation and adsorption of 2,4-D, atrazine, diazinon, and glyphosate in an agricultural soil from Yucatan state, Mexico. *Water Air Soil Poll.* **2019**, *230* (6). <https://doi.org/10.1007/s11270-019-4177-y>.
 - (31) Su, L.; Sivey, J. D.; Dai, N. Sunlight photolysis of 2,4-D herbicides in systems simulating leaf surfaces. *Environ. Sci. Processes Impacts.* **2018**, *20* (8), 1123–1135. <https://doi.org/10.1039/c8em00186c>.

- (32) Peterson, M. A.; McMaster, S. A.; Riechers, D. E.; Skelton, J.; Stahlman, P. W. 2,4-D past, present, and future: A review. *Weed Tech.* **2016**, *30* (2), 303–345. <https://doi.org/10.1614/wt-d-15-00131.1>.
- (33) Tominack, R. L. Herbicide formulations. *Clinical Toxicology* **2000**, *38* (2), 129–135.
- (34) Polli, E. G.; Alves, G. S.; de Oliveira, J. V.; Kruger, G. R. Physical–chemical properties, droplet size, and efficacy of dicamba plus glyphosate tank mixture influenced by adjuvants. *Agronomy* **2021**, *11* (7). <https://doi.org/10.3390/agronomy11071321>.
- (35) Walters, J. Environmental fate of 2,4-dichlorophenoxyacetic acid <http://citeseerx.ist.psu.edu/viewdoc/download?doi=10.1.1.639.4289&rep=rep1&type=pdf> (accessed 2020-05-15).
- (36) Moody, M. L.; Les, D. H. Evidence of hybridity in invasive watermilfoil (*Myriophyllum*) populations. *PNAS*. **2002**, *99* (23), 14867–14871. <https://doi.org/10.1073/pnas.172391499>.
- (37) Parks, S. R.; McNair, J. N.; Hausler, P.; Tynning, P.; Thum, R. A. Divergent responses of cryptic invasive watermilfoil to treatment with auxinic herbicides in a large Michigan lake. *Lake and Resvr. Mange.* **2016**, *32* (4), 366–372. <https://doi.org/10.1080/10402381.2016.1212955>.
- (38) Larue, E. A.; Zuellig, M. P.; Netherland, M. D.; Heilman, M. A.; Thum, R. A. Hybrid watermilfoil lineages are more invasive and less sensitive to a commonly used herbicide than their exotic parent (Eurasian watermilfoil). *Evol. Applic.* **2013**, *6* (3), 462–471. <https://doi.org/10.1111/eva.12027>.
- (39) Zepp, R. G.; Wolfe, N. L.; Gordon, J. A.; Baughman, G. L. Dynamics of 2,4-D esters in surface waters: Hydrolysis, photolysis, and vaporization. *Environ. Sci. Technol.* **1975**, *9* (13), 1144–1150. <https://doi.org/10.1021/es60111a001>.
- (40) Bekbölet, M.; Yenigün, O.; Yücel, I. Sorption studies of 2,4-D on selected soils. *Water Air Soil Poll.* **1999**, *111* (1–4), 75–88. <https://doi.org/10.1023/A:1005089612111>.
- (41) Ogram, A. v.; Jessup, R. E.; Ou, L. T.; Rao, P. S. C. Effects of sorption on biological degradation rates of (2,4-dichlorophenoxy)acetic acid in soils. *Appl. Environ. Micro.* **1985**, *49* (3), 582–587. <https://doi.org/10.1128/aem.49.3.582-587.1985>.
- (42) Crosby, D. G.; Tutass, H. O. Photodecomposition of 2,4-dichlorophenoxyacetic acid. *J. Agric. Food Chem.* **1966**, *14* (6), 596–599. <https://doi.org/10.1021/jf60148a012>.
- (43) U.S. EPA. Reregistration Eligibility Decision for 2,4-D https://archive.epa.gov/pesticides/reregistration/web/pdf/24d_red.pdf (accessed 2020 -05 -15).
- (44) Benitez, F. J.; Acero, J. L.; Real, F. J.; Roman, S. Oxidation of MCPA and 2,4-D by UV radiation, ozone, and the combinations UV/H₂O₂ and O₃/H₂O₂. *J. Environ. Sci. Health. B.* **2004**, *39* (3), 393–409. <https://doi.org/10.1081/PFC-120035925>.
- (45) Mabury, S. A.; Crosby, D. G. Pesticide reactivity toward hydroxyl and its relationship to field persistence. *J. Agric. Food Chem.* **1996**, *44* (7), 1920–1924. <https://doi.org/10.1021/jf950423y>.
- (46) Remucal, C. K. The role of indirect photochemical degradation in the environmental fate of pesticides: A review. *Environ. Sci. Processes Impacts.* **2014**, *16* (4), 628–653. <https://doi.org/10.1039/c3em00549f>.
- (47) Maizel, A. C.; Li, J.; Remucal, C. K. Relationships between dissolved organic matter composition and photochemistry in lakes of diverse trophic status. *Environ. Sci. Technol.* **2017**, *51* (17), 9624–9632. <https://doi.org/10.1021/acs.est.7b01270>.

- (48) Boreen, A. L.; Arnold, W. A.; McNeill, K. Photodegradation of pharmaceuticals in the aquatic environment: A review. *Aquat. Sci.* **2003**, *65* (4), 320–341. <https://doi.org/10.1007/s00027-003-0672-7>.
- (49) Berg, S. M.; Whiting, Q. T.; Herrli, J. A.; Winkels, R.; Wammer, K. H.; Remucal, C. K. The role of dissolved organic matter composition in determining photochemical reactivity at the molecular level. *Environ. Sci. Technol.* **2019**, *53* (20), 11725–11734. <https://doi.org/10.1021/acs.est.9b03007>.
- (50) Brucha, G.; Aldas-Vargas, A.; Ross, Z.; Peng, P.; Atashgahi, S.; Smidt, H.; Langenhoff, A.; Sutton, N. B. 2,4-Dichlorophenoxyacetic acid degradation in methanogenic mixed cultures obtained from Brazilian Amazonian soil samples. *Biodegradation* **2021**, *32* (4), 419–433. <https://doi.org/10.1007/s10532-021-09940-3>.
- (51) Serbent, M. P.; Rebelo, A. M.; Pinheiro, A.; Giongo, A.; Tavares, L. B. B. Biological agents for 2,4-dichlorophenoxyacetic acid herbicide degradation. *Appl. Micro. and Biotech.* **2019**, *103* (13), 5065–5078. <https://doi.org/10.1007/s00253-019-09838-4>.
- (52) Soulas, G. Evidence for the existence of different physiological groups in the microbial community responsible for 2,4-D mineralization in soil. *Soil Bio. Biochem.* **1993**, *25* (4), 443–449. [https://doi.org/10.1016/0038-0717\(93\)90069-N](https://doi.org/10.1016/0038-0717(93)90069-N).
- (53) Lerch, T. Z.; Dignac, M. F.; Nunan, N.; Bardoux, G.; Barriuso, E.; Mariotti, A. Dynamics of soil microbial populations involved in 2,4-D biodegradation revealed by fame-based stable isotope probing. *Soil Bio. Biochem.* **2009**, *41* (1), 77–85. <https://doi.org/10.1016/j.soilbio.2008.09.020>.
- (54) de Liphay, J. R.; Tuxen, N.; Johnsen, K.; Hansen, L. H.; Albrechtsen, H. J.; Bjerg, P. L.; Aamand, J. In situ exposure to low herbicide concentrations affects microbial population composition and catabolic gene frequency in an aerobic shallow aquifer. *App. Environ. Micro.* **2003**, *69* (1), 461–467. <https://doi.org/10.1128/AEM.69.1.461-467.2003>.
- (55) Nicolaisen, M. H.; Bælum, J.; Jacobsen, C. S.; Sørensen, J. Transcription dynamics of the functional *tfdA* gene during MCPA herbicide degradation by *Cupriavidus necator* AEO106 (pRO101) in agricultural soil. *Environ. Micro.* **2008**, *10* (3), 571–579. <https://doi.org/10.1111/j.1462-2920.2007.01476.x>.
- (56) Aly, O. M.; Faust, S. D. Studies on the fate of 2,4-D and ester derivatives in natural surface waters. *J. Agric. Food Chem.* **1964**, *12* (6), 541–546. <https://doi.org/10.1021/jf60136a016>.
- (57) de Liphay, J. R.; Aamand, J.; Barkay, T. Expression of *tfdA* genes in aquatic microbial communities during acclimation to 2,4-dichlorophenoxyacetic acid. *FEMS Micro. Eco.* **2006**, *40* (3), 205–214. <https://doi.org/10.1111/j.1574-6941.2002.tb00953.x>.
- (58) Laemmli, C. M.; Leveau, J. H. J.; Zehnder, A. J. B.; Roelof Van Der Meer, J. Characterization of a second *tfd* gene cluster for chlorophenol and chlorocatechol metabolism on plasmid pJP4 in *Ralstonia eutropha* JMP134(pJP4). *J. Bact.* **2000**, *182* (15), 4165–4172. <https://doi.org/10.1128/JB.182.15.4165-4172.2000>.
- (59) Ledger, T.; Pieper, D. H.; González, B. Chlorophenol hydroxylases encoded by plasmid pJP4 differentially contribute to chlorophenoxyacetic acid degradation. *Appl. Environ. Micro.* **2006**, *72* (4), 2783–2792. <https://doi.org/10.1128/AEM.72.4.2783-2792.2006>.
- (60) Lerch, T. Z.; Dignac, M. F.; Barriuso, E.; Bardoux, G.; Mariotti, A. Tracing 2,4-D metabolism in *Cupriavidus necator* JMP34 with ¹³C-labelling technique and fatty acid profiling. *J. Micro. Methods* **2007**, *71* (2), 162–174. <https://doi.org/10.1016/j.mimet.2007.08.003>.

- (61) Fukumori, F.; Hausinger, R. P. *Alcaligenes eutrophus* JMP134 “2,4-dichlorophenoxyacetate monooxygenase” is an α -ketoglutarate-dependent dioxygenase. *J. Bact.* **1993**, *175* (7), 2083–2086. <https://doi.org/10.1128/jb.175.7.2083-2086.1993>.
- (62) Bælum, J.; Jacobsen, C. S. TaqMan probe-based real-time PCR assay for detection and discrimination of class I, I, and III *tfdA* genes in soils treated with phenoxy acid herbicides. *Appl. Environ. Micro.* **2009**, *75* (9), 2969–2972. <https://doi.org/10.1128/AEM.02051-08>.
- (63) Bælum, J.; Nicolaisen, M. H.; Holben, W. E.; Strobel, B. W.; Sørensen, J.; Jacobsen, C. S. Direct analysis of *tfdA* gene expression by indigenous bacteria in phenoxy acid amended agricultural soil. *ISME* **2008**, *2* (6), 677–687. <https://doi.org/10.1038/ismej.2008.21>.
- (64) Winfield Solutions, LLC. Shredder Amine 4 chemical label <http://www.cdms.net/ldat/ldAOS000.pdf> (accessed 2021-10-24).
- (65) Teasdale, P. R.; Batley, G. E.; Apte, S. C.; Webster, I. T. Pore water sampling with sediment peepers. *Trends Analyt. Chem.* **1995**, *14* (6), 250–256. [https://doi.org/10.1016/0165-9936\(95\)91617-2](https://doi.org/10.1016/0165-9936(95)91617-2).
- (66) Bulman, D. M.; P. Mezyk, S.; K. Remucal, C. The impact of pH and irradiation wavelength on the production of reactive oxidants during chlorine photolysis. *Environ. Sci. Technol.* **2019**, *53* (8), 4450–4459. <https://doi.org/10.1021/acs.est.8b07225>.
- (67) Gueymard, C. A. Interdisciplinary applications of a versatile spectral solar irradiance model: A review. *Energy* **2005**, *30* (9), 1551–1576. <https://doi.org/10.1016/j.energy.2004.04.032>.
- (68) McConville, M. B.; Hubert, T. D.; Remucal, C. K. Direct photolysis rates and transformation pathways of the lampricides TFM and niclosamide in simulated sunlight. *Environ. Sci. Technol.* **2016**, *50* (18), 9998–10006. <https://doi.org/10.1021/acs.est.6b02607>.
- (69) Applied Biochemists. Navigate chemical label <http://www.lakerestoration.com/pdf/Navigatelabel.pdf> (accessed 2021-10-24).
- (70) Galbavy, E. S.; Ram, K.; Anastasio, C. 2-Nitrobenzaldehyde as a chemical actinometer for solution and ice photochemistry. *J. Photochem. Photobio. A: Chem* **2010**, *209* (2–3), 186–192. <https://doi.org/10.1016/j.jphotochem.2009.11.013>.
- (71) Laszakovits, J. R.; Berg, S. M.; Anderson, B. G.; O’Brien, J. E.; Wammer, K. H.; Sharpless, C. M. *p*-Nitroanisole/pyridine and *p*-nitroacetophenone/pyridine actinometers revisited: Quantum yield in comparison to ferrioxalate. *Environ. Sci. Technol. Lett.* **2017**, *4* (1), 11–14. <https://doi.org/10.1021/acs.estlett.6b00422>.
- (72) US EPA. Method 160.4: Residue, Volatile (Gravimetric, Ignition at 550°C) by Muffle Furnace www.epa.gov (accessed 2021-12-29).
- (73) Peleg, M.; Corradini, M. G.; Normand, M. D. The logistic (Verhulst) model for sigmoid microbial growth curves revisited. *Food Res. Int.* **2007**, *40* (7), 808–818. <https://doi.org/10.1016/j.foodres.2007.01.012>.
- (74) Peleg, M. A new look at models of the combined effect of temperature, pH, water activity, or other factors on microbial growth rate. *Food Engineering Reviews.* **2022**, *14*, 31–44. <https://doi.org/10.1007/s12393-021-09292-x>.
- (75) Tjørve, K. M. C.; Tjørve, E. The use of Gompertz models in growth analyses, and new Gompertz-model approach: An addition to the unified-Richards family. *PLoS ONE* **2017**, *12* (6). <https://doi.org/10.1371/journal.pone.0178691>.
- (76) Koseki, S.; Nonaka, J. Alternative approach to modeling bacterial lag time, using logistic regression as a function of time, temperature, pH, and sodium chloride concentration. *Appl. Environ. Microbiol.* **2012**, *78* (17), 6103–6112. <https://doi.org/10.1128/AEM.01245-12>.

- (77) Paris, D. F.; Steen, W. C.; Baughman, G. L.; Barnett, J. T. Second-Order Model to Predict Microbial Degradation of Organic Compounds in Natural Waters. *Appl. Environ. Microbiol.* **1981**, 41 (3), 603-609.
- (78) Kumar, A.; Trefault, N.; Olaniran, A. O. Microbial degradation of 2,4-dichlorophenoxyacetic acid: Insight into the enzymes and catabolic genes involved, their regulation and biotechnological implications. *Crit. Rev. Micro.* **2016**, 42 (2), 194–208. <https://doi.org/10.3109/1040841X.2014.917068>.
- (79) Magnoli, K.; Carranza, C. S.; Aluffi, M. E.; Magnoli, C. E.; Barberis, C. L. Herbicides based on 2,4-D: Its behavior in agricultural environments and microbial biodegradation aspects. A review. *Environmental Science and Pollution Research.* **2020**, 27, 38501 – 38512. <https://doi.org/10.1007/s11356-020-10370-6>/Published.
- (80) Huang, X.; He, J.; Yan, X.; Hong, Q.; Chen, K.; He, Q.; Zhang, L.; Liu, X.; Chuang, S.; Li, S.; Jiang, J. Microbial catabolism of chemical herbicides: microbial resources, metabolic pathways and catabolic genes. *Pest. Biochem. Physiol.* **2017**, 143, 272–297. <https://doi.org/10.1016/j.pestbp.2016.11.010>.
- (81) Wang, Y.; Roddick, F. A.; Fan, L. Direct and indirect photolysis of seven micropollutants in secondary effluent from a wastewater lagoon. *Chemosphere.* **2017**, 185, 297–308. <https://doi.org/10.1016/j.chemosphere.2017.06.122>.
- (82) Armbrust, K. L. Pesticide hydroxyl radical rate constants: Measurements and estimates of their importance in aquatic environments. *Environ. Toxicol. Chem.* **2000**, 19 (9), 2175–2180. <https://doi.org/10.1002/etc.5620190905>.
- (83) Vione, D.; Minero, C.; Housari, F.; Chiron, S. Photoinduced transformation processes of 2,4-dichlorophenol and 2,6-dichlorophenol on nitrate irradiation. *Chemosphere.* **2007**, 69 (10), 1548–1554. <https://doi.org/10.1016/j.chemosphere.2007.05.071>.
- (84) Ossola, R.; Jönsson, O. M.; Moor, K.; McNeill, K. Singlet oxygen quantum yields in environmental waters. *Chem. Rev.* **2021**, 121 (7), 4100–4146. <https://doi.org/10.1021/acs.chemrev.0c00781>.
- (85) Boivin, A.; Amellal, S.; Schiavon, M.; van Genuchten, M. T. 2,4-Dichlorophenoxyacetic acid (2,4-D) sorption and degradation dynamics in three agricultural soils. *Environ. Poll.* **2005**, 138 (1), 92–99. <https://doi.org/10.1016/j.envpol.2005.02.016>.
- (86) Gaultier, J.; Farenhorst, A.; Crow, G. Sorption-desorption of 2,4-dichlorophenoxyacetic acid by wetland sediments. *Wetlands.* **2009**, 29 (3), 837–844. <https://doi.org/10.1672/08-42.1>.
- (87) Li, Z.; McLachlan, M. S. Biodegradation of chemicals in unspiked surface waters downstream of wastewater treatment plants. *Environ. Sci. Technol.* **2019**, 53 (4), 1884–1892. <https://doi.org/10.1021/acs.est.8b05191>.
- (88) Wickham, P.; Pandey, P.; Harter, T.; Sandoval-Solis, S. UV light and temperature induced fluridone degradation in water and sediment and potential transport into aquifer. *Environ. Poll.* **2020**, 265, 114750. <https://doi.org/10.1016/j.envpol.2020.114750>.
- (89) Chalifour, A.; Walser, J. C.; Pomati, F.; Fenner, K. Temperature, phytoplankton density and bacteria diversity drive the biotransformation of micropollutants in a lake ecosystem. *Water Res.* **2021**, 202, 117412. <https://doi.org/10.1016/j.watres.2021.117412>.
- (90) Macur, R. E.; Wheeler, J. T.; Burr, M. D.; Inskip, W. P. Impacts of 2,4-D application on soil microbial community structure and on populations associated with 2,4-D degradation. *Micro. Res.* **2007**, 162 (1), 37–45. <https://doi.org/10.1016/j.micres.2006.05.007>.

- (91) Peterson, B. D.; McDaniel, E. A.; Schmidt, A. G.; Lepak, R. F.; Janssen, S. E.; Tran, P. Q.; Marick, R. A.; Ogorek, J. M.; DeWild, J. F.; Krabbenhoft, D. P.; McMahon, K. D. Mercury methylation genes identified across diverse anaerobic microbial guilds in a eutrophic sulfate-enriched lake. *Environ. Sci. Technol.* **2020**, *54*, 15840. <https://doi.org/10.1021/acs.est.0c05435>.
- (92) Gionfriddo, C. M.; Wymore, A. M.; Jones, D. S.; Wilpiseski, R. L.; Lynes, M. M.; Christensen, G. A.; Soren, A.; Gilmour, C. C.; Podar, M.; Elias, D. A. An improved *hgcAB* primer set and direct high-throughput sequencing expand Hg-methylator diversity in nature. *Frontiers Micro.* **2020**, *11*. <https://doi.org/10.3389/fmicb.2020.541554>.
- (93) Jones, D. S.; Walker, G. M.; Johnson, N. W.; Mitchell, C. P. J.; Coleman Wasik, J. K.; Bailey, J. V. Molecular evidence for novel mercury methylating microorganisms in sulfate-impacted lakes. *ISME*. **2019**, *13* (7), 1659–1675. <https://doi.org/10.1038/s41396-019-0376-1>.
- (94) Beach, N. K.; Noguera, D. R. Design and assessment of species-level qPCR primers targeting Comammox. *Frontiers Micro.* **2019**, *10*, 1–15. <https://doi.org/10.3389/fmicb.2019.00036>.
- (95) Kijima, K.; Mita, H.; Kawakami, M.; Amada, K. Role of *cadC* and *cadD* in the 2,4-dichlorophenoxyacetic acid oxygenase system of *Sphingomonas agrestis* 58-1. *J. Biosci. Bioengr.* **2018**, *125* (6), 649–653. <https://doi.org/10.1016/j.jbiosc.2018.01.003>.
- (96) Barbosa da Costa, N.; Fugère, V.; Hébert, M. P.; Xu, C. C. Y.; Barrett, R. D. H.; Beisner, B. E.; Bell, G.; Yargeau, V.; Fussmann, G. F.; Gonzalez, A.; Shapiro, B. J. Resistance, resilience, and functional redundancy of freshwater bacterioplankton communities facing a gradient of agricultural stressors in a mesocosm experiment. *Molec. Eco.* **2021**, *30* (19), 4771–4788. <https://doi.org/10.1111/mec.16100>.
- (97) Shade, A.; Read, J. S.; Youngblut, N. D.; Fierer, N.; Knight, R.; Kratz, T. K.; Lottig, N. R.; Roden, E. E.; Stanley, E. H.; Stombaugh, J.; Whitaker, R. J.; Wu, C. H.; McMahon, K. D. Lake microbial communities are resilient after a whole-ecosystem disturbance. *ISME*. **2012**, *6* (12), 2153–2167. <https://doi.org/10.1038/ismej.2012.56>.
- (98) Grossmann, K. Auxin herbicides: Current status of mechanism and mode of action. *Pest Mgmt. Sci.* **2010**, *66* (2), 113–120. <https://doi.org/10.1002/ps.1860>.
- (99) Wang, Y.; Jaw, C.; Chen, Y. Accumulation of 2,4-D and glyphosate in fish and water hyacinth. *Water Air Soil Poll.* **1994**, 397–403. <https://doi.org/10.1007/BF00479802>.
- (100) Benoit, P.; Barriuso, E.; Calvet, R. Biosorption characterization of herbicides, 2,4-D and atrazine, and two chlorophenols on fungal mycelium. *Chemosphere*. **1998**, *37* (7), 1271–1282. [https://doi.org/10.1016/S0045-6535\(98\)00125-8](https://doi.org/10.1016/S0045-6535(98)00125-8).
- (101) Boval, B.; Smith, J. M. Photodecomposition of 2,4-dichlorophenoxyacetic acid. *Chem. Engr. Sci.* **1973**, *28*, 1661–1675. [https://doi.org/10.1016/0009-2509\(73\)80020-X](https://doi.org/10.1016/0009-2509(73)80020-X).
- (102) McMartin, D. W.; Gillies, J. A.; Headley, J. v.; Peterson, H. G. Biodegradation kinetics of 2,4-dichlorophenoxyacetic acid (2,4-D) in South Saskatchewan River water. *Cand. Wat. Res. J.* **2000**, *25* (1), 81–92. <https://doi.org/10.4296/cwrj2501081>.
- (103) Zabaloy, M. C.; Gómez, M. A. Isolation and characterization of indigenous 2,4-D herbicide degrading bacteria from an agricultural soil in proximity of Sauce Grande River, Argentina. *Annals Micro.* **2014**, *64* (3), 969–974. <https://doi.org/10.1007/s13213-013-0731-9>.

Chapter 3

Expanded diversity of *tfdA* harboring bacteria across the natural and built environment

3.1 Details on Collaboration

This chapter is a collaboration between Amber M. White, Amarilys Gonzalez Vazquez, Elizabeth A. McDaniel, Benjamin D. Peterson, Paul Koch, Christina K. Remucal, Katherine D. McMahon. A.M.W. and A.G.V. conducted the field sampling, incubation experiments, qPCR, and TOPO cloning. E.A.M. conducted the metagenomic analysis. B. D. P. conducted Geneious analysis. A.M.W. wrote most of the paper with feedback from all co-authors.

3.2 Abstract

2,4-Dichlorophenoxyacetic acid (2,4-D) is an herbicide commonly used in aquatic and terrestrial environments that is degraded by bacteria through the TFD pathway, which is thought to be mainly carried on a plasmid. Previous work has relied on culture-based methods to study and develop primers for qPCR analysis of the gene cassette in environmental samples. In this study, we combined molecular and genomic analysis techniques to examine the accuracy of established *tfdA* qPCR primers on environmental samples and update the phylogeny of *tfdA* genes detected in bacterial genomes. We found most putative 2,4-D degraders are Proteobacteria but also found several novel degraders including members of the phyla *Candidatus* Rokubacteria and *Candidatus* Eremiobacteraeota. *In silico* analysis of established primers showed potential amplification of <

5% of putative degrader sequences but 52-100% of experimentally verified degraders when allowing for three and one mismatches between template and primer sequences, respectively. Overall, our work expands the diversity of putative 2,4-D degraders and demonstrates yet again the limitations of culture-based tools for investigating environmental community diversity.

3.3 Importance

Cultivation-based methods can misrepresent the diversity of environmental microorganisms. Our work showcases one example of how culture-based development of molecular tools underestimates the full spectrum of 2,4-D degrading microorganisms. Accurately identifying microorganisms with 2,4-D degradation potential is crucial for understanding the biodegradation potential of a commonly used herbicide across terrestrial, aquatic, and subsurface environments. Additionally, this work reinforces well-documented pitfalls associated with relying on cultured representatives when constructing primers and the challenges of translating findings from a few cultured representatives to understudied or unknown microorganisms in complex environments.

3.4 Introduction

The herbicide 2,4-dichlorophenoxyacetic acid (2,4-D) is used extensively to control invasive and nuisance plants in terrestrial and aquatic environments (1–4) but is a chemical of concern due to its toxicity and potential non-target effects (5, 6). As one of the most used and globally distributed herbicides (7–12), understanding the diversity and prevalence of bacteria with the potential to degrade 2,4-D is critical for understanding the fate and persistence of 2,4-D in the environment. 2,4-D is degraded by bacteria harboring the *tfd* gene cassette, named after the 2,4-D

compound (TFD) (12–16). Biodegradation is initiated by *tfdA* gene product, which encodes an alpha-ketoglutarate dependent oxygenase that uses Fe(II) to catalyze the reaction into 2,4-dichlorophenol, carbon dioxide, and succinate (17). Complete mineralization of 2,4-D proceeds via the associated *tfdBCDEF* gene products, which catalyze the transformation of 2,4-dichlorophenol into 3,5-dichlorocatechol; this product eventually being shuttled into the citric acid cycle (18). The reaction catalyzed by the *tfdA* gene product is considered the rate limiting step of biodegradation because it is transcribed separately from *tfdBCDEF*. There are also generally two copies of the *tfdBCDEF* gene cluster but only one copy of the *tfdA* gene (19). This duplication is likely due to the need for rapid degradation of 2,4-D transformation products that are toxic to bacteria (18).

The *tfd* gene is most often detected in plasmids (15, 18, 20, 21) but can occasionally be found on a chromosome (17–19, 22, 23). *tfdA*-dependent 2,4-D degradation via the TfdA enzyme has been extensively studied on plasmids in *Cupriavidus pinatubonesis*, previously named *Cupriavidus necator*, *Alcaligenes eutrophus*, and *Ralstonia eutropha* (17, 20, 24, 25). The gene is 819 bp long, and is well documented with strains belonging to Alpha, Beta, and Gammaproteobacteria isolated from soil systems (21, 25–27), including several strains capable of using 2,4-D as their sole carbon source (15, 16, 27). There are three recognized *tfdA* gene classes, but because the gene can be horizontally transferred (28) these classes are distributed throughout different bacterial phyla. Class I is located on transmissible plasmids and has been detected in Betaproteobacteria. Class II has 76% nucleotide identity to class I, has also been mostly detected in Betaproteobacteria (*Burkholderia* strains), and can also be found on the chromosome where it is referred to as *tfdA α* (22, 23). Lastly, class III has 77% and 80% nucleotide identity to class I and class II, respectively, and has been detected in Beta- and Gammaproteobacteria (28). Phylogenetic

analysis of *tfdA* genes sequenced from 31 confirmed 2,4-D degraders found that while there is diversity among the *tfdA* sequences that can be attributed to the different gene classes, gene sequences within the classes are relatively well conserved (25).

Previously, a set of qPCR primers were developed for the quantitative detection of *tfdA* in pure cultures and from the environment (29). Two primer sets that amplify an 81 or 215 bp fragment are expected to amplify all three gene classes. These primers have been applied with variable success in soil (20, 30), sediments (31), aquifer solids (32), and glacial ice (33), but have been limitedly applied in aquatic environments (4, 34, 35). Despite a wide range of environmental applications, the qPCR primers were developed from cultured representatives of soil environments that may miss other environmental representatives. Additionally, to the best of our knowledge no previous studies have applied metagenomic analyses to the *tfdA* gene, suggesting the diversity of the gene at present is limited to what has been detected through culturing, potentially misrepresenting the complete diversity of the degrading population.

In this study, we combined molecular and metagenomic approaches to examine the accuracy of established *tfdA* qPCR primers on environmental samples and update the *tfdA* phylogeny. Established *tfdA* primers failed to amplify clean PCR products when applied to environmental samples known to degrade 2,4-D. We also identified over 1000 genomes containing the *tfdA* marker from publicly available isolate genomes and metagenome-assembled genomes (MAGs) belonging to over a dozen different phyla from several different environmental sources. Importantly, we found several putative 2,4-D degraders belonging to phyla that, to our knowledge, have not previously been characterized as 2,4-D degraders. Lastly, a predictive *in silico* PCR analysis found extremely poor amplification of *tfdA* gene fragments from environmental samples, while genomes of cultured and experimentally verified representatives were indeed predicted to

yield PCR products. This work underscores the pitfalls associated with relying on cultured representatives when constructing primers and the challenges of translating findings from a few cultured representatives to understudied or unknown microorganisms in complex environments.

3.5 Results

3.5.1 Confirming Specificity of 81 and 215 bp Primers in *tfdA* Reference Genes

Amplification of the standard template for all three gene classes using the 215 bp primer produced products of expected size when visualized on a 1.5% agarose gel (**Figure B.1**). Analysis with BLASTN versus the NCBI database also confirmed the sequence of the *tfdA* gene product using the 215 bp primers (**Supplementary Data**). However, initial efforts to amplify *tfdA* using both 81 and 215 bp primers in sediment and soil samples previously exposed to and known to degrade 2,4-D (**Table 3.1**) yielded non-specific products from extracted sample DNA as evidenced by smearing on agarose gels, even though the positive control produced products of expected size (**Figure 3.1a**, **Figure 3.2**). We first hypothesized that co-extracted constituents were interfering with PCR and investigated further amplification interference with two experiments.

Table 3.1. Characteristics of four environmental samples used in TOPO cloning including environmental origin, number of colonies sequenced from each parent sample, and primer used for PCR amplification.

Environment	Experimental 2,4-D half-life (days)	Colonies sampled	Primer used for PCR
Soil	< 7	S	81 bp
Soil	< 7	T,U,V,W	81 bp
Water	24	A,D,E,F,G,H,I,J,K,L,M,N,O	215 bp
Sediment	24	B,C,P,Q,R	215 bp

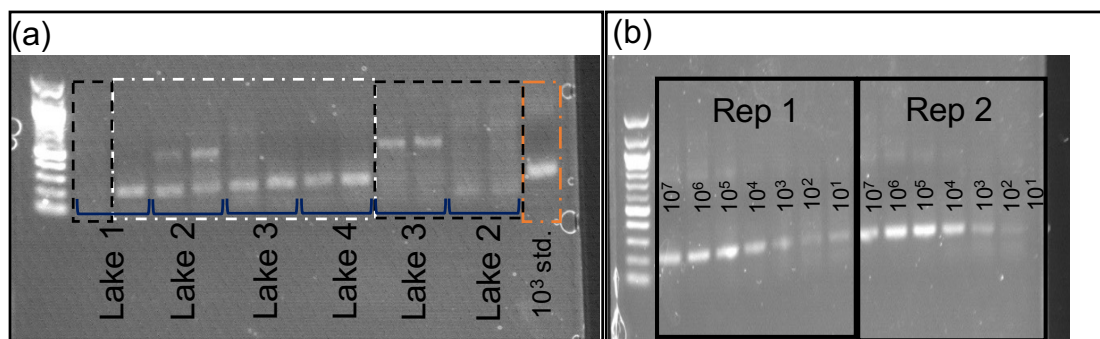


Figure 3.1. Gel of sediment recovery experiment using a serial dilution of *tfdA* class I gene standard from 10^7 (most left) to 10^1 (most right) (a). Gel of lake sediments and spiked with 10^3 gene copies (white boxes) and unspiked sediments (black boxes) as well as a 10^3 standard (orange box) (b). Ladder in both (a) and (b) is New England biotech 100 bp ladder. Band size is approximately 215 bp.

To evaluate interference by impurities co-extracted from sediments, serial dilutions of the class I *tfdA* gene from 10^7 to 10^1 copies were spiked into duplicate 0.5 g wet sediment aliquots previously unexposed to 2,4-D, extracted, and amplified with the 215 bp primer. High spiked gene copies (10^5 and $10^{2.5}$ after correcting concentration for saturated sediments) had a percent recovery of 96-107% (**Table 3.2**), indicating successful recovery by DNA extraction and amplification of the standard. However, poor percent recoveries were observed at low copies (below $10^{2.5}$). Gene products visualized using a 1.5% v/v agarose gel showed some smearing and additional bands for all products (**Figure 3.1b**, **Figure 3.2**). At high concentrations, a prominent band was present at around 200 bp, which aligns with the expected fragment size of 215 bp. However, the band was less clear at $10^{2.5}$ copies and below, which also had poor calculated recoveries. This suggests, even with the standard derived from cultured representatives, low concentrations of the *tfdA* gene were not selectively amplified using the primers when the template DNA was present at relatively low abundance.

We conducted additional recovery experiments with sediment from four lakes unexposed to 2,4-D (4) with varying organic carbon concentrations to test organic matter interference. We

10^3 copies of the *tfdA* gene and amplifying with the 215 bp primer (**Figure 3.1a**). Sediments with the added standard had a clear product band at ~200 bp, but the unspiked sediments had no clear band at 200 bp. Rather, these unspiked sediments had some smearing and light bands at 500 bp. This confirmed the finding that the primers could amplify the standard when found at relatively high levels in the extracted DNA, but that native *tfdA*, if present in the samples, was not selectively amplified. Instead, another non-specific product was being amplified.

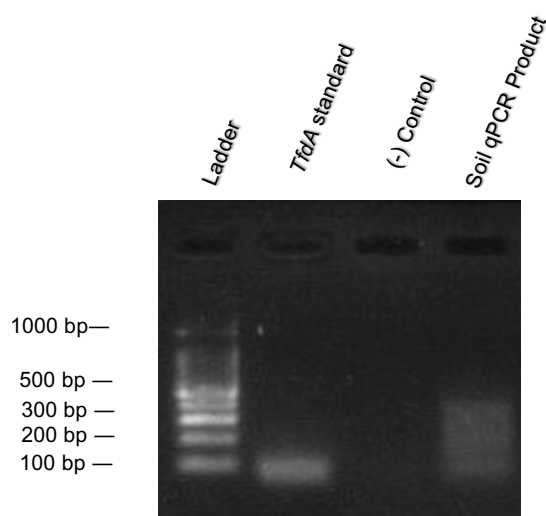


Figure 3.2. Electrophoresis gel of a qPCR amplification product of *tfdA* class I 81 bp primer in soil sample collected from the growth chamber study with 100 bp ladder.

Table 3.2. Recovery of *tfdA* class I gene in sediments unexposed to 2,4-D. Expected gene recoveries are calculated based on sediment mass and water content.

Log10 gene copies Expected	Log10 gene copies Rep 1	Log10 gene copies Rep 2	Rep 1 recovery	Rep 2 recovery	Average recovery	SD recovery
5.73	5.64	5.47	0.98	0.95	0.97	0.02
4.40	4.73	4.66	1.08	1.06	1.07	0.01
3.54	3.67	3.62	1.04	1.02	1.03	0.01
2.51	2.66	2.74	1.06	1.09	1.08	0.02
1.42	2.02	1.94	1.42	1.36	1.39	0.04
-0.565	1.49	1.73	-2.69	-3.06	-2.85	0.30
-0.229	1.63	1.54	-7.10	-6.71	-6.90	0.28
0.000	1.59	1.65				

Additional attempts to optimize the reaction did not improve amplification results. First, we attempted to adjust annealing temperatures by running a temperature gradient from 60 - 70°C and separately changing annealing time from 15 seconds to 30 seconds. We also tested doubling and tripling primer concentrations as well as lowering template concentrations to 0.5x and 0.25x of the standard protocol. Lastly, we performed additional clean up steps with phenol-chloroform and salt/alcohol precipitation to remove additional interferences prior to amplification. None of these troubleshooting steps generated clean bands on a gel from environmental samples. As a result, we cloned and sequenced PCR products to determine what, if anything, was being amplified.

3.5.2 Failed Amplicon Cloning and Sequencing of PCR Products

We constructed clone libraries to sequence individual amplicons from two soil (81 bp primer), one water (215 bp primer), and one sediment (215 bp primer) sample (**Table 3.1**). We selected 23 colonies for sequencing (5 from soil, 13 from water, 5 from sediment, **Table 3.1**).

Following plasmid prep and amplification using M13 primers, visualization of 19 plasmid insert-derived PCR products from the sediment and water samples generated bands of approximately 200 bp each, which is shorter than the expected product of 215 bp. Amplified plasmid inserts from the remaining four clones from soil samples showed a band size between 200 and 500 bp (**Figure 3.3**). Analysis with *blastn* versus the NCBI nr database confirmed the sequences from samples A-S (water, sediment, and soil derived colonies) were fragments of the cloning vector rather than the *tfdA* gene product. For samples T-W (soil only) the insert sequence had less than 20% alignment with the best hits. Only 6 to 18%, 5 to 17%, and 5 to 17%, for class I, II, and III, respectively was calculated as the percent query coverage (**Table B.2**). Sequences producing significant alignments did not exhibit any predicted functions with similarities to TfdA.

Our work here shows the *tfdA* qPCR primers failed to detect 2,4-D degrading microorganisms in environmental samples, which is consistent with other studies that have demonstrated challenges in applying primers created from cultured representatives to environmental samples (36–39). A potential explanation for the failed amplification results in environmental samples could be the presence of the *cad* pathway, which can degrade 2,4-D and has predominantly been found in *Burkholderia* (40–42). Additionally, the isolation technique used can influence what class of *tfdA* is recovered, suggesting primers created from isolates may miss parts of the degrading community solely based on how the strains were isolated (43). Thus, we further investigated if extensive *tfdA* sequence divergence at the primer binding site could explain why the primers failed on our environmental samples using non-isolation-based tools.

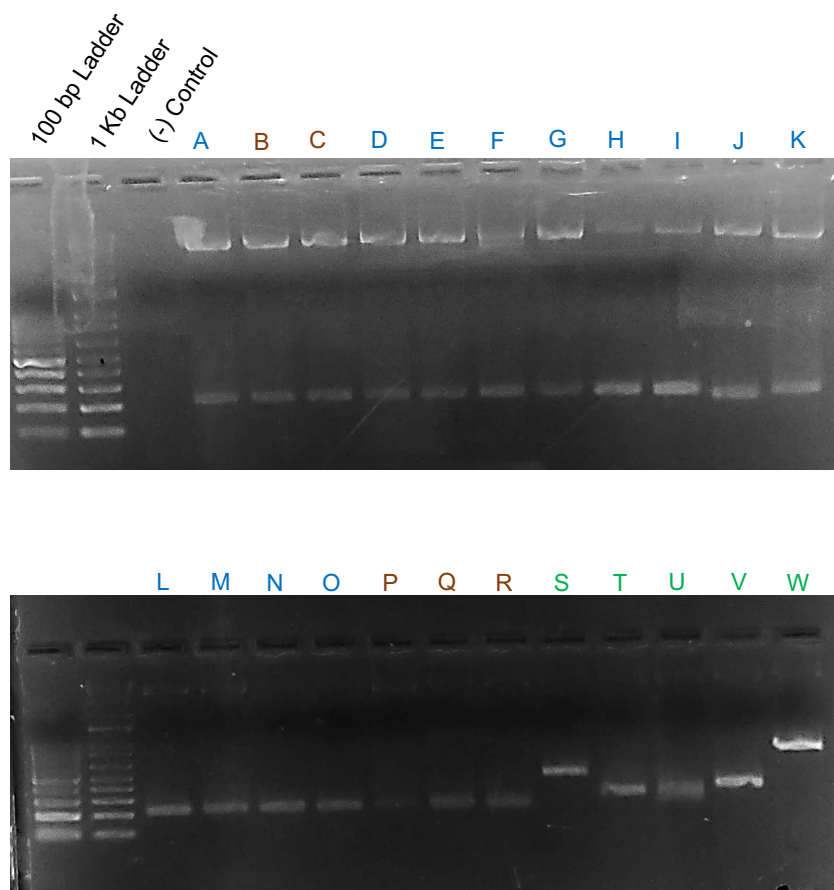


Figure 3.3. Gel of colonies with gene product from two soil (green letters), one sediment (brown letters), and one water sample (blue letters) after TOPO cloning, incubation in LB and plates at 37°C, and amplified using M13 primers. Expected product size of 215 bp for samples A-R and 81 bp for samples S-W. Ladder size indicated on gel is 100 bp and 1 kbp from left to right.

3.5.3 Phylogenetic Analysis Leads to Discovery of Putative Degraders

We searched for *tfdA* homologs using a custom Hidden Markov Model (HMM) in more than 200,000 publicly available isolate genomes and MAGs available in Genbank at the time of the search and found 1,035 putative 2,4-D degraders spanning over a dozen phyla and several different environmental sources (**Figure 3.4, Metadata file**). 90% of identified putative degraders belong to *Proteobacteria*, specifically the *Alpha-*, *Beta-*, *Gamma-*, *Deltaproteobacteria* classes and otherwise unresolved *Proteobacteria* (**Figure 3.4b and 3.4c**), groups which have previously

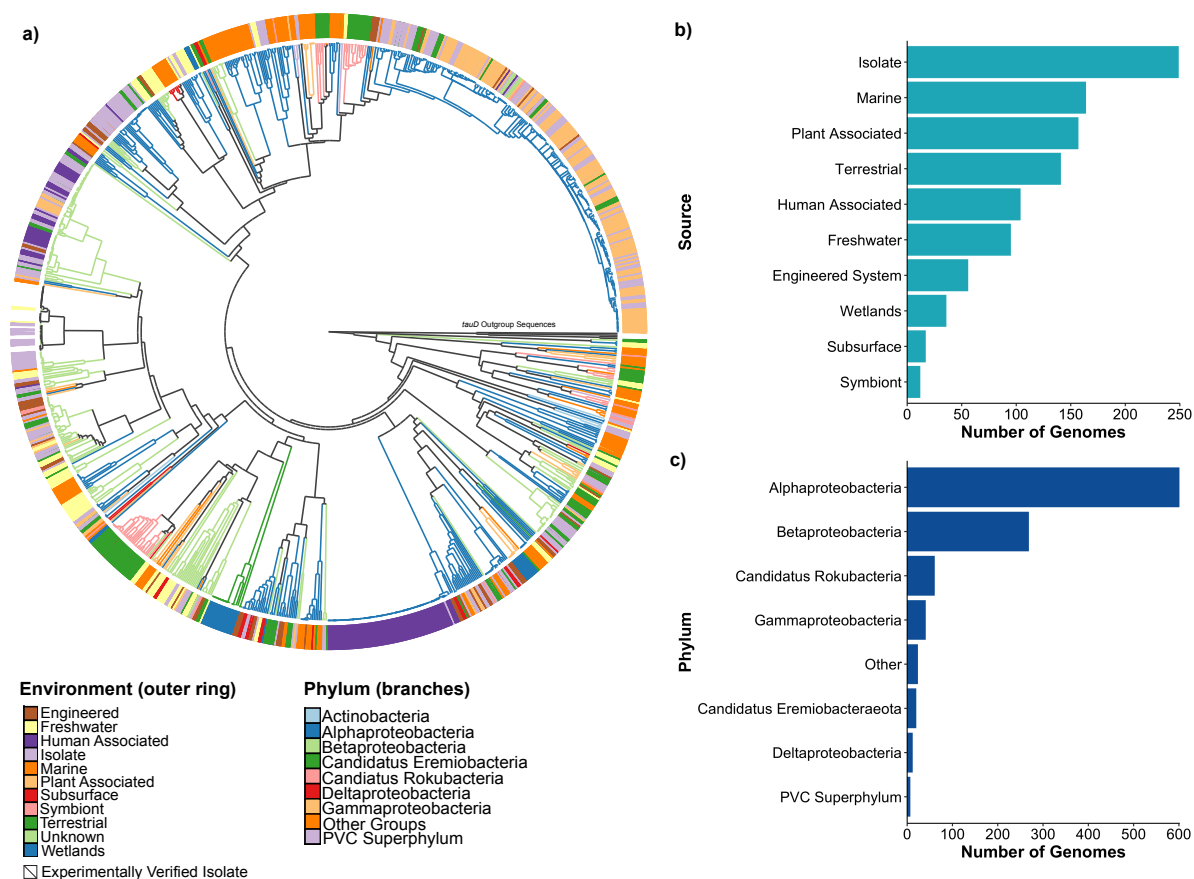


Figure 3.4. Phylogenetic tree of putative *tfdA* degraders (a). Tree color corresponds to phylum and outer ring corresponds to environmental origin. Counts of sequences from each phyla of putative 2,4-D degraders (b). Counts of sequences from each environment of origin of putative 2,4-D degraders (c).

been identified to contain 2,4-D degraders. The remaining 103 novel putative degraders are classified within the Acidobacteria (1), Actinobacteria (5), Fibrobacteres (1), Gemmatimonadetes (2), and PVC Superphylum (7) as well as several recently described candidate phyla, including *Candidatus Eremiobacteraeota* (20), *Candidatus Latescibacteria* (1), *Candidatus Rokubacteria* (61), and *Candidatus Tectomicrobia* (4). Putative degrader genomes were recovered from marine, freshwater, and wetland aquatic environments in addition to the more well studied terrestrial and subsurface environments. The distribution of the putative degraders across all environments and

phyla aligns with evidence for horizontal gene transfer (28). Importantly, cultured and experimentally verified representatives clustered separately from the putative degraders, suggesting the gene is highly conserved among degraders that are easily isolated or can use 2,4-D as a sole carbon source.

We found putative 2,4-D degraders in Acidobacteria, Gemmatimonadetes, and the PVC superphylum that have been previously reported as degraders or members of the degrading community of the related phenoxyalkanoic acid herbicide (2-methyl-4-chlorophenoxy) propionic acid (MCPA) (44). While these phyla have not been shown to degrade 2,4-D, the structural similarity of MCPA to 2,4-D and the demonstrated ability of *tfdA* to degrade both herbicides (29, 30, 45) suggests these microbes have the potential to degrade 2,4-D as well.

Most of the novel putative degraders were members of *Candidatus* Rokubacteria in our search and contained representatives from marine, freshwater, soil, subsurface, and sediment environments. This is consistent with previous reports of the global diversity of Rokubacteria (46), which are also expected to play an important role in sulfur cycling (47, 48) and degradation of complex carbon compounds found in leaf litter or root exudates (48–50). Previous work demonstrating uncultured microbes like Rokubacteria may use alternative metabolic pathways that prevent their culturing under typical conditions (46, 51, 52) highlights the power of non-culture-based methods in exploring community structure and function and the limits of historic cultured-based primer development methods for environmental analyses.

Wetland-derived putative degraders are predominantly from *Candidatus* Eremiobacteraeota, specifically found in arctic peatlands. Another uncultured phylum, Eremiobacteraeota are described as “heterotrophic scavengers” (53) found in polar/alpine environments (54–57) as well as polychlorinated biphenyl- and fracking-contaminated

environments (58, 59). All instances of *Candidatus* Eremiobacteraeota in our study were derived from the arctic wetland environment. Other wetland-derived putative degraders include *Acetobacteraceae*, *Rhizobiales*, and *Rhodospirillales* (Alphaproteobacteria), *Burkholderiales* (Betaproteobacteria), nine unresolved Gammaproteobacteria, and one unresolved Deltaproteobacteria.

Several of the putative degraders from all environments have been found to survive in heavily contaminated environments. For example, *Sphingomonadaceae* (Alphaproteobacteria) are known to have several members that can tolerate or degrade contaminants, including 2,4-D (25, 28, 60, 61), and have been found in gasoline (62), polyaromatic hydrocarbon (63), hexachlorocyclohexane (64), copper-mine (65), and electronic-waste (66) contaminated soils and sediments. We found *Sphingomonadaceae* in all sampled environments, including a large group of human-associated isolates from building infrastructure and patient cultures during an investigation of an outbreak of multiple-drug resistant *S. koreensis* at the NIH Clinical Center from 2006-2016 (67). We found several other *tfdA* carrying representatives in drinking water samples, specifically a member of the family *Bradyrhizobiaceae* (68, 69), *Variovorax paradoxus* (70), and other Proteobacteria representatives (69). Additional putative 2,4-D degraders known to tolerate contaminants include the isoprene-degrading *Variovorax* (71), heavy metal-resistant *Altererythrobacter atlanticus* (72), and the previously described *Eremiobacteraeota* (58, 59).

The variety in origin and diversity of putative 2,4-D degraders suggests they can be found nearly ubiquitously across natural and built environments and supports previous evidence that the gene can be horizontally transferred. Many of the degraders identified here, both established and putative, are associated with complex carbon cycling, such as the Eremiobacteraeota and Rokubacteria. This finding aligns with previous evidence that *tfd* genes or ancestral *tfd* genes were

used to degrade naturally occurring compounds that are structurally similar to 2,4-D (73–75). Additionally, the large number of putative degraders found in contaminated or engineered environments implies the gene or plasmid is resilient or conveys advantageous traits in stressful environments, even if 2,4-D or MCPA is not present.

3.5.4 Failed *in silico* Amplification With qPCR Primers on Putative Degraders

Given the wide distribution of the *tfdA* gene across all environments sampled here, we investigated the *in silico* amplification using the 81 and 215 bp primers from putative degrader genomes as compared to the confirmed 2,4-D degrader sequences, to investigate primer accuracy. Applying the 81 and 215 bp primers to the curated sequences of putative degraders resulted in poor rates of *in silico* amplification, even when allowing for one and three mismatches (**Figure 3.5a**). The 81 bp forward and reverse primer found zero matches for 1604 sequences when allowing for zero mismatches. Allowing for one mismatch amplified 10 sequences while further allowing for three mismatches resulted in 55 amplified sequences, (i.e., 3.4% success rate). The 215 bp primer had slightly better success with 8 amplified sequences assuming zero mismatches. Increasing the number of allowable mismatches to one and three resulted in 9 and 83 (i.e., 5.2% success rate) amplified sequences, respectively (**Figure 3.5a**).

In contrast, applying both primer sets to experimentally verified and cultured 2,4-D degraders (25) resulted in 52% amplification with zero mismatches and 100% amplification for one mismatch (**Figure 3.5b**). These results, combined with the previously described tree, show the diversity of the *tfdA* gene is much larger than previously described using *tfdA* sequences obtained from microorganisms predominantly cultivated from soil environments.

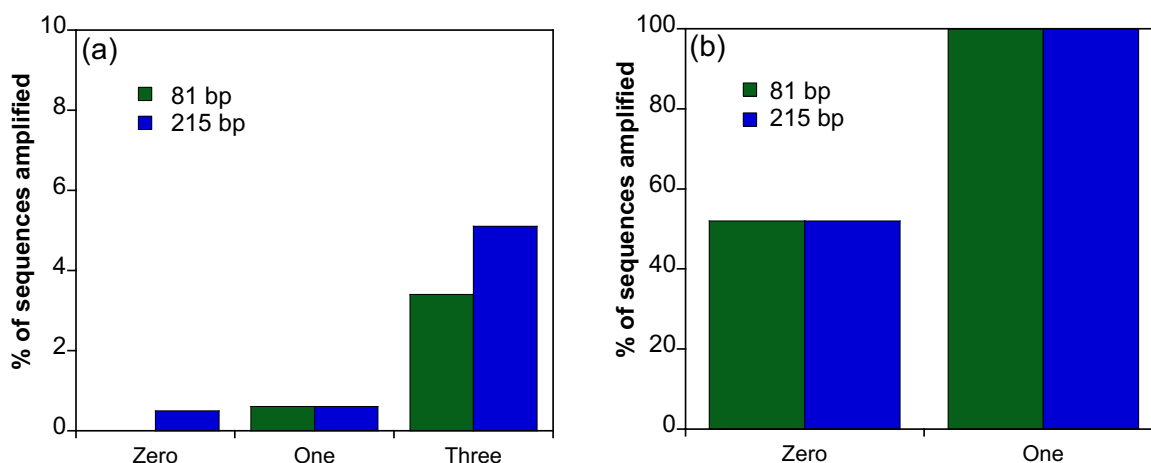


Figure 3.5. (a) Amplification success rates using 1604 sequences of putative 2,4-D degraders tested with 81 and 215 bp primers. Zero, one, and three mismatches were allowed. (b) Amplification success rates of 29 experimentally verified 2,4-D degraders with 81 and 215 bp primers.

3.6 Conclusions

In this study we expanded the diversity of known putative 2,4-D degraders using genome-resolved metagenomics and evaluated the accuracy of published qPCR primers commonly used to quantify the amount of *tfdA* gene in environmental samples. Our study found a significant gap between amplification of experimentally verified degraders and putative environmental degraders, which demonstrates how the use of cultured representatives to develop quantitative molecular tools has been known to underestimate the diversity of gene-carrying microorganisms in natural environments (51). Additionally, many of the putative degrader sequences were within phyla or families containing experimentally verified degraders, groups known to degrade similar phenoxyacid herbicides, or groups known to degrade other organic contaminants across the natural and built environment, suggesting the gene is more widespread than previously described.

Understanding *tfdA* gene distribution and prevalence across the natural environment is critical for understanding natural herbicide biodegradation, which is especially important for relatively persistent compounds such as 2,4-D. Our study evaluated established qPCR primers for the *tfdA* gene through molecular and computational techniques and found these primers missed a large portion of the potential 2,4-D degrading community. We did not evaluate PCR primers that predated the development of the qPCR primers (34, 76) nor did we explore the more recently reported *cad* genes (41). Our results underscore the importance of using caution when applying qPCR primers developed from a small number of sequences from cultured representatives to environmental samples because they are likely to misrepresent true environmental diversity. Additionally, further investigation into the 2,4-D degrading community is critical to understand the true environmental impact of phenoxyacid herbicides or other persistent halogenated compounds that are prevalent in the environment. The combination of targeted molecular techniques and genome-resolved metagenomics is a powerful way to link quantitative data to qualitative community and function data for a holistic understanding of microbial community response to anthropogenic stressors and both should be considered when designing future studies.

3.7 Methods

3.7.1 Environmental Sample Collection

Lake water and sediment were collected from several Wisconsin Lakes undergoing large-scale (i.e., lake wide concentrations $>0.45 \mu\text{M}$) treatments, described in detail in (4). Water and sediment used in TOPO cloning were from Random Lake, which had whole-lake treatments in 2018 and 2019. The water column biomass and sediment used in TOPO cloning were collected May 20th and 29th, 2019, respectively. These samples were chosen for additional analysis because

of a low Ct-value relative to other samples in preliminary qPCR tests. Water samples were collected via grab sampling from the epilimnion of the deepest point of the lake (< 1 m sampling depth) and stored on ice until processing. 1.5 L of water was filtered through a 0.22 μm polyethersulfone filter in a Sterivex filter unit (Millipore Sigma) and stored in a -20°C freezer. Lake sediment samples were collected by hand using a 5 cm diameter PVC core tube. Three individual sediment cores (top 0-4 cm) were homogenized in a sterile plastic bag and transferred to a 50 mL falcon tube for long term storage in a -20°C freezer. Soil samples were collected using a 100 mm PVC diameter soil core at a depth of 200 mm from OJ Noer Turfgrass Research Station in Madison, Wisconsin, on July 30th, 2020. 2,4-D formulation was applied to field plots using a nozzle pressure of 40 psi using a CO₂ pressurized boom sprayer with two XR Teejet AI8004 nozzles. The herbicide was agitated by hand and applied at a rate equivalent to 0.35 mL / m² of the commercial 2,4-D product with an initial concentration of 11.9 μM . Soil subsamples from each core were then collected in the following regions: upper soil (top 5 cm) and lower soil (15-20 cm depth) using a stainless-steel soil core sampler.

3.7.2 qPCR Amplification

Sediment, water, and soil samples exposed to 2,4-D were collected and amplified as described previously in (4) and (77). DNA was extracted using an MP Bio Fast DNA Spin Kit and quantified for DNA concentration using an Invitrogen Qubit 3.0 fluorimeter. Amplification was attempted using non-class specific *tdA* primers intended to amplify an 81bp or 215bp fragment (29, 30).

Primer sequences and thermocycle conditions adapted from Baelum et al. 2008 (30). For the 215 bp product, the forward primer was 5'-GAGCACTACGCRCTGAAYTCCCG-3' and the

reverse primer was 5'-GTCGCGTGCTCGAGAAG-3'. Amplification was done using a BioRad Thermocycler with initial heating for 10 minutes at 95°C and 40 cycles of 15 seconds at 95°C; 30 seconds at 64°C, and 30 seconds at 72°C. For the 81 bp product, forward primer was 5'-GAGCACTAC GCRCTGAAYTCCCG-3' and the reverse primer was 5'-SACCGGMGGCATSGCATT-3'. The reaction conditions were as follows: 3 min at 95°C for enzyme activation, followed by 35 cycles of 15 s at 95°C and 1 min at 62°C in a Bio-Rad CFX96 Touch Real-Time PCR Detection System. Amplified product melt curves were inspected to assess product homogeneity and visualized using agarose gel electrophoresis (1-1.5% wt/vol) to confirm product length.

3.7.3 Bacterial Strains and *tfdA* Reference Genes

tfdA class I gene, originally from *R. eutropha* pJP4(JMP134), *tfdA* Class II and Class III genes originated from *Burkholderia* strain RASC and *Burkholderia cepacia* strain 2a pIJB1, respectively, were synthesized by Integrated DNA Technologies in a pUCIDT- AMP cloning vector and transformed into *E. coli* AMP-resistant competent cells and processed as described in Gonzalez-Vasquez 2021. Cultures of each class were grown overnight at 37°C on Luria Bertani (LB) medium containing 500 mg/L ampicillin. According to the manufacturer's protocol, DNA plasmid isolations were performed using E.Z.N.A. Plasmid DNA Kit (Omega Bio Tek, Radnor, PA). Plasmid DNA, including *tfdA* class I, II, and III gene fragments, were quantified using a NanoDrop ND-1000 spectrophotometer (ThermoFisher Scientific, Waltham, MA). Plasmids were serially diluted and used as standards for quantitative real-time PCR (29).

3.7.4 TOPO Cloning

TOPO cloning using an Invitrogen TOPO[®]-TAcloning (Invitrogen, Karlsruhe, Germany) kit with One Shot TOP10 chemically competent *Escherichia coli* cells was conducted on two soil, one sediment, and one water sample amplified with either the 81 bp or 215 bp primer set. To set up the TOPO[®] reaction, 4 μ L of fresh qPCR product, 1 μ L salt solution and 1 μ L of the pCR^{TM4}-TOPO[®] vector were combined. Fresh PCR product was inserted into the provided plasmids and transformed into the chemically competent cells. Cells were spread on LB Agar plates with 50 mg/mL kanamycin, incubated overnight at 37°C. Colonies grown on overnight plates were transferred to LB broth with 50 mg/mL kanamycin and incubated at 37°C overnight again. Aliquots of liquid cultures were extracted using an Invitrogen PureLink Quick Plasmid Miniprep kit. Plasmids were then amplified with IDT ReadyMade M13 (-20) forward primers. Product sizes were evaluated using gel electrophoresis (1.5% agarose) with SYBR Safe DNA Gel Stain (Fisher Scientific, Chicago, IL) and purified using a Qiagen PCR Purification Kit (Qiagen, Hilden, Germany). Final products were quantified using a NanoDrop 1000 (Thermo Fisher Scientific, Waltham, MA) and sequenced on a 3730XL Genetic Analyzer (ThermoFisher) for Sanger sequencing in the Biotechnology Center at the University of Wisconsin-Madison. Obtained sequences were processed using A Plasmid Editor (ApE) (78) and analyzed using NCBI NucleotideBLAST (blastn) and blastx.

3.7.5 Accessed Datasets

We used a combination of publicly available sequenced isolates and metagenome-assembled genomes (MAGs) to survey *tfdA* diversity. All publicly available isolates and MAGs were accessed from Genbank in August 2019, resulting in more than 200,000 genomes to search

for *tfdA*. We also included MAGs assembled from three freshwater lakes, Lake Tanganyika in the East African Rift Valley (79), Trout Bog near Minocqua, WI, and Lake Mendota in Madison, WI (80). Samples from Trout Bog and Lake Mendota were sequenced, and population genomes assembled as described previously (80). Samples were sequenced, and population genomes were also assembled from two stations in Lake Tanganyika, Kegoma and Mahale, as described previously (79).

3.7.6 Identification of Putative 2,4-D Degraders

We constructed a Hidden Markov Model (HMM) of the TfdA protein using a collection of 30 reference TfdA protein sequences from experimentally verified isolates with 2,4-D degradation activity (25). Reference protein sequences were aligned with MUSCLE and an HMM built with the hmmbuild function of the HMMER suite (81). The constructed HMM profile was used to then identify putative 2,4-D degraders among over 1000 publicly available genomes, including pure culture isolates and metagenome assembled genomes (MAGs). For all genome sequences, open reading frames and protein-coding genes were predicted with Prodigal (82). We used hmmsearch as part of the HMMER program to search all predicted proteins for putative TfdA sequences with an e-value cutoff of $1e-50$ (81). All sequence hits were aligned with MUSCLE and visualized using AliView to manually check for specific conserved residues (83, 84). Based on the predicted positions of active site residues of TfdA in *Cupriavidus pinatubonensis* JMP134 (previously known as *Cupriavidus necator* JMP134 and *Ralstonia eutropha* JMP134), we checked for the presence of residues at His263 and Arg278 that appeared to be required for degradation and mostly conserved among the majority of sequences (75, 85, 86). Any sequences without these residues aligned with the corresponding positions of *C. pinatubonensis* were discarded.

3.7.7 Phylogenetic Diversity of Putative 2,4-D Degraders and Functional Annotations

A phylogenetic tree of all TfdA protein sequences was created from the alignment of all confident TfdA hits and constructed with RAxML (87). The tree was rooted using TauD sequences as an outgroup, as these sequences are from a related family of dioxygenases as TfdA (61, 88, 89). TauD sequences from *Mycobacterium marinum* strain M (ACC39598), *Burkholderia pseudomallei* 1710b (ABA48168), *Escherichia coli* K12 (BAE76149.1), and *Yersinia pestis* CO92 (CAL18870.1) were used as outgroup dioxygenases, as these were also used in Gonod et al. 2006 (88). These outgroups sequences were used to root the tree, and any putative TfdA sequences that did not fall within a monophyletic clade outside of the root were removed. The environmental or isolation source was overlaid on the tree as described by the project type for the associated BioProject for each strain or MAG in Genbank. The tree and associated metadata were visualized using EMPress v1.1.0 (90), and a full phylogenetic tree with bootstrap values is provided in the Supplementary Data.

3.7.8 Primer Analysis

Primer specificity was evaluated using the Geneious (Biomatters, New Zealand) primer mapper. Both the 215 and 81 bp forward and reverse primer sets were mapped against a database of *tfdA* sequences from cultured organisms and environmental MAGs. Mapping was done with different stringency criteria, allowing for 0, 1, and 3 mismatches. Sequences that were not matched by the primers when three mismatches were allowed were considered unlikely to be amplified by the primers in environmental samples.

3.8 Data availability statement

All data files and supplementary information available at https://figshare.com/projects/Expanded_diversity_of_tfdA_harboring_bacteria_across_the_natural_and_built_environment/145275. Metadata, HMM, phylogenetic tree with bootstraps, and alignment files for curated sequences well as Sanger sequencing results for 215 bp primer verification and TOPO cloning are available. A PDF Supplementary File with Table S1 and Figure S1 is also available. All code available at <https://github.com/elizabethmcd/tfdA>.

3.9 Acknowledgements

Thank you to Dr. Jan Roelof van der Meer from the University of Lausanne, Switzerland for supplying cultures for creation of the qPCR standards. We acknowledge valuable input from Angela Magness and Naila Barbosa da Costa in the qPCR and sequencing for this project. This research was performed in part using the Wisconsin Energy Institute computing cluster, which is supported by the Great Lakes Bioenergy Research Center as part of the U.S. Department of Energy Office of Science (DE-SC0018409), as well as the Center for High-Throughput Computing (CHTC) at UW-Madison in the Department of Computer Sciences. CHTC is supported by UW-Madison, the Advanced Computing Initiative, the Wisconsin Alumni Research Foundation, the Wisconsin Institute for Discovery, and the National Science Foundation. Additional funding provided by the National Institute of Food and Agriculture, United States Department of Agriculture Hatch/Evans-Allen/McIntire Stennis project #1013114, Wisconsin Department of Natural Resources, National Science Foundation Graduate Research Fellowship (A.M.W. and B.D.P), UW-Madison Department of Bacteriology Predoctoral Fellowship (E.A.M), and an Anna Grant Birge Memorial Award (A.M.W.).

3.10 References

1. Peterson MA, McMaster SA, Riechers DE, Skelton J, Stahlman PW. 2016. 2,4-D past, present, and future: A review. *Weed Tech* 30:303–345.
2. Nault ME, Netherland MD, Mikulyuk A, Skogerboe JG, Asplund T, Hauxwell J, Toshner P. 2014. Efficacy, selectivity, and herbicide concentrations following a whole-lake 2,4-D application targeting Eurasian watermilfoil in two adjacent northern Wisconsin lakes. *Lake and Resvr. Mänge* 30:1–10.
3. Góngora-Echeverría VR, Martin-Laurent F, Quintal-Franco C, Lorenzo-Flores A, Giacomán-Vallejos G, Ponce-Caballero C. 2019. Dissipation and Adsorption of 2,4-D, Atrazine, Diazinon, and Glyphosate in an Agricultural Soil from Yucatan State, Mexico. *Water, Air, Soil Poll* 230:131.
4. White AM, Nault ME, McMahan KD, Remucal CK. 2022. Synthesizing Laboratory and Field Experiments to Quantify Dominant Transformation Mechanisms of 2,4-Dichlorophenoxyacetic Acid (2,4-D) in Aquatic Environments. *Environ Sci Technol* 56:10838–10848.
5. Dehnert GK, Freitas MB, DeQuattro ZA, Barry T, Karasov WH. 2018. Effects of low, subchronic exposure of 2,4-Dichlorophenoxyacetic acid (2,4-D) and commercial 2,4-D formulations on early life stages of fathead minnows (*Pimephales promelas*). *Environ. Toxicol. Chem* 37:2550–2559.
6. Dehnert GK, Freitas MB, Sharma PP, Barry TP, Karasov WH. 2021. Impacts of subchronic exposure to a commercial 2,4-D herbicide on developmental stages of multiple freshwater fish species. *Chemosphere* 263:127638.
7. Zuanazzi NR, Ghisi N de C, Oliveira EC. 2020. Analysis of global trends and gaps for studies about 2,4-D herbicide toxicity: A scientometric review. *Chemosphere* 241:125016.
8. Liu W, Li H, Tao F, Li S, Tian Z, Xie H. 2013. Formation and contamination of PCDD/Fs, PCBs, PeCBz, HxCBz and polychlorophenols in the production of 2,4-D products. *Chemosphere* 92:304–308.
9. Islam F, Wang J, Farooq MA, Khan MSS, Xu L, Zhu J, Zhao M, Muñoz S, Li QX, Zhou W. 2018. Potential impact of the herbicide 2,4-dichlorophenoxyacetic acid on human and ecosystems. *Environment International* 111:332–351.
10. Atwood D, Paisley-Jones C. 2017. US EPA - Pesticides Industry Sales and Usage 2008 - 2012. https://www.epa.gov/sites/default/files/2017-01/documents/pesticides-industry-sales-usage-2016_0.pdf (accessed 27-06-2022)
11. Barbosa AMC, Solano M de LM, Umbuzeiro G de A. 2015. Pesticides in Drinking Water – The Brazilian Monitoring Program. *Front Public Health* 3:246.
12. Paszko T, Muszyński P, Materska M, Bojanowska M, Kostecka M, Jackowska I. 2016. Adsorption and degradation of phenoxyalkanoic acid herbicides in soils: A review. *Environ. Toxicol. Chem* 35:271–286.
13. Chavez Rodriguez L, Ingalls B, Schwarz E, Streck T, Uksa M, Pagel H. 2020. Gene-centric model approaches for accurate prediction of pesticide biodegradation in soils. *Environ. Sci. Technol* 54:13638–13650.
14. Ogram A v., Jessup RE, Ou LT, Rao PSC. 1985. Effects of sorption on biological degradation rates of (2,4-dichlorophenoxy)acetic acid in soils. *Appl Environ Micro* 49:582–587.

15. Han L, Zhao D, Li C. 2015. Isolation and 2,4-D-degrading characteristics of *Cupriavidus campinensis* BJ71. *Braz J Microbiol* 46:433–441.
16. Zabaloy MC, Gómez MA. 2014. Isolation and characterization of indigenous 2,4-D herbicide degrading bacteria from an agricultural soil in proximity of Sauce Grande River, Argentina. *Annals Micro* 64:969–974.
17. Fukumori F, Hausinger RP. 1993. *Alcaligenes eutrophus* JMP134 “2,4-dichlorophenoxyacetate monooxygenase” is an α -ketoglutarate-dependent dioxygenase. *J Bact* 175:2083–2086.
18. Kumar A, Trefault N, Olaniran AO. 2016. Microbial degradation of 2,4-dichlorophenoxyacetic acid: Insight into the enzymes and catabolic genes involved, their regulation and biotechnological implications. *Crit Rev Micro* 42:194–208.
19. Laemmlli CM, Leveau JHJ, Zehnder AJB, Roelof Van Der Meer J. 2000. Characterization of a second *tfd* gene cluster for chlorophenol and chlorocatechol metabolism on plasmid pJP4 in *Ralstonia eutropha* JMP134(pJP4). *J Bact* 182:4165–4172.
20. Nicolaisen MH, Bælum J, Jacobsen CS, Sørensen J. 2008. Transcription dynamics of the functional *tfdA* gene during MCPA herbicide degradation by *Cupriavidus necator* AEO106 (pRO101) in agricultural soil. *Environ Micro* 10:571–579.
21. Chaudhry GR, Huang GH. 1988. Isolation and characterization of a new plasmid from a *Flavobacterium* sp. which carries the genes for degradation of 2,4-Dichlorophenoxyacetate. *J Bact* 170:9.
22. Suwa Y, Wright AD, Fukimori F, Nummy KA, Hausinger RP, Holben WE, Forney LJ. 1996. Characterization of a Chromosomally Encoded 2,4-Dichlorophenoxyacetic Acid/-Ketoglutarate Dioxygenase from *Burkholderia* sp. Strain RASC. *Appl Environ Microbiol* 62:2464–2469.
23. Matheson VG, Forney LJ, Suwa Y, Nakatsu CH, Sextstone AJ, Holben WE. 1996. Evidence for Acquisition in Nature of a Chromosomal 2,4-Dichlorophenoxyacetic Acid/-Ketoglutarate Dioxygenase Gene by Different *Burkholderia* spp. *Appl Environ Microbiol* 62:2457–2463.
24. Lerch TZ, Dignac MF, Barriuso E, Bardoux G, Mariotti A. 2007. Tracing 2,4-D metabolism in *Cupriavidus necator* JMP134 with ¹³C-labelling technique and fatty acid profiling. *J Micro Methods* 71:162–174.
25. Baelum J, Jacobsen CS, Holben WE. 2010. Comparison of 16S rRNA gene phylogeny and functional *tfdA* gene distribution in thirty-one different 2,4-dichlorophenoxyacetic acid and 4-chloro-2-methylphenoxyacetic acid degraders. *Systematic and Applied Microbiology* 33:67–70.
26. Marron-Montiel E, Ruiz-Ordaz N, Rubio-Graados C, Juarez-Ramirez C, Galindez-Mayer CJ. 2006. Isolation, kinetic characterization in batch and continuous culture and application for bioaugmenting an activated sludge microbial community. *Process Biochemistry* 41:1521–1528.
27. Musarrat J, Bano N. 2000. Isolation and characterization of 2,4-dichlorophenoxyacetic acid-catabolizing bacteria and their biodegradation efficiency in soil. *Word Jrnl Micro Biotech* 16:495–497.
28. McGowan C, Fulthorpe R, Wright A, Tiedje JM. 1998. Evidence for interspecies gene transfer in the evolution of 2,4-dichlorophenoxyacetic acid degraders. *Appl Environ Microbiol* 64:4089–4092.

29. Bælum J, Jacobsen CS. 2009. TaqMan probe-based real-time PCR assay for detection and discrimination of class I, II, and III *tfdA* genes in soils treated with phenoxy acid herbicides. *Appl Environ Micro* 75:2969–2972.
30. Bælum J, Nicolaisen MH, Holben WE, Strobel BW, Sørensen J, Jacobsen CS. 2008. Direct analysis of *tfdA* gene expression by indigenous bacteria in phenoxy acid amended agricultural soil. *ISME* 2:677–687.
31. Batoğlu-Pazarbaşı M, Milosevic N, Malaguerra F, Binning PJ, Albrechtsen HJ, Bjerg PL, Aamand J. 2013. Discharge of landfill leachate to streambed sediments impacts the mineralization potential of phenoxy acid herbicides depending on the initial abundance of *tfdA* gene classes. *Environmental Pollution* 176:275–283.
32. Batioğlu-Pazarbaşı M, Bælum J, Johnsen AR, Sørensen SR, Albrechtsen HJ, Aamand J. 2012. Centimetre-scale vertical variability of phenoxy acid herbicide mineralization potential in aquifer sediment relates to the abundance of *tfdA* genes. *FEMS Micro. Eco.* 80:331–341.
33. Stibal M, Bælum J, Holben WE, Sørensen SR, Jensen A, Jacobsen CS. 2012. Microbial degradation of 2,4-dichlorophenoxyacetic acid on the Greenland ice sheet. *Appl Environ Microbiol* 78:5070–5076.
34. de Liphay JR, Aamand J, Barkay T. 2006. Expression of *tfdA* genes in aquatic microbial communities during acclimation to 2,4-dichlorophenoxyacetic acid. *FEMS Micro. Eco.* 40:205–214.
35. de Liphay JR, Tuxen N, Johnsen K, Hansen LH, Albrechtsen HJ, Bjerg PL, Aamand J. 2003. In situ exposure to low herbicide concentrations affects microbial population composition and catabolic gene frequency in an aerobic shallow aquifer. *Appl Environ Microbiol* 69:461–467.
36. Peterson BD, McDaniel EA, Schmidt AG, Lepak RF, Janssen SE, Tran PQ, Marick RA, Ogorek JM, DeWild JF, Krabbenhoft DP, McMahan KD. 2020. Mercury methylation genes identified across diverse anaerobic microbial guilds in a eutrophic sulfate-enriched lake. *Environ Sci Technol* 54:15840.
37. Gionfriddo CM, Wymore AM, Jones DS, Wilpiseski RL, Lynes MM, Christensen GA, Soren A, Gilmour CC, Podar M, Elias DA. 2020. An improved *hgcAB* primer set and direct high-throughput sequencing expand Hg-methylator diversity in nature. *Front Microbiol* 11:541554.
38. Jones DS, Walker GM, Johnson NW, Mitchell CPJ, Coleman Wasik JK, Bailey J v. 2019. Molecular evidence for novel mercury methylating microorganisms in sulfate-impacted lakes. *ISME* 13:1659–1675.
39. Beach NK, Noguera DR. 2019. Design and assessment of species-level qPCR primers targeting Comammox. *Front Microbiol* 10:1–15.
40. Itoh K, Kanda R, Sumita Y, Kim H, Kamagata Y, Suyama K, Yamamoto H, Hausinger RP, Tiedje JM. 2002. *tfdA*-like genes in 2,4-dichlorophenoxyacetic acid-degrading bacteria belonging to the *Bradyrhizobium-Agromonas-Nitrobacter-Afipia* cluster in α -Proteobacteria. *Appl Environ Microbiol* 68:3449–3454.
41. Kijima K, Mita H, Kawakami M, Amada K. 2018. Role of *CadC* and *CadD* in the 2,4-dichlorophenoxyacetic acid oxygenase system of *Sphingomonas agrestis* 58-1. *J Biosci Bioengr* 125:649–653.

42. Nielsen TK, Xu Z, Gözdereliler E, Aamand J, Hansen LH, Sørensen SR. 2013. Novel insight into the genetic context of the *cadAB* genes from a 4-chloro-2-methylphenoxyacetic acid-degrading *Sphingomonas*. *PLoS ONE* 8:e83346.
43. Lee TH, Kurata S, Nakatsu CH, Kamagata Y. 2005. Molecular analysis of bacterial community based on 16S rDNA and functional genes in activated sludge enriched with 2,4-dichlorophenoxyacetic acid (2,4-D) under different cultural conditions. *Microbial Ecology* 49:151–162.
44. Liu YJ, Liu SJ, Drake HL, Horn MA. 2011. Alphaproteobacteria dominate active 2-methyl-4-chlorophenoxyacetic acid herbicide degraders in agricultural soil and rhizosphere. *Environ Micro* 13:991–1009.
45. Rodríguez-Cruz MS, Bælum J, Shaw LJ, Sørensen SR, Shi S, Aspray T, Jacobsen CS, Bending GD. 2010. Biodegradation of the herbicide mecoprop-p with soil depth and its relationship with class III *tfdA* genes. *Soil Biology and Biochemistry* 42:32–39.
46. Becraft ED, Woyke T, Jarett J, Ivanova N, Godoy-Vitorino F, Poulton N, Brown JM, Brown J, Lau MCY, Onstott T, Eisen JA, Moser D, Stepanauskas R. 2017. Rokubacteria: Genomic giants among the uncultured bacterial phyla. *Front Microbiol* 8:2264.
47. Anantharaman K, Hausmann B, Jungbluth SP, Kantor RS, Lavy A, Warren LA, Rappé MS, Pester M, Loy A, Thomas BC, Banfield JF. 2018. Expanded diversity of microbial groups that shape the dissimilatory sulfur cycle. *ISME* 12:1715–1728.
48. Hug LA, Thomas BC, Sharon I, Brown CT, Sharma R, Hettich RL, Wilkins MJ, Williams KH, Singh A, Banfield JF. 2016. Critical biogeochemical functions in the subsurface are associated with bacteria from new phyla and little studied lineages. *Environ Micro* 18:159–173.
49. Wang Y, Li T, Li C, Song F. 2020. Differences in microbial community and metabolites in litter layer of plantation and original Korean pine forests in north temperate zone. *Microorganisms* 8:1–23.
50. Butterfield CN, Li Z, Andeer PF, Spaulding S, Thomas BC, Singh A, Hettich RL, Suttle KB, Probst AJ, Tringe SG, Northen T, Pan C, Banfield JF. 2016. Proteogenomic analyses indicate bacterial methylotrophy and archaeal heterotrophy are prevalent below the grass root zone. *PeerJ* 4:e2687.
51. Rinke C, Schwientek P, Sczyrba A, Ivanova NN, Anderson IJ, Cheng J-F, Darling A, Malfatti S, Swan BK, Gies EA, Dodsworth JA, Hedlund BP, Tsiamis G, Sievert SM, Liu W-T, Eisen JA, Hallam SJ, Kyrpides NC, Stepanauskas R, Rubin EM, Hugenholtz P, Woyke T. 2013. Insights into the phylogeny and coding potential of microbial dark matter. *Nature* 499:431–437.
52. Brown CT, Hug LA, Thomas BC, Sharon I, Castelle CJ, Singh A, Wilkins MJ, Wrighton KC, Williams KH, Banfield JF. 2015. Unusual biology across a group comprising more than 15% of domain Bacteria. *Nature* 523:208–211.
53. Sheremet A, Jones GM, Jarett J, Bowers RM, Bedard I, Culham C, Eloë-Fadrosh EA, Ivanova N, Malmstrom RR, Grasby SE, Woyke T, Dunfield PF. 2020. Ecological and genomic analyses of candidate phylum WPS-2 bacteria in an unvegetated soil. *Environ Microbiol* 22:3143–3157.
54. Frindte K, Pape R, Werner K, Löffler J, Knief C. 2019. Temperature and soil moisture control microbial community composition in an arctic-alpine ecosystem along elevational and micro-topographic gradients. *ISME* 13:2031–2043.

55. Ferrari BC, Bissett A, Snape I, van Dorst J, Palmer AS, Ji M, Siciliano SD, Stark JS, Winsley T, Brown M v. 2016. Geological connectivity drives microbial community structure and connectivity in polar, terrestrial ecosystems. *Environ Microbiol* 18:1834–1849.
56. Frey B, Rime T, Phillips M, Hajdas I, Widmer F, Hartmann M. 2016. Microbial diversity in European alpine permafrost and active layers. *FEMS Micro. Eco.* 92:18.
57. Pointing SB, Gillor O, Fulthorpe R, Lazzaro A, Hilfiker D, Zeyer J. 2015. Structures of Microbial Communities in Alpine Soils: Seasonal and Elevational Effects. *Front Microbiol* 6:1330.
58. Nogales B, Moore ERB, Llobet-Brossa E, Rossello-Mora R, Amann R, Timmis KN. 2001. Combined Use of 16S Ribosomal DNA and 16S rRNA to Study the Bacterial Community of Polychlorinated Biphenyl-Polluted Soil. *Appl Environ Microbiol* 67:1874–1884.
59. Trexler R, Solomon C, Brislawn CJ, Wright JR, Rosenberger A, McClure EE, Grube AM, Peterson MP, Keddache M, Mason OU, Hazen TC, Grant CJ, Lamendella R, Saikaly P, Abdullah K. 2014. Assessing impacts of unconventional natural gas extraction on microbial communities in headwater stream ecosystems in Northwestern Pennsylvania. *Front Microbiol* 5:1–13.
60. Vallaeys T, Persello-Cartieaux F, Rouard N, Lors C, Laguerre G, Soulas G. 2006. PCR-RFLP analysis of 16S rRNA, *tfdA* and *tfdB* genes reveals a diversity of 2,4-D degraders in soil aggregates. *FEMS Micro. Eco.* 24:269–278.
61. Han L, Liu Y, He A, Zhao D. 2014. 16S rRNA gene phylogeny and *tfdA* gene analysis of 2,4-D-degrading bacteria isolated in China. *World Journal of Microbiology and Biotechnology* 30:2567–2576.
62. Park YJ, Kim KH, Han DM, Lee DH, Jeon CO. 2019. *Sphingobium terrigena* sp. Nov., isolated from gasoline-contaminated soil. *International Journal of Systematic and Evolutionary Microbiology* 69:2459–2464.
63. Leys NMEJ, Ryngaert A, Bastiaens L, Verstraete W, Top EM, Springael D. 2004. Occurrence and Phylogenetic Diversity of Sphingomonas Strains in Soils Contaminated with Polycyclic Aromatic Hydrocarbons. *App Environ Micro* 70:1944–1955.
64. Niharika N, Moskalikova H, Kaur J, Khan F, Sedlackova M, Hampel A, Damborsky J, Prokop Z, Lal R. 2013. *Sphingobium czechense* sp. nov., isolated from a hexachlorocyclohexane dump site. *International Journal of Systematic and Evolutionary Microbiology* 63:723–728.
65. Li L, Liu H, Shi Z, Wang G. 2013. *Sphingobium cupriresistens* sp. nov., a copper-resistant bacterium isolated from copper mine soil, and emended description of the genus *Sphingobium*. *International Journal of Systematic and Evolutionary Microbiology* 63:604–609.
66. Chen X, Wang H, Xu J, Song D, Sun G, Xu M. 2016. *Sphingobium hydrophobicum* sp. nov., a hydrophobic bacterium isolated from electronic-waste-contaminated sediment. *International Journal of Systematic and Evolutionary Microbiology* 66:3912–3916.
67. Johnson RC, Deming C, Conlan S, Zellmer CJ, Michelin A v., Lee-Lin S, Thomas PJ, Park M, Weingarten RA, Less J, Dekker JP, Frank KM, Musser KA, McQuiston JR, Henderson DK, Lau AF, Palmore TN, Segre JA. 2018. Investigation of a Cluster of *Sphingomonas koreensis* Infections. *New England Journal of Medicine* 379:2529–2539.
68. Kantor RS, Miller SE, Nelson KL. 2019. The water microbiome through a pilot scale advanced treatment facility for direct potable reuse. *Front Microbiol* 10:993.

69. Pinto AJ, Marcus DN, Ijaz UZ, Bautista-de Iose Santos QM, Dick GJ, Raskin L. 2016. Metagenomic Evidence for the Presence of Comammox *Nitrospira*-Like Bacteria in a Drinking Water System. *mSphere* 1:e00054-15.
70. Gomez-Alvarez V, Pfaller S, Revetta RP. 2016. Draft genome sequence of two *Sphingopyxis* sp. strains, dominant members of the bacterial community associated with a drinking water distribution system simulator. *Genome Announcements* 4:e0018316.
71. Crombie AT, Larke-Mejia NL, Emery H, Dawson R, Pratscher J, Murphy GP, McGenity TJ, Murrell JC. 2018. Poplar phyllosphere harbors disparate isoprene-degrading bacteria. *PNAS* 115:13081–13086.
72. Wu YH, Cheng H, Zhou P, Huo YY, Wang CS, Xu XW. 2015. Complete genome sequence of the heavy metal resistant bacterium *Altererythrobacter atlanticus* 26DY36T, isolated from deep-sea sediment of the North Atlantic Mid- Ocean ridge. *Marine Genomics* 24:289–292.
73. Hogan DA, Buckley DH, Nakatsu CH, Schmidt TM, Hausinger RP. 1997. Distribution of the *tfdA* gene in soil bacteria that do not degrade 2,4-dichlorophenoxyacetic acid (2,4-D). *Microbial Ecology* 34:90–96.
74. Dunning Hotopp JC, Hausinger RP. 2001. Alternative substrates of 2,4-dichlorophenoxyacetate/-ketoglutarate dioxygenase. *Journal of Molecular Catalysis B: Enzymatic* 15:155–162.
75. Dunning Hotopp JC, Hausinger RP. 2002. Probing the 2,4-dichlorophenoxyacetate/ α -ketoglutarate dioxygenase substrate-binding site by site-directed mutagenesis and mechanism-based inactivation. *Biochemistry* 41:9787–9794.
76. Amy PS, Schulke JW, Frazier LM, Seidler RJ. 1985. Characterization of aquatic bacteria and cloning of genes specifying partial degradation of 2,4-dichlorophenoxyacetic acid. *Appl Environ Microbiol* 49:1237–1245.
77. Gonzalez Vazquez AE. 2021. Impact of Seasonal Environmental Variations on 2,4-D Fate and Metabolism in Urban Landscapes. PhD. University of Wisconsin-Madison, Madison.
78. Davis MW, Jorgensen EM. 2022. ApE, A Plasmid Editor: A freely available DNA manipulation and visualization program. *Front Bioinform* 2:818619.
79. Tran PQ, Bachand SC, McIntyre PB, Kraemer BM, Vadeboncoeur Y, Kimirei IA, Tamatamah R, McMahan KD, Anantharaman K. 2021. Depth-discrete metagenomics reveals the roles of microbes in biogeochemical cycling in the tropical freshwater Lake Tanganyika. *ISME* 15:1971–1986.
80. Linz AM, He S, Stevens SLR, Anantharaman K, Rohwer RR, Malmstrom RR, Bertilsson S, McMahan KD. 2018. Freshwater carbon and nutrient cycles revealed through reconstructed population genomes. *PeerJ* 2018:1–24.
81. Eddy SR. 2011. Accelerated profile HMM searches. *PLoS Computational Biology* 7:e1002195.
82. Hyatt D, Chen G-L, Locascio PF, Land ML, Larimer FW, Hauser LJ. 2010. Prodigal: prokaryotic gene recognition and translation initiation site identification. *BMC Bioinformatics* 11:119.
83. Larsson A. 2014. AliView: A fast and lightweight alignment viewer and editor for large datasets. *Bioinformatics* 30:3276–3278.
84. Edgar RC. 2004. MUSCLE: A multiple sequence alignment method with reduced time and space complexity. *BMC Bioinformatics* 5:113.

85. Han L, Liu Y, Li C, Zhao D. 2015. Cloning, expression, characterization and mutational analysis of the *tfdA* gene from *Cupriavidus campinensis* BJ71. *World Journal of Microbiology and Biotechnology* 31:1021–1030.
86. Hogan DA, Smith SR, Saari EA, McCracken J, Hausinger RP. 2000. Site-directed mutagenesis of 2,4-dichlorophenoxyacetic acid/ α -ketoglutarate dioxygenase. Identification of residues involved in metallocenter formation and substrate binding. *Journal of Biological Chemistry* 275:12400–12409.
87. Stamatakis A. 2014. RAxML version 8: A tool for phylogenetic analysis and post-analysis of large phylogenies. *Bioinformatics* 30:1312–1313.
88. Gonod LV, Martin-Laurent F, Chenu C. 2006. 2,4-D impact on bacterial communities, and the activity and genetic potential of 2,4-D degrading communities in soil. *FEMS Micro. Eco.* 58:529–537.
89. Gazitúa MC, Slater AW, Melo F, González B. 2010. Novel α -ketoglutarate dioxygenase *tfdA*-related genes are found in soil DNA after exposure to phenoxyalkanoic herbicides. *Environ Microbiol* 12:2411–2425.
90. Cantrell K, Fedarko MW, Rahman G, McDonald D, Yang Y, Zaw T, Gonzalez A, Janssen S, Estaki M, Haiminen N, Beck KL, Zhu Q, Sayyari E, Morton JT, Armstrong G, Tripathi A, Gauglitz JM, Marotz C, Matteson NL, Martino C, Sanders JG, Carrieri AP, Song J, Swafford AD, Dorrestein PC, Andersen KG, Parida L, Kim H-C, Vázquez-Baeza Y, Knight R. 2021. EMPress Enables Tree-Guided, Interactive, and Exploratory Analyses of Multi-omic Data Sets. *mSystems* 6:1–10.

Chapter 4

Aquatic transformation of the novel herbicide florpyrauxifen-benzyl generates more persistent degradation product florpyrauxifen

4.1 Details on Collaboration

Chapter 4 is a collaboration between Amber White, Sydney Van Frost, Angela Magness, Josie Jauquet, Katherine McMahon, and Christina Remucal. A.W. designed the project structure and goals. A.W., S.V.F., A.M., and J.J. carried out the field work and laboratory work experiments. A.W. wrote the manuscript with input from K.M. and C.R.

4.2 Abstract

The transformation of polar organic compounds can produce multiple transformation products with unknown the toxicity and persistence. Here, we investigated the photodegradation, biodegradation, and hydrolysis of the herbicide florpyrauxifen-benzyl (FPB) in field and laboratory experiments as well as formation and fate of several transformation products. FPB persisted 5 to 7 days after application in five Wisconsin lakes with an in-lake half-life of < 2 days. The transformation product florpyrauxifen was detectable for 20-30 days post-FPB application at high conversion rates from FPB to the product florpyrauxifen. Paired laboratory studies demonstrated that FPB is degraded to florpyrauxifen via hydrolysis, and that photodegradation transformation pathways generate unique transformation products not found in the field campaign.

Mass balance calculations found that FPB can be completely hydrolyzed to florpyrauxifen and the microbially degraded to X11966341, which is further degraded into an unknown product. Additional bulk carbon analyses of surface water during treatments were used to characterize inert herbicide formulation components, which had a quantifiable impact on whole-lake carbon concentration and composition. This is the first reported quantification of FPB and florpyrauxifen in aquatic environments, as well as measurements of transformation processes affecting both FPB and florpyrauxifen. These results show how the combined use of field and laboratory studies can be used to identify transformation products that warrant further investigation for polar organic compounds.

4.3 Introduction

The accumulation of micropollutants in the aquatic environment poses a risk to the health of aquatic ecosystems.^{1,2} The mixture of organic chemicals found in the aquatic environment contains intentionally released compounds (e.g., pesticides), unintentionally released compounds (e.g., pharmaceuticals and personal care products from wastewater treatment facilities), and their products produced by biotic and abiotic degradation. Additionally, these transformation products may retain or increase persistence or toxicity once in the environment, suggesting transformation does not lead to a reduction of toxicity of aquatic micropollutants.³⁻⁶

However, the laboratory studies used to investigate the transformation of pesticides and other polar organic compounds for regulatory risk assessment often fall short of accurately replicating environmental conditions.⁷⁻¹⁰ Photodegradation studies do not require modeling for all compounds under environmental conditions or quantification of potential indirect photodegradation, or which can be an important environmental pathway.¹¹⁻¹³ Biodegradation is

isolated to either water or sediment microbial communities, which oversimplifies sediment-water dynamics and disrupts the ambient nutrients, oxygen, and light trends the microbial populations may have been conditioned before.¹⁴⁻¹⁷ Techniques used to keep incubations oxygenated, such as shaking or stirring sediments, as well as high ratios of sediment to water can influence how chemicals of interest and their degradation products sorb in a way that is not environmentally relevant.^{14,18,19}

Laboratory transformation studies are designed to inform regulation of the compound of concern and are not typically conducted to study the transformation product behavior.²⁰ Furthermore, commercial solutions of these chemicals are applied in a mixture of active ingredients that carry out the specific function of the product and inactive ingredients that support the delivery or effectiveness of the product and can change the environmental fate of the compound.²¹⁻²⁴ These inactive ingredients are often also not subjected to as strict regulatory testing and simply listed as “inert” or “other” on product labels.^{25,26} Thus, the emphasis of regulatory study on the active ingredient may inadequately describe the complete fate and transport of the actual applied solution.

Florpyrauxifen-benzyl (FPB) is an auxin mimic herbicide registered in 2017 predominantly for use in aquatic environments.²⁷ Commonly used to combat hydrilla, Eurasian watermilfoil, and other broadleaf plants, FPB was developed to address increasing tolerance to previously used herbicides²⁸ such as 2,4-D, an auxin mimic targeting different binding sites than FPB,²⁹⁻³² and fluridone, a photobleaching agent.³³⁻³⁵ FPB is an active ingredient in at least seven commercial formulations ranging from 1.3 - 26.2% FPB in each formulation.³⁶⁻⁴² Interestingly, aquatic application of FPB in spot treatments is allowed up to 114 nM (i.e., 50 ppb) despite a low solubility

of 34 nM (i.e., 15 ppb),^{27,40,43} suggesting the inactive ingredients help increase the solubility of FPB.

FPB is understudied in laboratory and field settings with most existing information about the fate and transformation reported in EPA registration, product labels, and SDS sheets, and promotional materials. FPB is highly sorptive with a octanol-water partitioning coefficient ($\log K_{ow}$) of 5.5 and partitioning coefficient ($\log K_{oc}$) of 4.53 mL g⁻¹.⁴⁴ FPB is expected to undergo rapid photodegradation ($t_{1/2} = 0.07$ days at 40 °N latitude in pH 4) and has negligible volatilization.⁴⁴ Hydrolysis at pH 7 is slow ($t_{1/2} = 111$ days), but significantly faster at pH 9 ($t_{1/2} = 1.3$ days).⁴³ Aerobic and anaerobic microbial degradation is expected to be faster at low and neutral pH with aquatic metabolism half-lives of 2-6 days.^{27,44} Thus, the existing laboratory data suggest rapid transformation of FPB via several pathways in aquatic environments.

Five degradation products of FPB have been identified in laboratory studies investigating photo- and biodegradation (**Table C.1, Figure 4.7**).^{27,45,46} The primary degradation product in water-sediment systems is florpyrauxifen, which is also herbicidal.^{46,47} Authentic standards and common names for the remaining four products are not available. They are instead identified as X11966341 and X12300837, which are also likely to form in water-sediment systems, and X12131932 and X12393505 which are expected to form predominantly through photodegradation.⁴⁶ The suggestion that different pathways form different products means transformation mechanisms could be identified in the environment based on product formation but has yet to be tested. Importantly, the lack of field data quantifying transformation of FPB or the persistence of these potential degradation products makes decision making difficult for resource managers.⁴⁸

The goal of this study was to use the aquatic herbicide FPB as a tool to study micropollutant transformation in aquatic environments with competing transformation mechanisms through combined laboratory and field degradation studies. We also investigated the bulk composition and fate of the inactive portions of herbicide solution in the field campaign due to the high fraction of these ingredients (97.3%)⁴⁰ to understand how the inactive ingredients transform in the aquatic environment. These two goals combined will provide insight to the complete transformation of the end-use FPB formulation and potential effects on lake chemistry from the active ingredients, inert ingredients, and transformation products.

4.4 Materials and Methods

4.4.1 Chemicals

Chemicals were used as received and are described in detail in **Section C.1**. All commercial FPB solutions used in lake treatments were ProcellaCOR EC, which consists of 2.7% FPB and 97.3% inactive ingredients (2.1% ethylhexanol, 0.9% methanol, 94.3% unknown).^{40,43} ¹³C-labeled florpyrauxifen-benzyl and florpyrauxifen, as well as unnamed potential degradation products X12300837, X11966341, X12131932, and X12393505, were obtained from Corteva Agriscience. Ultrapure water (18.2 MΩ cm) was obtained from an ultrapure water purification system.

4.4.2 FPB Sample Preservation and Processing

Water samples for FPB analysis were preserved with methanol (50:50 methanol:water ratio) and 0.1% formic acid prior to syringe filtering through a 0.22 μm PES filter. A ¹³C-labeled florpyrauxifen-benzyl internal standard was added at 1 ppb (field campaign) or 5 ppb (hydrolysis and microcosm experiments) to account for loss during processing and storage.

4.4.3 Field Sampling

Five FPB treatments were studied during May-August 2021 and 2022 (**Table 4.1, Figure C.1**). These treatments applied FPB to areas of high-density Eurasian watermilfoil but had the potential to mix completely throughout the lake. Lakes were selected in collaboration with the Wisconsin Department of Natural Resources (WIDNR) to study lakes with potential lake wide FPB concentrations high enough to detect several orders of magnitude of loss.

Table 4.1. Summary of sampled lakes including waterbody identification code (WBIC), herbicide application area, treatment date, target concentration, and treatment history. Trophic status is designated as eutrophic (E), mesotrophic (M), or oligotrophic (O). Target 2,4-D concentration is from treatment permit application. When not stated on permit application, target concentration was calculated from lake/bay volume and amount of herbicide applied as listed on treatment record.

Lake (WBIC)	Herbicide application area (m ²)	Lake Surface area (m ²)	Trophic Status	Treatment Date	Water temp (°C)	pH	Potential lake wide conc. (nM)/(ppb)
South Twin Lake 31623700	234,718	2,541,000	O	June 9th, 2021	24	8.6	0.93/0.41
Muskellunge Lake 1596600	80,128	1,093,000	E	June 23 rd , 2021	24	7.2	0.48/0.21
Silver Lake 555700	60,703	1,283,000	O-M	June 23 rd , 2021	22	7.2	0.36/0.16
Lilly Lake 740900	42,492	343,983	O	May 23 rd , 2022	17	8	2.16/0.95
Kettle Moraine Lake 43900	72,843	845,793	M	June 3 rd , 2022	21	8.8	1.28/0.56

Pretreatment surface water and sediment were collected from the epilimnion and nearshore area ≤ 2 hours prior to treatment and stored at 4°C until processing (**Section C2**). Pretreatment samples were used for bulk water chemistry measurements (**Section C3**), photochemical irradiations (**Section C4**), microcosm incubations (**Section C5**), and hydrolysis experiments (**Section C6**). Water samples were collected at three sites on each lake, with at least one site in treatment area, one outside of treatment area (i.e., not intended to be treated) to monitor advective transport out of treatment area, and one site at the deepest point of the lake. Samples were collected immediately after FPB application (<1 hour after application) and at 3- to 4-hour intervals for 12 hours after treatment, every 1 to 2 days after treatment for one week after treatment, and then weekly thereafter. Additional depth discrete samples were collected with a Van Dorn sampler at 2 or 3 m intervals the deep hole of Muskellunge and Silver Lakes. At each sampling event, surface water was analyzed for all six described compounds. Additional samples not preserved with methanol were collected for organic carbon analysis and UV-vis spectroscopy.

Sediment for sorption analysis was collected by Eckman dredge or hand-coring at the nearshore site (**Section C2**). Samples collected during the treatment were stored on ice and in the dark until processing, typically on site (i.e., within 1 hour of collection) but no more than 24 hours after collection and preserved with methanol and formic acid as described above.

4.4.4 Photochemical Irradiation Experiments

Photodegradation experiments were conducted in a Rayonet merry-go-round photoreactor equipped with sixteen bulbs that emit light at 311 nm (± 22 nm width at half-max), which is within the absorbance spectra of FPB (**Figure C2**), to quantify direct and indirect FPB photodegradation. Irradiation experiments in borosilicate glass tubes were conducted in triplicate using 45 nM (10

ppb) FPB in buffered (pH 7, 10 mM phosphate buffer) ultrapure water (direct photodegradation) or 3 mg-C L⁻¹ lake water (indirect photodegradation) alongside dark controls. Light intensity during the experiment was quantified using 2-nitrobenzaldehyde⁴⁹ as a chemical actinometer. This FPB concentration is representative of the maximum FPB application concentration in spot treatments.

The direct quantum yield of FPB was calculated relative to the actinometer as described previously.^{7,50–52} The calculated quantum yield was combined with solar irradiance modeling using the Simple Model of Atmospheric Transfer of Sunshine (SMARTS)⁵³ to calculate FPB half-lives in sunlight (**Section C4**).

4.4.5 Microcosm Incubations

Water and sediment were collected from two study lakes (Kettle Moraine and Lilly Lakes) in the field campaign for microcosm biodegradation studies of FPB and florpyrauxifen (**Section C5**). Glass 4 L amber bottles were used to reduce sorption. Microcosms were stored at room temperature (21–28 °C) in the Water Science and Engineering Laboratory in Madison, WI. Degradation by the water column microbial community was quantified in triplicate microcosms with unfiltered lake water (3 L) while degradation by the sediment microbial community was quantified in microcosms with filtered lake water (2 L) and sediment (1 kg). Abiotic loss processes were assessed in control microcosms with filtered lake water (2 L). Microcosms were incubated with 45 nM (10 ppb). Samples were collected for up to 150 days, preserved as described above, and analyzed for FPB and five degradation products.

4.4.6 Hydrolysis Experiment

Ultrapure water and water from five study lakes was spiked at 45 nM and buffered at pH 4-10 (ultra-pure water) or ambient pH (study lakes, 0.45 μ m filtered) using 10 mM acetate (pH 4-5), phosphate (6-7), or borate buffer (pH 8-10). Triplicate 250 mL glass amber bottles were stored at room temperature (20-25 °C) in the dark and sampled at a regular frequency, ranging from every three hours for high pH conditions to weekly/biweekly for low pH conditions. Samples were collected for up to 100 days, preserved as previously above, and analyzed for FPB and degradation products using liquid chromatography tandem mass spectrometry (LC-MS/MS).

4.4.7 Analytical Methods

FPB, floryrauxifen, ^{13}C -FPB, ^{13}C -floryrauxifen, X12300837, X11966341, X12131932, and X12393505 were measured using liquid LC-MS/MS. 2-Nitrobenzaldehyde was quantified using high-performance liquid chromatography using a diode-array detector. Ultraviolet-visible light spectra for each lake were collected from 200-800 nm to calculate specific absorbance at 254 nm (SUVA_{254})⁵⁴ and the ratio of absorbance 250 nm to 365 nm ($E_2:E_3$).⁵⁵ Dissolved organic carbon concentrations were quantified using a Shimadzu total organic carbon analyzer. Methods details are provided in **Section C7**.

4.4.8 Mass Balance Calculations

A mass balance was carried out to calculate the recovery of FPB as a degradation product in both the lake treatments and hydrolysis experiment. For the lake treatments, an estimate of time of lake mixing, specifically when lake wide concentrations began to stabilize, was made within

the first 12-48 hours based on [FPB] concentrations at all three sampling sites in a lake (**Figures C.8-C.12**). Percent recovery was calculated using Equation 4.1:

$$\% \text{FPB}_{\text{lake}} \text{ recovery} = \frac{[\text{FPB}]_{\text{mixed}} + [\text{product(s)}]_{\text{mixed}}}{\text{Expected lake wide } [\text{FPB}]}$$
 Eq. 4.1

where $[\text{FPB}]_{\text{mixed}}$ is the average of [FPB] at all sampling stations and $[\text{product(s)}]_{\text{mixed}}$ is the average concentration of any degradation product at all three stations found in the lake at the time of mixing. The expected lake wide [FPB] is found on the herbicide treatment plan or calculated using lake volume⁵⁶ and mass of FPB applied from treatment record.

For the hydrolysis experiments, FPB recovery was calculated using Equation 4.2:

$$\% \text{FPB}_{\text{hydrolysis}} \text{ recovery} = \frac{[\text{florpyrauxifen}]_t}{[\text{FPB}]}$$
 Eq. 4.2

where $[\text{florpyrauxifen}]_t$ is florpyrauxifen at time t normalized to the initial [FPB] added to the reactor.

4.5 Results and Discussion

4.5.1 FPB Degradation and Florpyrauxifen Formation in Lakes

FPB was quantified in five Wisconsin lakes undergoing treatments (**Table 4.1, Figure C.1**). [FPB] ranged from < 0.07 to 32 nM and was below the detection limit (LOD = 0.07 nM) after day 7. [FPB] in treatment areas immediately after treatment reached up to 32 nM, which is close to the solubility of 34 nM.⁴⁴ However, within 4-6 hours after treatment, FPB quickly moved from the site of application to the non-treated sites of all lakes except Kettle Moraine (**Figure 4.1a, 4.2a, C.8-C.12**). This movement of FPB from the treatment area to all other sites demonstrates that FPB does not remain localized to the treatment area even within 6 hours after treatment, suggesting appropriate dosing measures and considerations of non-target impacts should be made

for the whole lake. Advective transport occurs rapidly over the first 12-48 hours after treatment, after which a lake-wide homogenous concentration is achieved (**Figure C.8-C.12**). FPB half-lives are estimated using lake-wide average [FPB] and visually estimating when a consistent loss occurs over one half-life (i.e., concentrations appear mixed throughout the lake), and range <1 day to 3 days (**Figure 4.1a, Table 4.2**).

Table 4.2. Half-lives of FPB in field study and laboratory experiments.

Lake	In lake recovery of FPB	Lake half-life (days)	Photodeg. Half-life (days)	Microcosm half-life (days)			Hydrolysis half-life (days)
				Abiotic	Water only	Water-Sediment	
South Twin Lake	160%	1	0.08	-	-	-	5.5
Muskellunge Lake	112%	2	0.08	-	-	-	14
Silver Lake	126%	3	0.08	-	-	-	18
Lilly Lake	103%	0.17	0.08	6.6	7.3	2.5	n/a
Kettle Moraine Lake	257%	1	0.08	6.5	8.5	1.8	n/a

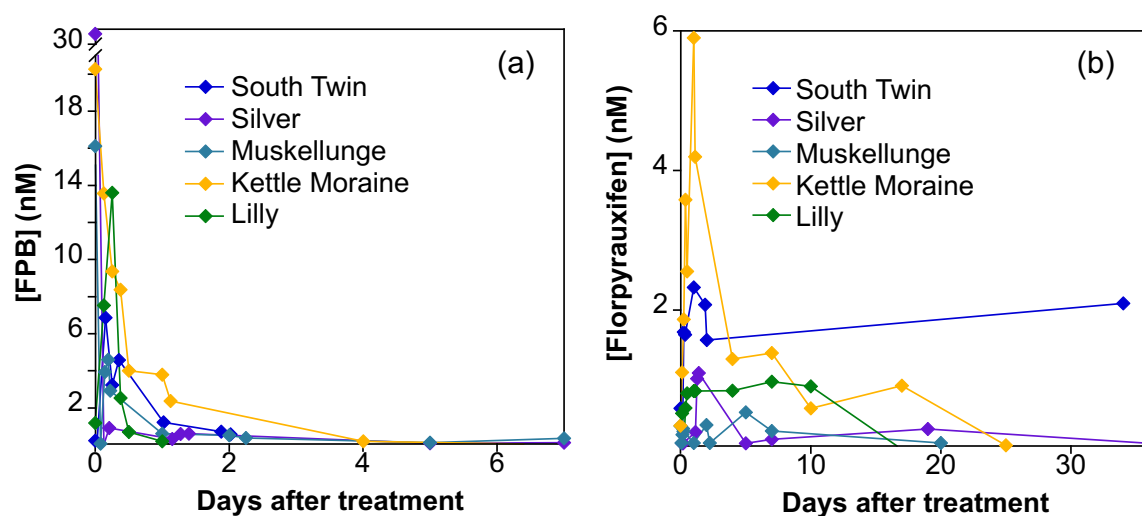


Figure 4.1. (a) [FPB] and (b) [florpyrauxifen] in the treatment zone of all treated lakes.

While advective transport is important in initial loss of FPB from the treatment area, the degradation product florpyrauxifen is generated nearly immediately after FPB treatment, suggesting transformation is occurring on the same timescale as physical transport. [Florpyrauxifen] ranges < 0.09 to 3 nM in all lakes and persists 2-3 times as long in each lake as FPB (**Figure 4.1b** and **4.2b**). The only other degradation product detected was X11966341 starting at days 4 and 7 in Kettle Moraine (**Figure 4.2b**) and Lilly Lakes (**Figure C.12**) respectively, which persisted until 25 days after treatment.

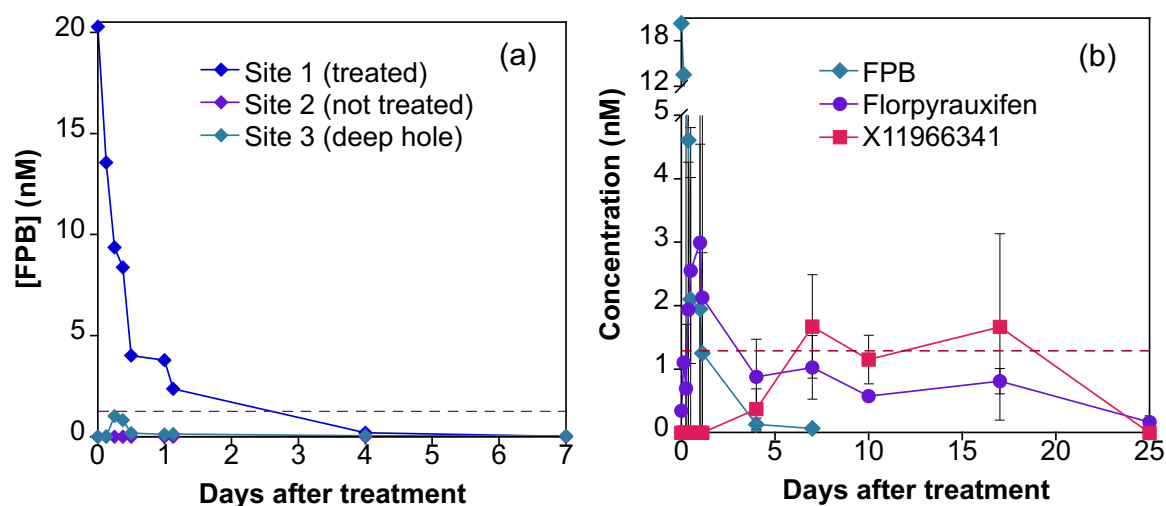


Figure 4.2. (a) [FPB] at three sites and (b) epilimnion wide average [FPB], [florpyrauxifen], and [X11966341] in Kettle Moraine Lake. Error bars in (b) represent standard deviation of all epilimnion samples.

The magnitude of florpyrauxifen accumulation in the lakes suggests florpyrauxifen is the primary environmental degradation product and a large proportion of the added FPB is converted to florpyrauxifen in the early stages of treatment. Mass balance calculations using Equation 4.1, epilimnion-wide average [FPB] and [florpyrauxifen] and expected lake-wide [FPB] based on added herbicide were used to calculate a recovery of FPB 12-48 hours after treatment in all 5 lakes. We calculated a recovery range of 103-257%, with an average recovery of 151% (**Table 4.2**).

Kettle Moraine Lake had the highest recovery of 257%, but also did not experience complete mixing throughout the waterbody (**Figure 4.2a**) which likely caused the epilimnetic volume used in the calculation to be inaccurate and excessively overestimate recovery. While these calculations all overestimate the expected lake-wide concentration, this is likely due to averaging across the epilimnion while FPB and florpyrauxifen are both still mixing throughout the waterbody. Interestingly, florpyrauxifen accounts for 48% of added FPB 19 days after treatment in Silver Lake and 56% of added FPB 20 days after treatment in Muskellunge Lake. Thus, we conclude that the primary environmental transformation product in aquatic systems is florpyrauxifen (**Figure 4.7**) and predict a complete transformation of FPB to florpyrauxifen is possible based on these calculations. However, the formation and persistence of florpyrauxifen in the lakes alone cannot be used to identify the transformation pathway.

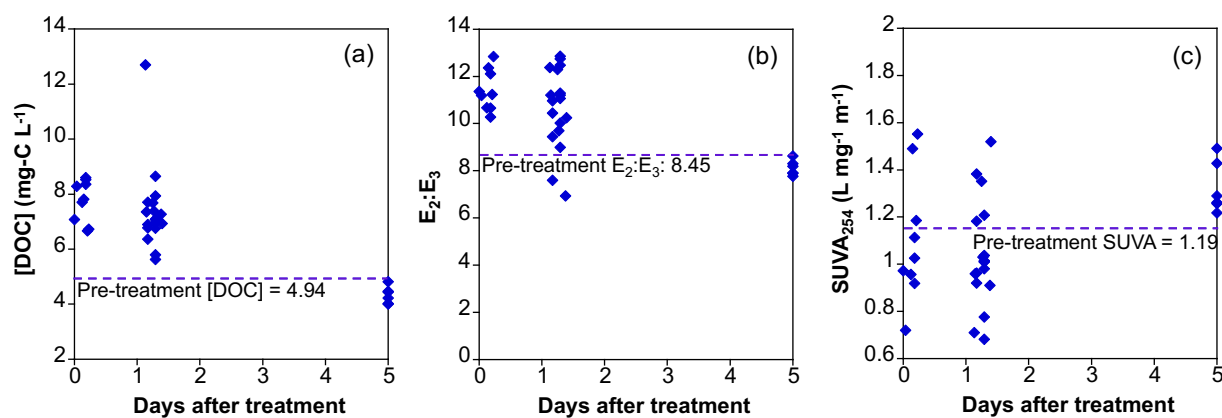


Figure 4.3. Silver Lake (a) [dissolved organic carbon] (DOC), (b) ratio of absorbance at 265 and 350 nm (b), and (c) SUVA₂₅₄ during 2021 herbicide treatment. Purple dashed lines represent pretreatment values of 4.94, 8.5, and 0.8 for [DOC], E₂:E₃, and SUVA₂₅₄ respectively.

While FPB and florpyrauxifen are present in part-per-billion concentrations, surface water dissolved organic carbon (DOC) changes by several parts-per-million during the treatment (**Figure 4.3**). Silver Lake had 4.94 mg-C L⁻¹ prior to treatment but experiences elevated DOC

concentrations ranging from 5.38 to 8.65 mg-C L⁻¹ during the first 48 hours after treatment at both the treated and non-treated sites. E₂:E₃ (**Figure 4.3b**), which is inversely related to apparent molecular weight,^{55,57} increases from 8.45 before treatment to 8.9 to 12.8 during the same period. Similarly, SUVA₂₅₄ (**Figure 4.3c**), an indicator of aromaticity,⁵⁴ decreases from 1.89 to 0.68 L mg⁻¹ m⁻¹. Combined, the increases in [DOC] and E₂:E₃ and decrease in SUVA₂₅₄ suggests the inactive ingredient of the applied herbicide product contains a high concentration of small, aliphatic organic compounds. The ProcellaCOR EC SDS document describes as ethylhexanol and methanol as two components of the full herbicide mixture, which is consistent with these bulk carbon composition measurements. However, these two compounds only make up 3% of the whole solution while another 94% is unknown. The remaining solution is likely additional short chain carbons, but a full identification is beyond the scope of this paper. While FPB and florpyrauxifen persist for days and weeks, respectively, [DOC] returned to pre-treatment levels approximately 2-5 days after treatment, suggesting any effects of the added carbon-solution are transient. Combined, this data but illustrates three different fate and transport scenarios (i.e., FPB degradation, florpyrauxifen generation, and DOC concentration and composition changes) associated with the application of one mixed herbicide solution, of which differently regulatory/investigative processes were applied to each component of the product despite a measurable and likely compounding change to the lake by all three components.

The field data demonstrates that FPB is subject to both advective transport and degradation on similar timescales once in aquatic systems. However, the field data alone cannot be used to identify what transformation pathways generate florpyrauxifen or X11966341. Laboratory studies isolating photodegradation, biodegradation, and hydrolysis of FPB were used to identify

transformation rates and additional products for these reactions in a controlled setting to identify what process(es) are dominant in lakes.

4.5.2 Photochemical Irradiations and Environmental Photodegradation Modeling

FPB undergoes direct photodegradation under 311 nm irradiation with an observed first-order loss rate constant of $(1.0 \pm 0.1) \times 10^{-2} \text{ s}^{-1}$ ($t_{1/2} = 70$ seconds; **Figure C.3**), which corresponds to a quantum yield (Φ) of $(2.3 \pm 0.3) \times 10^{-2}$, which is the first reported quantum yield for this compound. The observed photodegradation rate constants in the presence of dissolved organic matter were slower than the direct photodegradation rate constant with an average value of $(7.5 \pm 0.6) \times 10^{-3} \text{ s}^{-1}$ ($t_{1/2} = 93$ seconds) after correcting for light screening, suggesting that indirect photodegradation is negligible. Furthermore, the slower photodegradation rate in the presence of lake water may be due to the dissolved organic matter acting as an antioxidant.⁵⁸⁻⁶⁰ Thus, direct photodegradation is dominant in aquatic environments.

Irradiation of FPB produced two degradation products: X12131932 and X12393505 (**Figure 4.4** and **Figure 4.7**), which is consistent with the European Food Safety review document.⁴⁶ Interestingly, photodegradation of FPB did not generate florpyrauxifen or X11966341, which were the two measurable environmental degradation products (**Figure 4.1** and **Figure 4.2**)⁴⁶ and X1239505 is only generated in lake water irradiations (**Figure 4.4c**). However, both products appear to undergo photodegradation on similar timescales as FPB, suggesting they may degrade too quickly to accumulate in the environment (**Figure 4.4b** and **Figure 4.4c**).

Modeling of *in situ* depth integrated photodegradation using sunlight intensity from Vilas County, WI at noon on June 9th, 2019 (12 hours of sunlight a day) estimates a half-life of 1.9 hours (0.08 days), which is consistent with registration documentation reports of 0.07 days (**Section**

C.4).^{43,44,61} Despite this rapid predicted lake photodegradation rate, field observations did not find an accumulation of either of the photodegradation products or direct evidence of in-lake photodegradation. This suggests photodegradation is not responsible for the transformation of FPB to florpyrauxifen, the primary environmental degradation product identified.

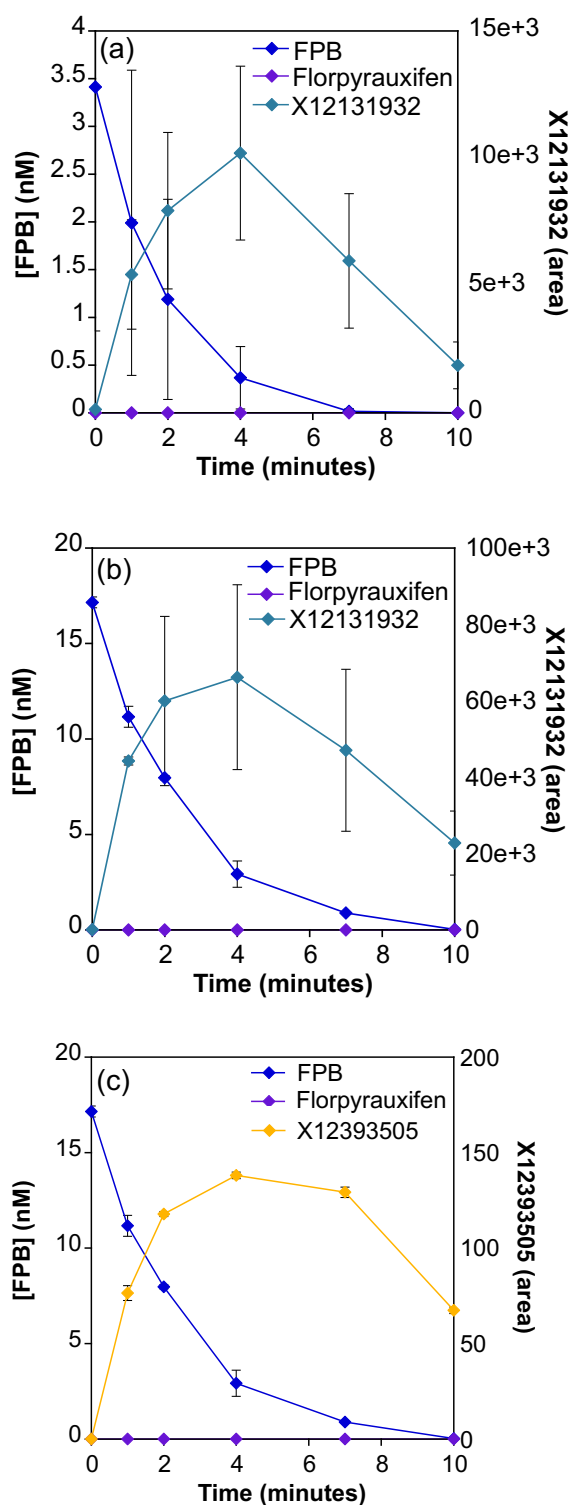


Figure 4.4 311 nm irradiation of FPB in (a) ultrapure water and (b,c) Muskellunge Lake water. [FPB] and [florpyrauxifen] on left axis and degradation products (b) X12131932 and (c) X12393505 on right axis, presented as area. Error bars represent standard deviation of triplicate samples.

4.5.3 Microcosm Incubations

FPB loss is observed in microcosm incubations under all control and experimental conditions (Table 4.2, Figure 4.5). Loss is fastest in the sediment-water microcosm incubations, while loss in the water-only microcosms (filtered and unfiltered water) were nearly the same for both lakes. All microcosms had loss of FPB, generation of florpyrauxifen, and loss of florpyrauxifen over 30-35 days. Loss in the microcosms followed pseudo-first order loss with no significant lag time and thus FPB half-life was calculated by finding the slope of the line of $\ln([FPB]_t/[FPB]_0)$ versus time (Figure C.4).

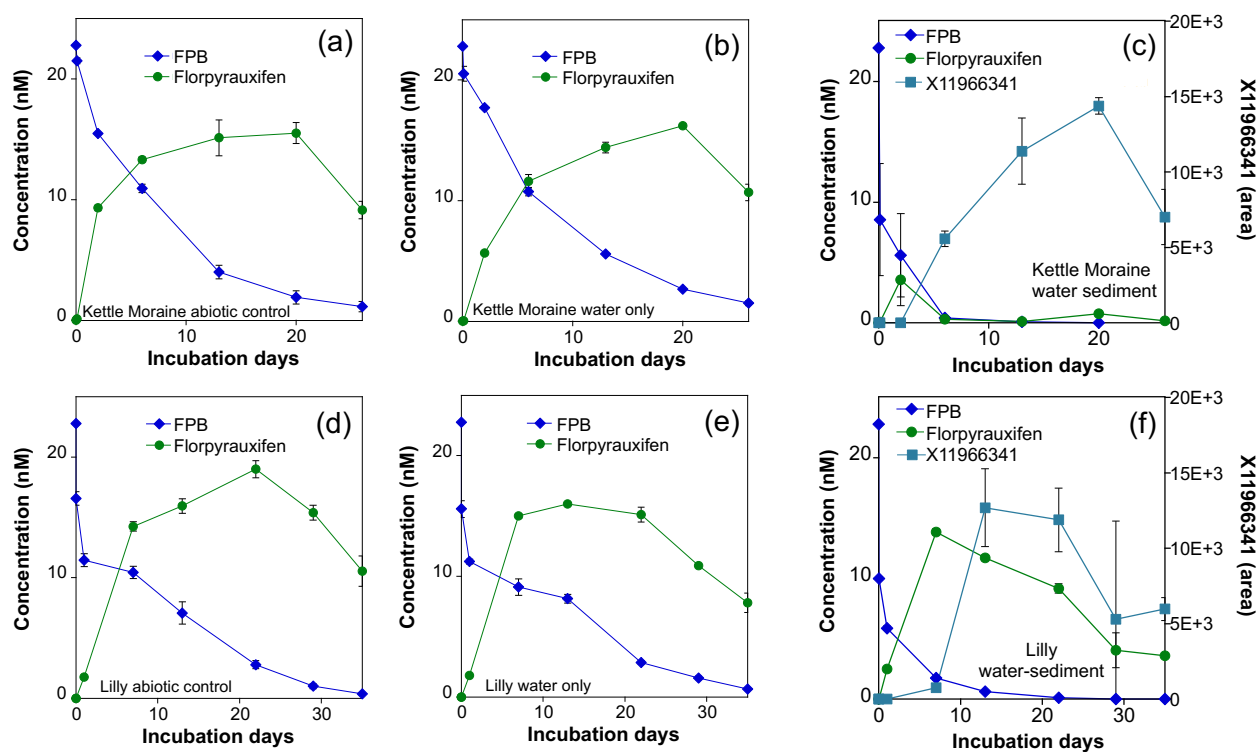


Figure 4.5. Microcosms incubated with FPB in (a-c) Kettle Moraine Lake and (d-f) Lilly Lake. (a, d) Abiotic controls are 0.2 μm filter sterilized, while (b, e) water only microcosms are unfiltered lake water and no sediment. (c, f) Sediment microcosms contain area of degradation product X11966341 due to issues with quantification on LC-MS/MS. Error bars represent the standard deviation of samples from triplicate microcosms.

Rapid sorption of FPB to solids is likely responsible for a decrease in initial [FPB] of 8.5 nM and 9.9 nM in microcosms constructed using sediments from Lilly and Kettle Moraine, respectively, from the spiked 23 nM. It is important to note that while wet sediment was used in this experiment, attempts to reduce water added to microcosms from the sediments were made by pouring off excess water as it settled out of sediments. FPB half-lives in the sediment-water microcosms were 2.5 and 1.8 days in Lilly and Kettle Moraine Lakes, respectively. Abiotic microcosms (**Figure 4.5a, 4.5d**) had an FPB half-life of 6.6 days for both Lilly and Kettle Moraine Lakes (**Table 4.2**). This is nearly the same as the unfiltered water incubations, which have an FPB half-life of 7.3 and 8.5 days in Lilly and Kettle Moraine Lakes (**Figure 4.5b, 4.5e**).

Given the predominance of florpyrauxifen in the lakes, a second set of microcosms were incubated with florpyrauxifen (**Figure C.5**). Since the florpyrauxifen microcosms have yet to experience the 2 logs of loss required for kinetic calculations, florpyrauxifen half-life is estimated by visually inspecting the graph and finding the time when [florpyrauxifen] decreases by half. Like the FPB microcosms, florpyrauxifen is lost in both the filtered water control and unfiltered water microcosms with similar half-lives (20-23 days in Kettle Moraine Lake and 15 days in Lilly Lake). The product X11966341 is also generated in the sediment microcosms, demonstrating that this compound is a biodegradation product of florpyrauxifen. Both FPB and florpyrauxifen degraded fastest in the sediment-water microcosms, likely due to higher microbe concentrations in the sediment, a result consistent with other polar organic compounds ^{7,10,18} that underscores the importance of using relevant microbial concentrations in laboratory experiments investigating micropollutant fate of saturated systems. ^{17,62}

In all microcosms, FPB degrades to florpyrauxifen. This degradation occurs at the same rate in abiotic and biotic water-only microcosms (**Table 4.2, Figure 4.5**), suggesting abiotic loss is an important transformation pathway for FPB. We hypothesized this is mostly likely a hydrolysis reaction due to 1) nearly complete conversion of FPB to florpyrauxifen ruling out significant sorption or volatilization from water, 2) use of glass amber incubation bottles and lack of photodegradation products, and 3) florpyrauxifen forming as a product is structurally consistent with the hydrolysis of a carboxylic acid esters, which is commonly susceptible to hydrolysis.⁶³

X11966341 was generated in both FPB and florpyrauxifen microcosms, but only in the presence of sediment (**Figures 4.5c, 4.5f, C5**). Thus, we hypothesized FPB degradation occurred in two steps in the sediment microcosm and lake: FPB to florpyrauxifen and then to X11966341 (**Figure 4.7**). If FPB was degraded into X11966341 without first degrading to florpyrauxifen, we would have seen an accumulation of X12300837 prior to the accumulation of X11966341 (potentially through hydrolysis of X12300837) but instead we saw florpyrauxifen first. Additionally, we only see the generation of X11966341 in the sediment microcosms in both FPB and florpyrauxifen microcosms, which suggests this is a biodegradation product generated by the sediment microbial community. We thus carried out hydrolysis experiments in ultrapure water and lake water to confirm the rate and product of FPB hydrolysis.

4.5.4 Hydrolysis of FPB

FPB hydrolysis rates were quantified in buffered ultrapure water from pH 4-10 and three lake waters over 65 days (**Figure 4.6a, C.6**). Hydrolysis rate increased with pH, suggesting a base catalyzed reaction. Our measured hydrolysis rates at low pH are much faster than current registration documentation (i.e., 37 days in this study versus 913 days in registration documents at

pH 4 and 18 days versus 111 days at pH 7) but were the same at pH 9 (i.e., 1.3 days).⁴³ Lakes typically have a pH of 6-8, which suggests that FPB applications in lakes with pH less than 8 would likely not undergo hydrolysis fast enough to disrupt the required exposure time of ~24 hours,^{47,64} but resource managers working in elevated pH environments should consider this degradation pathway more seriously.

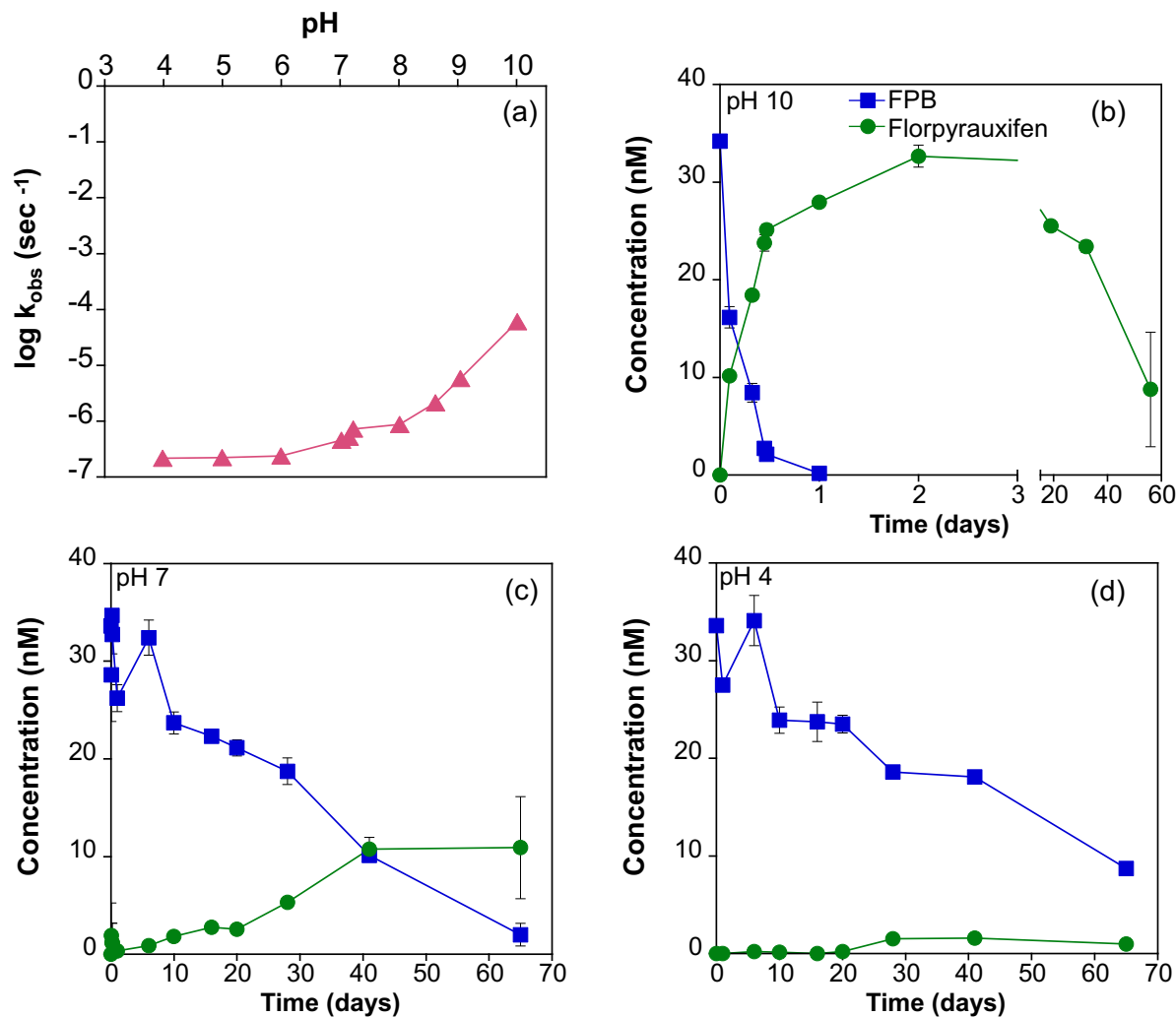


Figure 4.6. Observed (a) hydrolysis rates plotted against pH for all tested conditions and [FPB] and [florpyrauxifen] at (b) pH 10, (c) pH 7, and (d) pH 4. Error bars represent the standard deviation of samples taken from triplicate reactors.

Florpyrauxifen is the only degradation product detected during the hydrolysis experiments and accounts for 89% and 99% of added FPB at pH 9 and 10, respectively (**Figure 4.6c**, **Figure 4.6d**, **Figure C.6**). Interestingly, florpyrauxifen also degrades in the hydrolysis experiment, but no other product is measured. This suggests some additional abiotic process is driving the loss of florpyrauxifen. We hypothesize this is likely to be hydrolysis, even though florpyrauxifen does not have a functional group typically associated with hydrolysis,⁶³ and rather than volatilization or sorption due to a pK_a of 3.1 and a negative charge under our conditions (**Figure C.7**).

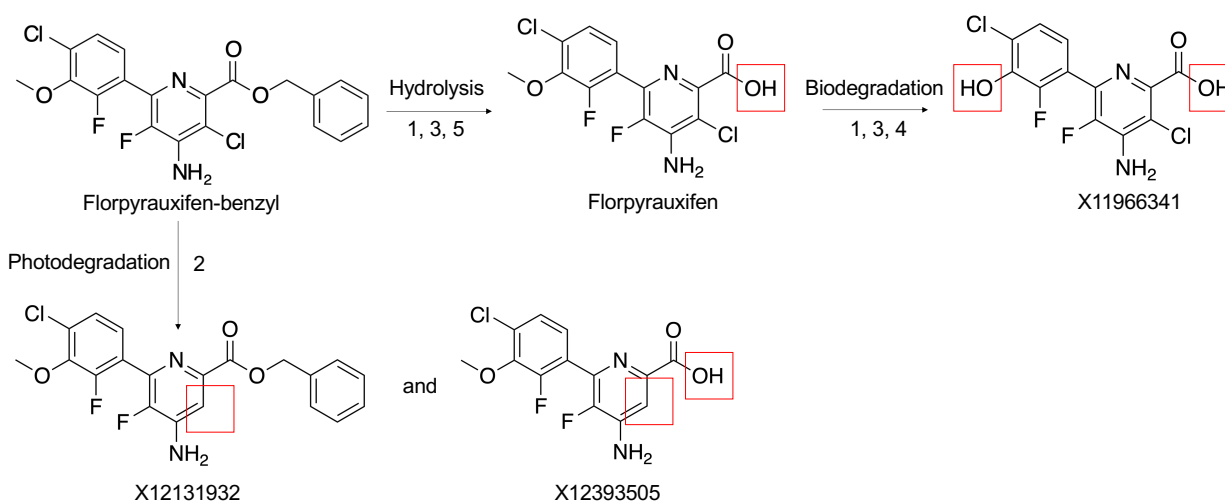


Figure 4.7. Proposed FPB degradation schematic in aquatic environments. Product identified in each reaction by number as follows: 1- field campaign; 2- photodegradation experiments; 3- FPB incubated microcosms; 4- florpyrauxifen incubated microcosm, 5- hydrolysis experiment. Red boxes represent changed functional group after reaction.

While the identification of florpyrauxifen in lakes suggests that hydrolysis is an important transformation pathway in aquatic environments, the FPB half-life observed in the field campaign and sediment microcosms is much shorter than the hydrolysis experiments and water-only microcosms (**Table 4.2**). For example, FPB half-life in Kettle Moraine is about 1 day in the lake and 1.8 days in the water-sediment suspension, but 6-8 days in the water only microcosms despite

a similar pH across all experiments. This discrepancy in half-life suggests the hydrolysis of FPB can be catalyzed through a mechanism not captured in the microcosm experiments or through sediment interaction.⁶⁵ Specifically, hydrolysis via aquatic plants as part of the uptake and toxicity mechanism has been described for both FPB and the predecessor to FPB, halauxifen-methyl, which suggests the rapid hydrolysis in the lakes could be due to uptake of FPB and release of florpyrauxifen by the targeted plant community.^{28,66}

Future investigation into the sorption of FPB to sediments is needed to provide additional detail in the mass balances described here. While lake mass balance calculations account for nearly all the added FPB (**Table 4.2**), the high K_{oc} and rapid sorption in the sediment-water microcosms suggests sorption could occur rapidly in aquatic systems, which have both sediments and suspended solids. Photodegradation experiments with florpyrauxifen will also provide transformation rates and degradation products of florpyrauxifen, which can contextualize florpyrauxifen degradation beyond the microcosms. While the microcosm and lake data suggest florpyrauxifen is degraded into X11966341 biotically, irradiation experiments will identify the rates and products of photodegradation for a comprehensive understanding of florpyrauxifen fate and transport, which is critical given the extended lifetime of florpyrauxifen in lakes.

4.6 Environmental Implications

We combined field and laboratory studies to investigate the fate and transport of an herbicide intentionally added to aquatic environments for the control of nuisance plants, including the degradation products formed *in situ* following treatment and the inactive components of the commercial herbicide solution. Our study combined kinetics and product tracking to determine the

mechanism responsible for degrading FPB into florpyrauxifen at nearly a 1:1 ratio in aquatic environments, as well as the biodegradation of florpyrauxifen into the product X11966341.

Our study demonstrates the limitations of laboratory experiments in predicting environmental fate of polar organic compounds. While photodegradation experiments and modeling predict rapid *in situ* photodegradation of FPB, the predominance of florpyrauxifen after treatment suggests a different mechanism is likely more dominant. Additionally, isolating different transformation pathways in laboratory experiments may miss combinations of transformation pathways that occur in the environment, such as the proposed biotically catalyzed hydrolysis of FPB to florpyrauxifen and subsequent microbial degradation of florpyrauxifen to X11966341.

Our results show that regulatory studies that only focus on the active ingredient of an intentionally applied chemical mixture may overlook the degradation products or inactive ingredients that have a measurable impact on water chemistry. While our study focused on the chemical fate and transport of these compounds, additional studies are needed to understand how the concentration and lifetime of these compounds can impact aquatic or plant life, which is beyond the scope of this paper. Additionally, more research is needed to investigate the effects of mixtures of compounds, such as combination herbicide treatments using triclopyr and FPB or wastewater treatment plant discharge that can have dozens of compounds present. As such, the current approach to regulatory studies relying on active ingredients alone should be revisited from a holistic environmental fate perspective.

4.7 Acknowledgements

The authors would like to thank Onterra, LLC., Lilly Lake Resort, Tiki Beach Resort on Kettle Moraine Lake, Camp Birch Knoll, and the homeowners and lake associations of all five

study lakes for their assistance carrying out sampling. The Wisconsin Department of Natural Resources provided immense logistical and technical support during treatments, especially Michelle Nault, Scott Van Egeren, and Ty Krajewski. Field equipment provided by University of Wisconsin-Madison Center for Limnology and Trout Lake Station. Funding provided by the Wisconsin Department of Natural Resources, National Science Foundation Graduate Research Fellowship Program (A.M.W.), Midwest Aquatic Plant Management Society, Anna Grant Birge Memorial Award (S.V.F.), and the United States Air Force (A.M.M.).

4.8 References

- (1) Schwarzenbach, R. P.; Escher, B. I.; Fenner, K.; Hofstetter, T. B.; Johnson, C. A.; von Gunten, U.; Wehrli, B. The challenge of micropollutants in aquatic systems. *Science*. **2006**, *313* (5790), 1072–1077. <https://doi.org/10.1126/science.1127291>.
- (2) Yang, Y.; Zhang, X.; Jiang, J.; Han, J.; Li, W.; Li, X.; Yee Leung, K. M.; Snyder, S. A.; Alvarez, P. J. J. Which micropollutants in water environments deserve more attention globally? *Environ. Sci. Technol.* **2022**, *56* (1), 13–29. <https://doi.org/10.1021/acs.est.1c04250>.
- (3) Sinclair, C. J.; Boxall, A. B. A. Assessing the ecotoxicity of pesticide transformation products. *Environ. Sci. Technol.* **2003**, *37* (20), 4617–4625. <https://doi.org/10.1021/es030038m>.
- (4) Tian, Z.; Zhao, H.; Peter, K. T.; Gonzalez, M.; Wetzel, J.; Wu, C.; Hu, X.; Prat, J.; Mudrock, E.; Hettinger, R.; Cortina, A. E.; Biswas, R. G.; Vinicius, F.; Kock, C.; Soong, R.; Jenne, A.; Du, B.; Hou, F.; He, H.; Lundeen, R.; Gilbreath, A.; Sutton, R.; Scholz, N. L.; Davis, J. W.; Dodd, M. C.; Simpson, A.; McIntyre, J. K.; Kolodziej, E. P. A ubiquitous tire rubber-derived chemical induces acute mortality in coho salmon. *Science*. **2021**, *371*, 185–189.
- (5) Cwiertny, D. M.; Snyder, S. A.; Schlenk, D.; Kolodziej, E. P. Environmental designer drugs: When transformation may not eliminate risk. *Environ. Sci. Technol.* **2014**, *48* (20), 11737–11745. <https://doi.org/10.1021/es503425w>.
- (6) Puhlmann, N.; Olsson, O.; Kümmerer, K. Transformation products of sulfonamides in aquatic systems: Lessons learned from available environmental fate and behaviour data. *Sci. Total Environ.* **2022**, *830*, 154744. <https://doi.org/10.1016/j.scitotenv.2022.154744>.
- (7) White, A. M.; Nault, M. E.; McMahon, K. D.; Remucal, C. K. Synthesizing laboratory and field experiments to quantify dominant transformation mechanisms of 2,4-dichlorophenoxyacetic acid (2,4-D) in aquatic environments. *Environ. Sci. Technol.* **2022**, *56* (15), 10838–10848. <https://doi.org/10.1021/acs.est.2c03132>.

- (8) Honti, M.; Fenner, K. Deriving persistence indicators from regulatory water-sediment studies - Opportunities and limitations in OECD 308 data. *Environ. Sci. Technol.* **2015**, *49* (10), 5879–5886. <https://doi.org/10.1021/acs.est.5b00788>.
- (9) Fenner, K.; Canonica, S.; Wackett, L. P.; Elsner, M. Evaluating pesticide degradation in the environment: blind spots and emerging opportunities. *Science*. **2013**, *341*, 752–758.
- (10) Zhi, H.; Miannecki, A. L.; Kolpin, D. W.; Klaper, R. D.; Iwanowicz, L. R.; LeFevre, G. H. Tandem field and laboratory approaches to quantify attenuation mechanisms of pharmaceutical and pharmaceutical transformation products in a wastewater effluent-dominated stream. *Water Res.* **2021**, *203*. <https://doi.org/10.1016/j.watres.2021.117537>.
- (11) McConville, M. B.; Mezyk, S. P.; Remucal, C. K. Indirect photodegradation of the lampricides TFM and niclosamide. *Environ. Sci. Processes Impacts*. **2017**, *19* (8), 1028–1039. <https://doi.org/10.1039/c7em00208d>.
- (12) McConville, M. B.; Cohen, N. M.; Nowicki, S. M.; Lantz, S. R.; Hixson, J. L.; Ward, A. S.; Remucal, C. K. A field analysis of lampricide photodegradation in Great Lakes tributaries. *Environ. Sci. Processes Impacts*. **2017**, *19* (7), 891–900. <https://doi.org/10.1039/c7em00173h>.
- (13) Remucal, C. K. The role of indirect photochemical degradation in the environmental fate of pesticides: A review. *Environ. Sci. Processes Imp.* **2014**, *16* (4), 628–653. <https://doi.org/10.1039/c3em00549f>.
- (14) Honti, M.; Hahn, S.; Hennecke, D.; Junker, T.; Shrestha, P.; Fenner, K. Bridging across OECD 308 and 309 data in search of a robust biotransformation indicator. *Environ. Sci. Technol.* **2016**, *50* (13), 6865–6872. <https://doi.org/10.1021/acs.est.6b01097>.
- (15) Li, J.; Shimizu, K.; Sakharkar, M. K.; Utsumi, M.; Zhang, Z.; Sugiura, N. Comparative study for the effects of variable nutrient conditions on the biodegradation of microcystin-LR and concurrent dynamics in microcystin-degrading gene abundance. *Bioresource Technology*. **2011**, *102* (20), 9509–9517. <https://doi.org/10.1016/j.biortech.2011.07.112>.
- (16) Trigo, A.; Valencia, A.; Cases, I. Systemic approaches to biodegradation. *FEMS Microbiology Reviews*. **2009**, *33* (1), 98–108. <https://doi.org/10.1111/j.1574-6976.2008.00143.x>.
- (17) Thouand, G.; Durand, M. J.; Maul, A.; Gancet, C.; Blok, H. New concepts in the evaluation of biodegradation/persistence of chemical substances using a microbial inoculum. *Front. Microbiol.* **2011**, *2*. 1-6. <https://doi.org/10.3389/fmicb.2011.00164>.
- (18) Seller, C.; Honti, M.; Singer, H.; Fenner, K. Biotransformation of chemicals in water-sediment suspensions: influencing factors and implications for persistence assessment. *Environ. Sci. Technol. Lett.* **2020**, *7* (11), 854–860. <https://doi.org/10.1021/acs.estlett.0c00725>.
- (19) Shrestha, P.; Junker, T.; Fenner, K.; Hahn, S.; Honti, M.; Bakkour, R.; Diaz, C.; Hennecke, D. Simulation studies to explore biodegradation in water-sediment systems: From OECD 308 to OECD 309. *Environ. Sci. Technol.* **2016**, *50* (13), 6856–6864. <https://doi.org/10.1021/acs.est.6b01095>.
- (20) Escher, B. I.; Fenner, K. Recent advances in environmental risk assessment of transformation products. *Environ. Sci. Technol.* **2011**, *45* (9), 3835–3847. <https://doi.org/10.1021/es1030799>.
- (21) Reinert, K. H.; Rodgers, J. H. Fate and persistence of aquatic herbicides. *Rev. of Environ. Cont. and Tox.* **1987**, 61–89. https://doi.org/10.1007/978-1-4612-4700-5_3.
- (22) Tominack, R. L. Herbicide formulations. *Clinical Toxicology* **2000**, *38* (2), 129–135.

- (23) Peterson, M. A.; McMaster, S. A.; Riechers, D. E.; Skelton, J.; Stahlman, P. W. 2,4-D past, present, and future: A review. *Weed Tech.* **2016**, *30* (2), 303–345. <https://doi.org/10.1614/wt-d-15-00131.1>.
- (24) Polli, E. G.; Alves, G. S.; de Oliveira, J. V.; Kruger, G. R. Physical–chemical properties, droplet size, and efficacy of dicamba plus glyphosate tank mixture influenced by adjuvants. *Agronomy* **2021**, *11* (7). <https://doi.org/10.3390/agronomy11071321>.
- (25) Cox, C.; Sorgan, M. Unidentified inert ingredients in pesticides: Implications for human and environmental health. *Environmental Health Perspectives* **2006**, *114* (12), 1803–1806. <https://doi.org/10.1289/ehp.9374>.
- (26) Straw, E. A.; Thompson, L. J.; Leadbeater, E.; Brown, M. J. F. Inert ingredients are understudied, potentially dangerous to bees and deserve more research attention. *Proc. R. Soc. B.* **2022**, *289*, 20212353. <https://doi.org/10.1098/rspb.2021.2353>.
- (27) USEPA. Final Registration Decision on the New Active Ingredient Florpyrauxifen-benzyl <https://www.regulations.gov/document/EPA-HQ-OPP-2016-0560-0065> (accessed 2022 -07 -25).
- (28) Epp, J. B.; Alexander, A. L.; Balko, T. W.; Buysse, A. M.; Brewster, W. K.; Bryan, K.; Daeuble, J. F.; Fields, S. C.; Gast, R. E.; Green, R. A.; Irvine, N. M.; Lo, W. C.; Lowe, C. T.; Renga, J. M.; Richburg, J. S.; Ruiz, J. M.; Satchivi, N. M.; Schmitzer, P. R.; Siddall, T. L.; Webster, J. D.; Weimer, M. R.; Whiteker, G. T.; Yerkes, C. N. The discovery of arylex™ active and rinskor™ active: two novel auxin herbicides. *Bioorganic and Medicinal Chemistry* **2016**, *24* (3), 362–371. <https://doi.org/10.1016/j.bmc.2015.08.011>.
- (29) Busi, R.; Goggin, D. E.; Heap, I. M.; Horak, M. J.; Jugulam, M.; Masters, R. A.; Napier, R. M.; Riar, D. S.; Satchivi, N. M.; Torra, J.; Westra, P.; Wright, T. R. Weed resistance to synthetic auxin herbicides. *Pest Mgmt. Sci.* **2018**, *74* (10), 2265–2276. <https://doi.org/10.1002/ps.4823>.
- (30) Richardson, R. J. Aquatic plant management and the impact of emerging herbicide resistance issues. *Weed Tech.* **2008**, *22* (1), 8–15. <https://doi.org/10.1614/wt-07-034.1>.
- (31) Moody, M. L.; Les, D. H. Evidence of hybridity in invasive watermilfoil (*Myriophyllum*) populations. *PNAS.* **2002**, *99* (23), 14867–14871. <https://doi.org/10.1073/pnas.172391499>.
- (32) Larue, E. A.; Zuellig, M. P.; Netherland, M. D.; Heilman, M. A.; Thum, R. A. Hybrid watermilfoil lineages are more invasive and less sensitive to a commonly used herbicide than their exotic parent (Eurasian watermilfoil). *Evolutionary Applications* **2013**, *6* (3), 462–471. <https://doi.org/10.1111/eva.12027>.
- (33) Berger, S. T.; Netherland, M. D.; MacDonald, G. E. Laboratory documentation of multiple-herbicide tolerance to fluridone, norflurazon, and topamazone in a hybrid watermilfoil (*Myriophyllum spicatum* × *M. sibiricum*) population. *Weed Sci.* **2015**, *63* (1), 235–241. <https://doi.org/10.1614/ws-d-14-00085.1>.
- (34) Netherland, M. D.; Jones, D. Fluridone-resistant hydrilla (hydrilla verticillate) is still dominant in the Kissimmee Chain of Lakes, FL. *Invasive Plant Science and Management.* **2015**, *8* (2), 212–218. <https://doi.org/10.1614/ipsm-d-14-00071.1>.
- (35) Mallory-Smith, C. A.; Retzinger Jr., E. J. Revised classification of herbicides by site of action for weed resistance management strategies. *Weed Tech.* **2003**, *17* (3), 605–619. [https://doi.org/10.1614/0890-037x\(2003\)017\[0605:rcohbs\]2.0.co;2](https://doi.org/10.1614/0890-037x(2003)017[0605:rcohbs]2.0.co;2).
- (36) SePRO. ProcellaCOR_SC--Label <https://www.sepro.com/aquatics/procellacor-product#LabelButton> (accessed 2022 -07 -25).

- (37) Corteva Agriscience. TerraVue specimen label <https://www.corteva.us/products-and-solutions/land-management/terravue.html> (accessed 2022 -07 -25).
- (38) Corteva Agriscience. Agixa Rinskor active label <https://www.corteva.com.au/products-and-solutions/crop-protection/agixa-rinskor-active.html> (accessed 2022 -07 -25).
- (39) Corteva Agriscience. Ubeniq® Rinskor® active www.corteva.com.au.
- (40) SePRO. ProcellaCOR EC https://sepro.com/Documents/ProcellaCOR_EC--Label.pdf (accessed 2022 -07 -25).
- (41) Corteva Agriscience. Loyant Label <https://www.corteva.us/products-and-solutions/crop-protection/loyant.html> (accessed 2022 -07 -25).
- (42) Corteva Agriscience. Novixid label https://s3-us-west-1.amazonaws.com/agrian-cg-fs1-production/pdfs/Novixid1d_with_Rinskor_active_Label.pdf (accessed 2022 -07 -25).
- (43) SePRO. ProcellaCOR EC SDS https://sepro.com/Documents/ProcellaCOR_EC--SDS.pdf (accessed 2022 -08 -15).
- (44) Corteva Agriscience. Rinskor Active Technical Bulletin https://www.corteva.com/content/dam/dpagco/corteva/global/corporate/general/files/active-ingredients/DF_Rinskor-TechBulletin_12-14-18.pdf (accessed 2022 -07 -25).
- (45) Battelle. Independent Laboratory Validation of a Dow AgroSciences Method for the Determination of XDE-848 Benzyl Ester and Five Metabolites (X11438848, X12300837, X11966341, X12131932 and X12393505) in Water https://www.epa.gov/sites/production/files/2017-09/documents/ilv_-_florpyrauxifen-benzyl_degradates_in_water_-_mrid_49677802.pdf. (accessed 2020 -05 -25).
- (46) Arena, M.; Auteri, D.; Barmaz, S.; Brancato, A.; Brocca, D.; Bura, L.; Carrasco Cabrera, L.; Chaideftou, E.; Chiusolo, A.; Civitella, C.; Court Marques, D.; Crivellente, F.; Ctverackova, L.; de Lentdecker, C.; Egsmose, M.; Erdos, Z.; Fait, G.; Ferreira, L.; Goumenou, M.; Greco, L.; Ippolito, A.; Istace, F.; Jarrah, S.; Kardassi, D.; Leuschner, R.; Lostia, A.; Lythgo, C.; Magrans, J. O.; Medina, P.; Mineo, D.; Miron, I.; Molnar, T.; Padovani, L.; Parra Morte, J. M.; Pedersen, R.; Reich, H.; Sacchi, A.; Santos, M.; Serafimova, R.; Sharp, R.; Stanek, A.; Streissl, F.; Sturma, J.; Szentes, C.; Tarazona, J.; Terron, A.; Theobald, A.; Vagenende, B.; van Dijk, J.; Villamar-Bouza, L. Peer review of the pesticide risk assessment of the active substance florpyrauxifen (variant assessed florpyrauxifen-benzyl). *EFSA Journal* **2018**, *16* (8). <https://doi.org/10.2903/j.efsa.2018.5378>.
- (47) Netherland, M. D.; Richardson, R. J. Evaluating sensitivity of five aquatic plants to a novel arylpicolinate herbicide utilizing an organization for economic cooperation and development protocol. *Weed Sci.* **2016**, *64* (1), 181–190. <https://doi.org/10.1614/ws-d-15-00092.1>.
- (48) Northeast Aquatic Research. Tuxedo Lake, Wee Wah, and Little Wee Wah Aquatic Plant Sampling Report http://www.tpfyi.com/docs/NEAR_Aquatic_Plant_SamplingReport_1-24-2020.pdf. (accessed 2020 -05 -25).
- (49) Galbavy, E. S.; Ram, K.; Anastasio, C. 2-nitrobenzaldehyde as a chemical actinometer for solution and ice photochemistry. *J. Photochem. Photobio. A: Chem.* **2010**, *209* (2–3), 186–192. <https://doi.org/10.1016/j.jphotochem.2009.11.013>.
- (50) Bulman, D. M.; P. Mezyk, S.; K. Remucal, C. The impact of pH and irradiation wavelength on the production of reactive oxidants during chlorine photolysis. *Environ. Sci. Technol.* **2019**, *53* (8), 4450–4459. <https://doi.org/10.1021/acs.est.8b07225>.

- (51) Berg, S. M.; Whiting, Q. T.; Herrli, J. A.; Winkels, R.; Wammer, K. H.; Remucal, C. K. The role of dissolved organic matter composition in determining photochemical reactivity at the molecular level. *Environ. Sci. Technol.* **2019**, *53* (20), 11725–11734. <https://doi.org/10.1021/acs.est.9b03007>.
- (52) McConville, M. B.; Hubert, T. D.; Remucal, C. K. Direct photolysis rates and transformation pathways of the lampricides TFM and niclosamide in simulated sunlight. *Environ. Sci. Technol.* **2016**, *50* (18), 9998–10006. <https://doi.org/10.1021/acs.est.6b02607>.
- (53) Gueymard, C. A. Interdisciplinary applications of a versatile spectral solar irradiance model: A review. *Energy* **2005**, *30* (9), 1551–1576. <https://doi.org/10.1016/j.energy.2004.04.032>.
- (54) Weishaar, J. L.; Aiken, G. R.; Bergamaschi, B. A.; Fram, M. S.; Fujii, R.; Mopper, K. Evaluation of specific ultraviolet absorbance as an indicator of the chemical composition and reactivity of dissolved organic carbon. *Environ. Sci. Technol.* **2003**, *37* (20), 4702–4708. <https://doi.org/10.1021/es030360x>.
- (55) Helms, J. R.; Stubbins, A.; Ritchie, J. D.; Minor, E. C.; Kieber, D. J.; Mopper, K. Absorption spectral slopes and slope ratios as indicators of molecular weight, source, and photobleaching of chromophoric dissolved organic matter. *Limnol. Oceanogr.* **2009**, *54* (3), 1023. <https://doi.org/10.4319/lo.2009.54.3.1023>.
- (56) Wisconsin DNR. Wisconsin Lake Finder. <https://dnr.wi.gov/lakes/findalake/> (accessed 2022-08-10).
- (57) Maizel, A. C.; Remucal, C. K. Molecular composition and photochemical reactivity of size-fractionated dissolved organic matter. *Environ. Sci. Technol.* **2017**, *51* (4), 2113–2123. <https://doi.org/10.1021/acs.est.6b05140>.
- (58) Wenk, J.; Graf, C.; Aeschbacher, M.; Sander, M.; Canonica, S. Effect of solution pH on the dual role of dissolved organic matter in sensitized pollutant photooxidation. *Environ. Sci. Technol.* **2021**, *55* (22), 15110–15122. <https://doi.org/10.1021/acs.est.1c03301>.
- (59) Wenk, J.; Canonica, S. Phenolic antioxidants inhibit the triplet-induced transformation of anilines and sulfonamide antibiotics in aqueous solution. *Environ. Sci. Technol.* **2012**, *46* (10), 5455–5462. <https://doi.org/10.1021/es300485u>.
- (60) Aeschbacher, M.; Graf, C.; Schwarzenbach, R. P.; Sander, M. Antioxidant properties of humic substances. *Environ. Sci. Technol.* **2012**, *46* (9), 4916–4925. <https://doi.org/10.1021/es300039h>.
- (61) DOW. Rinskor Active Technical Bulletin http://storage.dow.com.edgesuite.net/dowagro/rinskor/Rinskor_Tech_Bulletin.pdf. (accessed 2020 -05 -25).
- (62) Kowalczyk, A.; Martin, T. J.; Price, O. R.; Snape, J. R.; van Egmond, R. A.; Finnegan, C. J.; Schäfer, H.; Davenport, R. J.; Bending, G. D. Refinement of biodegradation tests methodologies and the proposed utility of new microbial ecology techniques. *Ecotoxicology and Environmental Safety* **2015**, *111*, 9–22. <https://doi.org/10.1016/j.ecoenv.2014.09.021>.
- (63) Schwarzenbach, R. P.; Gschwend, P. M.; Imboden, D. M. *Environmental Organic Chemistry*, 3rd ed.; 2017.
- (64) Blanke, C.; Mikulyuk, A.; Nault, M.; Provost, S.; Schaal, C.; Egeren, S. van; Williams, M.; Mednick, A. Strategic Analysis of Aquatic Plant Management in Wisconsin

https://dnr.wi.gov/topic/EIA/documents/APMSA/APMSA_Final_2019-06-14.pdf
(accessed 2020 -05 -15).

- (65) Haag, W. R.; Mill, T. Effect of a subsurface sediment on hydrolysis of haloalkanes and epoxides. *Environ. Sci. Technol.* **1988**, 22 (6), 658–663.
- (66) Deboer, G. J.; Satchivi, N. Comparison of translocation properties of insecticides versus herbicides that leads to efficacious control of pests as specifically illustrated by Isoclast™ active, a new insecticide, and Arylex™ active, a new herbicide. *Retention, Uptake, and Translocation of Agrochemicals in Plants.* **2014**, 4, 7-93. <https://doi.org/10.1021/bk-2014-1171.ch004>

Chapter 5

Photodegradation and biodegradation of fluridone in laboratory experiments

5.1 Contribution Statement

This chapter is a collaboration between Amber M. White, Sydney Van Frost, Angela M. Magness, Katherine D. McMahon, and Christina K. Remucal. A.M.W wrote the paper and did photodegradation modeling, A.M.M. conducted biodegradation microcosm, and S. V. F. did photodegradation irradiations and sediment sorption analyses.

5.2 Abstract

Fluridone is used commonly to treat invasive and nuisance plants in lakes. However, required exposures times are very long, often exceeding 100 days. Thus, understanding the mechanisms responsible for degrading fluridone in lakes is critical for supporting effective herbicide treatments. We used laboratory studies to quantify the direct and indirect photodegradation rates of fluridone, as well microbial degradation rates in water and sediment microcosms. Irradiation studies found fluridone is susceptible to direct photodegradation with negligible indirect photodegradation. Modeling with natural sunlight intensities predict in-lake photodegradation half-life to be 11 days in 10 cm of water and 102 days in 1 meter of water. Biodegradation only occurred in the sediment microcosm after a 170 day lag period. Lastly, sorption to solids accounted for 10% of fluridone loss in microcosm experiments. Combined, these

results demonstrate the importance of direct photodegradation and sorption on fluridone fate in lakes and can be used to help resource managers apply herbicides to waterbodies in a responsible manner.

5.3 Introduction

Aquatic herbicides are popular for their effective semi-selective control of several invasive plant species.¹⁻⁵ Herbicide treatments are only effective when specific concentrations and exposure times are met, which are often successfully achieved through whole-lake exposures.⁶⁻⁸ However, variable herbicide degradation rates can cause what would be a successful treatment to fail, prompting additional treatments at even higher concentrations. Furthermore, extensive use of similar mode of action herbicides has contributed to more prevalent herbicide tolerance and resistance.⁹⁻¹² Not only does extensive herbicide use impact efficacy of herbicidal control on nuisance plant populations, but herbicide applications can negatively impact the native plant community.¹³ Thus, understanding the specific degradation pathways of aquatic herbicides is crucial to responsible herbicide use to both prevent the rise of herbicide resistance/tolerance but also protect native plant populations.

Fluridone is a commonly used systemic herbicide that prevents the synthesis of important biomolecules that protect the plant from photobleaching.^{2,14} For fluridone to be effective, a low concentration (6-26 nM)¹⁵⁻¹⁷ is applied for an entire growing season, which often requires multiple applications to maintain an effective concentration.¹⁷⁻²⁰ It is also a popular alternative to auxin-mimic herbicides, such as 2,4-dichlorophenoxyacetic acid (2,4-D), for treating the 2,4-D tolerant hybrid watermilfoil (*Myriophyllum spicatum* × *Myriophyllum sibiricum*, HWM).^{11,21} While fluridone has shown control of both EWM and HWM,^{1,15,17,22,23} preliminary documented fluridone

tolerance by HWM⁹ and Hydrilla (*Hydrilla verticillate*)²⁴ underscores the importance of highly responsible herbicide applications to preserve fluridone as a viable herbicide tool.

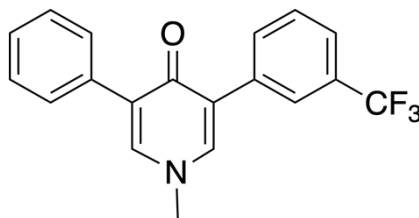


Figure 5.1. Chemical structure of fluridone.

In lakes, fluridone is expected to undergo rapid photolysis with reported half-lives of 28 hours – 12 days in Milli-Q and lake water, respectively (**Table 5.1**).^{25–27} Few laboratory studies have investigated fluridone degradation in lake water, but all have demonstrated the photolability of the compound. However, these studies have not specifically described how dissolved organic carbon in a lake may enhance (i.e., through indirect photodegradation) or hinder fluridone degradation.^{26,27} Indirect photodegradation is the mechanism through which dissolved organic carbon becomes sensitized by sunlight, causing a chain of reactions that can increase degradation of chemicals such as fluridone.^{28–30} Thus, a thorough investigation into possible indirect photodegradation is critical for understanding fluridone fate in lakes.

Microbial degradation of fluridone has also been observed but is expected to be slower than photolysis. Additionally, no specific microbes or metabolic pathways have been associated with its degradation.^{20,31,32} Fluridone also has a high affinity for binding to sediments³³ and has been found to persist for up to a year following initial treatment, suggesting sediments are a possible sink for unreacted fluridone that is available for future resuspension or uptake.^{20,34,35} Field

observations of fluridone treatments have reported half-lives in the range of hours to hundreds of days (**Table 5.1**),^{20,36} with some instances of fluridone persisting more than a year in the water column,¹⁷ indicating a need for additional investigation of the specific degradation mechanisms of fluridone.

The extended exposure time requirement of fluridone in lakes requires a mechanistic understanding of the environmental transformation process that degrade fluridone to better inform herbicide application strategies. Thus, the goal of this study is to quantify the photodegradation, biodegradation, and sorption of fluridone through laboratory studies. The results of this study will be used to inform strategic fluridone herbicide applications in lakes to ensure successful treatments and minimize potential effects to the non-target community.

5.4 Materials and Methods

5.4.1 Chemicals

Chemicals were used as received. Fluridone (99.5%) was purchased ChemService, Inc. Dibasic potassium phosphate (ACS, 98%), monobasic potassium phosphate (ReagentPlus(R)), were purchased from Sigma Aldrich. Acetonitrile (HPLC grade), formic acid (ACS, 88%) were purchased from Fisher Chemical. 2-Nitrobenzaldehyde (99%) was purchased from Acros Organics. Ultrapure water (18.2 MΩ cm) for all analyses and photochemical irradiations was obtained from Milli-Q water purification system. Calibration solutions for the pH meter were obtained from Aqua Solutions.

Table 5.1. Summary of literature reports of field, photodegradation, biodegradation, and sorption studies of fluridone.

Half-life	Study type	Ref.
Field Studies		
2-11 days	Three ponds and one lake in MI, NY, FL, & Panama Canal	37
4 – 7 days	Small ponds in Manitoba, Canada	35
6-50 days	Ponds in TX, WV, MO, CA, IN, and FL	20
30-50 days	Small- medium ponds in Greenfield, Indiana	14
8 months	Lake, Silver Lake, Wisconsin	17
Photodegradation Studies		
15-36 hours	Ultrapure water, natural light, filtered > 297 nm	27
23 hours	Ultrapure water, simulated sunlight 280-365 nm	37
28-55 hours	Ultrapure water, simulated sunlight 280-365 nm	26
35 hours	Ultrapure water, natural sunlight, 325-355 nm	27
8.8 days	Ultrapure water, simulated sunlight, 310-380 nm	27
7 days	Well water, natural sunlight	25
12 days	Ultrapure & lake water, natural sunlight	26
33 days	Well water, natural sunlight, 290 - 320 nm light filtered out	25
Biodegradation Studies		
50 days	Microcosms with silty and sandy soil, saturated with tap water	38
>150 days	Microcosm with lake sediment	31
>150 days	Cultures enriched from lake sediments	31
Sorption studies		
10% sorbed in 30 days	Silty and sandy soil, saturated with tap water	38
16-27% sorbed in 28 days	Pond application in New York and Florida	37
14-52% sorbed in over 150 days	Pond sediments in Manitoba, Canada	34
K_{oc} : 883- 2462 L kg ⁻¹	Pond sediments in Manitoba, Canada	35

5.4.2 Photochemical Irradiation Experiments

Photodegradation experiments were conducted in a Rayonet merry-go-round photoreactor equipped with sixteen bulbs that emit light at 311 nm (\pm 22 nm width at half-max). This is both within the environmental irradiance spectrum ($>$ 290 nm) and in the absorbance spectrum of fluridone (**Figure 5.2**). Irradiation experiments in borosilicate glass tubes were conducted in

triplicate using 20 μM (6.58 ppm) fluridone in 10 mM pH 7 buffered ultrapure water to measure direct photodegradation. Indirect photodegradation was measured in lake water diluted to 3 mg-C L^{-1} from six lakes. South Twin and Muskellunge Lake water was also irradiated at ambient dissolved organic carbon concentrations of 3.8 and 6.9 mg-C L^{-1} , respectively. Light intensity was quantified using 2-nitrobenzaldehyde³⁹ as a chemical actinometer. [Fluridone] used in irradiations is much higher than typical fluridone applications but was better for detection over several orders of magnitude of loss and to account for sorption during the experiment.

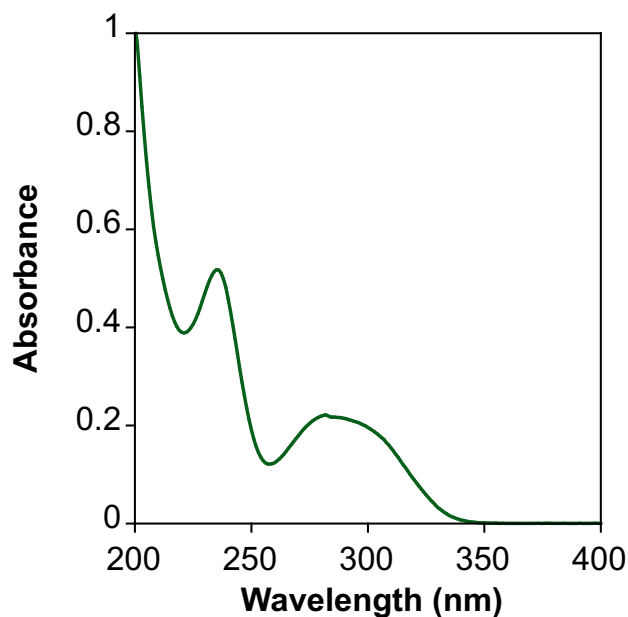


Figure 5.2. Absorbance spectra of 20 μM fluridone in ultrapure water.

The direct quantum yield of fluridone was calculated relative to the actinometer as described previously using Equation 5.1:⁴⁰⁻⁴³

$$\Phi_{Fluridone} = \frac{k_{screened,direct,fluridone}}{k_{direct,act}} \times \frac{k_{abs,act}}{k_{abs,fluridone}} \times \Phi_{act} \quad \text{Eq. 5.1}$$

where $k_{screened,direct,fluridone}$ is direct photodegradation rate constant for the direct control corrected for light screening (s^{-1}), $k_{direct,act}$ is the photodegradation rate constant of the actinometer (s^{-1}), $k_{abs,act}$ (s^{-1}) is the rate of light absorbance of the actinometer, $k_{abs,fluridone}$ (s^{-1}) is the rate of light absorption for fluridone and $\Phi_{act} = 0.41$ for 2-nitrobenzaldehyde.³⁹

The calculated quantum yield was combined with solar irradiance modeling using the Simple Model of Atmospheric Transfer of Sunshine (SMARTS)⁴⁴ to calculate fluridone half-life in sunlight in lakes using Equation 5.2:

$$k_{photodegradation} = k_{abs,sun} \times \Phi_{Fluridone} \quad \text{Eq. 5.2}$$

where $k_{abs,sun}$, is a light absorbance rate constant was calculated for the horizontal global irradiance spectrum for Vilas County, WI, on June 9th 2019. A depth integrated photodegradation^{29,42} rate was calculated as described previously. Briefly, we calculated the photodegradation rate in 1 cm intervals through a 1-meter-deep water column (i.e., at 1 cm, 2 cm, 3 cm ... 100 cm) and averaged the rates through the water column. The depth integrated rate was then used to calculate an in-lake photodegradation half-life using Equation 5.3, assuming first-order loss:

$$t_{1/2} = \frac{\ln 2}{k_{photodegradation,1m}} \quad \text{Eq. 5.3}$$

where $k_{photodegradation,1m}$ is the modeled aquatic photodegradation rate calculated in Eq. 5.2 and averaged through the 1 meter-water column.

5.4.3 Microcosm Incubations

Water and sediment were collected from Lake Mendota, Madison, WI, USA for microcosm incubations quantifying fluridone biodegradation. 10 L LDPE cubitainers were incubated at 12°C in the Microbial Sciences Building. Degradation by the water column microbial community was quantified in triplicate microcosms with unfiltered lake water (5 L) while

degradation by the sediment microbial community was quantified in microcosms with filtered lake water (2 L) and sediment (1 kg). Abiotic loss processes were assessed in control microcosms with filtered lake water (2 L). Microcosms were incubated with 3 μM (998 ppb) fluridone and incubated for 250 days. Water and sediment samples were collected bi-weekly during the first three months and then monthly thereafter. Water samples were filtered through a 0.45 nylon filter and stored in a 4°C fridge prior to analysis. Sediment samples were collected using a serological pipette and stored in a 2.5 mL PCR tube in a -20°C freezer until analysis.

5.4.4 Sediment Fluridone Extractions

Sediment extractions were conducted using 100 mg of microcosm sediment, dried it at 100°C for at least 8 hours. Dried samples were placed in falcon tubes with 10 mL of a 50:50 methanol:water extraction solution, shaken for 2 hours, centrifuged, and syringe filtered (0.45 μm) into clean 2 mL glass amber vial for analysis. Additionally, sediment and water spiked with fluridone over the range of 1 to 12 μM was used to calculate a sediment-water partition coefficient (K_d) and water-organic carbon partitioning coefficient (K_{oc}) using Equation 5.4:

$$K_d = K_{oc} \times f_{oc} \quad \text{Eq. 5.4}$$

where K_d is the sediment-water partitioning coefficient (L kg^{-1}), K_{oc} is the water-carbon partitioning coefficient (L kg^{-1}), and f_{oc} is the fraction of sediment that is comprised of organic carbon.⁴⁵

5.4.5 Analytical Methods

Fluridone and 2-nitrobenzaldehyde were analyzed via high performance liquid chromatography (HPLC). All methods used an Agilent Technologies 1260 Infinity instrument equipped a diode array detector, an Agilent InfinityLab C-18 Poroshell 120 column, and an aqueous buffer composed of 10% acetonitrile and 0.1% formic acid in ultrapure water for the aqueous phase (A) and 100% acetonitrile for the mobile phase (B). Fluridone was analyzed using a gradient method (**Table 5.2 and 5.3**)⁴⁶ and 2-nitrobenzaldehyde was analyzed using an isocratic method.

Table 5.2. Time segments for gradient method used to analyze fluridone on HPLC.

Time (minutes)	A%	B%
0	60	40
0.8	100	0
1.25	0	100
1.30	60	40
3.5	60	40

Table 5.3. Instrument parameters for detection of 2-nitrobenzaldehyde and fluridone in water.

Compound	% Aqueous Buffer	Flow (mL min ⁻¹)	Detection wavelength (nm)	Retention Time (min)	Purpose	LOD (μM)
2-nitrobenzaldehyde	80	0.5	231	2.9	311 nm actinometer	0.5
Fluridone	See Table 5.2	0.8	313	1.8	Herbicide	0.6

5.5 Results and Discussion

5.5.1 Photodegradation of Fluridone in Lake Water

Irradiation of fluridone at 311 nm (**Figure 5.3**) followed first-order kinetics with a direct photodegradation rate constant in buffered ultrapure water (k_{direct}) of $(4.27 \pm 0.5) \times 10^{-4} \text{ s}^{-1}$ ($t_{1/2} = 27$ minutes). The measured direct photodegradation rate constant corresponds to a quantum yield (Φ), or reaction efficiency, of $(5.6 \pm 0.58) \times 10^{-4}$. This is a factor of two higher than previous measurements of quantum yield of 2.7 to 6.7×10^{-5} in ultrapure water.²⁶

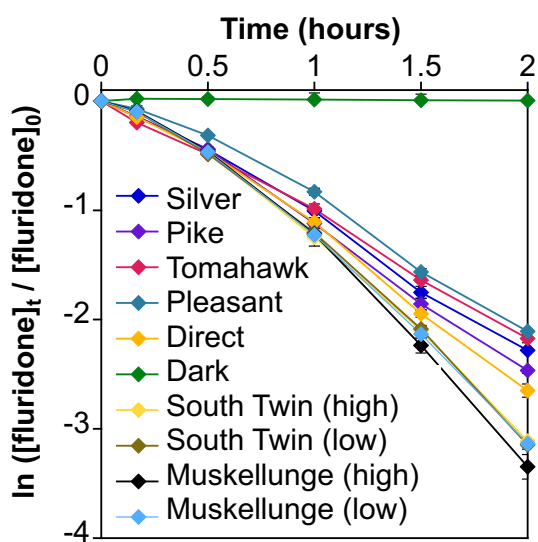


Figure 5.3. Irradiation at 311 nm for direct degradation control and six different lake waters including the high (undiluted lake water) and low (diluted to 3 mg-C L^{-1}) dissolved organic carbon concentrations.

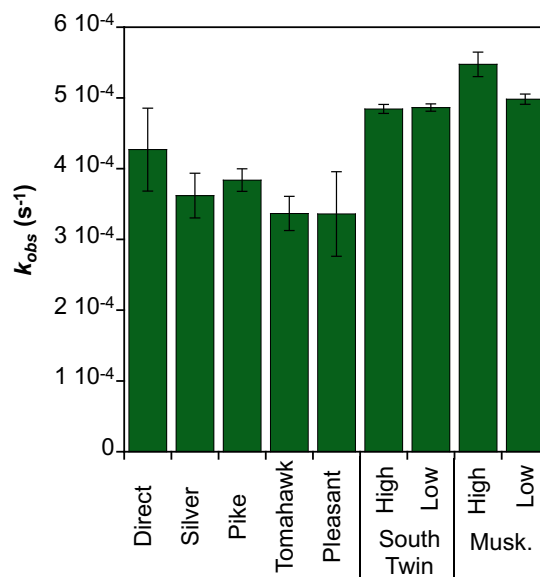


Figure 5.4. Rate constants measured during 311 nm irradiation experiments in ultrapure and natural water (corrected for light screening). Error bars represent standard deviation of triplicate samples.

Irradiation of fluridone in lake water also followed first order kinetics (**Figure 5.3**). k_{obs} in lake water was similar to the direct photodegradation rate constants when corrected for light screening (**Figure 5.4**), even between the diluted and undiluted South Twin and Muskellunge Lake waters, with an average rate constant across all irradiated samples of $k_{obs} = (4.38 \pm 0.81) \times 10^{-4}$ (sec^{-1}). The similarity of rate constants across all irradiated samples suggests fluridone is susceptible to direct photodegradation and that indirect photodegradation is negligible under these conditions. Previous literature has described similar photodegradation rates between ultrapure water and one natural water sample in sunlight.^{26,37} Therefore, our study confirms the dominance of direct photodegradation by testing several different natural waters as well as comparing photodegradation rates across the same waters (i.e., South Twin and Muskellunge) but varying dissolved organic carbon concentrations.

In-lake photodegradation modeling using sunlight intensity in Vilas County, WI on June 9th, 2019, and the calculated quantum yield estimates an aquatic photodegradation half-life of 2 days in the top 1 cm of surface water and 11 days when integrated through the top 10 cm of water. However, half-life increases steeply to 102 days when integrated through 100 cm (i.e., 1 meter). Previous studies report an environmental fluridone photodegradation half-life of 7 to 12 days in 57 cm deep uncovered concrete outdoor mesocosms²⁵ and 100 mL glass bottles irradiated in sunlight,²⁶ which is consistent with our modeled half-life of 11 days.

While our 10 cm depth integrated modeled photodegradation half-life agrees with previous photodegradation studies in natural sunlight, there are some notable differences. First, the bottle study was irradiated in summer sunlight in Indiana while the mesocosm experiment was conducted in Florida, which means light intensity is not consistent across all three studies. Additionally, both sunlight irradiated studies experienced varying light intensity throughout the day, which suggests our constant noontime sunlight intensity is like an overestimate.⁴⁷ Lastly, the pathlength (i.e., depth of “water”) of our and the two reported studies is different. Our 10 cm deep half-life estimate is smaller than the 57 cm pathlength in the Florida mesocosm study, but more representative of the aquatic environment than the irradiated glass bottles that let light pass through all sides. Thus, while our modeled photodegradation rate compares to two reported sunlight irradiations, more research is needed on the effect of water depth, diurnal light intensity, and water clarity to better understand aquatic photodegradation of fluridone.

5.5.2 *Microcosm Incubations*

The fluridone concentration fluctuated frequently over 236 days of fluridone incubation in the abiotic control, unfiltered water, and water-sediment microcosms (**Figure 5.5a**). We

hypothesize this variability is due to analytical issues across two HPLC instruments and several columns during a 250-day study. Because these fluctuations were consistent across all microcosms, including the abiotic control, [fluridone] in the unfiltered water (i.e., water only) microcosm and water-sediment microcosm were normalized to the abiotic control microcosm (**Figure 5.5b**). Normalizing concentrations in the experimental microcosms to the abiotic control reduced the variability over time and allowed interpretation of the data to draw conclusions about biodegradation.

Normalized fluridone concentrations in unfiltered water microcosm remained consistent across the 236 days of incubation, with most concentration fluctuations remaining within the standard deviation of previously analyzed samples. Because the ratio of fluridone between unfiltered water: filtered water stayed close to one for the duration of the study, this means both the abiotic control and the unfiltered water experienced no loss of fluridone throughout the study. However, fluridone concentrations in the water-sediment microcosms were not consistent throughout the duration of the study. While fluridone concentrations remained consistent until ~170 days after incubation, fluridone degradation started shortly after and continued until below detection limit (0.6 μM). The degradation of fluridone only in the sediment microcosms is consistent with several other polar organic compounds (e.g., 2,4-D and FPB) and is likely due to a higher concentration of microbes or additional nutrients in the sediments.^{43,48–52} The extended lag period and then onset of faster degradation is also common for persistent polar organic compounds.^{53,54}

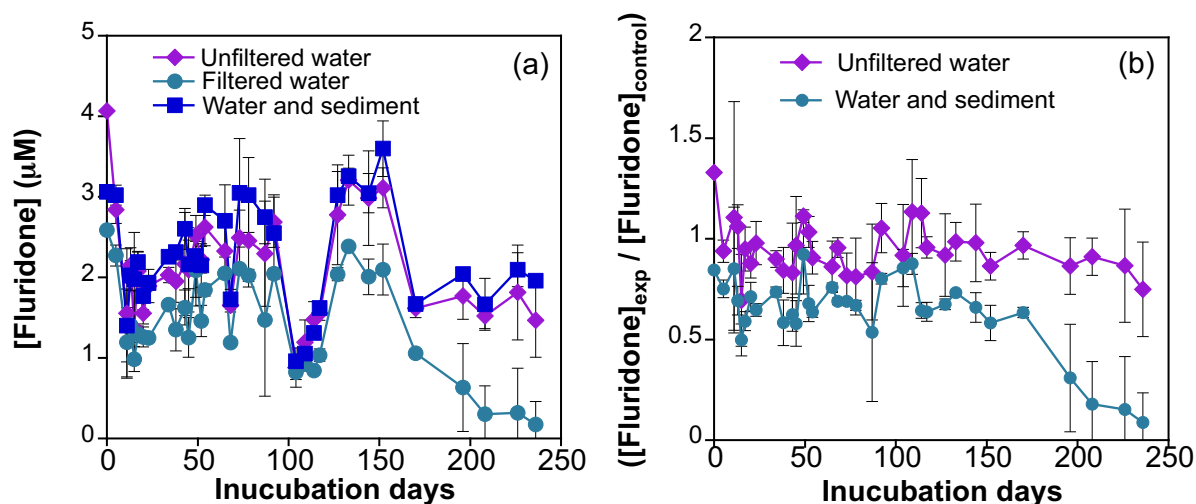


Figure 5.5. (a) [Fluridone] in microcosms incubated with relevant environmental inocula at an initial concentration of 3 μM . (b) [Fluridone] in unfiltered lake water and water and sediment microcosms normalized to abiotic control [fluridone]. Error bars in (a) represent the standard deviation of triplicate microcosms measurements and in (b) are the standard deviation of the triplicate concentration ratios.

Because of the inconsistencies in fluridone concentrations throughout the experiment, no half-life was calculated for the biodegradation of fluridone. However, the extended lag time and persistence of fluridone in the microcosms for over 200 days suggests fluridone is not easily biodegraded in the environment. This conclusion is consistent with biodegradation studies that did not see significant fluridone loss after 150 days³¹ (**Table 5.1**) and, given the long lag time, suggests biodegradation is slower than our modeled photodegradation, especially in shallower waters. While fluridone is degraded slowly in the sediment microcosms over 236 days, fluridone persisted for 200+ days in the water only microcosms, suggesting fluridone is highly stable in water alone in the absence of sunlight.

There is an immediate decrease in dissolved fluridone concentration from initial sampling through the end of the experiment in the sediment microcosms compared to the unfiltered water

and abiotic control microcosms (**Figure 5.5b**). This consistent offset in fluridone concentration is potentially due to sediment sorption in the microcosm. Thus, measurements of sediment fluridone concentrations are needed to quantify the amount of fluridone lost to the sediments throughout the experiment.

5.5.3 Sediment fluridone extractions

Sediment fluridone extractions using methanol and water consistently achieved an average of 103% recovery over a fluridone concentration range of 1 to 20 μM (**Table 5.4**). This suggests the extraction protocol is sensitive and reliable for microcosm sediment quantification. Thus, nine sediment samples from the water and sediment microcosms were extracted using this validated protocol to quantify the amount of sorption to solids (**Table 5.5**). Sediment microcosm extractions found an average recover of $10.8\% \pm 5\%$ across nine sediment samples from the first 26 days of microcosm incubation. This average sorption percentage is consistent with previous studies reporting 10-27%^{37,38} of added fluridone partitioning to the solid phase.

Table 5.4. Recovery and standard deviation of triplicate fluridone sediment extractions measured during method development.

Sample	Spiked concentration (μM)	Recovery concentration (μM)	Average Recovery (%)	Standard deviation
1-3	1	1.00	100.1	0.12
4-6	5	5.80	116.1	0.32
7-9	10	10.95	109.5	0.38
10-12	15	15.10	100.6	1.92
13-15	20	17.94	89.7	0.34

Table 5.5. Recovery and standard deviation of triplicate fluridone sediment extractions measured in microcosms. Each microcosm had 1 kg of sediment was incubated with a total of 6 μM fluridone.

Incubation day	[Fluridone] $\mu\text{M g}^{-1}$	[Fluridone] $\mu\text{M kg}^{-1}$	Percent of fluridone recovered	Standard deviation
0	0.00E+00	0	0.0%	0
7	6.52E-04	0.65	10.9%	5.52E-05
11	6.87E-04	0.69	11.4%	6.09E-05
13	7.17E-04	0.72	12.0%	2.53E-05
15	1.53E-04	0.15	2.6%	9.96E-06
17	5.86E-04	0.59	9.8%	2.36E-05
20	7.13E-04	0.71	11.9%	4.16E-06
23	1.05E-03	1.05	17.5%	1.23E-04
26	6.26E-04	0.63	10.4%	2.89E-05

Given the importance of sediment sorption to fluridone fate in the microcosms, we calculated a solid-water partitioning coefficient (K_d ; **Figure 5.6**). We measured partitioning over a range of 1 to 12 μM and found a K_d of $145.14 \pm 3.4 \times 10^{-5} \text{ L kg}^{-1}$. Because the sediment used in this experiment contained an organic carbon fraction (f_{oc}) of 0.39, we calculated a K_{oc} of $366 \pm 8.8 \times 10^{-5} \text{ L kg}^{-1}$. This calculated K_{oc} is lower than literature values of 883 – 2,462 L kg^{-1} , although these measurements were made using field sediments in experimental ponds, which could introduce uncharacterized variability from other transformation reactions, temperature changes, and water mixing compared to our measurements.³⁵

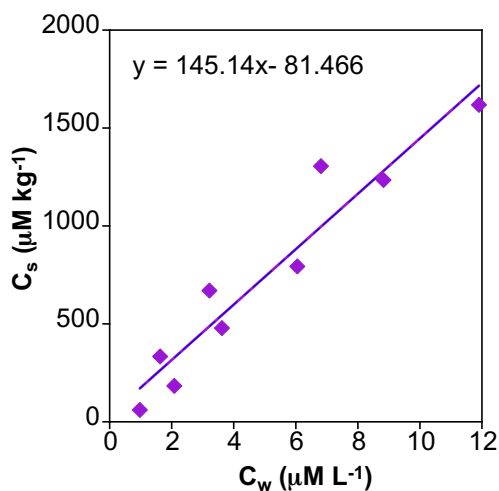


Figure 5.6. Sorption isotherm for fluridone over concentration range of 1-12 μM . C_w is the concentration in the water and C_s is concentration on the solid.

5.6 Conclusions and Future Directions

Our work quantified the photodegradation, biodegradation, and sorption of fluridone in laboratory experiments. These laboratory experiments are critical to isolating specific transformation pathways under controlled conditions, which can be used to contextualize field data and aid in the design of field studies investigating fluridone fate. Our results found fluridone is susceptible to photodegradation and biodegradation, although the water depth and water clarity of a treated water body will be critical for determining what degradation process is dominant. Sediment sorption accounted for a 10% loss of fluridone in the microcosms nearly immediately after spiking with fluridone, suggesting sorption can happen quickly. Our measured degradation rates are much slower than reported field half-lives, suggesting a loss mechanism not characterized here is responsible for the loss of fluridone, such as plant uptake⁵⁵ or discharge from lakes.⁴³ Additionally, the importance of photodegradation in shallow waters and sediment sorption suggests physical lake parameters such as sediment surface area, average depth, or surface area to volume ratios may be important in understanding the in-lake degradation mechanisms of fluridone.

5.7 Acknowledgements

This work was funded by the Midwest Aquatic Plant Management Society Robert L. Johnson Memorial Grant (A.M.W), Anna Grant Birge Memorial Award (A.M.W. and A.M.M.) and a National Science Foundation Graduate Research Fellowship. Thanks to Josie Jauquet for assistance conducting laboratory experiments.

5.8 References

- (1) Slade, J. G.; Poovey, A. G.; Netherland, M. D. Efficacy of fluridone on Eurasian and hybrid watermilfoil. *J. Aquat. Plant Manage.* **2007**, *45* (2), 116–118.
- (2) Bartels, P. G.; Watson, C. W. Inhibition of carotenoid synthesis by fluridone and norflurazon. *Weed Sci* **1978**, *26* (2), 198–203. <https://doi.org/10.1017/s0043174500049675>.
- (3) Koschnick, T. J.; Haller, W. T.; Vandiver, V. v; Santra, U. Efficacy and residue comparisons between two slow-release formulations of fluridone. *J. Aquat. Plant Manage* **2003**, *41*, 25–27.
- (4) Peterson, M. A.; McMaster, S. A.; Riechers, D. E.; Skelton, J.; Stahlman, P. W. 2,4-D past, present, and future: A review. *Weed Tech.* **2016**, *30* (2), 303–345. <https://doi.org/10.1614/wt-d-15-00131.1>.
- (5) Netherland, M. D.; Sisneros, D.; Fox, A. M.; Haller, W. T. *Field Evaluation of Low-Dose Metering and Polymer Endothall Applications and Comparison of Fluridone Degradation from Liquid and Slow Release-Pellet Applications*. **1998**. <https://erdc-library.erdcdren.mil/jspui/bitstream/11681/6301/1/8745.pdf> (accessed 2022- 08-10)
- (6) Wagner, K. I.; Hauxwell, J.; Rasmussen, P. W.; Koshere, F.; Toshner, P.; Aron, K.; Helsel, D. R.; Toshner, S.; Provost, S.; Gansberg, M.; Masterson, J.; Warwick, S. Whole-lake herbicide treatments for Eurasian watermilfoil in four Wisconsin lakes: Effects on vegetation and water clarity. *Lake and Resvr. Mange.* **2007**, *23* (1), 83–94. <https://doi.org/10.1080/07438140709353912>.
- (7) Nault, M. E.; Netherland, M. D.; Mikulyuk, A.; Skogerboe, J. G.; Asplund, T.; Hauxwell, J.; Toshner, P. Efficacy, selectivity, and herbicide concentrations following a whole-lake 2,4-D application targeting Eurasian watermilfoil in two adjacent northern Wisconsin lakes. *Lake and Resvr. Mange.* **2014**, *30* (1), 1–10. <https://doi.org/10.1080/10402381.2013.862586>.
- (8) Getsinger, K. D.; Madsen, J. D.; Koschnick, T. J.; Netherland, M. D. Whole-lake fluridone treatments for selective control of Eurasian watermilfoil: I. Application strategy and herbicide residues. *Lake and Resvr. Mange.* **2002**, *18* (3), 181–190. <https://doi.org/10.1080/07438140209354147>.
- (9) Berger, S. T.; Netherland, M. D.; MacDonald, G. E. Laboratory documentation of multiple-herbicide tolerance to fluridone, norflurazon, and topramazone in a hybrid watermilfoil (*Myriophyllum spicatum* × *M. sibiricum*) population. *Weed Sci.* **2015**, *63* (1), 235–241. <https://doi.org/10.1614/ws-d-14-00085.1>.

- (10) Mallory-Smith, C. A.; Retzinger Jr., E. J. Revised classification of herbicides by site of action for weed resistance management strategies. *Weed Tech.* **2003**, *17* (3), 605–619. [https://doi.org/10.1614/0890-037x\(2003\)017\[0605:rcobhs\]2.0.co;2](https://doi.org/10.1614/0890-037x(2003)017[0605:rcobhs]2.0.co;2).
- (11) Nault, M. E.; Barton, M.; Hauxwell, J.; Heath, E.; Hoyman, T.; Mikulyuk, A.; Netherland, M. D.; Provost, S.; Skogerboe, J.; van Egeren, S. Evaluation of large-scale low-concentration 2,4-D treatments for eurasian and hybrid watermilfoil control across multiple wisconsin lakes. *Lake and Resvr. Mange.* **2018**, *34* (2), 115–129. <https://doi.org/10.1080/10402381.2017.1390019>.
- (12) Richardson, R. J. Aquatic plant management and the impact of emerging herbicide resistance issues. *Weed Tech.* **2008**, *22* (1), 8–15. <https://doi.org/10.1614/wt-07-034.1>.
- (13) Mikulyuk, A.; Kujawa, E.; Nault, M. E.; van Egeren, S.; Wagner, K. I.; Barton, M.; Hauxwell, J.; Vander Zanden, M. J. Is the cure worse than the disease? Comparing the ecological effects of an invasive aquatic plant and the herbicide treatments used to control it. *Facets* **2020**, *5* (1), 353–366. <https://doi.org/10.1139/FACETS-2020-0002>.
- (14) Arnold, W. R. Fluridone: A new aquatic herbicide. *J. Aquat. Plant. Manage.* **1979**, *17*, 30–33.
- (15) Netherland, M. D.; Getsinger, K. D.; Skogerboe, J. D. Mesocosm evaluation of the species-selective potential of fluridone. *J. Aquat. Plant. Manage.* **1997**, *35* (2), 41–50.
- (16) Netherland, M. D.; Getsinger, K. D.; Turner, E. G. Fluridone concentration and exposure time requirements for control of Eurasian watermillfoil and hydrilla. *J. Aquat. Plant. Manage.* **1993**, *31*, 189–194.
- (17) Onterra. Silver Lake Management Plan. https://www.townshipofmarion.com/wp-content/uploads/2018/01/SilverWaushara_HWMmonitorReport2017_v1-1.pdf. (accessed 2020-05-20)
- (18) Blanke, C.; Mikulyuk, A.; Nault, M.; Provost, S.; Schaal, C.; Egeren, S. van; Williams, M.; Mednick, A. Strategic Analysis of Aquatic Plant Management in Wisconsin https://dnr.wi.gov/topic/EIA/documents/APMSA/APMSA_Final_2019-06-14.pdf (accessed 2020 -05 -15).
- (19) Osborne, J. A.; West, S. D.; Cooper, Raymond, B.; Schmitz, D. C.; Cooper B., R.; Schmitz, D. C. Fluridone and *N*-methylformaide residue determination in ponds. *J. Aquat. Plant. Manage.* **1989**, *27*, 74–78.
- (20) West, S. D.; Burger, R. O.; Poole, G. M.; Mowrey, D. H. Bioconcentration and field dissipation of the aquatic herbicide fluridone and its degradation products in aquatic environments. *J. Agric. Food Chem.* **1983**, *31* (3), 579–585. <https://doi.org/10.1021/jf00117a028>.
- (21) Larue, E. A.; Zuellig, M. P.; Netherland, M. D.; Heilman, M. A.; Thum, R. A. Hybrid watermilfoil lineages are more invasive and less sensitive to a commonly used herbicide than their exotic parent (Eurasian watermilfoil). *Evolutionary Applications.* **2013**, *6* (3), 462–471. <https://doi.org/10.1111/eva.12027>.
- (22) Valley, R. D.; Crowell, W.; Welling, C. H.; Proulx, N. Effects of a low-dose fluridone treatment on submersed aquatic vegetation in a eutrophic Minnesota lake dominated by Eurasian watermilfoil and coontail. *J. Aquat. Plant. Manage.* **2006**, *44*, 19–25.
- (23) Madsen, J. D.; Getsinger, K. D.; Stewart, R. M.; Owens, C. S. Whole Lake fluridone treatments for selective control of Eurasian watermilfoil: II. Impacts on submersed plant communities. *Lake and Resvr. Mange.* **2002**, *18* (3), 191–200. <https://doi.org/10.1080/07438140209354148>.

- (24) Netherland, M. D.; Jones, D. Fluridone-resistant hydrilla (*Hydrilla verticillata*) is still dominant in the Kissimmee Chain of Lakes, Fl. *Invasive Plant Science and Management*. **2015**, *8* (2), 212–218. <https://doi.org/10.1614/ipsm-d-14-00071.1>.
- (25) Macdonald, G. E.; Haller, W. T.; Shilling, D. G. UV-B filtration to reduce photolysis of fluridone in experimental tanks. *J. Aquat. Plant. Manage.* **1996**, *34* (2), 78–80.
- (26) Saunders, D. G.; Mosier, J. W. Photolysis of the aquatic herbicide fluridone in aqueous solution. *J. Agric. Food Chem.* **1983**, *31* (2), 237–241. <https://doi.org/10.1021/jf00116a013>.
- (27) Mossler, M. A.; Shilling, D. G.; Haller, W. T. Photolytic degradation of fluridone. *J. Aquat. Plant. Manage.* **1989**, *27*, 69–73.
- (28) Remucal, C. K. The role of indirect photochemical degradation in the environmental fate of pesticides: A review. *Environ. Sci. Processes Impacts* **2014**, *16* (4), 628–653. <https://doi.org/10.1039/c3em00549f>.
- (29) McConville, M. B.; Mezyk, S. P.; Remucal, C. K. Indirect photodegradation of the lampricides TFM and niclosamide. *Environ. Sci. Processes Impacts* **2017**, *19* (8), 1028–1039. <https://doi.org/10.1039/c7em00208d>.
- (30) Maizel, A. C.; Li, J.; Remucal, C. K. Relationships between dissolved organic matter composition and photochemistry in lakes of diverse trophic status. *Environ. Sci. Technol.* **2017**, *51* (17), 9624–9632. <https://doi.org/10.1021/acs.est.7b01270>.
- (31) Mossler, M. A.; Shillings, D. G.; Albrecht, S. L.; Haller, W. T. Microbial degradation of fluridone. *J. Aquat. Plant. Manage.* **1991**, *29*, 77–80.
- (32) Schroeder, J.; Banks, P. A. Persistence of fluridone in five Georgia soils. *Weed Sci* **1986**, *34* (4), 612–616. <https://doi.org/10.1017/s0043174500067539>.
- (33) Mossler, M. A.; Shilling, D. G.; Milgram, K. E.; Haller, W. T. Interaction of formulation and soil components on the aqueous concentration of fluridone. *J. Aquat. Plant. Manage.* **1993**, pp 257–260.
- (34) Muir, D. C. G.; Grift, N. P. Fate of fluridone in sediment and water in laboratory and field experiments. *J. Agric. Food Chem.* **1982**, *30* (2), 238–244. <https://doi.org/10.1021/jf00110a006>.
- (35) Muir, D.; Grift, N. P.; Blouw, A. P.; Lockhart, W. L. Persistence of fluridone in small ponds. **1980**, *9* (1), 151–156.
- (36) Wickham, P.; Pandey, P.; Harter, T.; Sandoval-Solis, S. UV light and temperature induced fluridone degradation in water and sediment and potential transport into aquifer. *Environ. Poll.* **2020**, *265*, 114750. <https://doi.org/10.1016/j.envpol.2020.114750>.
- (37) West, S. D.; Day, E. W.; Burger, R. O. Dissipation of the experimental aquatic herbicide fluridone from lakes and ponds. *J. Agric. Food Chem.* **1979**, *27* (5), 1067–1072.
- (38) Marquis, L. Y.; Comes, R. D.; Yang, C. P. Degradation of fluridone in submersed soils under controlled laboratory conditions. *Pesticide Biochem. and Phys.* **1982**, *17*, 68–75.
- (39) Galbavy, E. S.; Ram, K.; Anastasio, C. 2-Nitrobenzaldehyde as a chemical actinometer for solution and ice photochemistry. *J. Photochem. Photobio. A: Chem* **2010**, *209* (2–3), 186–192. <https://doi.org/10.1016/j.jphotochem.2009.11.013>.
- (40) Bulman, D. M.; P. Mezyk, S.; K. Remucal, C. The impact of pH and irradiation wavelength on the production of reactive oxidants during chlorine photolysis. *Environ. Sci. Technol.* **2019**, *53* (8), 4450–4459. <https://doi.org/10.1021/acs.est.8b07225>.
- (41) Berg, S. M.; Whiting, Q. T.; Herrli, J. A.; Winkels, R.; Wammer, K. H.; Remucal, C. K. The role of dissolved organic matter composition in determining photochemical reactivity

- at the molecular level. *Environ. Sci. Technol.* **2019**, *53* (20), 11725–11734. <https://doi.org/10.1021/acs.est.9b03007>.
- (42) McConville, M. B.; Hubert, T. D.; Remucal, C. K. Direct photolysis rates and transformation pathways of the lampricides TFM and niclosamide in simulated sunlight. *Environ. Sci. Technol.* **2016**, *50* (18), 9998–10006. <https://doi.org/10.1021/acs.est.6b02607>.
- (43) White, A. M.; Nault, M. E.; McMahan, K. D.; Remucal, C. K. Synthesizing laboratory and field experiments to quantify dominant transformation mechanisms of 2,4-dichlorophenoxyacetic acid (2,4-D) in aquatic environments. *Environ. Sci. Technol.* **2022**, *56* (15), 10838–10848. <https://doi.org/10.1021/acs.est.2c03132>.
- (44) Gueymard, C. A. Interdisciplinary applications of a versatile spectral solar irradiance model: A review. *Energy* **2005**, *30* (9), 1551–1576. <https://doi.org/10.1016/j.energy.2004.04.032>.
- (45) Schwarzenbach, R. P.; Gschwend, P. M.; Imboden, D. M. *Environmental Organic Chemistry*, 3rd ed.; 2017.
- (46) Cozzola, A. J.; Dehnert, G. K.; White, A. M.; Karasov, W. H. Effects of subchronic exposure to environmentally relevant concentrations of a commercial fluridone formulation on fathead minnows (*Pimephales promelas*). *Aquat. Tox.* **2022**, *244*. <https://doi.org/10.1016/j.aquatox.2022.106098>.
- (47) McConville, M. B.; Cohen, N. M.; Nowicki, S. M.; Lantz, S. R.; Hixson, J. L.; Ward, A. S.; Remucal, C. K. A field analysis of lampricide photodegradation in great lakes tributaries. *Environ. Sci. Processes Impacts.* **2017**, *19* (7), 891–900. <https://doi.org/10.1039/c7em00173h>.
- (48) Mezzanotte, V.; Bertani, R.; Innocenti, F. D.; Tosin, M. Influence of inocula on the results of biodegradation tests. *Polymer Degradation and Stability.* **2005**, *87* (1), 51–56. <https://doi.org/10.1016/j.polymdegradstab.2004.06.009>.
- (49) Ott, A.; Martin, T. J.; Snape, J. R.; Davenport, R. J. Increased cell numbers improve marine biodegradation tests for persistence assessment. *Sci. Total Environ.* **2020**, *706*. <https://doi.org/10.1016/j.scitotenv.2019.135621>.
- (50) Zhi, H.; Miannecki, A. L.; Kolpin, D. W.; Klaper, R. D.; Iwanowicz, L. R.; LeFevre, G. H. Tandem field and laboratory approaches to quantify attenuation mechanisms of pharmaceutical and pharmaceutical transformation products in a wastewater effluent-dominated stream. *Water Res.* **2021**, *203*. <https://doi.org/10.1016/j.watres.2021.117537>.
- (51) Seller, C.; Honti, M.; Singer, H.; Fenner, K. Biotransformation of chemicals in water-sediment suspensions: Influencing factors and implications for persistence assessment. *Environ. Sci. Technol. Lett.* **2020**, *7* (11), 854–860. <https://doi.org/10.1021/acs.estlett.0c00725>.
- (52) Seller, C.; Özel Duygan, B. D.; Honti, M.; Fenner, K. Biotransformation of chemicals at the water–sediment interface—Toward a robust simulation study setup. *ACS Environ. Au* **2021**, *1* (1), 46–57. <https://doi.org/10.1021/acsenvironau.1c00006>.
- (53) Koseki, S.; Nonaka, J. Alternative approach to modeling bacterial lag time, using logistic regression as a function of time, temperature, pH, and sodium chloride concentration. *Appl. Environ. Microbiol.* **2012**, *78* (17), 6103–6112. <https://doi.org/10.1128/AEM.01245-12>.
- (54) Tjørve, K. M. C.; Tjørve, E. The use of gompertz models in growth analyses, and new gompertz-model approach: An addition to the unified-richards family. *PLoS ONE* **2017**, *12* (6). <https://doi.org/10.1371/journal.pone.0178691>.

- (55) Vassios, J. D.; Nissen, S. J.; Koschnick, T. J.; Hielman, M. A. Fluridone, penoxsulam, and triclopyr absorption and translocation by Eurasian watermilfoil (*Myriophyllum spicatum*) and hydrilla (*Hydrilla verticillata*). *J. Aquat. Plant Manage.* **2017**, *55*, 58–64.

Chapter 6

Conclusions

6.1 Summary

The primary goal of this dissertation was to investigate the environmental fate and transformation of three aquatic herbicides and use these three herbicides as a tool to relate laboratory degradation studies to environmental fate. Most of the research described in this dissertation combined laboratory-based degradation studies that quantified photodegradation, biodegradation, hydrolysis, and/or sorption under isolated and controlled conditions. When possible, paired field campaigns quantified herbicide degradation following direct applications to lakes and were used to contextualize the laboratory data. The variety of required exposure times, effective concentrations, and physical-chemical properties of each herbicide allowed for an investigation into more transformation reactions than one herbicide alone would have allowed. These results were used to determine the primary transformation mechanisms acting on each herbicide in the aquatic environment, but also draw broader conclusions about laboratory-based descriptions of environmental fate of polar organic compounds.

2,4-Dichlorophenoxyacetic acid (2,4-D) is susceptible to photodegradation and biodegradation, but the combined laboratory and field studies demonstrated that sediment bacteria are responsible for 2,4-D loss in aquatic environments (Chapter 2). Laboratory photodegradation studies found 2,4-D is degraded through direct photodegradation, with negligible indirect photodegradation. Modeling of aquatic photodegradation, however, resulted in a photodegradation half-life much longer than any 2,4-D half-lives quantified in the field campaign. Laboratory biodegradation microcosms only quantified 2,4-D loss in the presence of sediment, with a wide

range of half-lives comparable to those observed in the field campaigns. However, 2,4-D loss in the lakes was also strongly affected by lake physical parameters not captured by the laboratory studies. For example, physical discharge of unreacted 2,4-D through lake outlets also contributed to 2,4-D loss while stratification mid-treatment changed degradation kinetics such that epilimnion and hypolimnion had different degradation rates. Ultimately, mass balance modeling that included advective transport, biodegradation, and photodegradation was most representative of [2,4-D] observed in the field studies, underscoring the importance of including physical waterbody properties or considerations in translating laboratory data to the environment.

Because of the importance of bacteria to the degradation of 2,4-D, we tried to quantify the abundance of 2,4-D degradation gene copies in the laboratory and field studies (Chapter 3). However, poor accuracy of established qPCR primers for amplifying the *tfd* gene was found to be a consistent problem across aquatic, terrestrial, and subsurface environments. Metagenomic analysis of publicly available genomes discovered over 1,000 putative 2,4-D degraders, which included bacterial phyla not previously cultured. These results demonstrate the limitations of applying culture-based molecular tools to the environment and that attempts to do so should be appropriately verified prior to environmental application.

Our work expanded to another auxin mimic herbicide in Chapter 4: florpyrauxifen-benzyl (FPB). FPB which was developed to target a different binding site than other auxin mimic herbicides, like 2,4-D, to combat herbicide resistance in aquatic plant populations.^{1,2} We found FPB should photodegrade rapidly when photodegradation is modeled in lake water with natural sunlight intensity. However, field quantification of FPB also measured an accumulation of the product florpyrauxifen, which was produced in hydrolysis experiments and all three microcosm conditions. A second product, X11966341, was measured in lake water and sediment microcosms,

including microcosms spiked only with florpyrauxifen, suggesting that FPB can be hydrolyzed to florpyrauxifen and microbially degraded to X1199641. While FPB hydrolysis is a base catalyzed reaction, FPB degradation in lakes was still faster than any hydrolysis or microcosm experiment at the same pH. We hypothesize this discrepancy in degradation rate is due to plant catalyzed hydrolysis in the lake, which is listed as part of the toxicity mechanism of FPB.^{1,3}

While the laboratory experiments were able to identify the likely transformation pathway in lakes by tracking transformation products across field and laboratory experiments, documentation of plant-catalyzed hydrolysis of similar compounds suggests that transformation rate in the lake is likely dependent on physical lake parameters (e.g., plant density) missed by the laboratory studies. Additionally, changes in lake carbon concentration and composition were measured following the application of FPB, which is applied in a solution of mostly inactive ingredients.⁴ The focus of laboratory studies on transformation of active ingredients in herbicides overlooks potential compounding effects of the complete end use product formulation.

Fluridone (Chapter 5) is another aquatic herbicide that is predominantly degraded via direct photodegradation and is likely photodegraded in aquatic systems based on photodegradation modeling and resistance to biodegradation in microcosm experiments. Like 2,4-D and FPB, biodegradation was only observed in the presence of sediment, albeit after a 170-day lag period. Additionally, sorption to solids accounted for 10% of added fluridone in the. While no field treatments occurred during the 2021 field season in Wisconsin, lake physical parameters such as average water depth, water clarity, and sediment-water surface are likely critical to understanding fluridone fate given the high potential for photodegradation and sorption.

6.2 Suggestions for Future Research

The research in this dissertation demonstrated the complexities of translating laboratory studies to environmental fate, especially when transformation mechanisms not captured by the laboratory studies are important to environmental fate. Based on the findings of this research, there are several questions remaining that can be explored to better understand specific herbicide fate and continue connecting laboratory experiments to environmental fate.

6.2.1 FPB Degradation in Plants

In Chapter 4, a hypothesis that FPB is hydrolyzed in plants in the lakes is proposed based on documentation describing the discovery of FPB (referred to under trade name Rinskor Active) that the toxicity mechanism relies on “phloem trapping” to transport and trap the active ingredient in the plant.¹ This mechanism works by designing an herbicide to be easily absorbed by plants. Once inside the plant, this compound can degrade into a charged or more polar active compound, which makes it difficult to pass back out of the plant so it can accumulate and cause the toxic effect.^{1,3} One potential area of future research could investigate the accumulation of FPB or florpyrauxifen in plants being treated to estimate FPB uptake both quantity and rate and confirm if florpyrauxifen is produced in the plant structure. In our study, we found most FPB was quickly converted to florpyrauxifen after treatment and that most FPB added to the lake was converted to florpyrauxifen. If the transformation of FPB to florpyrauxifen is mediated by plants, understanding the kinetics of this reaction is important to future treatment design. Additional work to relate plant parameters in the lakes, such as plant density, biomass, growth rate, etc., to degradation rate would also be useful for comprehensively understanding FPB fate and risk to non-target organisms.

6.2.2 Florpyrauxifen Fate and Transformation

Chapter 4 documented that the persistence of florpyrauxifen is significantly longer than FPB in all study lakes. As such, investigating the fate and transformation of florpyrauxifen is an important next step for understanding the complete transformation of FPB post-herbicide treatments. Florpyrauxifen also has herbicidal activity,^{2,5} yet most research and regulation has focused on FPB instead of florpyrauxifen, likely because FPB is the active ingredient. Additional research into the photodegradation or potential hydrolysis of florpyrauxifen is important given the aquatic persistence of this compound. Lastly, investigation into potential effects of florpyrauxifen on the non-target community would be ideal for a complete risk assessment of FPB as an aquatic herbicide. Previous work has demonstrated that transformation of one toxic chemical to a degradation product does not necessarily eliminate toxicity,⁶⁻¹⁰ and thus the extended lifetime of florpyrauxifen, which is known to have herbicidal activity² requires additional investigation into the toxicity, fate, and transport of this chemical.

6.2.3 Incorporation of Microbiology Community Analysis Into Standardized Biodegradation

Tests

Chapters 2 and 4 demonstrate the importance of the microbial community to herbicide degradation while Chapter 3 describes several tools that can be used to characterize the microbial community associated contaminant degradation, specifically 2,4-D degradation. However, standardized laboratory biodegradation tests do not include characterization of the microbial community beyond inoculum source and concentrations.¹¹⁻¹³ While identifying specific genes or bacterial strains that can degrade a contaminant is likely not a feasible approach for every chemical risk assessment, incorporating molecular tools like 16S rRNA sequencing could be used to

describe community structure and diversity of inocula used in biodegradation experiments.^{12,14,15} Metagenomic or metatranscriptomic data could be used to characterize community metabolism as a “finger print” to associate with biodegradation studies,^{16–18} while measurements of increased abundance or transcription of genes associated negative health outcomes like antibiotic resistance genes¹⁹ or cyanotoxin production^{20,21} could be screened as part of the environmental fate and transformation studies. A systemic investigation of these microbiology tools coupled to a suite of chemical kinetic studies could be used to develop new laboratory biodegradation tests that explain or eliminate high variability across biodegradation tests^{22,23} or better predict microbial degradation of polar organic compounds in the environment.

6.3 References

- (1) Epp, J. B.; Alexander, A. L.; Balko, T. W.; Buysse, A. M.; Brewster, W. K.; Bryan, K.; Daeuble, J. F.; Fields, S. C.; Gast, R. E.; Green, R. A.; Irvine, N. M.; Lo, W. C.; Lowe, C. T.; Renga, J. M.; Richburg, J. S.; Ruiz, J. M.; Satchivi, N. M.; Schmitzer, P. R.; Siddall, T. L.; Webster, J. D.; Weimer, M. R.; Whiteker, G. T.; Yerkes, C. N. The discovery of ArylexTM active and RinskorTM active: Two novel auxin herbicides. *Bioorganic and Medicinal Chemistry*. **2016**, *24* (3), 362–371. <https://doi.org/10.1016/j.bmc.2015.08.011>.
- (2) Netherland, M. D.; Richardson, R. J. Evaluating sensitivity of five aquatic plants to a novel arylpicolinate herbicide utilizing an organization for economic cooperation and development protocol. *Weed Sci*. **2016**, *64* (1), 181–190. <https://doi.org/10.1614/ws-d-15-00092.1>.
- (3) Deboer, G. J.; Satchivi, N. Comparison of translocation properties of insecticides versus herbicides that leads to efficacious control of pests as specifically illustrated by IsoclastTM active, a new insecticide, and ArylexTM active, a new herbicide. *Retention, Uptake, and Translocation of Agrochemicals in Plants*. **2014**, *4*, 7-93. <https://doi.org/10.1021/bk-2014-1171.ch004>
- (4) SePRO. ProcellaCOR EC https://sepro.com/Documents/ProcellaCOR_EC--Label.pdf (accessed 2022 -07 -25).
- (5) Beets, J.; Heilman, M.; Netherland, M. D. Large-scale mesocosm evaluation of florpyrauxifen-benzyl, a novel arylpicolinate herbicide, on eurasian and hybrid watermilfoil and seven native submersed plants. *J. Aquat. Plant. Manage*. **2019**, *57*, 49–55.
- (6) Tian, Z.; Zhao, H.; Peter, K. T.; Gonzalez, M.; Wetzel, J.; Wu, C.; Hu, X.; Prat, J.; Mudrock, E.; Hettlinger, R.; Cortina, A. E.; Biswas, R. G.; Vinicius, F.; Kock, C.; Soong, R.; Jenne, A.; Du, B.; Hou, F.; He, H.; Lundeen, R.; Gilbreath, A.; Sutton, R.; Scholz, N. L.; Davis, J.

- W.; Dodd, M. C.; Simpson, A.; McIntyre, J. K.; Kolodziej, E. P. A ubiquitous tire rubber-derived chemical induces acute mortality in coho salmon. *Science*. **2021**, *371*, 185–189.
- (7) Wiener, E. A.; Lefevre, G. H. White rot fungi produce novel tire wear compound metabolites and reveal underappreciated amino acid conjugation pathways. *Environ. Sci. Technol. Lett.* **2022**. <https://doi.org/10.1021/acs.estlett.2c00114>.
- (8) Unice, K.; Bare, J.; Kreider, M.; Panko, J. Experimental methodology for assessing the environmental fate of organic chemicals in polymer matrices using column leaching studies and OECD 308 water/sediment systems: application to tire and road wear particles. *Sci. Total Environ.* **2015**, *533*, 476–487. <https://doi.org/10.1016/j.scitotenv.2015.06.053>.
- (9) Sinclair, C. J.; Boxall, A. B. A. Assessing the ecotoxicity of pesticide transformation products. *Environ. Sci. Technol.* **2003**, *37* (20), 4617–4625. <https://doi.org/10.1021/es030038m>.
- (10) Cwiertny, D. M.; Snyder, S. A.; Schlenk, D.; Kolodziej, E. P. Environmental designer drugs: When transformation may not eliminate risk. *Environ. Sci. Technol.* **2014**, *48* (20), 11737–11745. <https://doi.org/10.1021/es503425w>.
- (11) OECD. *Test No. 309: Aerobic Mineralization in Surface Water – Simulation Biodegradation Test*; OECD, 2004. <https://doi.org/10.1787/9789264070547-en>.
- (12) Kowalczyk, A.; Martin, T. J.; Price, O. R.; Snape, J. R.; van Egmond, R. A.; Finnegan, C. J.; Schäfer, H.; Davenport, R. J.; Bending, G. D. Refinement of biodegradation tests methodologies and the proposed utility of new microbial ecology techniques. *Ecotoxicology and Environmental Safety* **2015**, *111*, 9–22. <https://doi.org/10.1016/j.ecoenv.2014.09.021>.
- (13) OECD. *Test No. 308: Aerobic and Anaerobic Transformation in Aquatic Sediment Systems*; OECD, 2002. <https://doi.org/10.1787/9789264070523-en>.
- (14) Thouand, G.; Durand, M. J.; Maul, A.; Gancet, C.; Blok, H. New concepts in the evaluation of biodegradation/persistence of chemical substances using a microbial inoculum. *Front. Microbiol.* **2011**, *2*, 1-6. <https://doi.org/10.3389/fmicb.2011.00164>.
- (15) Linz, A.; Shade, A.; Owens, S.; Jack, G.; Knight, R.; McMahon, K. Bacterial community composition and dynamics spanning five years in freshwater bog lakes. *mSphere* **2017**, *2* (June), 1–15. <https://doi.org/10.1128/mSphere.00169-17>.
- (16) Tran, P. Q.; Bachand, S. C.; McIntyre, P. B.; Kraemer, B. M.; Vadeboncoeur, Y.; Kimirei, I. A.; Tamatamah, R.; McMahon, K. D.; Anantharaman, K. Depth-discrete metagenomics reveals the roles of microbes in biogeochemical cycling in the tropical freshwater lake Tanganyika. *ISME* **2021**, *15* (7), 1971–1986. <https://doi.org/10.1038/s41396-021-00898-x>.
- (17) Linz, A. M.; He, S.; Stevens, S. L. R.; Anantharaman, K.; Rohwer, R. R.; Malmstrom, R. R.; Bertilsson, S.; McMahon, K. D. Freshwater carbon and nutrient cycles revealed through reconstructed population genomes. *PeerJ* **2018**, *2018* (12), 1–24. <https://doi.org/10.7717/peerj.6075>.
- (18) Peterson, B. D.; McDaniel, E. A.; Schmidt, A. G.; Lepak, R. F.; Janssen, S. E.; Tran, P. Q.; Marick, R. A.; Ogorek, J. M.; DeWild, J. F.; Krabbenhoft, D. P.; McMahon, K. D. Mercury methylation genes identified across diverse anaerobic microbial guilds in a eutrophic sulfate-enriched lake. *Environ. Sci. Technol.* **2020**, *54*, 15840. <https://doi.org/10.1021/acs.est.0c05435>.
- (19) Xi, C.; Zhang, Y.; Marrs, C. F.; Ye, W.; Simon, C.; Foxman, B.; Nriagu, J. Prevalence of antibiotic resistance in drinking water treatment and distribution systems. *Appl. Environ. Microbiol.* **2009**, *75* (17), 5714–5718. <https://doi.org/10.1128/AEM.00382-09>.

- (20) Kaebernick, M.; Neilan, B. A. Ecological and molecular investigations of cyanotoxin production. *FEMS Micro. Eco.* **2006**, *35* (1), 1–9. <https://doi.org/10.1111/j.1574-6941.2001.tb00782.x>.
- (21) Boopathi, T.; Ki, J. S. Impact of environmental factors on the regulation of cyanotoxin production. *Toxins*. **2014**, (6) 7, 1951 -1978. <https://doi.org/10.3390/toxins6071951>.
- (22) Seller, C.; Honti, M.; Singer, H.; Fenner, K. Biotransformation of chemicals in water-sediment suspensions: Influencing factors and implications for persistence assessment. *Environ. Sci. Technol. Lett.* **2020**, *7* (11), 854–860. <https://doi.org/10.1021/acs.estlett.0c00725>.
- (23) Wennberg, A. C.; Meland, S.; Grung, M.; Lillicrap, A. Unravelling reasons for variability in the OECD 306 marine biodegradation test. *Chemosphere*. **2022**, *300*, 134476. <https://doi.org/10.1016/j.chemosphere.2022.134476>.

Appendix A

Supplementary Material for Chapter 2

Section A.1. Bio- and Photodegradation Transformation Pathways and Products

Several potential degradation products are associated with the bio- and photodegradation of 2,4-dichlorophenoxyacetic acid (2,4-D). 2,4-Dichlorophenol is expected to be produced as a primary photodegradation product¹⁻³ (**Figure A.1**) before being transformed into 2-chloro-1,4-benzoquinone.⁴

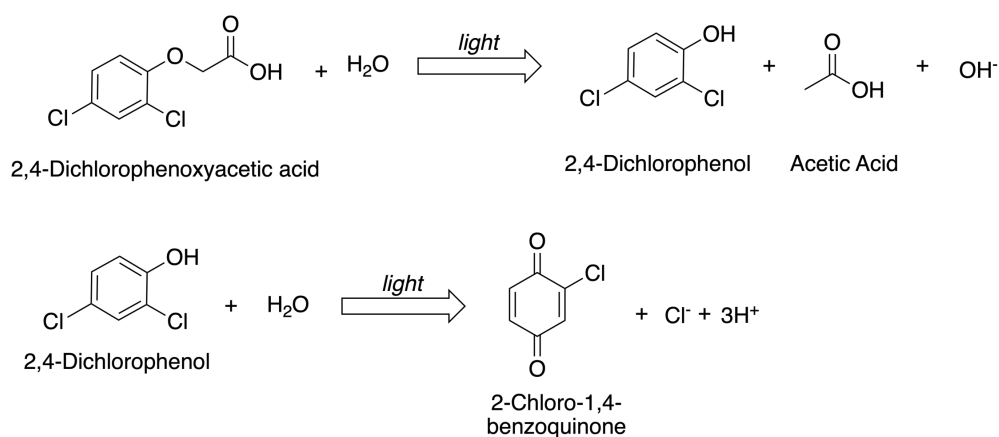


Figure A.1. Degradation schematic for photodegradation of 2,4-D. The primary product, 2,4-dichlorophenol, can be photodegraded into 2-chloro-1,4-benzoquinone.

Initial biodegradation of 2,4-D via *tfda* gene product uses alpha-ketoglutarate to produce 2,4-dichlorophenol, glyoxylate, succinate, and carbon dioxide (**Figure A.2**).^{1,5,6} However, 2,4-dichlorophenol is toxic to microbes and is quickly transformed into 3,5-dichlorocatechol by *tfdb* gene product,^{6,7} suggesting no build-up of 2,4-dichlorophenol will occur during biodegradation.

Thus, we used 2,4-dichlorophenol as an indicator of photodegradation and 3,5-dichlorocatechol as an indicator for biodegradation.

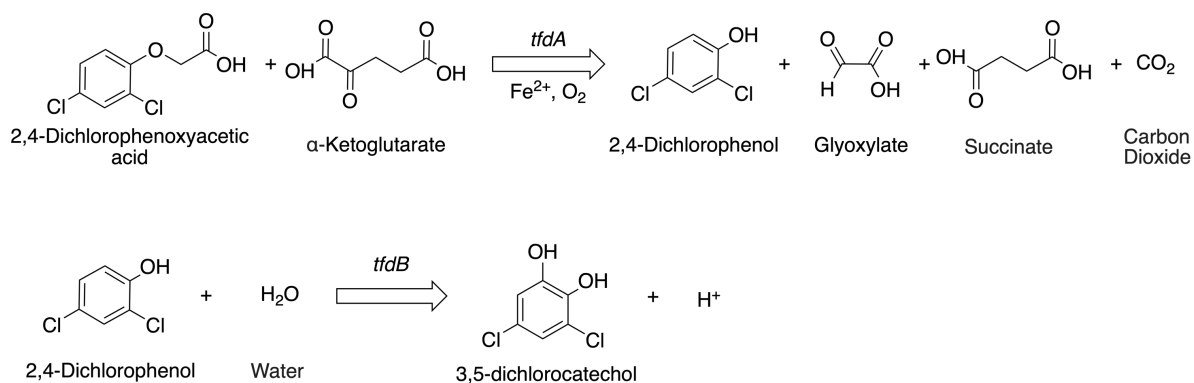


Figure A.2. Biodegradation schematic for 2,4-D via the *tfdA* and *tfdB* genes products. Primary degradation products formed include 2,4-dichlorophenol, glyoxylate, succinate, and carbon dioxide before 2,4-dichlorophenol is further oxidized to 3,5-dichlorocatechol.^{5,7}

Table A.1. Summary of 2,4-D transformation pathways and rates for field and lab studies. Half-lives, formulation, and study type with important details are summarized. All studies were completed using the 2,4-D anion except the field studies, which used a 2,4-D dimethylamine salt formulation that dissociates immediately.^{8,9} Asterisk indicates two half-lives provided that are not directly applicable to our study system based on experimental conditions but are included for completeness.

Half-Life	Study type	Ref.
Field Studies		
4 – 76 days	Field study, large-scale treatment	10
34 to 41 days	Field study, large-scale treatment	11
Photodegradation Studies		
50 minutes*	Laboratory, 254 nm, ultrapure water	1
2.3 hours*	Laboratory, 254 nm, ultrapure water	12
38.5 hours	Laboratory, 290-800 nm, secondary wastewater treatment plant effluent with 'OH	13
12.9 days	Laboratory, ultrapure water, modeled in aquatic half-life with 12 hours of sunlight a day	9
13 days	Laboratory, 300-800 nm, ultrapure water, constant light	13
32 days	Laboratory, simulated sunlight, ultrapure water	13
Biodegradation Studies		
24-60 hours	Cultures isolated from soil using 2,4-D as sole carbon source, complete degradation by 72 hours	15
30-40 hours	Unfiltered river water microcosm, 18-day acclimation	16
48 hours	Soil microcosm, 3-day acclimation. rapid loss from days 3-8 but slowed from days 8-150	17
48 hours	<i>C. necator</i> culture, one half-life achieved, maximum loss of 59% by day 10	18
7-38 days	Soil microcosms	19
10-30 days	Soil microcosms	20
12-25 days	Sediment microcosms	21
25-50 days	Sediment microcosms	1
> 120 days	Lake water microcosms	1

Section A.2. Materials

Dibasic potassium phosphate (ACS, 98%), monobasic potassium phosphate (ReagentPlus(R)), and 3,5-dichlorocatechol (97%) were purchased from Sigma Aldrich. Acetonitrile (HPLC grade), formic acid (ACS, 88%) were purchased from Fisher Chemical. 2,4-Dichlorophenoxyacetic acid (98%) and 2,4-dichlorophenol (99%) were purchased from Alfa Aesar. *para*-Nitroanisole (PNA, 99%) and 2-nitrobenzaldehyde (99%) were purchased from Acros Organics. All chemicals were used as received.

Ultrapure water (18.2 M Ω cm) for all analyses and photochemical irradiations was obtained from Milli-Q water purification system. Calibration solutions for the pH meter were obtained from Aqua Solutions. The dissolved organic carbon (DOC) analyzer was calibrated using potassium hydrogen phthalate (99.8%) purchased from Tokyo Chemical Industry.

Section A.3. Field Sampling Methods

Water. Surface water was collected from the epilimnion in the center of each lake prior to treatment using either four-liter combusted glass amber bottles for chemical analysis or ten-liter high-density polyethylene cubitainers for microcosm construction and pre-treatment *tfdA* quantification. Additional pre-treatment surface water samples were collected into cubitainers from a nearshore site and hypolimnion (when possible) to collect microbial filters for *tfdA* analysis.

Following 2,4-D applications, water samples were collected immediately after treatment, 1, 3, 5, and 7 days after treatment, and approximately weekly thereafter. At each sampling event, water samples were collected in ten-liter high density polyethylene cubitainers from the epilimnion in the middle of the lake, a nearshore site, and the hypolimnion for 2,4-D and *tfdA* quantification. Additional spatially discrete samples were collected using a 50 mL plastic syringe and immediately filtered through a 0.45 μm nylon syringe filter (Agilent) into 15 mL plastic Falcon tubes to quantify herbicide drift from treatment area and to monitor complete mixing in the lake. Depth profiles of temperature and dissolved oxygen were measured from the center of the lake using a multiparameter sonde (YSI Incorporated, Yellow Springs, OH). Secchi depths were recorded during each sampling event

For all sampling points, surface water samples were collected via grab sampling and all deep-water samples were collected using a Van Dorn sampler. Samples were stored on ice in a dark cooler and transported back to the lab. Grab samples were filtered using a 0.22 μm polyethersulfone filter in a Sterivex filter unit (Millipore Sigma). All samples were stored at 4 °C in the dark until analysis.

Homeowners on the treated lakes collected water samples in between regular weekly sampling. Samples were collected in 15 mL Falcon tubes after rinsing the tubes three times with

lake water and stored at 4 °C in the dark. Homeowners recorded the time and date of sample collection on a sample log sheet. Samples were collected from homeowners during weekly sampling visits, filtered through a 0.45 µm nylon syringe filter, and stored at 4 °C until analysis.

Microbial community samples. Samples for *tfdA* quantification were collected prior to treatment and at each sampling event. Ten liters of water were collected and filtered in triplicate using a 0.22 µm Sterivex polyethersulfone inline filter and stored in a -20 °C freezer until DNA extraction. Sediment samples were collected using a 1.5-inch diameter PVC pipe sediment corer. Three sediment cores were collected into a sterile plastic bag, homogenized, and transferred to a 50 mL falcon tube prior to storage in a -20 °C freezer.

Flow. Flow out of the lake was measured at a point of discharge in the middle of the water column using a Marsh McBirney Flo-Mate Model 2000 portable flowmeter to calculate 2,4-D flux out of the lake. A corresponding 2,4-D water sample was collected at the culvert for flow calculation (**Section A.8**).



Figure A.3. Location of all lakes sampled in Wisconsin, USA. All maps were created using ArcGIS software (10.6.1) by Esri. Data provided by the National Atlas of the United States, USGS.

Table A.2. Summary of all sample types collected during field campaign.

Sample Type	When	Where	Volume	Preservation	Purpose
Surface water	Prior to treatment	Epilimnion; middle of the lake	4 L	0.22 μm polyethersulfone filter (Sterivex)	Water used for photochemical irradiations and bulk water characterization. Filter used for DNA analysis
Surface water	Prior to treatment	Epilimnion; middle of the lake	30 L	4 °C fridge	Microcosms
Sediment	Prior to treatment	Shore	19 L	4 °C fridge	Microcosms
Surface water	During treatment at every sampling event	Epilimnion, hypolimnion, and shore location	10 L	0.22 μm polyethersulfone filter (Sterivex)	Water used for 2,4-D quantification Filter used for DNA analysis
Surface water	During treatment at every sampling event	Various locations throughout epilimnion	15 mL	0.45 μm nylon syringe filter	2,4-D quantification
Sediment	During treatment at every sampling event	Shore	0.5 L	-20°C freezer	DNA analysis

Section A.4. Bulk Water Chemistry

Dissolved organic carbon (DOC) was measured using a GE Sievers M5310 TOC analyzer. Calibration check solutions were made from analytical grade potassium hydrogen phthalate ranging from 0 - 10 mg-C L⁻¹. Ultraviolet-visible light spectra for each lake were collected using a Shimadzu 2401PC recording spectrophotometer in 1 nm increments from 200-800 nm. Anions were measured using ion chromatography using a Thermo Dionex 1100. Cations and metals were measured using an Agilent 5110 VDV inductively coupled plasma-optical emission spectrometer (ICP-OES). All samples were filtered through 0.2 µm syringe filter and acidified to 2% nitric acid. Calibration solutions were made from 1000 mg L⁻¹ SPEX CertiPrep solutions.

Table A.3. Dissolved carbon, E₂:E₃ (absorbance at 250 nm divided by absorbance at 365 nm),²² and SUVA₂₅₄ (specific UV absorbance at 254 nm)²³ for all lakes visited during field sampling.

Lake	[DOC] (mg L⁻¹)	E₂:E₃	SUVA₂₅₄ (L mg-C⁻¹ m⁻¹)
Eagle	3.4	7.7	1.5
McCarry	5.2	5.7	2.4
Okauchee	7.9	8.4	2.1
Pike	7.2	9.2	1.8
Pleasant	6.2	9.6	0.9
Random	5.6	8.7	2.1
Round	3.2	15.0	0.9
Bony	3.2	16.1	0.8

Table A.4. Bulk water chemistry for all lakes visited during the field campaign. ND indicates concentrations were below the limit of detection.

Lake	[Ca²⁺] (ppm)	[K⁺] (ppm)	[Mg²⁺] (ppm)	[Na⁺] (ppm)	[SO₄²⁻] (ppm)	[Cl] (ppm)	[NO₃⁻] (ppm)
Eagle	13.19	0.55	3.87	3.04	2.25	4.82	ND
McCarry	15.32	0.63	4.11	4.58	2.07	9.70	0.17
Okauchee	40.32	1.52	31.59	21.45	13.00	50.42	ND
Pike	36.07	2.09	33.76	41.36	13.44	79.96	ND
Pleasant	26.66	1.36	30.23	18.29	20.22	51.69	0.41
Random	48.22	1.57	28.13	23.61	22.06	55.38	1.23
Round	11.90	0.49	3.54	1.93	1.23	2.42	ND
Bony	14.64	0.51	3.70	3.52	2.82	5.63	ND

Section A.5. Photodegradation Experiments and Modeling

Irradiation Experiments. Irradiation experiments carried out using either 311 ± 22 nm (width at half-max) or 365 ± 10 nm (width at half-max) bulbs to test the direct and indirect photodegradation of 2,4-D, 2,4-dichlorophenol, and 3,5-dichlorocatechol. Experiments using the 311 nm bulbs were conducted alongside a 2-nitrobenzaldehyde actinometer,²⁴ while experiments using the 365 nm bulbs used the *para*-nitroanisole/pyridine actinometer.²⁵ 2,4-Dichlorophenol and 3,5-dichlorocatechol experiments were only conducted at 311 nm.

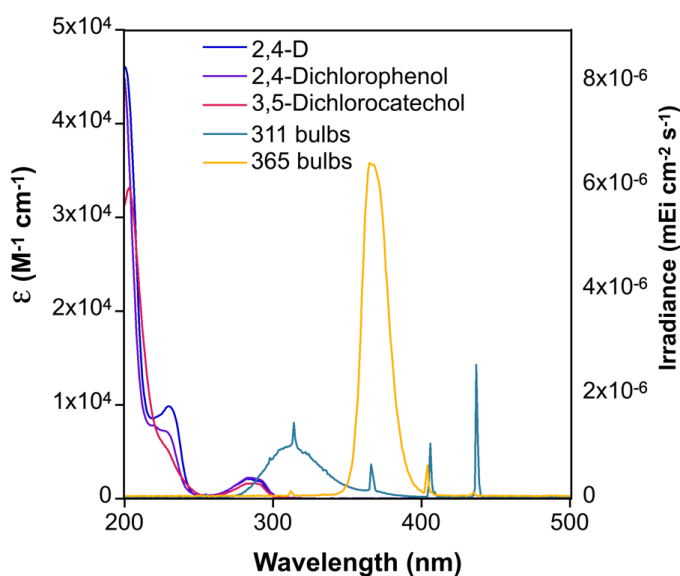


Figure A.4. Molar absorptivity of 2,4-D, 2,4-dichlorocatechol, and 3,5-dichlorocatechol on left y-axis. Bulb intensity of 311 and 365 nm bulbs on right y-axis.

Quantum yield calculations. The observed 2,4-D, 2,4-dichlorophenol, and 3,5-dichlorocatechol photodegradation rate constants (k_{obs}) were corrected for light screening in all solutions using by calculating a screening factor at each wavelength (S_λ):

$$S_{\lambda} = \frac{1-10^{-\alpha_{\lambda} * l}}{2.303 * -\alpha_{\lambda} * l} \quad \text{Eq. A1}$$

where α_{λ} is the solution decadic absorbance measured using a UV-vis spectrophotometer and l is the pathlength of the cuvette (1 cm). An average weighted screening factor (S_{weighted}) was calculated over the from 250-455 nm for the 311 bulbs and 300-455 nm for the 365 bulbs. The weighted screening factor was used to correct the observed degradation rate constants for all lake waters and the direct control using the Equation A2:

$$k_{\text{screened}} = \frac{k_{\text{obs}}}{S_{\text{weighted}}} \quad \text{Eq. A2}$$

The light absorbance rate constant (k_{abs}) was calculated using Equation A3:

$$k_{\text{abs}} = \Sigma \frac{2.303 \times I_{\lambda} \times \alpha_{\lambda} \times S_{\lambda}}{[C] \times j} \quad \text{Eq. A3}$$

where I_{λ} is the intensity of light ($\text{mEi cm}^{-2} \text{ s}^{-1}$), α_{λ} is the solution decadic absorbance, S_{λ} is the weighted screening factor, $[C]$ is 2,4-D, 2,4-dichlorophenol, or 3,5-dichlorocatechol concentration (μM), and j is a conversion factor of $1 \text{ einstein-mol}^{-1}$.²⁶

The quantum yield (Φ) was then calculated using Equation A4:^{27,28}

$$\Phi_{\text{unk}} = \frac{k_{\text{screened,direct}}}{k_{\text{direct,act}}} \times \frac{k_{\text{abs,act}}}{k_{\text{abs,unk}}} \times \Phi_{\text{act}} \quad \text{Eq. A4}$$

where $k_{\text{screened,direct}}$ is the light screening corrected direct photodegradation rate constant for the direct control (s^{-1}), $k_{\text{direct,act}}$ is the photodegradation rate constant of the actinometer (s^{-1}), $k_{\text{abs,act}}$ (s^{-1}) is the rate of light absorbance of the actinometer, $k_{\text{abs,unk}}$ (s^{-1}) is the rate of light absorption for either 2,4-D, 2,4-dichlorophenol, or 3,5-dichlorocatechol, and Φ_{act} is the quantum yield for the relevant actinometer ($\Phi_{\text{act}} = 0.41$ for 2-nitrobenzaldehyde; ²⁴ $\Phi_{\text{act}} = 3.19 \times 10^{-4}$ for PNA/pyridine).²⁵

Table A.5. Measured quantum yields for 2,4-D, 2,4-dichlorophenol, and 3,5-dichlorocatechol at pH 7. Quantum yields are calculated from 311 nm exposures using the ultrapure water (direct degradation) control.

Compound	Quantum Yield
2,4-D	$(3.12 \pm 0.01) \times 10^{-3}$
2,4-Dichlorophenol	$(7.9 \pm 0.3) \times 10^{-2}$
3,5-Dichlorocatechol	$(5.5 \pm 0.16) \times 10^{-2}$

In-lake photodegradation modeling. The calculated quantum yield was coupled with solar irradiance modeling using the Simple Model of Atmospheric Transfer of Sunshine (SMARTS)²⁹ to calculate 2,4-D half-lives in Wisconsin lakes. Using the horizontal global irradiance spectrum for I (**Figure A.4**), a light absorbance rate constant $k_{abs,sun}$ for direct photodegradation was calculated using Equation A3. $k_{abs,sun}$ was then used to calculate direct photodegradation rates in lakes with site-specific solar intensity using Equation A5:

$$k_{photodegradation} = k_{abs,sun} \times \Phi_{2,4-D} \quad \text{Eq. A5}$$

The $k_{photodegradation}$ for 2,4-D was used in mass balance modeling described in **Section A.6**.

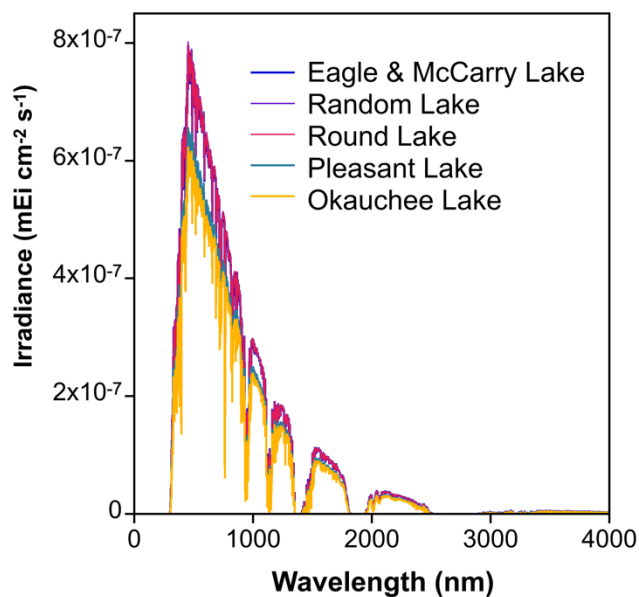


Figure A.5. Irradiance data for the global horizontal irradiance spectra generated using SMARTS. Early summer treatments show slightly higher intensities than fall treatments.

Table A.6. SMARTS Modeling input parameters for the in-lake photolysis degradation of 2,4-D. Each lakes modeling conditions, such as date, time, and location of treatment, is included. CO₂ concentration is from measurements from January 2019.

Card Number/ Description	Random	Eagle	McCarry	Round	Pleasant	Okauchee
1. Comment	'Random'	'Eagle Lake'	'McCarry Lake'	'Round Lake'	'Pleasant Lake'	'Okauchee Lake'
1. Manually input pressure	1	1	1	1	1	1
2a. Pressure, surface altitude, and height	989.7 0.271 0	972 0.37 0	972 0.37 0	957.3 0.363 0	988.9 0.300 0	984 0.269 0
3. Option to use default atmosphere	1	1	1	1	1	1
3a. Midlatitude Summer	'MLS'	'MLS'	'MLS'	'MLS'	'MLS'	'MLS'
4. Use default Water vapor	1	1	1	1	1	1
5. Use default ozone abundance	1	1	1	1	1	1
6. Use default gas abundance except CO ₂	1	1	1	1	1	1
7. Carbon dioxide from January 2019	411	411	411	411	411	411
7a. Use default synthetic spectrum	0	0	0	0	0	0
8. Use continental aerosol model	'SRA_ CONTL'	'SRA_ CONTL'	'SRA_ CONTL'	'SRA_ CONT L'	'SRA_ CONTL'	'SRA_ CONTL'
9. Use aerosol	5	5	5	5	5	5

optical depth of 55 nm						
9a.	0.084	0.084	0.084	0.084	0.084	0.084
10. Select “water” for albedo	2	2	2	2	2	2
10b. ITILT	1	1	1	1	1	1
ITILT is an option for tilted surface calculations. Leave box unchecked	51 37. 180.	51 37. 180.	51 37. 180.	51 37. 180.	51 37. 180.	51 37. 180.
11. Minimal spectral range, max spectral range, variability in irradiance, and default solar constant.	280 4000 1.0 1366.1	280 4000 1.0 1366.1	280 4000 1.0 1366.1	280 4000 1.0 1366.1	280 4000 1.0 1366.1	280 4000 1.0 1366.1
12. Option to generate results with spreadsheet	2	2	2	2	2	2
12a: Interval for printing results	280 4000 1	280 4000 1	280 4000 1	280 4000 1	280 4000 1	280 4000 1
12b. Total number of outputs	5	5	5	5	5	5
12c. Outputs: (1) extraterrestrial spectrum, (2) direct normal irradiance, (3) diffuse horizontal irradiance, (4) global horizontal irradiance	1 2 3 4 5	1 2 3 4 5	1 2 3 4 5	1 2 3 4 5	1 2 3 4 5	1 2 3 4 5

and (5) direct horizontal irradiance						
13. Bypass circumsolar radiation	0	0	0	0	0	0
14. Bypass smoothing calculation	0	0	0	0	0	0
15. Illuminance using CIE photopic curve	1	1	1	1	1	1
16. No special UV calculations	0	0	0	0	0	0
17. Set inputs for card 17	3	3	3	3	3	3
17a. Year, month, day, hour, latitude, longitude, time zone.	2019 05 20 12.1 43.549815 - 87.955191 -6	2019 06 10 12.1 46.49804 9 - 91.35682 7 -6	2019 06 10 12.1 46.516587 - 91.371709 -6	2019 06 25 12.1 45.995 52 - 91.320 341 -6	2019 09 16 12.1 42.78957 4 - 88.54590 6 -6	2019 09 23 12.1 43.119245 - 88.545906 -6

Section A.6. Microbial Degradation and *tfdA* Quantification

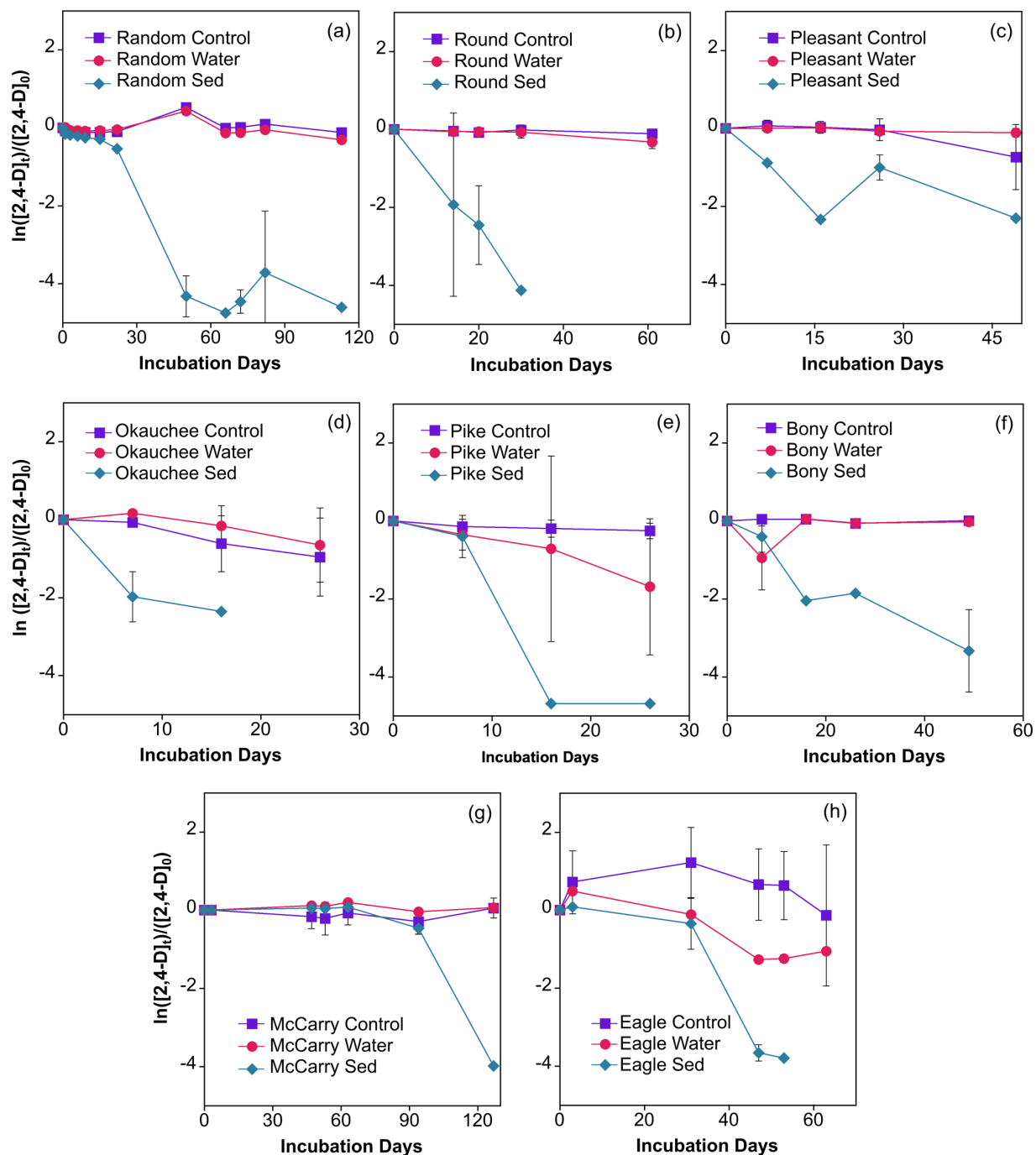


Figure A.6. 2,4-D degradation in microcosms. (a) Random, (b) Round, (c) Pleasant, and (d) Okauchee Lakes have been treated with 2,4-D previously, while (e) Pike, (f) Bony, (g) McCarry, and (h) Eagle Lakes have had no previous treatments. Two of three (h) Eagle water-only microcosms were destroyed during incubation so only one microcosm is shown after day 3. One replicate in the (e) Pike Lake water-only microcosm had loss, as shown in the large error bars at day 14 and 28. Error bars represent standard deviation of triplicate microcosms.

DNA extraction and *tfdA* quantification. DNA was extracted from samples collected from field sites. Sediment (0.5 g) and filters (1/2 filter) were extracted using an MP Bio Fast DNA Spin Kit and quantified for DNA concentration using an Invitrogen Qubit 3.0 fluorimeter. DNA was then qPCR amplified using the following forward and reverse general (non-class specific) *tfdA* primers intended to amplify a 215bp section. The forward primer was 5'-GAGCACTACGCRCTGAAYTCCCG-3' and the reverse primer was 5'-GTCGCGTGCTCGAGAAG-3'. Amplification was carried out on a BioRad thermocycler using the conditions in **Table A.7**.^{30,31} A vector containing a plasmid carrying the *tfdA* class I gene from *Ralstonia eutropha* was used to construct the standard curve, obtained originally from Dr. Jan Roelof van der Meer from the University of Lausanne, Switzerland by way of Dr. Lily Gonzalez Vazquez at the University of Wisconsin-Madison. The class I gene had been directly ligated into pGEM7-Ampicillin vector and transformed into *Escherichia coli* DH5 α competent cells. The PCR product from the standards was confirmed to be the expected length using a 1.5% agarose gel. The values obtained for *tfdA* abundance by qPCR in environmental samples were extremely low, corresponding to barely above the quantification limit (~10 copies per reaction). We also attempted to optimize the reaction by adjusting the annealing temperature, primer concentration, template concentration, and additional template clean-up steps but this was unsuccessful. This prompted us to verify that amplification products were truly *tfdA* gene fragments.

To confirm specific amplification of the *tfdA* gene fragment, we cloned the PCR products from two samples (one water column and one sediment from Random Lake) using an Invitrogen TOPO TA Cloning kit with One Shot TOP10 chemically competent *E. coli* cells. Fresh PCR product was inserted into the provided plasmids and transformed into the chemically competent

cells. Cells were spread on LB Agar plates with 50 µg/mL kanamycin and incubated overnight at 37 °C. Colonies grown on overnight plates were transferred to LB broth with 50 µg/mL kanamycin and incubated at 37 °C overnight again. Aliquots of 19 liquid cultures (total from both samples) were extracted using an Invitrogen PureLink Quick Plasmid Miniprep kit. Plasmids were then amplified with IDT ReadyMade M13 (-20) forward primers. Amplified plasmids were sent for Sanger sequencing University of Wisconsin-Madison Biotechnology Center. Obtained sequences were analyzed using NCBI NucleotideBLAST and blastx.

Chromatograms were processed using A plasmid Editor software³² (v. 3.0.7) to export fasta formatted sequences. None of the 19 sequences we obtained matched with any known *tfdA* in the NCBI nr database. The sequences only had “hits” to plasmid sequences related to the TOPO TA Cloning vector with ~97-100% nucleotide identity across ~ 50% of the query length (~180 bp). The other half of each sequence had no match using default settings.

Table A.7. Thermocycler conditions for qPCR amplification of a portion of the *tfdA* gene adapted from Baelum et al. 2008.^{30,31} Conditions were optimized for our thermocycler.

Step	Time	Temperature (°C)
Initial	10 minutes	95
Denaturation	15 seconds	95
Annealing	30 seconds	64
Elongation	30 seconds	72

Section A.7. Analytical Methods

Organic compound quantification. 2,4-D, 2,4-dichlorophenol, 3,5-dichlorocatechol, *p*-nitroanisole, and 2-nitrobenzaldehyde were quantified using an Agilent 1260 high-performance liquid chromatograph (HPLC) equipped with a diode-array detector. All methods used an Agilent InfinityLab Poroshell 120 EC-C18 (3.0 x 50 mm) column and a column temperature control of 30 °C. Samples were eluted using an isocratic method with acetonitrile as a mobile phase and an aqueous buffer of 90:10 ultrapure water: aqueous buffer of 10 % acetonitrile and 0.1% formic acid in ultra-pure water.

Table A.8. Flow rates, aqueous buffer ratios, and detection wavelengths for each compound analyzed via HPLC.

Compound	% Aqueous Buffer	Flow (mL min ⁻¹)	Detection wavelength (nm)	Retention Time (min)	Purpose	LOD (μM)
2,4-D	70	0.6	284	2.2	Herbicide	0.1
2,4-dichlorophenol	70	0.6	284	4.0	Degradation product	0.3
3,5-dichlorocatechol	70	0.6	284	1.8	Degradation product	0.8
2-nitrobenzaldehyde	80	0.5	231	2.9	311 nm actinometer	0.5
<i>para</i> -nitroanisole	60	0.5	314	1.4	365 nm actinometer	0.8

Analysis of low concentration (< 0.1 μM) 2,4-D samples used an Agilent Triple Quad 6460 liquid chromatograph-tandem mass spectrometer (LC-MS/MS). Samples were analyzed using an isocratic method of 80% aqueous buffer (10 % acetonitrile and 0.1% formic acid in ultra-pure water) and 20% acetonitrile at 0.3 mL min⁻¹ on an Agilent InfinityLab Poroshell 120 EC-C18 (3.0 x 50 mm) column with column temperature control of 30 °C. 2,4-D had an injection volume of 50 μL, retention time of 4.7 minutes, and detection limit of 0.047 μM.

LC-MS/MS running conditions:

Mode: Negative electrospray ionization
 Scan type: MRM
 Dwell time: 400
 Fragmentor voltage: 75
 Cell accelerator voltage: 7
 Gas temp: 300 °C
 Speed: 5 L/min
 Nebulizer pressure: 45 psi
 Sheath gas temperature: 250 °C
 Sheath gas flow rate: 11 L/min
 Precursor ion: 219 *m/z*
 Product: 161 *m/z*
 Product: 125 *m/z*
 Product: 89 *m/z*

Section A.8. Mass Balance

A mass balance for two lakes using photodegradation, biodegradation, and discharge rates modeled 2,4-D loss through each pathway. All loss is assumed to follow first-order kinetics and the overall mass balance is represented with Equation A6:

$$\frac{dC}{dt} = \frac{Q_{in}C_{in}}{V} - \frac{Q_{out}C_{lake}}{V} - k_{photodegradation}C_{lake} - k_{biodegradation}C_{lake} \quad \text{Eq. A6}$$

where Q is flow in (Q_{in}) and out (Q_{out}) in L day⁻¹, C_{in} is [2,4-D] flowing into the lake (μM), C_{lake} is the lake-wide [2,4-D] (μM), and $k_{photodegradation}$ and $k_{biodegradation}$ are reaction rate constants of photo- and biodegradation (day⁻¹), respectively. There are no new inputs of 2,4-D to the system after the treatment, so C_{in} is 0 after $t = 0$. Integrating the overall equation generates Equation S7 (i.e., Equation 1 in the manuscript) used in the mass balance model:

$$C_t = C_0 x e^{-\left(\frac{Q_{out}}{V} + k_{photodegradation} + k_{biodegradation}\right)t} \quad \text{Eq. A7}$$

where C_t (μM) is concentration at any time t (days) and C_0 (μM) is the initial lake-wide 2,4-D concentration.

Discharge for McCarry and Round Lakes was calculated using water depth, channel width (i.e., culvert width), and flow rate (**Tables A.9 and A.10**) at the middle of the water column using Equation A8:

$$Q = D \times W \times V \times j \quad \text{Eq. A8}$$

where Q is discharge (L day^{-1}), D is depth (m), W is culvert width (m), V is water velocity (m day^{-1}) and j is a conversion factor of converting m^3 to L (1000 L m^{-3}). We compared the average of all discharge observations versus using a weekly value and found no difference in modeled 2,4-D loss between the two approaches (**Figure A.7**). For simplicity, we used the average discharge for the overall mass balance.

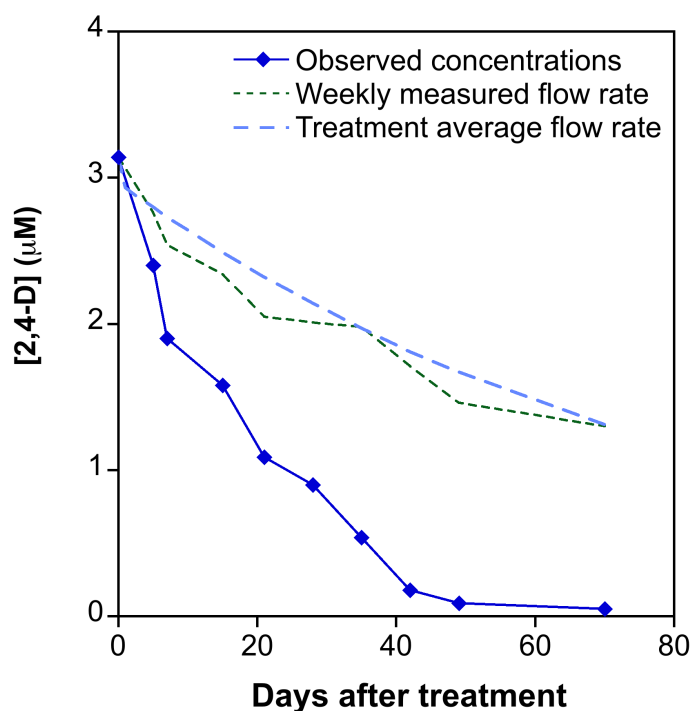


Figure A.7. Modeled [2,4-D] in McCarry Lake using weekly flow measurements compared to average discharge for 70 days of treatment.

The biodegradation rate constant ($k_{biodegradation}$, days⁻¹) was determined using the half-life observed in the microcosm incubations. Microcosm half-life was calculated from the day of 2,4-D addition to the day the concentration decreased to half the initial concentration. The only exception to this approach was McCarry Lake, in which degradation was only observed after a long lag phase. In this case, an adjusted time zero was used at day 67, which was the last time point before degradation started. The biodegradation half-lives ($t_{1/2}$) were used in Equation A9 to determine a biodegradation rate constant:

$$k_{biodegradation} = \frac{\ln 2}{t_{1/2}} \quad \text{Eq. A9}$$

The in-lake photodegradation rate constant ($k_{photodegradation}$) is calculated in Equation A5.

Table A.9. Water flow and depth observations at culvert discharging McCarry Lake.

Date	Water depth (m)	Flow (m/s)	Culvert width (m)
June 15	0.14	0.03	1.83
June 17	0.14	0.03	1.83
June 25	0.14	0.03	1.83
July 1	0.26	0.04	1.83
July 1	0.13	0.04	1.83
July 1	0.03	0.00	1.83
July 1	0.02	0.00	1.83
July 8	0.26	0.00	1.83
July 8	0.13	0.01	1.83
July 8	0.03	0.03	1.83
July 15	0.21	0.01	1.83
July 15	0.10	0.01	1.83
July 15	0.03	0.01	1.83
July 22	0.26	0.05	1.83
July 22	0.13	0.05	1.83
July 22	0.05	0.03	1.83
July 22	0.03	0.01	1.83
July 29	0.23	0.05	1.83
July 29	0.14	0.04	1.83
July 29	0.05	0.03	1.83
August 19	0.25	0.05	1.83
August 19	0.10	0.02	1.83
August 19	0.05	0.00	1.83

Table A.10. Water flow and depth observations at culvert discharging Round Lake.

Date	Water depth (m)	Flow (m/s)	Culvert width (m)
June 28	0.54	0.10	8.05
June 28	0.25	0.10	8.05
June 28	0.05	0.05	8.05
June 28	1.89	N/A	8.05
June 30	0.05	0.07	8.05
June 30	0.25	0.15	8.05
June 30	0.58	0.10	8.05
June 30	1.92	N/A	8.05
July 2	0.00	0.01	8.05
July 2	0.25	0.03	8.05
July 2	0.05	0.01	8.05
July 2	0.59	0.07	8.05
July 2	1.92	N/A	8.05
July 9	0.64	0.01	8.05
July 9	0.33	0.00	8.05
July 9	0.03	0.00	8.05
July 15	0.03	0.01	8.05
July 15	0.49	0.20	8.05
July 15	0.23	0.31	8.05
July 15	1.88	N/A	8.05
July 23	0.05	0.04	8.05
July 23	0.55	0.07	8.05
July 23	0.27	0.06	8.05
July 23	1.91	N/A	8.05

Section A.9. Treatment data

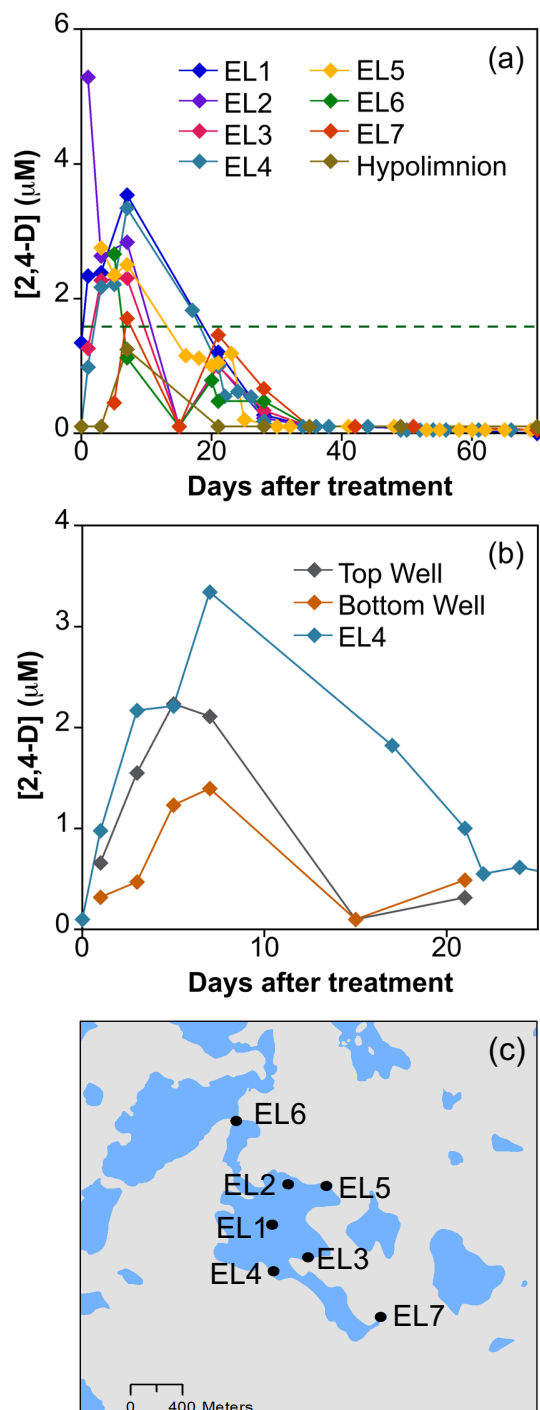


Figure A.8. [2,4-D] in (a) surface water and (b) porewater for (c) Eagle Lake. Hypolimnion samples were collected at EL1 and peepers were installed at site EL4. EL6 is a culvert under the road and was sampled to monitor advective transport back into Twin Bear Lake. EL7 is Murrays Dam at the outflow of Flynn Lake and was sampled to monitor advective transport downstream. Homeowner volunteers collected weekly samples at EL4 and EL5. Green dashed line in (a) represents application target whole lake concentration of 1.67 µM.

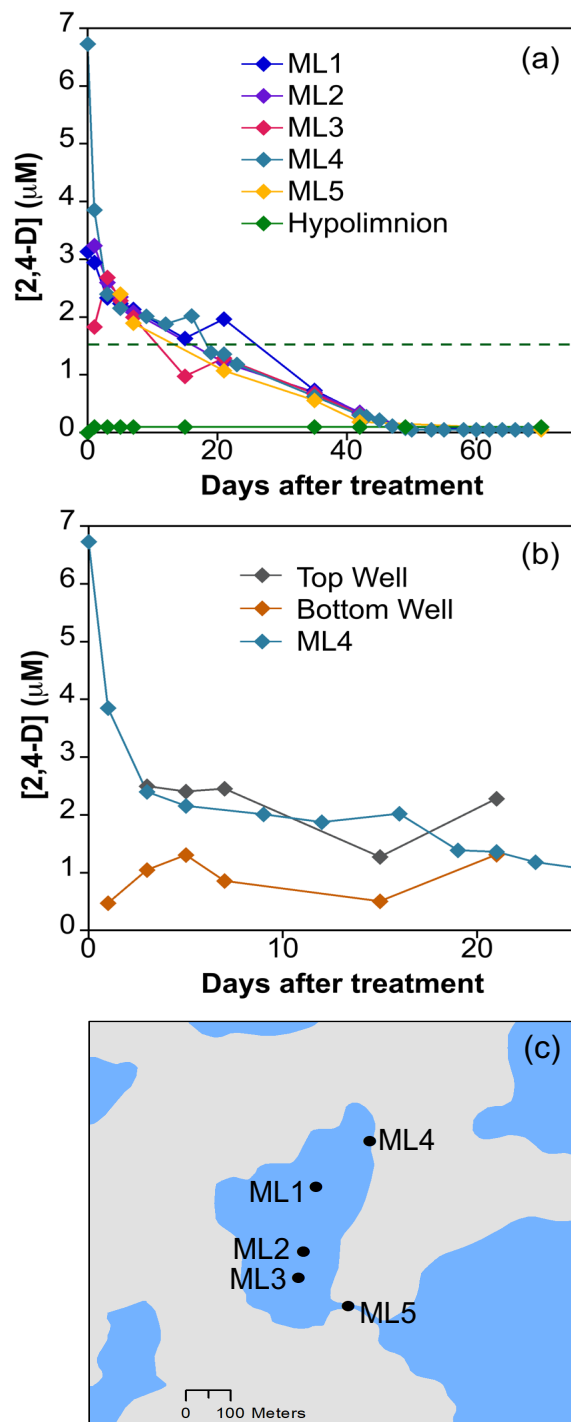


Figure A.9. [2,4-D] in (a) surface water and (b) porewater in (c) McCarry Lake. Hypolimnion collected at ML1. Peepers were installed and volunteer homeowner samples were collected at ML4. Green dashed line in (a) represents target whole lake concentration of 1.58 μM .

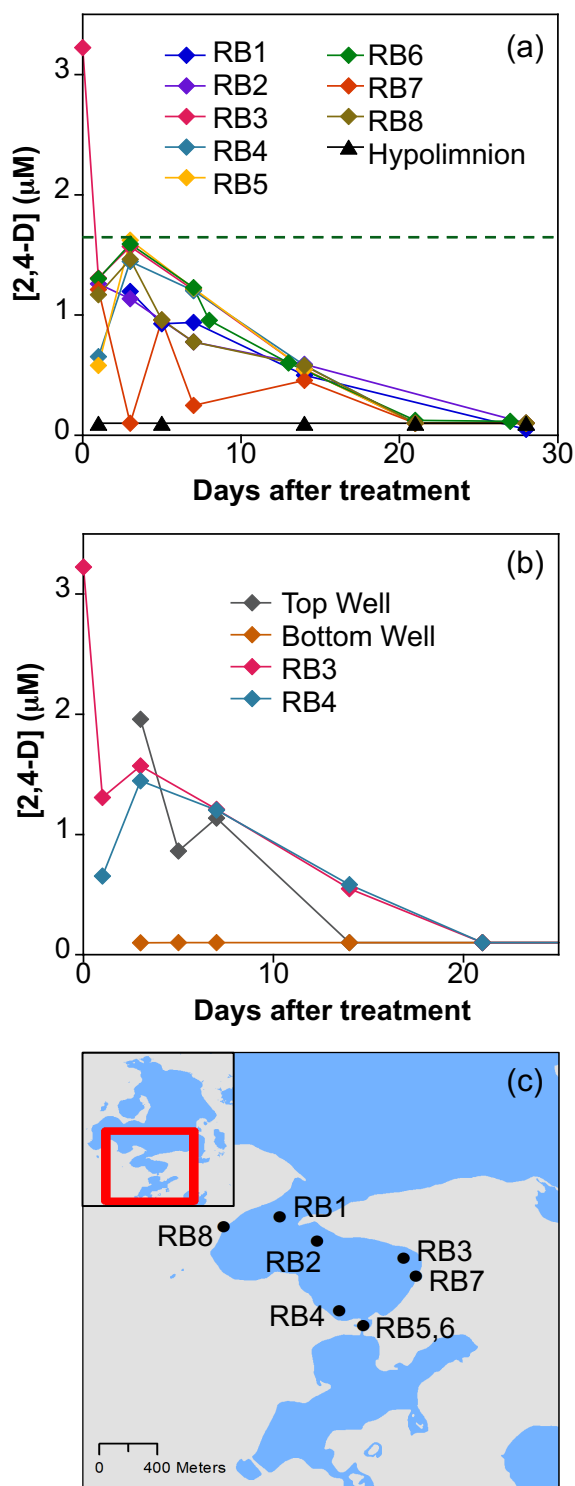


Figure A.10. [2,4-D] in (a) surface water and (b) porewater in (c) Round Lake. Hypolimnion samples were collected at RB1 and peepers were installed at RB7. Flow measurements and volunteer homeowner collected samples were made at RB5 and RB6. Green dashed line in (a) represents target bay-wide concentration of 1.63 µM.

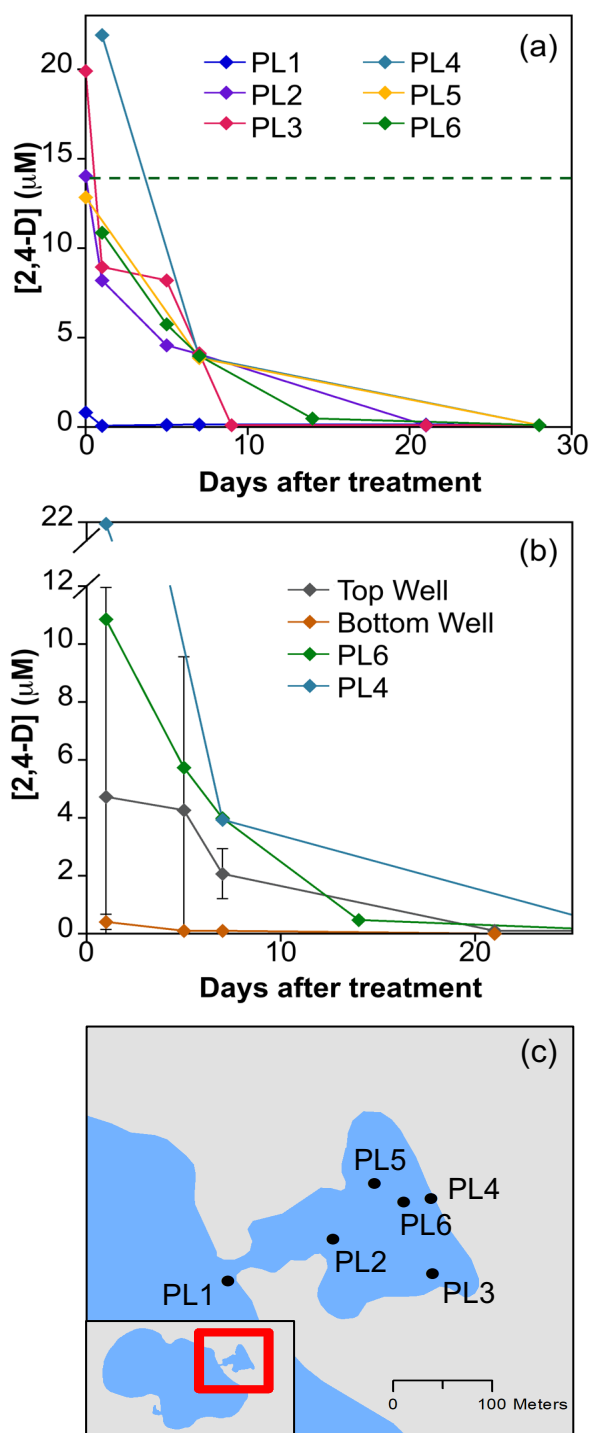


Figure A.11. [2,4-D] in (a) surface water and (b) porewater in (c) Pleasant Lake. Peepers were installed at site PL4. PL1 was used as reference for advective transport out of the treated bay. Green dashed line in (a) represents target bay-wide concentration of 14.2 μM . Large error bars in the top peeper wells for days 1, 5, and 7 is likely due to resettling of sediment and suspended solids following peeper placement given the shallowness (1.5 m) of the bay and unconsolidated nature of the sediment. Error bars represent the standard deviation of triplicate porewater samples.

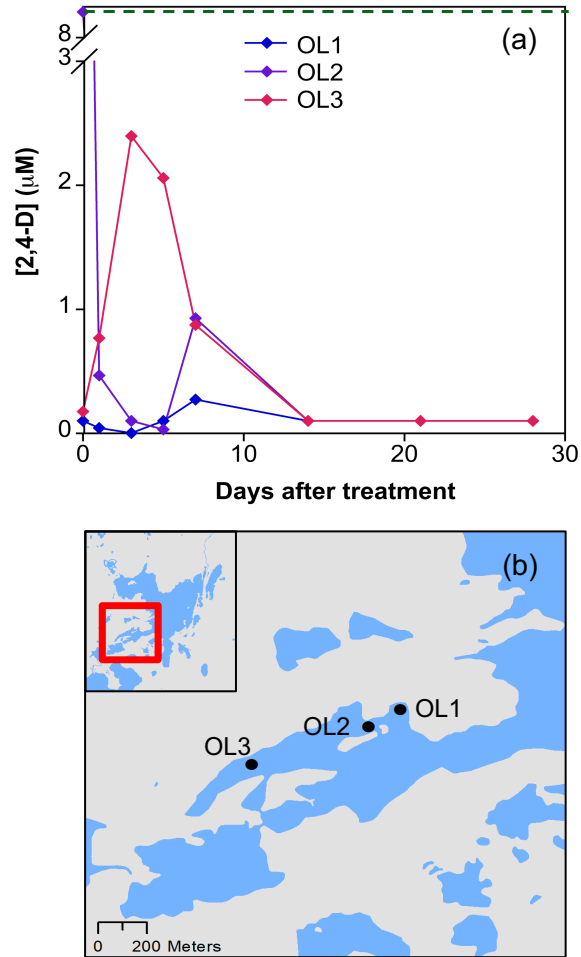


Figure A.12. (a) [2,4-D] in surface water at all sampling sites for (b) Okauchee Lake. Green dashed line in (a) represents target bay wide concentration of 9 μM . Peepers were not deployed in this lake.

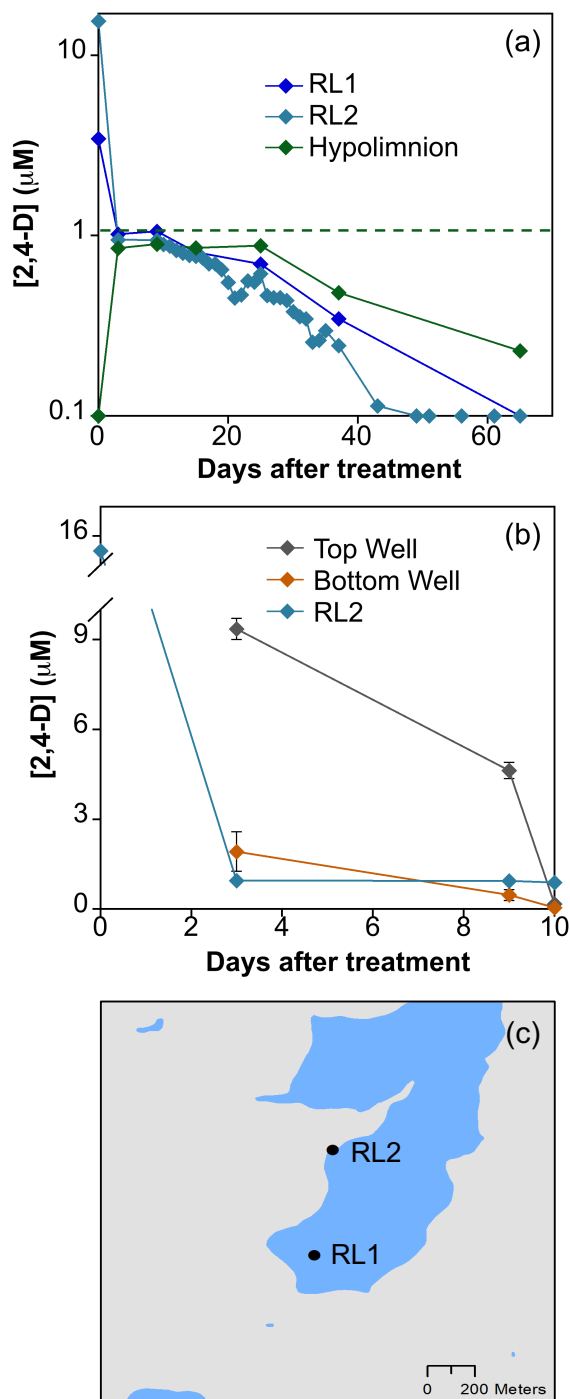


Figure A.13. [2,4-D] in (a) surface water and (b) porewater in (c) Random Lake. Hypolimnion sample were collected from RL1. Peepers were installed at RL2. Volunteer homeowner water samples and peepers were collected at RL2. Green dashed line in (a) represents target whole lake concentration of 1.17 μM . Three peepers were collected each sampling event for 15 days. Two peepers had a paired top and bottom sample while the third peeper was bottom only. Error bars represent the standard deviation of triplicate (bottom) or duplicate (top) samples.

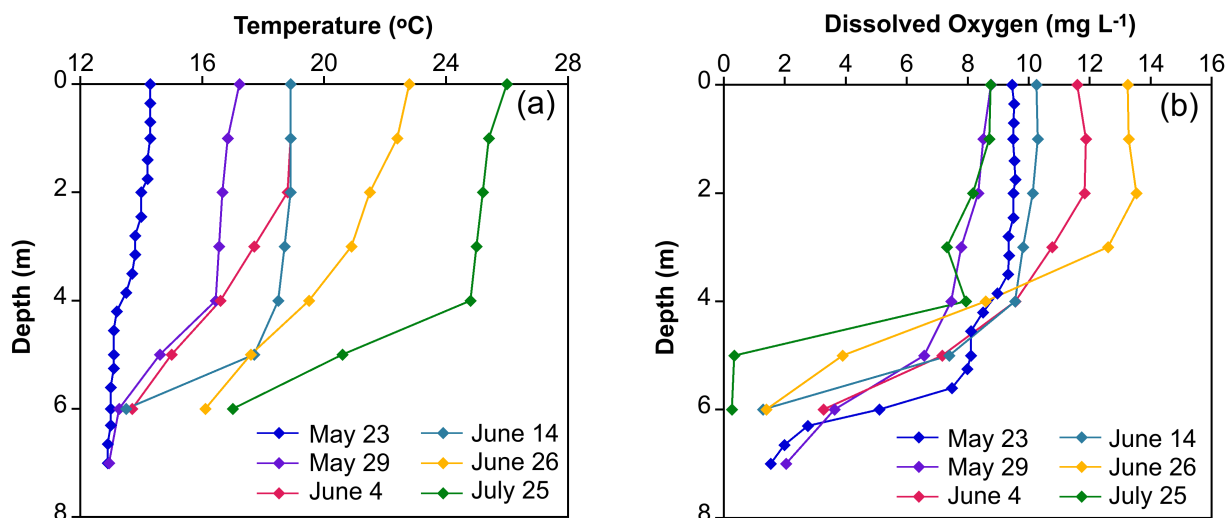


Figure A.14. (a) Temperature and (b) dissolved oxygen depth profiles for Random Lake. The lake was completely mixed at the beginning of treatment and began to stratify by May 29, 2019. Dissolved oxygen remained low in the hypolimnion throughout the entire treatment.

Table A.11. Predicted sediment [2,4-D] using lake/bay-wide 24-hour surface water [2,4-D], sediment organic carbon concentrations, and $K_{oc} = 61.7$ to 78 mL g^{-1} .^{9,20}

Lake	Organic carbon content (%)	Estimated [2,4-D] _{sediment} after 24 hours ($\mu\text{M g}^{-1}$)	Percent of 2,4-D lost to sediments
Eagle	12.0	0.01	0.84%
McCarry	3.0	0.01	0.21%
Pleasant	8.5	0.10	0.59%
Random	15.4	0.10	1.08%
Round	14.2	0.03	0.99%

Table A.12. Summary physical parameters distributions for each lake expressed as percent of lake area under 6 m and 1 m as well as mean depth.³³

Lake	Area under 6 m (%)	Area under 1 m (%)	Mean depth (m)
Random	96	14	1.8
Eagle	73	12	4.3
Round	69	9	5.2
McCarry	98	56	1.5
Pleasant	100	100	0.4
Okauchee	100	100	0.6

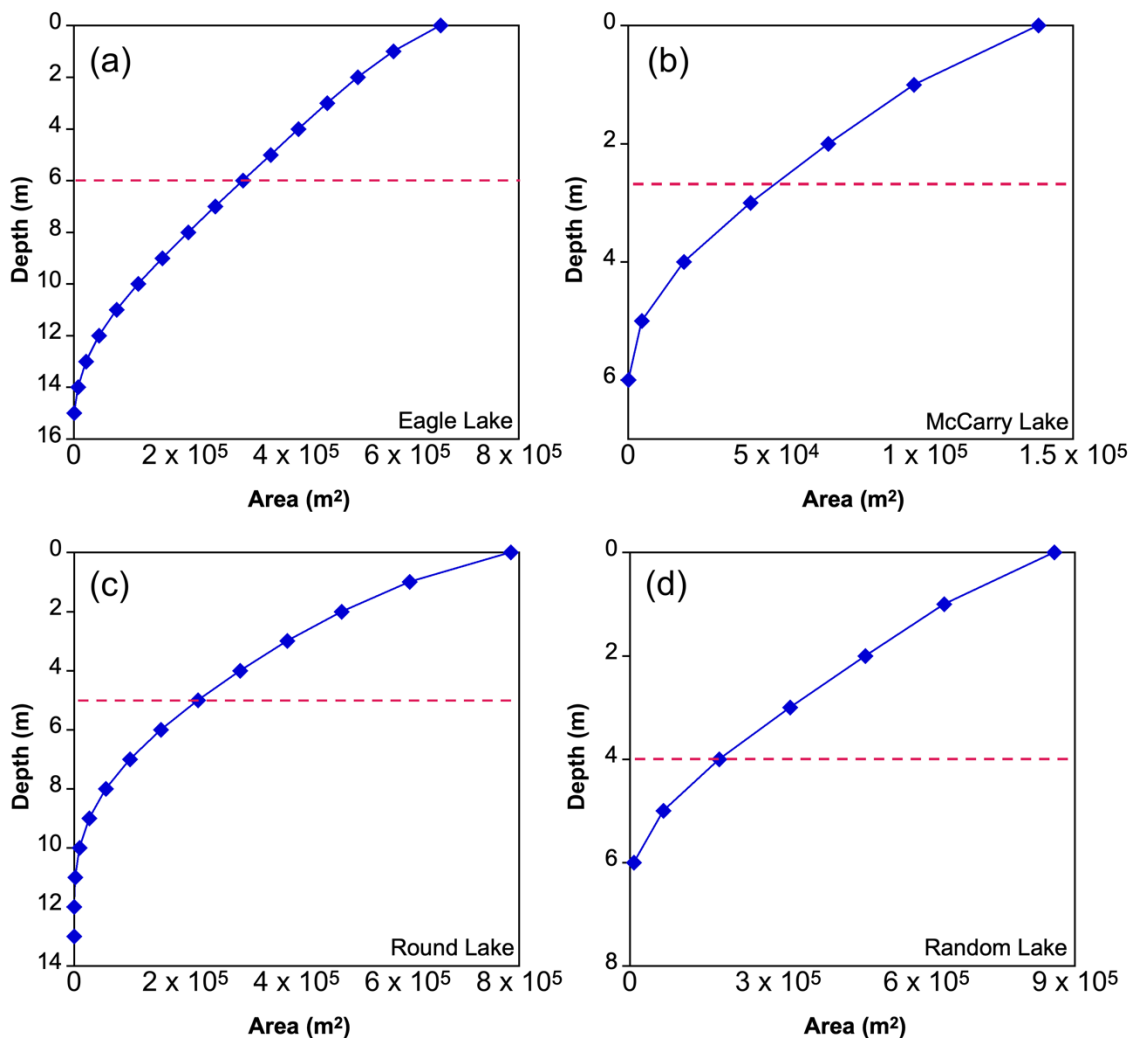


Figure A.15. Hypsographs for (a) Eagle, (b) McCarry, (c) Round, and (d) Random Lakes. Pink dashed line represents stratification depth. Area above pink curve represents sediment exposed to epilimnion, while area below the pink line is sediment isolated from epilimnion. Hypsographs³⁴ for each stratified lake were generated using the rLakeAnalyzer package in R Studio.^{35,36}

Section A.10. References

- (1) Aly, O. M.; Faust, S. D. Studies on the fate of 2,4-D and ester derivatives in natural surface waters. *J. Agric. Food Chem.* **1964**, *12* (6), 541–546. <https://doi.org/10.1021/jf60136a016>.
- (2) Crosby, D. G.; Tutass, H. O. Photodecomposition of 2,4-dichlorophenoxyacetic acid. *J. Agric. Food Chem.* **1966**, *14* (6), 596–599. <https://doi.org/10.1021/jf60148a012>.
- (3) Boval, B.; Smith, J. M. Photodecomposition of 2,4-dichlorophenoxyacetic acid. *Chem. Engr. Sci.* **1973**, *28*, 1661–1675. [https://doi.org/10.1016/0009-2509\(73\)80020-X](https://doi.org/10.1016/0009-2509(73)80020-X).
- (4) Vione, D.; Minero, C.; Housari, F.; Chiron, S. Photoinduced transformation processes of 2,4-dichlorophenol and 2,6-dichlorophenol on nitrate irradiation. *Chemosphere* **2007**, *69* (10), 1548–1554. <https://doi.org/10.1016/j.chemosphere.2007.05.071>.
- (5) Fukumori, F.; Hausinger, R. P. *Alcaligenes eutrophus* JMP134 “2,4-dichlorophenoxyacetate monooxygenase” is an α -ketoglutarate-dependent dioxygenase. *J. Bact.* **1993**, *175* (7), 2083–2086. <https://doi.org/10.1128/jb.175.7.2083-2086.1993>.
- (6) Kumar, A.; Trefault, N.; Olaniran, A. O. Microbial degradation of 2,4-dichlorophenoxyacetic acid: Insight into the enzymes and catabolic genes involved, their regulation and biotechnological implications. *Crit. Rev. Micro.* **2016**, *42* (2), 194–208. <https://doi.org/10.3109/1040841X.2014.917068>.
- (7) Laemmlli, C. M.; Leveau, J. H. J.; Zehnder, A. J. B.; Roelof Van Der Meer, J. Characterization of a second *tfd* gene cluster for chlorophenol and chlorocatechol metabolism on plasmid pJP4 in *Ralstonia eutropha* JMP134 (pJP4). *J. Bact.* **2000**, *182* (15), 4165–4172. <https://doi.org/10.1128/JB.182.15.4165-4172.2000>.
- (8) Walters, J. Environmental fate of 2,4-dichlorophenoxyacetic acid. **1999**. <https://doi.org/http://citeseerx.ist.psu.edu/viewdoc/download?doi=10.1.1.639.4289&rep=rep1&type=pdf> (accessed 2020-05-15).
- (9) U.S. EPA. *Reregistration Eligibility Decision for 2,4-D*; 2005. https://doi.org/https://archive.epa.gov/pesticides/reregistration/web/pdf/24d_red.pdf (accessed 2020 -05 -15).
- (10) Nault, M. E.; Barton, M.; Hauxwell, J.; Heath, E.; Hoyman, T.; Mikulyuk, A.; Netherland, M. D.; Provost, S.; Skogerboe, J.; van Egeren, S. Evaluation of large-scale low-concentration 2,4-D treatments for Eurasian and hybrid watermilfoil control across multiple Wisconsin lakes. *Lake Resvr. Mgmt.* **2018**, *34* (2), 115–129. <https://doi.org/10.1080/10402381.2017.1390019>.
- (11) Nault, M. E.; Netherland, M. D.; Mikulyuk, A.; Skogerboe, J. G.; Asplund, T.; Hauxwell, J.; Toshner, P. Efficacy, selectivity, and herbicide concentrations following a whole-lake 2,4-D application targeting Eurasian watermilfoil in two adjacent northern Wisconsin lakes. *Lake Resvr. Mgmt.* **2014**, *30* (1), 1–10. <https://doi.org/10.1080/10402381.2013.862586>.
- (12) Benitez, F. J.; Acero, J. L.; Real, F. J.; Roman, S. Oxidation of MPCA and 2,4-D by UV radiation, ozone, and the combinations UV/H₂O₂ and O₃/H₂O₂. *J. Environ. Sci. Health. B.* **2004**, *39* (3), 393–409. <https://doi.org/10.1081/PFC-120035925>.
- (13) Wang, Y.; Roddick, F. A.; Fan, L. Direct and indirect photolysis of seven micropollutants in secondary effluent from a wastewater lagoon. *Chemosphere.* **2017**, *185*, 297–308. <https://doi.org/10.1016/j.chemosphere.2017.06.122>.

- (14) Su, L.; Sivey, J. D.; Dai, N. Sunlight photolysis of 2,4-D herbicides in systems simulating leaf surfaces. *Environ. Sci. Processes Impacts*. **2018**, *20* (8), 1123–1135. <https://doi.org/10.1039/c8em00186c>.
- (15) Zabaloy, M. C.; Gómez, M. A. Isolation and characterization of indigenous 2,4-D herbicide degrading bacteria from an agricultural soil in proximity of Sauce Grande River, Argentina. *Annals Micro*. **2014**, *64* (3), 969–974. <https://doi.org/10.1007/s13213-013-0731-9>.
- (16) McMartin, D. W.; Gillies, J. A.; Headley, J. v.; Peterson, H. G. Biodegradation kinetics of 2,4-dichlorophenoxyacetic acid (2,4-D) in south Saskatchewan river water. *Cand. Wat. Res. J.* **2000**, *25* (1), 81–92. <https://doi.org/10.4296/cwrj2501081>.
- (17) Lerch, T. Z.; Dignac, M. F.; Nunan, N.; Bardoux, G.; Barriuso, E.; Mariotti, A. Dynamics of soil microbial populations involved in 2,4-D biodegradation revealed by fame-based stable isotope probing. *Soil Bio. Biochem.* **2009**, *41* (1), 77–85. <https://doi.org/10.1016/j.soilbio.2008.09.020>.
- (18) Lerch, T. Z.; Dignac, M. F.; Barriuso, E.; Bardoux, G.; Mariotti, A. Tracing 2,4-D metabolism in *Cupriavidus necator* JMP134 with ¹³C-labelling technique and fatty acid profiling. *J. Micro. Methods*. **2007**, *71* (2), 162–174. <https://doi.org/10.1016/j.mimet.2007.08.003>.
- (19) Bolan, N. S.; Baskaran, S. Biodegradation of 2,4-D herbicide as affected by its adsorption-desorption behaviour and microbial activity of soils. *Aust. J. Soil Res.* **1996**, *34*, 1041–1053. <https://doi.org/10.1071/SR9961041>.
- (20) Boivin, A.; Amellal, S.; Schiavon, M.; van Genuchten, M. T. 2,4-Dichlorophenoxyacetic acid (2,4-D) sorption and degradation dynamics in three agricultural soils. *Environ. Poll.* **2005**, *138* (1), 92–99. <https://doi.org/10.1016/j.envpol.2005.02.016>.
- (21) Chinalia, F. A.; Killham, K. S. 2,4-Dichlorophenoxyacetic acid (2,4-D) biodegradation in river sediments of northeast-Scotland and its effect on the microbial communities (PLFA and DGGE). *Chemosphere*. **2006**, *64* (10), 1675–1683. <https://doi.org/10.1016/j.chemosphere.2006.01.022>.
- (22) John, R. H.; Stubbins, A.; Ritchie, J. D.; Minor, E. C.; Kieber, D. J.; Mopper, K. Absorption spectral slopes and slope ratios as indicators of molecular weight, source, and photobleaching of chromophoric dissolved organic matter. *Limnol. Oceanogr.* **2009**, *54* (3), 1023. <https://doi.org/10.4319/lo.2009.54.3.1023>.
- (23) Weishaar, J. L.; Aiken, G. R.; Bergamaschi, B. A.; Fram, M. S.; Fujii, R.; Mopper, K. Evaluation of specific ultraviolet absorbance as an indicator of the chemical composition and reactivity of dissolved organic carbon. *Environ. Sci. Technol.* **2003**, *37* (20), 4702–4708. <https://doi.org/10.1021/es030360x>.
- (24) Galbavy, E. S.; Ram, K.; Anastasio, C. 2-Nitrobenzaldehyde as a chemical actinometer for solution and ice photochemistry. *J. Photochem. Photobio. A: Chem* **2010**, *209* (2–3), 186–192. <https://doi.org/10.1016/j.jphotochem.2009.11.013>.
- (25) Laszakovits, J. R.; Berg, S. M.; Anderson, B. G.; O'Brien, J. E.; Wammer, K. H.; Sharpless, C. M. *p*-Nitroanisole/pyridine and *p*-nitroacetophenone/pyridine actinometers revisited: Quantum yield in comparison to ferrioxalate. *Environ. Sci. Technol. Lett.* **2017**, *4* (1), 11–14. <https://doi.org/10.1021/acs.estlett.6b00422>.
- (26) Leifer, A. *The Kinetics of Environmental Aquatic Photochemistry: Theory and Practice*; American Chemical Society, 1988.

- (27) Remucal, C. K.; McNeill, K. Photosensitized amino acid degradation in the presence of riboflavin and its derivatives. *Environ. Sci. Technol.* **2011**, *45* (12), 5230–5237. <https://doi.org/10.1021/es200411a>.
- (28) McConville, M. B.; Hubert, T. D.; Remucal, C. K. Direct photolysis rates and transformation pathways of the lampricides TFM and niclosamide in simulated sunlight. *Environ. Sci. Technol.* **2016**, *50* (18), 9998–10006. <https://doi.org/10.1021/acs.est.6b02607>.
- (29) Gueymard, C. A. Interdisciplinary applications of a versatile spectral solar irradiance model: A review. *Energy* **2005**, *30* (9), 1551–1576. <https://doi.org/10.1016/j.energy.2004.04.032>.
- (30) Bælum, J.; Nicolaisen, M. H.; Holben, W. E.; Strobel, B. W.; Sørensen, J.; Jacobsen, C. S. Direct analysis of *tfdA* gene expression by indigenous bacteria in phenoxy acid amended agricultural soil. *ISME* **2008**, *2* (6), 677–687. <https://doi.org/10.1038/ismej.2008.21>.
- (31) Bælum, J.; Jacobsen, C. S. TaqMan probe-based real-time PCR assay for detection and discrimination of class I, II, and III *tfdA* genes in soils treated with phenoxy acid herbicides. *Appl. Environ. Micro.* **2009**, *75* (9), 2969–2972. <https://doi.org/10.1128/AEM.02051-08>.
- (32) Davis, M. W.; Jorgensen, E. M. ApE, a plasmid editor: A freely available DNA manipulation and visualization program. *Front. Bioinform.* **2022**, *2*. <https://doi.org/10.3389/fbinf.2022.818619>.
- (33) Wisconsin DNR. Wisconsin Lake Finder. <https://dnr.wi.gov/lakes/findalake/> (accessed 2020-05-15).
- (34) Johansson, H.; Brolin, A. A.; Håkanson, L. New approaches to the modelling of lake basin morphometry. *Environ. Model Assess.* **2007**, *12* (3), 213–228. <https://doi.org/10.1007/s10666-006-9069-z>.
- (35) Winslow, L.; Read, J.; Woolway, R.; Brentrup, J.; Leach, T.; Zwart, J.; Albers, S.; Collinge, D. RLakeAnalyzer: Lake physics tools. <https://CRAN.R-project.org/package=rLakeAnalyzer>. 2019.
- (36) R Core Team. R: A language and environment for statistical computing. <https://www.R-project.org/>. R Foundation for Statistical Computing.: Vienna, Austria. 2021.

Appendix B

Supplementary Material for Chapter 3

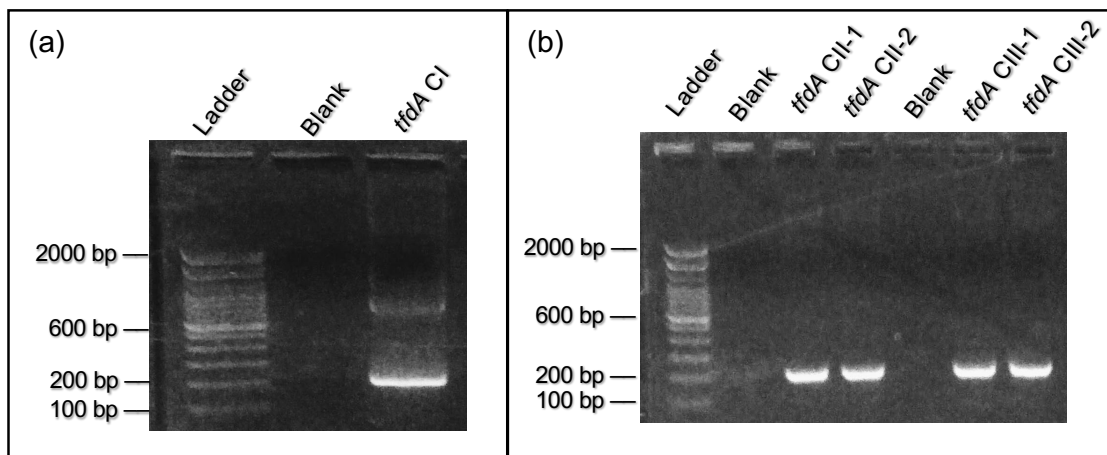


Figure B.1. Gel visualization of gene product of 215 bp *tfdA* primer on class I gene standard (a) as well as class II and class III standard (b) in duplicate.

Table B.1. NCBI BLAST hits for top pairwise alignments between *tfdA* classes I, II, and III genes and sequenced plasmids.

Reference Gene	Sample	Max Score	Total Score	Query Cover (%)	E-value	Identity (%)
R. eutropha (Class I)	S	38.3	71.1	10	6.00E-06	95.65
	T	35.6	70.2	18	1.00E-05	91.67
	U	32.8	32.8	7	1.00E-04	95.00
	V	42.8	80.1	15	1.00E-07	92.86
	W	38.3	71.1	6	1.00E-05	95.65
B. tropica (Class II)	S	33.7	85.9	12	7.00E-05	91.30
	T	40.1	69.3	17	1.00E-06	95.83
	U	27.4	27.4	6	6.00E-03	94.12
	V	37.4	37.4	8	4.00E-06	92.00
	W	33.7	61.2	5	1.00E-04	91.30
D. acidovorans (Class III)	S	33.7	85.9	12	7.00E-05	91.30
	T	40.1	69.3	17	1.00E-06	95.83
	U	27.4	27.4	6	6.00E-03	94.12
	V	37.4	37.4	8	4.00E-04	92.00
	W	33.7	61.2	5	1.00E-04	91.30

Appendix C

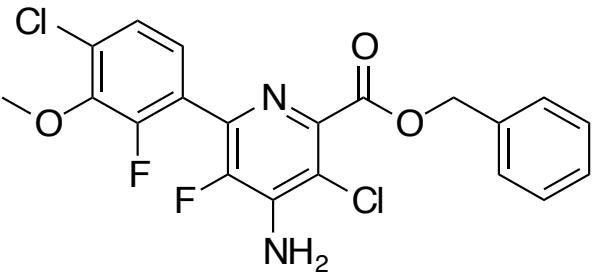
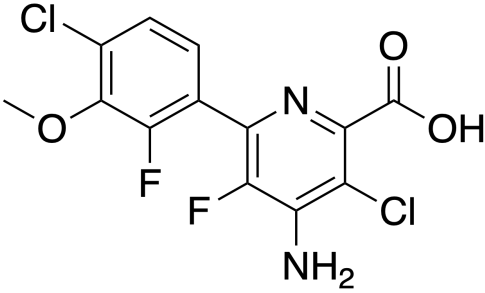
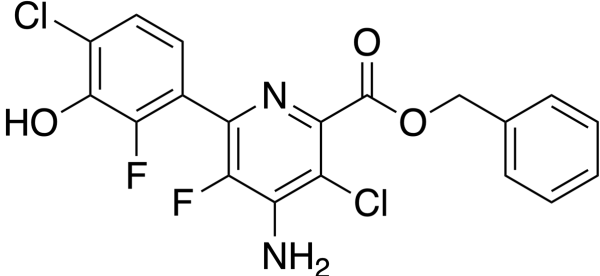
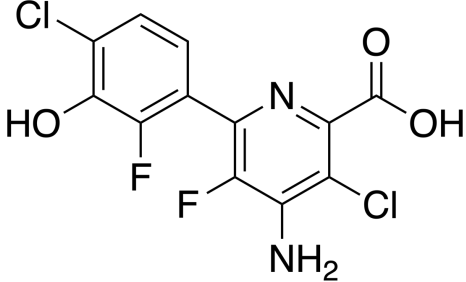
Supplementary Materials for Chapter 4

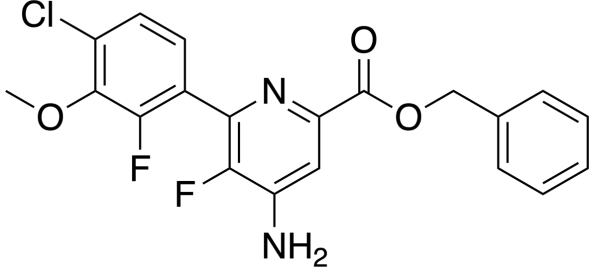
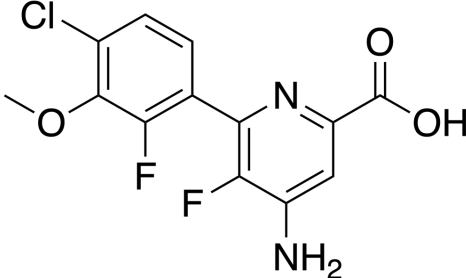
Section C.1. Materials and Chemical Structures

Dibasic potassium phosphate (ACS, 98%), monobasic potassium phosphate (ReagentPlus(R)), were purchased from Sigma Aldrich. Acetonitrile (HPLC grade), formic acid (ACS, 88%) were purchased from Fisher Chemical. 2-nitrobenzaldehyde (99%) was purchased from Acros Organics. Florpyrauxifen-benzyl (99.5%) was purchased from Chem Service, Inc. Florpyrauxifen (98.5%) was purchased from LGC Standards. Sodium Borate Buffer purchased from Amresco. Sodium Acetate (ACS purity) purchased from Alfa Aesar. Methanol (>99.8%) purchased from VWR. Standards for X12300837, X11966341, X12131932, X12393505 (**Table S1**) were not commercially available. Analytical standards were provided curtesy of Corteva Agrisciences. All chemicals were used as received.

Ultrapure water (18.2 MΩ cm) for all analyses and photochemical irradiations was obtained from Milli-Q water purification system. Calibration solutions for the pH meter were obtained from Aqua Solutions. The dissolved organic carbon (DOC) analyzer was calibrated using potassium hydrogen phthalate (99.8%) purchased from Tokyo Chemical Industry.

Table C.1. Chemical structures, formulas, and molecular weight of florpyrauxifen-benzyl and five degradation products. ¹⁻³

Chemical Name and Formula	Structure
<p>Florpyrauxifen-benzyl</p> <p>Molecular Formula: C₂₀H₁₄C₁₂F₂N₂O₃</p> <p>Molecular Weight: 439.24</p> <p>CAS Number: 1390661-72-9</p>	
<p>Florpyrauxifen</p> <p>Molecular Formula: C₂₀H₁₄C₁₂F₂N₂O₃</p> <p>Molecular Weight: 439.24</p> <p>CAS Number: 1390661-72-9</p>	
<p>X12300837</p> <p>Molecular Formula: C₁₉H₁₂C₁₂F₂N₂O₃</p> <p>Molecular Weight: 425.21</p>	
<p>X11966341</p> <p>Molecular Formula: C₁₂H₆C₁₂F₂N₂O₃</p> <p>Molecular Weight: 335.09</p>	

<p>X12131932</p> <p>Molecular Formula: C₂₀H₁₅ClF₂N₂O₃</p> <p>Molecular Weight: 404.79</p>	
<p>X12393505</p> <p>Molecular Formula: C₁₃H₉ClF₂N₂O₃</p> <p>Molecular Weight: 314.67</p>	

Section C.2. Field Sampling Methods

Five FPB treatments were studied during May-August 2021 and 2022 (**Table C.1, Figure C.1**). These treatments applied FPB to areas of high-density Eurasian watermilfoil but had the potential to mix completely throughout the lake. Lakes were selected in collaboration with the Wisconsin Department of Natural Resources (WIDNR).

Pretreatment surface water and sediment were collected from the epilimnion and nearshore area ≤ 2 hours prior to treatment and stored at 4°C until processing. Pretreatment samples were used for bulk water chemistry measurements and photochemical irradiations were collected in 4 L combusted glass amber bottles, filtered through a 0.45 μ M nylon filter, and preserved at 4°C until analysis. Water for microcosm incubations was collected with 10 L HDPE cubitainers and stored in the dark on ice until microcosm set up. Sediment for microcosm incubations was collected by Eckman dredge or hand-coring at a nearshore site of each, store in the dark on ice until microcosms set up.

Water samples collected during the treatment were stored on ice and in the dark until processing, typically on site (i.e., within 1 hour of collection) but no more than 24 hours after collection and preserved with methanol, formic acid, and the internal standard as described in the main text and in **Section C.7**.

Water samples were collected at three sites on each lake, with at least one site in treatment area, one outside of treatment area (i.e., not intended to be treated) to monitor advective transport out of treatment area, and one site at the deepest point of the lake. Samples were collected immediately after FPB application (<1 hour after application) and at 3- to-4-hour intervals for 12 hours after treatment, every 1 to 2 days after treatment for one week after treatment, and then weekly thereafter. Additional depth discrete samples were collected with a Van Dorn sampler at 2 or 3 m intervals the deep hole of Muskellunge and Silver Lakes. At each sampling event, surface water was analyzed for all six described compounds (**Table C.1**). Additional samples not preserved with methanol were collected for organic carbon analysis and UV-vis spectroscopy.



Figure C.1. Map of lakes sampled during 2021-2022 field campaign. All lakes selected in conjunction with Wisconsin Department of Natural Resources (WDNR). Map made using Leaflet package in RStudio.

Section C.3. Bulk Water Chemistry

Dissolved organic carbon (DOC) was measured using a GE Sievers M5310 TOC analyzer. Calibration check solutions from 0 - 10 mg-C L⁻¹. were made from analytical grade potassium hydrogen phthalate. Ultraviolet-visible light spectra for each lake were collected using a Shimadzu 2401PC recording spectrophotometer in 1 nm increments from 200-800 nm. Ultraviolet-visible light spectra for each lake were collected from 200-800 nm. Specific absorbance at 254 nm (SUVA₂₅₄)⁴ and the ratio of absorbance 250 nm to 365 nm (E₂:E₃)⁵ was calculated using UV-visible spectra and DOC measurements.

Section C.4. Photochemical Irradiations and Modeling

Irradiation Experiments. Irradiation experiments carried out using 311 ± 22 nm bulbs (width at half-max) alongside a 2-nitrobenzaldehyde actinometer.⁶ Lake water used for indirect photodegradation analysis was diluted to 3 mg-C L⁻¹.

Quantum yield calculations. The FPB quantum yield was calculated as described previously.^{7,8} Briefly, the observed FPB photodegradation rate constants (k_{obs}) were corrected for light screening in all solutions using by calculating a screening factor at each wavelength (S_{λ}):

$$S_{\lambda} = \frac{1 - 10^{-\alpha_{\lambda} * l}}{2.303 * -\alpha_{\lambda} * l} \quad \text{Eq. C1}$$

where α_{λ} is the solution decadic absorbance measured using a UV-vis spectrophotometer and l is the pathlength of the cuvette (1 cm). An average weighted screening factor ($S_{weighted}$) was calculated over the from 250-455 nm, which was used to correct the observed degradation rate constants for all lake waters and the direct control using the Equation C2:

$$k_{screened} = \frac{k_{obs}}{S_{weighted}} \quad \text{Eq. C2}$$

The light absorbance rate constant (k_{abs}) was calculated using Equation C3:

$$k_{abs} = \Sigma \frac{2.303 \times I_{\lambda} \times \alpha_{\lambda} \times S_{\lambda}}{[C] \times j} \quad \text{Eq. C3}$$

where I_{λ} is the intensity of light ($\text{mEi cm}^{-2} \text{ s}^{-1}$), α_{λ} is the solution decadic absorbance, S_{λ} is the weighted screening factor, $[C]$ is FPB concentration (molar), and j is a conversion factor of 1 einstein-mol⁻¹.⁹

The quantum yield (Φ) was then calculated using Equation SC: ^{7,8,10}

$$\Phi_{FPB} = \frac{k_{screened,direct,FPB}}{k_{direct,act}} \times \frac{k_{abs,act}}{k_{abs,FPB}} \times \Phi_{act} \quad \text{Eq. C4}$$

where $k_{screened,direct}$ is the light screening corrected direct photodegradation rate constant for the direct control (s^{-1}), $k_{direct,act}$ is the photodegradation rate constant of the actinometer (s^{-1}), $k_{abs,act}$ (s^{-1}) is the rate of light absorbance of the actinometer, $k_{abs,unk}$ (s^{-1}) is the rate of light absorption for FPB and $\Phi_{act} = 0.41$ for 2-nitrobenzaldehyde.⁶

In-lake photodegradation modeling. The calculated quantum yield was coupled with solar irradiance modeling using the Simple Model of Atmospheric Transfer of Sunshine (SMARTS)¹¹ to calculate FPB half-lives in the study lakes. A light absorbance rate constant, $k_{abs,sun}$, was calculated for the horizontal global irradiance spectrum for I^7 using Equation C3. $k_{abs,sun}$ was then used to calculate direct photodegradation rates in lakes with site-specific solar intensity using Equation S5:

$$k_{photodegradation} = k_{abs,sun} \times \Phi_{FPB} \quad \text{Eq. C5}$$

A depth integrated photodegradation rate was calculated by varying the pathlength (Eq. C1) to find a new $k_{photodegradation}$ at 10 cm intervals through a 10 m water column (i.e., 1 cm, 10 cm, 20 cm, ... 1000 cm). The depth discrete rates were then averaged together to find a depth integrated photodegradation rate.

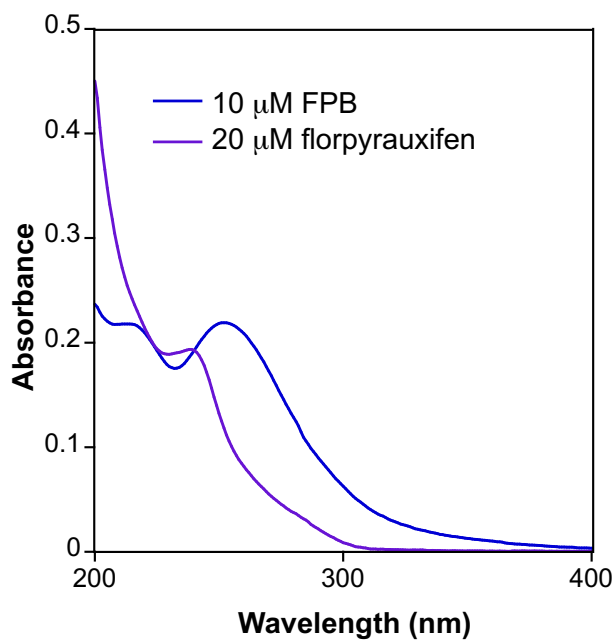


Figure C.2. Absorbance spectra of 10 μM FPB (blue) and 20 μM florypyrauxifen (purple).

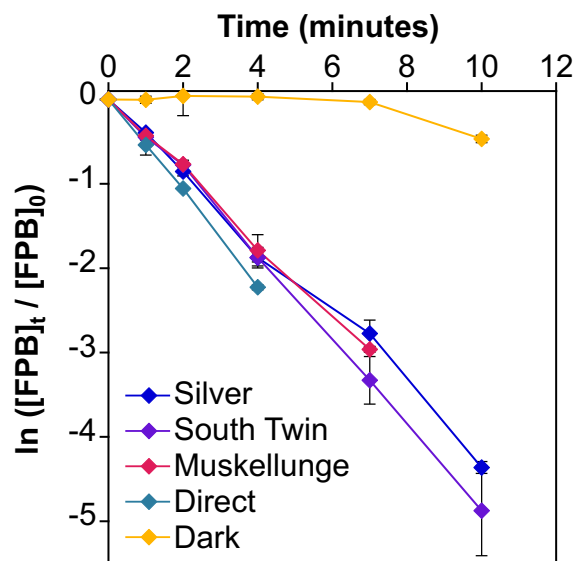


Figure C.3. Photochemical irradiation of FPB at 311 nm. Natural log of the ratio of [FPB] at time t to initial [FPB].

Section C.5. Microcosm Incubations

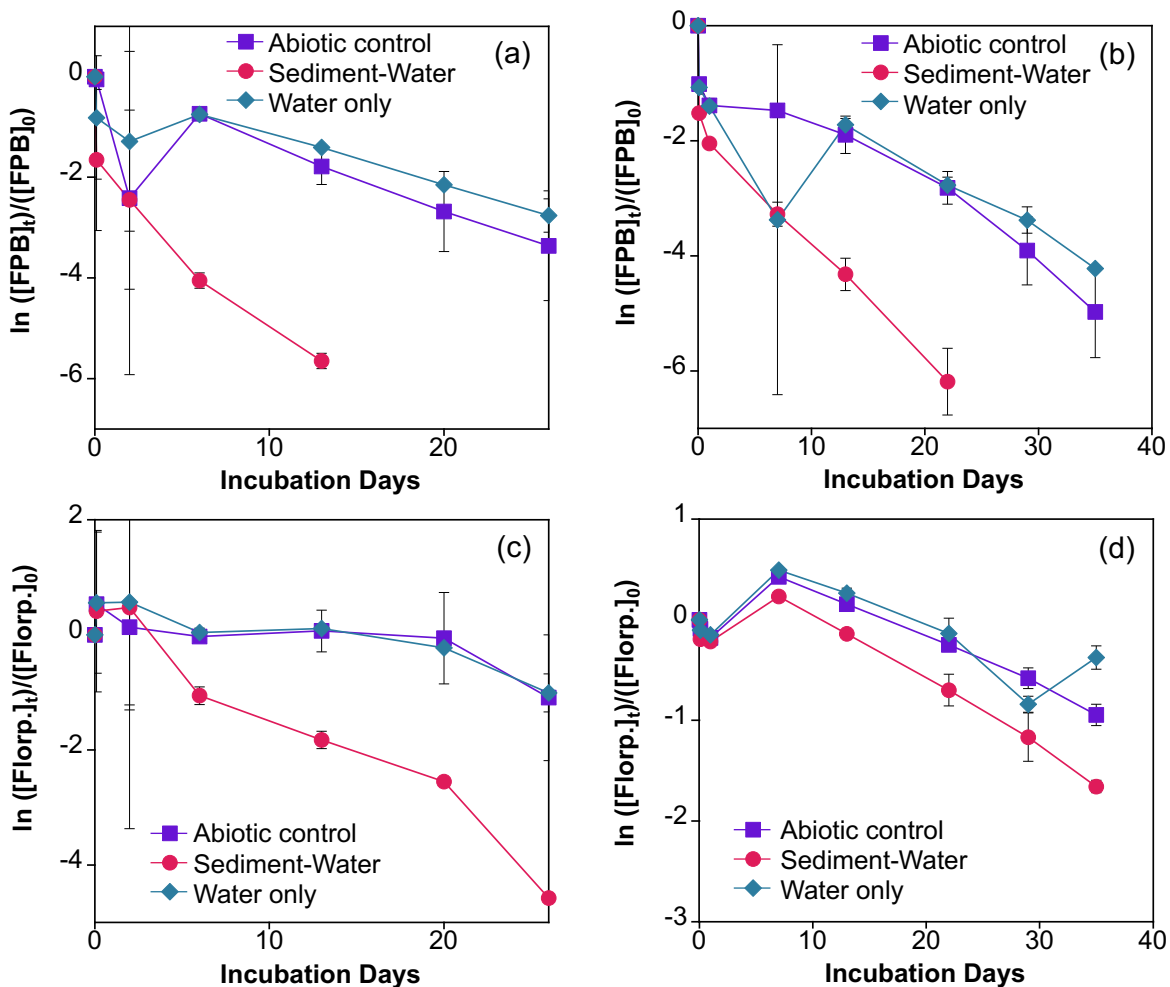


Figure C.4. Microcosms kinetics for FPB in (a) Kettle Moraine La and (b) Kettle Moraine Lake as well as floryprauxifen incubations in (c) Lilly Lake and (d) Kettle Moraine Lake. Error bars represent the standard deviation of triplicate reactors.

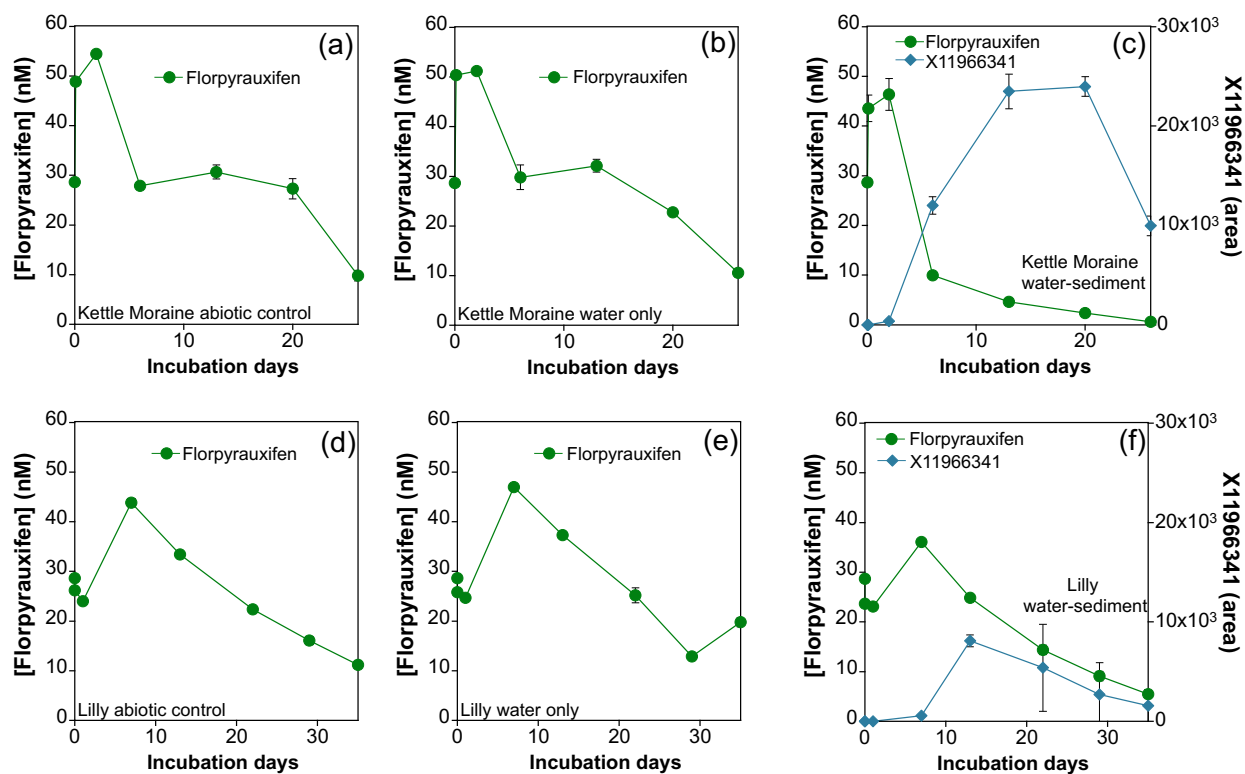


Figure C.5. Microcosms incubated with florpyrauxifen in (a-c) Kettle Moraine Lake and (d-f) Lilly Lake. (a, d) Abiotic controls are 0.2 μm filter sterilized while (b, e) water only microcosms are unfiltered lake water and no sediment. (c, f) Sediment microcosms contain area of degradation product X11966341 due to issues with quantification on LC-MS/MS. Error bars represent the standard deviation of samples from triplicate reactors.

Section C.6. Hydrolysis Experiments

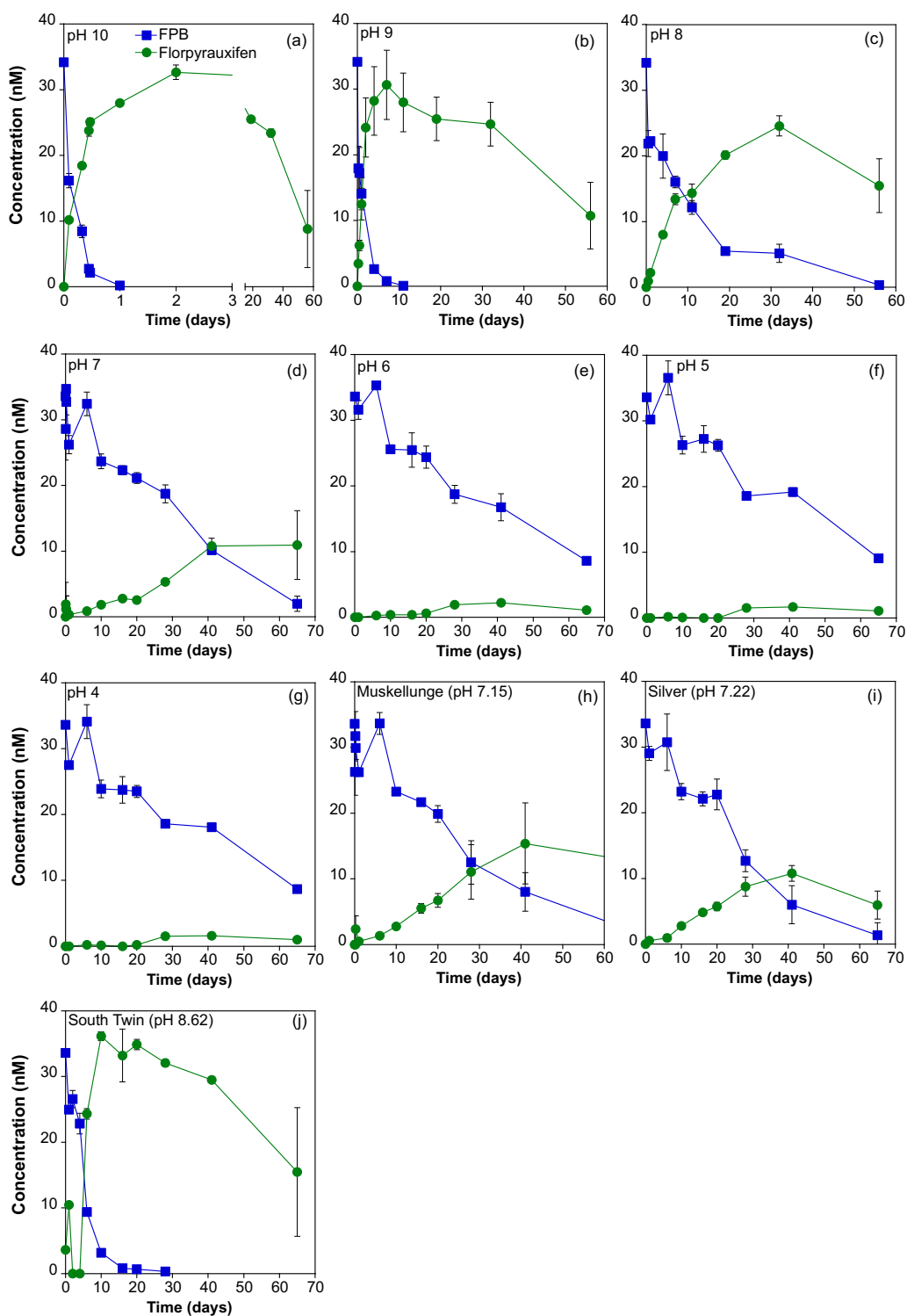


Figure C.6. [FPB] and [florpyrauxifen] in hydrolysis experiments at (a) pH 10, (b) pH 9, (c) pH 8, (d) pH 7, (e) pH 6, (f) pH 5, (g) pH 4. Three lake waters included at ambient pH: (h) Muskellunge (pH 7.15), (i) Silver Lake (pH 7.22), (j) South Twin Lake (pH 8.62). Error bars represent the standard deviation of triplicate reactors.

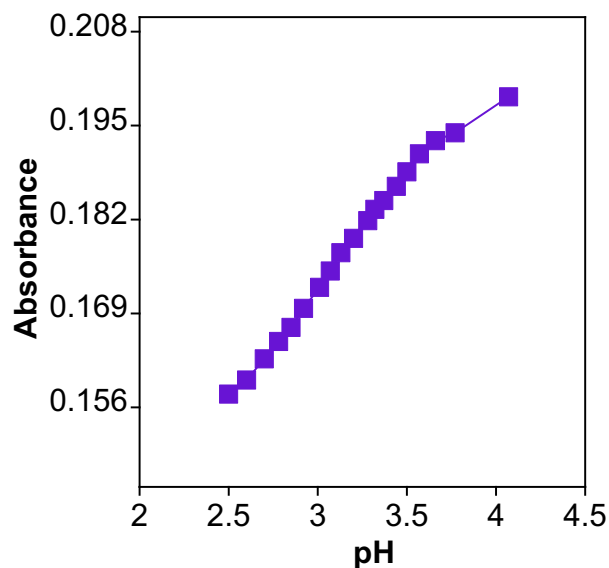


Figure C.7. Absorbance data for florpyrauxifen from pH 2.5-4. pK_a determined by measuring pH at different wavelengths and using least squares regression, which is at pH of 3.18.⁸

Section C.7. Analytical Methods

LC-MS/MS running conditions and method details for FPB and degradation products.

Mode: Positive electrospray ionization
Scan type: MRM
Gas temp: 400 °C
Speed: 13 L/min
Nebulizer pressure: 45 psi
Sheath gas temperature: 400 °C
Sheath gas flow rate: 12 L/min
Capillary voltage: 4500 V
Dwell: 100 msec

Table C.2. Precursor and product ion information for FPB, internal standard, and degradation products.

Compound	Retention Time (min)	Precursor <i>m/z</i>	Product <i>m/z</i>	Fragmentor voltage	Collision energy	Cell accelerator voltage	LOD (nM)
FPB	5.1	439	91	95	98	4	0.07
			65	95	110	4	
¹³ C FPB	5.1	445	91	95	98	4	0.07
			65	95	110	4	
Florpyrauxifen	4.2	349	268	96	25	7	0.09
			303	96	20	7	
¹³ C Florpyrauxifen	4.2	355	274	96	25	7	0.09
			309	96	20	7	
X12300837	4.8	425	91	102	50	7	Not calculated
			65	102	100	7	
X12131932	4.9	405	91	93	30	7	Not calculated
			65	93	100	6	
X11966341	2.9	335	289	12	21	5	Not calculated
			254	102	34	5	
X12393505	3.7	315	234	98	30	4	Not calculated
			191	98	60	4	

Samples were analyzed using a gradient method (**Table C.3**) of aqueous buffer (0.1% formic acid in ultra-pure water) and organic phase of 100% methanol at 0.35 mL min⁻¹ on an Agilent InfinityLab Poroshell 120 EC-C18 (3.0 x 50 mm).

Table C.3. Gradient chromatography details for analytical method of FPB, internal standard, and degradation products.

Time (minutes)	A%	B%
0.0	50	50
1	50	50
1.25	20	80
2	0	100
5.2	0	100
5.3	50	50
8.5	50	50

Table C.4. Method information for quantification of 2-nitrobenzaldehyde via high pressure liquid chromatography.

Compound	% Aqueous Buffer	Flow (mL min⁻¹)	Detection wavelength (nm)	Retention Time (min)	Purpose	LOD (μM)
2-nitrobenzaldehyde	80	0.5	231	2.9	311 nm actinometer	0.5

Section C.8. Treatment Data

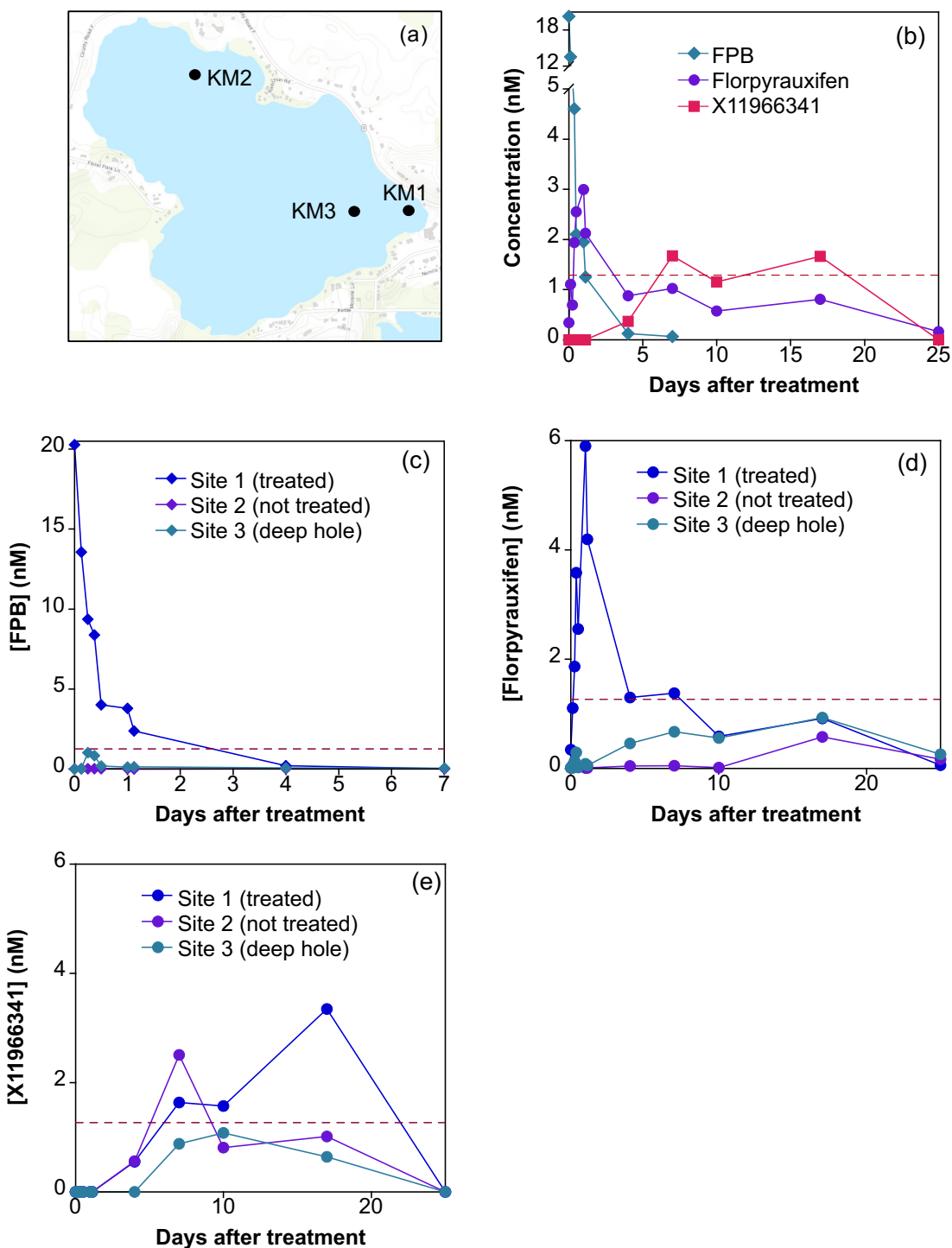


Figure C.8. (a) All sites on Kettle Moraine Lake, (b) [FPB], [florpyrauxifen], and [X11966341] of site KM1. (c) [FPB], (d) [florpyrauxifen], and [X11966341] in all sites. Dashed line is potential lake wide concentration of 1.28 nM. Standards for X11966341 and a quantitative method were only available for the 2022 lakes (Kettle Moraine Lake and Lilly Lake).

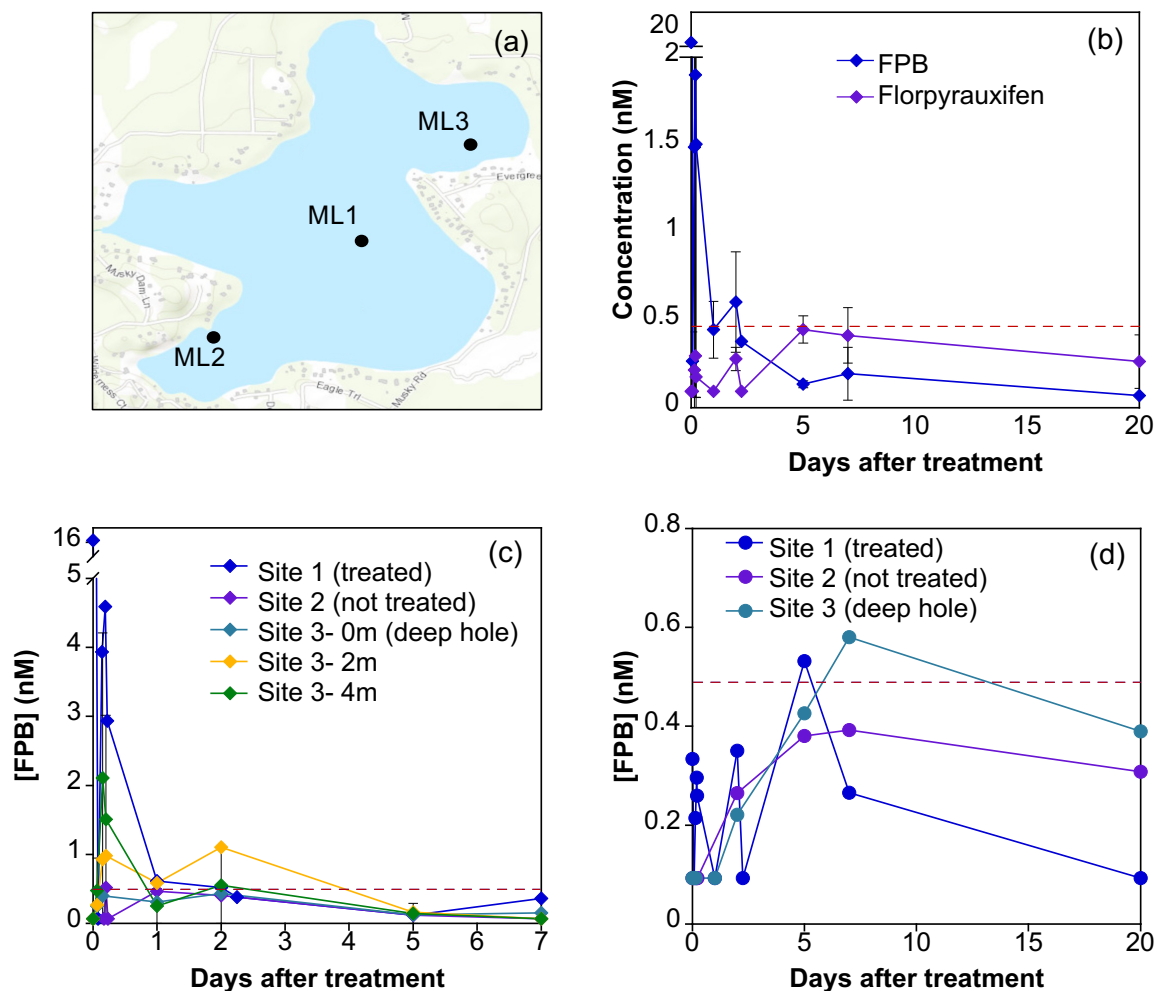


Figure C.9. (a) All sites on Muskellunge Lake, (b) lake wide average [FPB] and [florpyrauxifen]. (c) [FPB], (d) [florpyrauxifen] in all sites. Dashed line is potential lake wide concentration of 0.48 nM. Error bars in (b) represent standard deviation of three samples (one from each site) at each time point. Standards for X11966341 and a quantitative method were only available for the 2022 lakes (Kettle Moraine Lake and Lilly Lake).

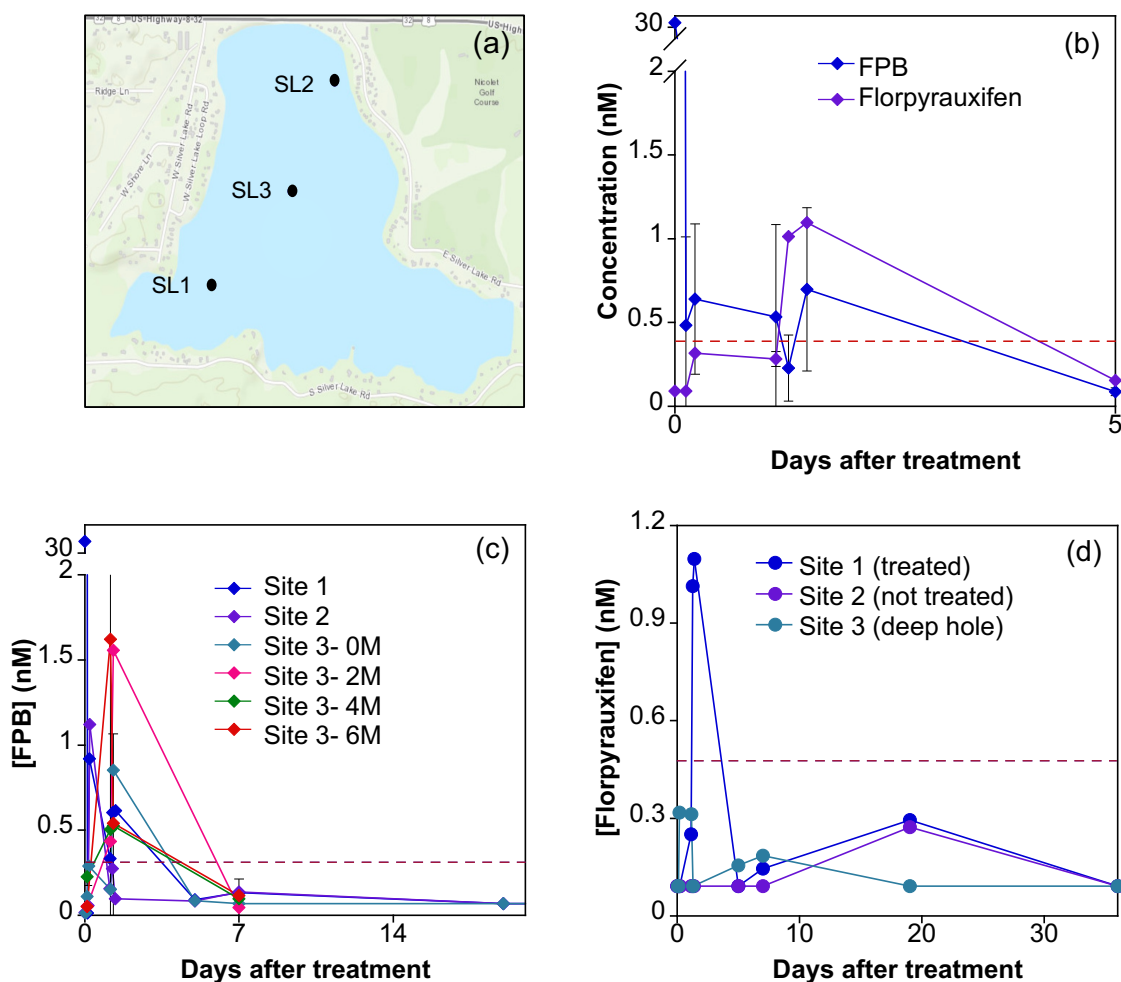


Figure C.10. (a) All sites on Silver Lake, (b) lake wide average [FPB] and [florpyrauxifen]. (c) [FPB], (d) [florpyrauxifen] in all sites. Dashed line is potential lake wide concentration of 0.36 nM. Error bars in (b) represent standard deviation of three samples (one from each site) at each time point. Standards for X11966341 and a quantitative method were only available for the 2022 lakes (Kettle Moraine Lake and Lilly Lake).

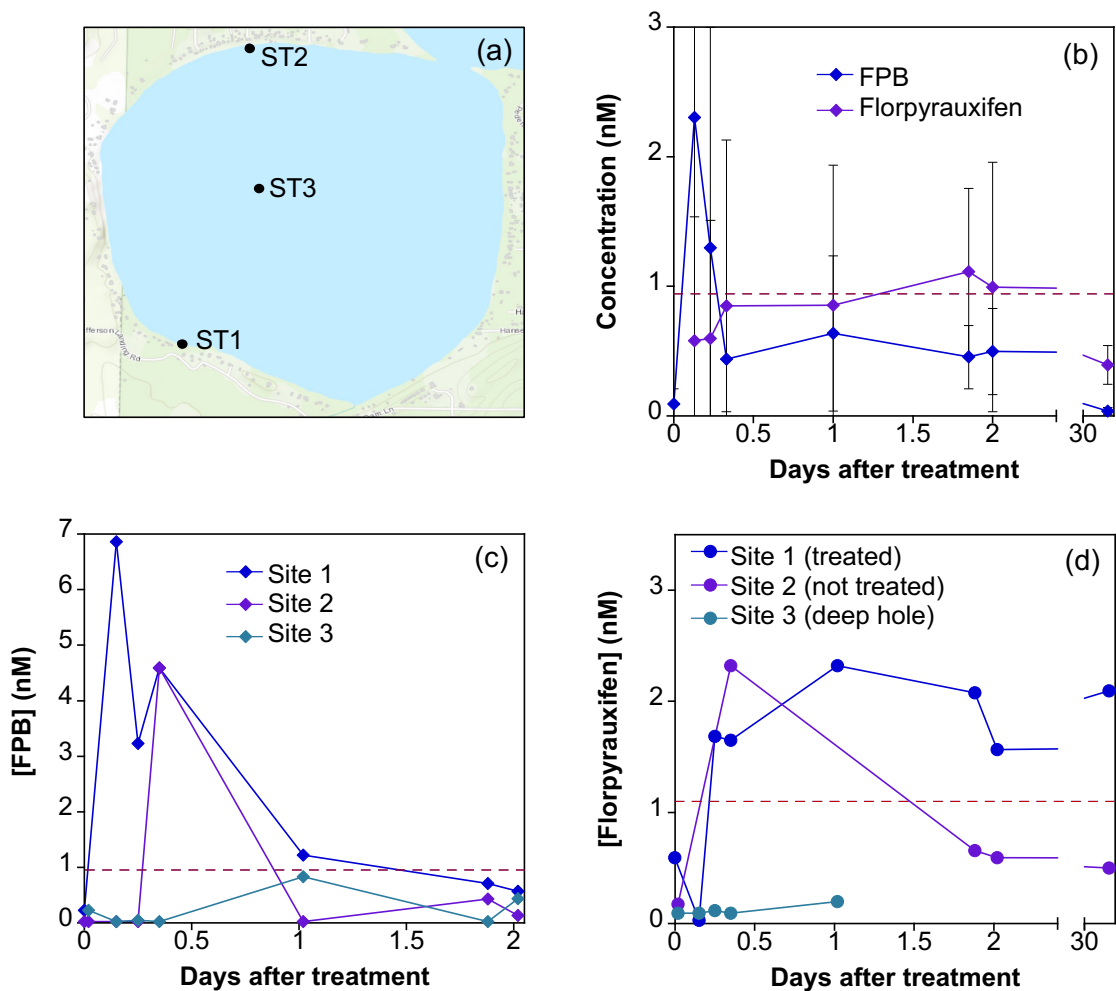


Figure C.11. (a) All sites on South Twin Lake, (b) lake wide average [FPB] and [florpyrauxifen]. (c) [FPB], (d) [florpyrauxifen] in all sites. Dashed line is potential lake wide concentration of 0.93 nM. Error bars in (b) represent standard deviation of three samples (one from each site) at each time point. Standards for X11966341 and a quantitative method were only available for the 2022 lakes (Kettle Moraine Lake and Lilly Lake).

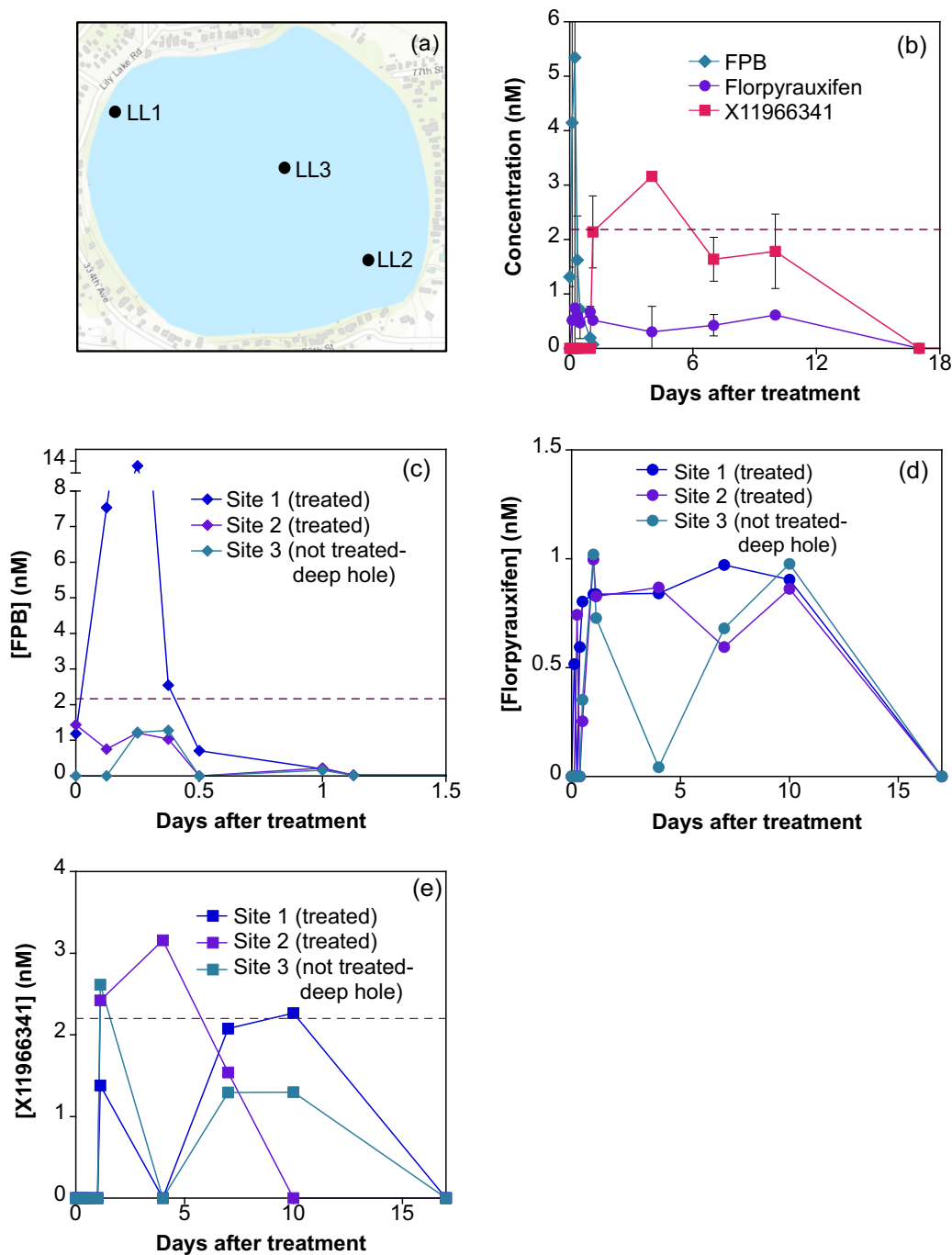


Figure C.12. (a) All sites on Lilly Lake, (b) lake wide average [FPB], [florpyrauxifen], and [X11966341]. (c) [FPB], (d) [florpyrauxifen] in all sites. Dashed line is potential lake wide concentration of 2.16 nM. Error bars in (b) represent standard deviation of three samples (one from each site) at each time point. Standards for X11966341 and a quantitative method were only available for the 2022 lakes (Kettle Moraine Lake and Lilly Lake).

Section C.9 References

- (1) Arena, M.; Auteri, D.; Barmaz, S.; Brancato, A.; Brocca, D.; Bura, L.; Carrasco Cabrera, L.; Chaideftou, E.; Chiusolo, A.; Civitella, C.; Court Marques, D.; Crivellente, F.; Ctverackova, L.; de Lentdecker, C.; Egsmose, M.; Erdos, Z.; Fait, G.; Ferreira, L.; Goumenou, M.; Greco, L.; Ippolito, A.; Istace, F.; Jarrah, S.; Kardassi, D.; Leuschner, R.; Lostia, A.; Lythgo, C.; Magrans, J. O.; Medina, P.; Mineo, D.; Miron, I.; Molnar, T.; Padovani, L.; Parra Morte, J. M.; Pedersen, R.; Reich, H.; Sacchi, A.; Santos, M.; Serafimova, R.; Sharp, R.; Stanek, A.; Streissl, F.; Sturma, J.; Szentes, C.; Tarazona, J.; Terron, A.; Theobald, A.; Vagenende, B.; van Dijk, J.; Villamar-Bouza, L. Peer review of the pesticide risk assessment of the active substance florpyrauxifen (variant assessed florpyrauxifen-benzyl). *EFSA Journal* **2018**, *16* (8).
- (2) Battelle. *Independent Laboratory Validation of a Dow AgroSciences Method for the Determination of XDE-848 Benzyl Ester and Five Metabolites (X11438848, X12300837, X11966341, X12131932 and X12393505) in Water*; 2013. https://www.epa.gov/sites/default/files/2017-09/documents/ilv_-_florpyrauxifen-benzyl_degradates_in_water_-_mrid_49677802.pdf (accessed 05-20-2020)
- (3) Battelle. *Independent Laboratory Validation of a Dow AgroSciences Method for the Determination of XDE-848 Benzyl Ester and Three Metabolites (X11438848, X12300837 and X11966341) in Soil*; 2013. https://www.epa.gov/sites/default/files/2017-09/documents/ilv_-_florpyrauxifen-benzyl_degradates_in_soil_-_mrid_49677776.pdf (accessed 05-20-2020)
- (4) Weishaar, J. L.; Aiken, G. R.; Bergamaschi, B. A.; Fram, M. S.; Fujii, R.; Mopper, K. Evaluation of specific ultraviolet absorbance as an indicator of the chemical composition and reactivity of dissolved organic carbon. *Environ. Sci. Technol.* **2003**, *37* (20), 4702–4708. <https://doi.org/10.1021/es030360x>.
- (5) Helms, J. R.; Stubbins, A.; Ritchie, J. D.; Minor, E. C.; Kieber, D. J.; Mopper, K. Absorption spectral slopes and slope ratios as indicators of molecular weight, source, and photobleaching of chromophoric dissolved organic matter. *Limnol. Oceanogr.* **2009**, *54* (3), 1023. <https://doi.org/10.4319/lo.2009.54.3.1023>.
- (6) Galbavy, E. S.; Ram, K.; Anastasio, C. 2-Nitrobenzaldehyde as a chemical actinometer for solution and ice photochemistry. *J. Photochem. Photobio. A: Chem* **2010**, *209* (2–3), 186–192. <https://doi.org/10.1016/j.jphotochem.2009.11.013>.
- (7) White, A. M.; Nault, M. E.; McMahan, K. D.; Remucal, C. K. Synthesizing laboratory and field experiments to quantify dominant transformation mechanisms of 2,4-dichlorophenoxyacetic acid (2,4-D) in aquatic environments. *Environ. Sci. Technol.* **2022**, *56* (15), 10838–10848. <https://doi.org/10.1021/acs.est.2c03132>.
- (8) McConville, M. B.; Hubert, T. D.; Remucal, C. K. Direct photolysis rates and transformation pathways of the lampricides TFM and niclosamide in simulated sunlight. *Environ. Sci. Technol.* **2016**, *50* (18), 9998–10006. <https://doi.org/10.1021/acs.est.6b02607>.
- (9) Leifer, A. *The Kinetics of Environmental Aquatic Photochemistry: Theory and Practice*; American Chemical Society, 1988.
- (10) Remucal, C. K.; McNeill, K. Photosensitized amino acid degradation in the presence of riboflavin and its derivatives. *Environ. Sci. Technol.* **2011**, *45* (12), 5230–5237. <https://doi.org/10.1021/es200411a>.

- (11) Gueymard, C. A. Interdisciplinary applications of a versatile spectral solar irradiance model: A review. *Energy* **2005**, *30* (9), 1551–1576. <https://doi.org/10.1016/j.energy.2004.04.032>.